MODULATION OF INSULINOTROPIC HORMONE BIOACTIVITY WITH A FOCUS ON GLUCOSE-DEPENDENT INSULINOTROPIC POLYPEPTIDE (GIP) AND ITS RECEPTOR

By

SIMON AMADEUS HINKE

B. Sc. (Hon.), The University of British Columbia, 1997

A THESIS SUBMITTED IN PARTIAL FULFILLMENT OF THE REQUIREMENTS FOR

THE DEGREE OF

DOCTOR OF PHILOSOPHY

In

THE FACULTY OF GRADUATE STUDIES

AND THE FACULTY OF MEDICINE,

DEPARTMENT OF PHYSIOLOGY

We accept this thesis as conforming to the required standard

UNIVERSITY OF BRITISH COLUMBIA

November 2002

In presenting this thesis in partial fulfilment of the requirements for an advanced degree at the University of British Columbia, I agree that the Library shall make it freely available for reference and study. I further agree that permission for extensive copying of this thesis for scholarly purposes may be granted by the head of my department or by his or her representatives. It is understood that copying or publication of this thesis for financial gain shall not be allowed without my written permission.

Department of Physiology

The University of British Columbia
Vancouver, Canada

Date Jan 27/03

ABSTRACT

Insulin secretory responses to oral glucose are compromised in type 2 diabetes. GIP receptor desensitization and internalization were studied as possible mechanisms for the blunted responsiveness to GIP in the human disease, employing *in vitro* cellular models. Using clonal insulin producing tumour cells (βTC-3) and rat GIP receptor transfected CHO-K1 cells, it was possible to characterize important aspects of receptor regulation. GIP receptor desensitization appeared to be slower than for other related receptors, and the rate appeared to parallel receptor internalization. Phosphorylation of receptor carboxyl terminal serine residues was implicated in both processes. Using co-transfection techniques and pharmacological agents, it was possible to partially delineate cellular proteins involved in GIP receptor desensitization and internalization.

Dipeptidyl peptidase IV cleaves dipeptides from the N-termini of GIP, GLP-1 and glucagon, all of which are insulinotropic peptides involved in glucose homeostasis. Using cells transfected with the cognate receptors for these hormones, it was possible to demonstrate the importance of this enzyme in the modulation of hormone bioactivity. Structure-activity relationships for the peptides were designed to characterize the N-terminally truncated peptides, as well as design enzyme resistant molecules predicted to have superagonist activity *in vivo*. Such analogues with enhanced bioactivity may have a use in the treatment of diabetic states (GIP and GLP-1) or cardiovascular complications (glucagon). *In vivo* bioassay of these peptides confirmed their increased potency and highlighted their therapeutic potential. Additionally, fragment analysis was performed on GIP in an attempt to minimize the bioactive domain of the molecule, thus generating small molecular weight GIP receptor agonists.

Table of Contents

List of Figures

List of Tables

List of Abbreviations

Amino Acids:	3 Letter Code	1 Letter Code
Alanine	Ala	A
Arginine	Arg	R
Asparagine	Asn	N
Aspartate	Asp	D
Cysteine	Cys	C
Glutamine	Gln	Q
Glutamate	Glu	E
Glycine	Gly	G
Histidine	His	H
Isoleucine	Ile	I
Leucine	Leu	L
Lysine	Lys	K
Methionine	Met	M
Phenylalanine	Phe	F
Proline	Pro	P
Serine	Ser	S
Threonine	Thr	T
Tryptophane	Try	W
Tyrosine	Tyr	Y
Valine	Val	V

PCR = polymerase chain reaction
RT-PCR = reverse-transcription PCR
ORF = open reading frame
mRNA = messenger ribonucleic acid
cDNA = complementary DNA
DNA = deoxyribonucleic acid
Da = Dalton (molecular mass)
HPLC = high pressure liquid chromatography/high performance liquid chrmatography
MALDI-TOF MS = matrix-assisted laser-desorption ionization-time of flight mass spectrometry
CT = carboxyl terminal (-COOH-terminal)
NT = amino terminal (-NH$_2$-terminal)
sp = synthetic porcine
np = natural porcine
sh = synthetic human
wt = wild type

EC$_{50}$ = effective concentration to achieve 50% of the maximal biological response
IC$_{50}$ = concentration inhibiting 50% of measured parameter (*e.g.* radioligand binding)
cpm = counts per minute (radioactivity)
AUC = area under the curve (integrated)

CHO = Chinese hamster ovary cells
CHL = Chinese hamster lung cells
HEK = Human embryonal kidney cells
COS = green monkey kidney cells
βTC = mouse insulinoma cells

EDTA = ethylenediaminetetraacetate
DMSO = dimethylsulfoxide
HEPES = *N*-2-hydroxyethylpiperazine-*N'*-2-ethane sulfonic acid
IBMX = 3-isobutyl-1-methylxanthine
BSA = bovine serum albumin
Ab = antibody
DPIV = dipeptidyl peptidase IV (CD26)

AVP = arginine vasopressin (anti-diuretic hormone, ADH)
GRP = gastrin releasing peptide
GLP-1 = glucagon-like peptide-1
GLP-2 = glucagon-like peptide-2
GIP = glucose-dependent insulinotropic polypeptide/gastric inhibitory polypeptide
VIP = vasoactive intestinal peptide
CCK = cholecystokinin
GHRH/GRF = growth hormone releasing hormone/growth hormone releasing factor
PHI/PHM = peptide histidine isoleucine/peptide histidine methionine
EGF = epidermal growth factor
PTH = parathyroid hormone/parathormone
THRH = thyroid hormone releasing hormone
LH = luteinizing hormone
FSH = follicle stimulating hormone
"R" following these abbreviations denote the hormone's receptor

GPCR = G-protein coupled receptor
GRK = G-protein coupled receptor kinase
G-protein = heterotrimeric guanosine triphosphate (GTP) binding proteins

ATP = adenosine 5'-triphosphate
ADP = adenosine 5'-diphosphate
cAMP = adenosine 3',5'-cyclic monophosphate
Ca^{2+} = cellular calcium
PIP_2 = phophotidylinositol 4,5,-bisphosphate
IP_3 = inositol 1,4,5-trisphosphate
DAG = diacylglycerol
CRE = cyclic AMP response element

AdC = adenylyl cyclase (forms cAMP from ATP)
PLC = phospholipase C (forms IP_3 and DAG from PIP_2)
MAPK/ERK = mitogen activating protein kinase/extracellular regulated kinase
PI3K = phosphotidylinositol 3' kinase
PKA = protein kinase A/cyclic AMP dependent protein kinase
PKC = protein kinase C
GEF = guanine-nucleotide exchange factor
GAP = GTPase-activating protein
PDE = phosphodiesterase (forms AMP from cAMP)

IV = intravenous
ICV = intracerebroventricular
IP = intraperitoneal
ID = intraduodenal
SC = subcutaneous

VDF = Vancouver diabetic fatty (Zucker rat)
Fa/? = homozygous/heterozygous dominant for functional leptin receptor = lean Zucker rat
fa/fa = homozygous recessive for non-functional leptin receptor = obese Zucker rat

Preface and Dedication

This thesis is dedicated to my high school teachers for their understanding and patience. In particular, Mrs. Broome, Ms. VanHeteren, and Mr. McCarthy inspired me to pursue science, and Jackie McDonald, with her friendship, instilled in me enthusiasm and faith in humanity.

Some of the work contained in this thesis has been published:

Hinke, SA, Gelling, R, Manhart, S, Lynn, F, Pederson, RA, Kühn-Wache, K, Rosche, F, Demuth, H-U, and CHS McIntosh, 2002. Structure-activity relationships of glucose-dependent insulinotropic polypeptide (GIP). *Biol. Chem.* (in press).

Hinke, SA, Gelling, RW, Pederson, RA, Manhart, S, Nian, C, Demuth, H-U, and CHS McIntosh, 2002. Dipeptidyl peptidase IV-resistant [D-Ala^2]glucose-dependent insulinotropic polypeptide (GIP) improves glucose tolerance in normal and obese diabetic rats. *Diabetes* 51:652-661.

Hinke, SA, Manhart, S, Pamir, N, Demuth, H-U, Gelling, RW, Pederson, RA, and CHS McIntosh, 2001. Identification of a bioactive domain in the amino-terminus of glucose-dependent insulinotropic polypeptide (GIP). *Biochim. Biophys. Acta* 1547:143-155.

Pospisilik, JA, Hinke, SA, Hoffmann, T, Rosche, F, Schlenzig, D, Heiser, U, Glund, K, McIntosh, CHS, Pederson, RA and H-U. Demuth, 2001. Metabolism of glucagon by dipeptidyl peptidase IV. *Regul. Pept.* 96:133-141.

Hinke, SA, Pauly, RP, Ehses, J, Kerridge, P, Demuth, H-U, McIntosh, CHS, and RA Pederson, 2000. Role of glucose in chronic desensitization of isolated rat islets and mouse insulinoma (βTC-3) cells to glucose-dependent insulinotropic polypeptide. *J. Endocrinol.* 165:281-291

Hinke, SA, Pospisilik, JA, Demuth, H-U, Manhart, S, Kühn-Wache, K, Hoffmann, T, Nishimura, E, Pederson, RA and CHS McIntosh, 2000. Dipeptidyl Peptidase IV Degradation of Glucagon : Characterization of Glucagon Degradation Products and DPIV Resistant Analogs. *J. Biol. Chem.* 275:3827-3834

Wheeler, MB, Gelling, RW, Hinke, SA, Tu, B, Pederson, RA, Lynn, F, Ehses, J, and CHS McIntosh, 1999. Characterization of the carboxyl-terminal domain of the rat glucose-dependent insulinotropic polypeptide (GIP) receptor. A role for serines 426 and 427 in regulating the rate of internalization. *J. Biol. Chem.* 274:24593-24624.

Acknowledgements

EPIGRAPH

CORPORA NON AGUNT NISI FIXATA – P. Ehrlich

Chapter 1: Introduction

1.1 Overview

GIP is a polypeptide hormone having structural similarities to the glucagon/secretin/vasoactive intestinal polypeptide superfamily of hormones. It is thought that GIP arose from a series of gene duplications occurring over the last 1,000 million years, derived from the ancestral gene for pituitary adenylyl cyclase activating polypeptide [1]. To date, GIP has yet to be identified in fish or birds, suggesting that the final gene duplication, resulting in the ancestral GIP gene, must have been prior to the divergence of modern mammals, 72 million years ago [1; 2].

Protein purification methods expanded in the 1960s and 1970s, and interest in gut hormones increased. Initially, GIP was identified for its enterogastrone (acid inhibitory) effects, hence the first term for the hormone, gastric inhibitory polypeptide. Large scale purification from pork intestine allowed the elucidation of the amino acid sequence of GIP. Based on sequence similarity to glucagon, it was hypothesized that GIP might have a role in glucose homeostasis. In contrast to the diabetogenic actions of glucagon, GIP acted to lower glycemia by augmenting nutrient stimulated insulin release from the pancreatic Islets of Langerhans. Thus came the second designation for GIP: glucose-dependent insulinotropic polypeptide, retaining the original acronym for the hormone [3].

Initial biochemical characterization of the GIP receptor was hindered by the apparent difficulty radiolabelling the hormone. Measurement of GIP by radioimmunoassay did not require biologically active GIP tracer, however, receptor binding studies did. Identification of the biologically active iodinated GIP product separated by high pressure liquid chromatography allowed these studies to begin in the mid 1980s [4]. During the same time, the first G-protein coupled receptor (GPCR) was cloned [5; 6]. Nearly a decade later, molecular biology techniques had advanced to the point where low-stringency screening of cDNA libraries was allowing the

1

cloning of families of receptors, based on conserved structural motifs. In 1991, the receptor for secretin was first cloned [7], and shortly thereafter, the receptor cDNAs for glucagon-like peptide-1 (GLP-1) [8], glucagon [9; 10], and GIP [11] were also obtained. The cloning of the GIP receptor has allowed three significant areas of research to advance: (1) Structure-activity relationships of synthetic GIP could be examined in an isolated model, (2) the signal transduction cascades utilized by the receptor could be dissected more easily, and (3) site-directed mutagenesis of the receptor allowed the molecular characterization of receptor binding, activation, and regulation.

1.2 The Discovery of GIP

1.2.1 History: Enterogastrone Effects & Gastric Inhibitory Polypeptide

Early studies on impure hog intestine mucosal extracts containing cholecystokinin-pancreozymin (CCK-PZ) established the role of CCK-PZ in stimulating enzyme release from the exocrine pancreas and contraction of the gall bladder, however, when looking at gastrointestinal (GI) motility or acid secretion, contradictory results were obtained [12]. When two preparations of CCK-PZ with differing purities, 200 Ivy dog units/mg ("10% pure") and 1,500 Ivy dog units/mg ("40% pure"), were examined in a multiparameter study in conscious dogs, evidence for a second contaminating hormone emerged. When CCK-PZ activity was held constant (0.2 IDU/kg/min) at sub-maximal doses for gall bladder contraction (measured using a bioassay in guinea pig), infusion into dogs gave equivalent changes in intra-gallbladder pressure, antral motor activity, and possibly pepsin secretion, however, significant differences in acid secretion from denervated fundic (Heidenhain) pouches were measured [13]. Brown and Pederson proposed two possibilities for these observations: either they had concentrated a gastric stimulant during purification or an acid inhibitory molecule was proportionately removed during the purification protocol. These hypotheses were later tested using a similar canine model with

2

mucosal extracts having undergone a series of gel chromatography separations and precipitation steps; fractions were tested for CCK-PZ activity using a bioassay, and all fractions not having significant guinea pig gallbladder contracting ability were pooled. Thus, it was demonstrated that it was possible to purify a polypeptide having the ability to potently inhibit both acetylcholine- and pentagastrin-stimulated acid secretion [12; 14; 15]. While results were preliminary, the authors suggested that this purified polypeptide was the enterogastrone (gastric inhibitory) substance described by Kosaka and Lim some thirty-nine years earlier [16]. It wasn't until Brown published the amino acid composition and tryptic peptides of the purified polypeptide that he officially dubbed the molecule "Gastric Inhibitory Polypeptide," giving the acronym GIP [17].

1.3 GIP Sequence

1.3.1 Peptide Sequence and mRNA Isolation

Not long after the initial isolation of GIP from pig intestinal mucosa, Brown published the first amino acid sequence data for the newly discovered peptide [17]. Using gel filtration chromatography and high voltage paper electrophoresis, fragments of GIP generated by enzymatic cleavage with trypsin or chymotrypsin, or chemically cleaved with cyanogen bromide (CNBr) were separated, and amino acid analyses and partial peptide sequencing were performed. Quantitative amino acid analysis suggested a molecule of 42 or 43 amino acid residues – it was uncertain as to the number of Glx residues present. Later the same year, the complete amino acid sequence was published; the Edman degradation sequencing method had been applied to all of the GIP fragments [18]. Unfortunately, the uncertainty in number of Gln residues was not entirely resolved; the sequence in question, tryptic fragment Tr-3b, was difficult to analyze due to low yields and amino acid composition. Comparisons between natural and early synthetic analogues were unable to confirm the original published structure, and the hypothesis was put

3

forward that the original sequence of Brown and Dryburgh was incorrect [19]. Upon reinvestigation, Jörnvall and colleagues used HPLC to separate GIP fragments generated by CNBr or N-chlorosuccinimide (cleaving GIP after each of its two tryptophane residues), as well as trypsin, prior to Edman sequencing. Hence, it was confirmed that indeed, one too many Gln residues was inserted at position 30 of the molecule, and in fact, GIP was only a 42 amino acid polypeptide [19].

Isolation and peptide sequencing of human GIP showed that only minor species variations existed between pig and man – Arg^{18} and Ser^{34} from the porcine sequence were replaced with His and Asn in *Homo sapiens*, respectively [20]. The same year, the sequence of cow GIP was also reported, differing at only one residue from the pig isoform (Table 1) [21]. The sequence of human GIP was later confirmed upon the isolation of an intestinal cDNA encoding the human isoform [22], and the cloning of the human GIP gene [23]. Sequences of rodent GIP isoforms have been entirely deduced from DNA sequences; three groups published the rat cDNA sequence in 1992 and 1993 [24-27], and the mouse cDNA sequence was published in 1996 [28]. Comparing isoforms from all species, very little variation exists – the sequences sharing greater than 90% sequence identity among mammals. GIP has yet to be isolated from fish, amphibians, birds or invertebrates, thus little is known about the molecular evolution of the molecule [1; 2].

Table 1: Amino acid sequence alignments of GIP from different species

	1-----------------10-----------------20-----------------30-----------------40--42
Human	Y-A-E-G-T-F-I-S-D-Y-S-I-A-M-D-K-I-H-Q-Q-D-F-V-N-W-L-L-A-Q-K-G-K-K-N-D-W-K-H-N-I-T-Q
Pig	Y-A-E-G-T-F-I-S-D-Y-S-I-A-M-D-K-I-R-Q-Q-D-F-V-N-W-L-L-A-Q-K-G-K-K-S-D-W-K-H-N-I-T-Q
Cow	Y-A-E-G-T-F-I-S-D-Y-S-I-A-M-D-K-I-R-Q-Q-D-F-V-N-W-L-L-A-Q-K-G-K-K-S-D-W-I-H-N-I-T-Q
Hamster	Y-A-E-G-T-F-I-S-D-Y-S-I-A-M-D-K-I-R-Q-Q-D-F-V-N-W-L-L-A-Q-K-G-K-K-N-D-W-K-H-N-I-T-Q
Rat	Y-A-E-G-T-F-I-S-D-Y-S-I-A-M-D-K-I-R-Q-Q-D-F-V-N-W-L-L-A-Q-K-G-K-K-N-D-W-K-H-N-L-T-Q
Mouse	Y-A-E-G-T-F-I-S-D-Y-S-I-A-M-D-K-I-R-Q-Q-D-F-V-N-W-L-L-A-Q-R-G-K-K-S-D-W-K-H-N-I-T-Q

Human [20], porcine [17-19] and bovine [21] sequences were first obtained by protein sequencing. Molecular cloning techniques allowed the deduction of rodent GIP sequences from genomic [25] or mRNA sequences [24; 26-29]. The human sequence was confirmed with the cloning of the GIP gene and isolation of an intestinal cDNA encoding GIP [22; 23]. Shadowed amino acids represent variations from the porcine sequence.

1.3.2 The GIP Gene

Inagaki and colleagues [23] were the first to report the structure of the human GIP gene, isolating clones from a human genomic phage library using a cDNA probe. DNA sequencing of three overlapping clones indicated that the human GIP gene consisted of six exons encoding GIP mRNA, with five intervening introns [23]. Mature processed GIP_{1-42} was encoded within exons 3 and 4, whereas the unprocessed translated product of GIP mRNA, preproGIP, was encoded by exons 2, 3, 4 and 5, and the 5'-untranslated region and 3'untranslated region/polyadenosine tail were in exons 1 and 6, respectively (Figure 1). Chromosomal localization indicated the GIP gene mapped to chromosome 17q [23; 30; 31]. Analysis of human cDNA clones showed a 459 base pair open reading frame encoding a 153 amino acid protein (preproGIP) with a predicted molecular weight of approximately 17 KDa [22]. Removal of the signal peptide following Gly^{21} and proteolytic processing to mature GIP by unidentified convertases following single arginine residues indicate production of a putative 21 amino acid signal peptide, a 30 residue NH_2-terminal peptide and a 60 residue COOH-terminal peptide, with GIP's 42 amino acid sequence in between (Figure 1). The rat genomic GIP sequence has also been shown to consist of 6 exons and 5 introns, with the mRNA encoded within exons 2-5, and mature GIP_{1-42} split between exons 3 and 4 [25], following a pattern similar to the human gene (Figure 1). Analysis of rodent GIP mRNA sequences suggest a putative preproGIP similar to that predicted in humans: a 432 base pair open reading frame encoding the unprocessed 144 amino acid product, with a 21 amino acid signal sequence, a 22 amino acid NH_2-terminal peptide, the 42 amino acid hormone, and a 59 amino acid COOH-terminal peptide. Due to the existence of a Gly^{31}-Lys^{32}-Lys^{33} sequence in all forms of mature GIP_{1-42}, it has been suggested that cellular processing may result in the production of $GIP_{1-30NH2}$ *in vivo* [28; 32], although its existence has not been confirmed experimentally.

5

A. genomic DNA

1 Kb

Exon 1   Exon 2   Exon 3   Exon 4 Exon 5   Exon 6

5' ———□——————▨—————————————■——————————▨———▨————————□——————— 3'

B. mRNA

0.1 Kb

Signal$_{1-21}$ GIP$_{52-93}$

| 5'-UT | ▨▨▨ | ■■■ | ▨▨▨ | 3'-UT | poly-A |

NT$_{22-51}$ CT$_{94-153}$

preproGIP$_{1-153}$

C. Protein

Signal$_{1-21}$

NT$_{1-30}$ GIP$_{1-42}$ CT$_{1-60}$
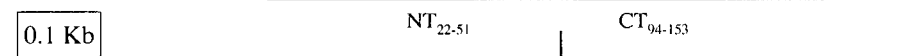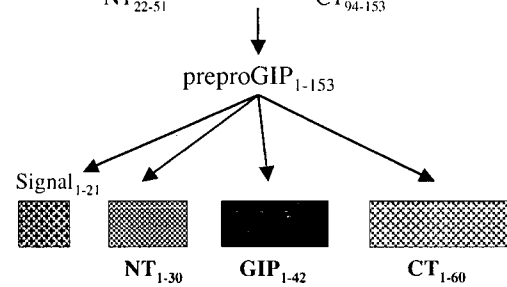
Figure 1: The human GIP gene, mRNA and post-translational processing
Adapted from [20; 22; 23].

6

1.3.3 Gene Regulation and GIP Expression

The 5'-upstream sequence from the human GIP gene was also determined, in order to gain insight into the potential regulation of GIP gene transcription; a TATA motif and consensus sequences for transcription factors Sp1, Ap-1, Ap-2 and a CRE element were identified, implicating regulation by cyclic AMP and protein kinases A and C [23]. Basal promoter activity of human GIP mRNA transcription was found to require the DNA sequence -180 to +14 (relative to the transcriptional initiation site), whereas inducible transcription was primarily mediated by one of two CRE elements in the regions -164 to -149, and *c-Jun* was capable of repressing transcription [33]. Several transcription factor motifs were identified in the rat GIP promoter [25]; delineation of regulatory domains of the rat promoter indicated a proximal and distal promoter, with cell-specific expression mediated by a GATA motif in the distal promoter, between -193 and -182 from the transcriptional start site [34].

Rat duodenal GIP mRNA transcripts have been detected as early as days 18-21 of embryogenesis [35; 36], but it is unclear as to whether low levels are present until birth, followed by a post-natal increase in transcription [36], or whether GIP mRNA transcripts steadily increase until birth, whereupon they reach adult levels [35]. It has been reported that in rats, 2 day starvation either nearly doubled [27] or halved [37] GIP mRNA levels. Clarification of this finding is necessary, as the question remains whether absence of nutrient stimulation acts as an anticipatory signal to promote biosynthesis of GIP for the next meal, or alternately, that biosynthesis of GIP during starvation is an expendible process during a time where energy should be conserved. Glucose has been reported to promote GIP transcript abundance in cell lines and rodents, with mild increases measured in immunoreactive GIP content after oral or *ID* glucose [28; 37; 38]. However, in hyperglycemic diabetic animals no changes in either GIP mRNA or protein content could be measured [39]. Gastric administration of peptone was found to have no influence on duodenal GIP gene transcription, but was able to increase intestinal GIP

content; this effect was reversed by omeprazole, indicating that peptone-induced effects were mediated via stimulation of acid secretion. Confirmation of this hypothesis was shown by perfusing rat duodenum with 0.1 M HCl, which increased both GIP transcription and immunoreactive GIP content [38; 40]. Dietary fat has also been reported to increase GIP mRNA levels [26; 37], but did not result in increased duodenal GIP peptide levels [37]. Hence, GIP expression is regulated developmentally and by dietary intake.

Early histological studies defined the intestinal mucosal cells containing immunoreactive (IR) GIP. These cells were determined to belong to the APUD (amine precursor uptake and decarboxylation) type, but distinct from other enteroendocrine cells; GIP containing cells were identified to be the K-cell [41-43]. Original studies found K-cells to have a distribution with greatest quantities in the duodenum and upper jejunum, distinctly different from L-cells containing gut glucagons, which were primarily in the jejunum and ileum [41; 43]. Recent studies have suggested that a population of L-cells in the jejunum exists that are co-localized with K-cells [44; 45], but this remains to be confirmed. Radioimmunoassay of extractable GIP from tissues compares well with mRNA expression profiles. GIP mRNA and IR-GIP are found in highest amounts in the proximal small intestine, and are present in decreasing amounts distally in the bowel [3].

The only convincingly confirmed regions in which GIP has been detected outside of the gut are in ductal cells of the submandibular salivary gland and in a specific population of endocrine cells in the stomach [26; 29; 35]. In addition to using the traditional methods of PCR detection, *in situ* hybridization and immunocytochemistry to define the stomach and intestinal populations of GIP-positive cells, Yeung *et al* [29] generated mice with a herpes simplex thymidine kinase gene driven by the human GIP promoter region, and examined tissue enzyme activity. This technique revealed significant enzyme activity in the stomach and pancreas, however, activity was not detected in the small intestine. The absence of enzyme activity in the duodenum, a well

8

established GIP expressing tissue, may be due to species differences controlling gene expression (*i.e.* human promoter in mice), or the GIP promoter construct was incomplete, and additional 5' upstream or intronic sequence is necessary for intestinal transgene expression. A similar transgenic approach employing the rat GIP promoter resulted in transgene expression in both stomach and duodenum [46]. Both the rat and human promoters were able to drive gene transcription in the insulinoma cell line, HIT-T15, to a certain degree, but this was extremely small compared to the level seen in the enteroendocrine tumor line, STC-1 [33; 34]. Most studies show that GIP is not expressed in esophagus, stomach, gastric antrum, gastric fundus, gastric cardia, colon, cecum, rectum, liver, gall bladder, pancreas, kidney, spleen, lung, heart, muscle, ovary, brain, hypothalamus, pituitary, spinal cord, or thyroid [22-24; 26; 27; 29; 39; 46; 47]. Apart from enriched primary cultures of K-cells [48] or *E. coli* transformed with a synthetic GIP expression plasmid [49], expression of GIP *in vitro* has been limited to only human embryonic intestinal 407 cells, STC-1 cells or derivatives of this tumor line, among a host of cell types tested, including cells derived from the salivary gland [28; 34; 50].

1.4 GIP Measurement and Release

1.4.1 Radioimmunoassay and Complications

Since the first development of a radioimmunoassay for GIP in 1974 [51], studies have been performed in a variety of species, including python, amphibians, pig, dog, rat, cow, sheep, goat, horse, and human, but many of these are complicated by the cross-reactivity of antibodies raised against natural source GIP [3; 52; 53]. Generally, antibodies have been raised against an epitope of GIP within amino acids 15-42 of the primary sequence; unfortunately, this same sequence is the region in which the greatest species differences in GIP occur (Table 1), thus resulting in inconsistent results when used for measuring GIP levels in other animals [52; 54]. Furthermore, these antibodies differentially recognize 4 or 5 immunoreactive species, only one of which is the

5 KDa peptide responsible for the known biological effects of GIP [3; 52; 53; 55; 56]. In a study designed to compare several antibodies in parallel, Jorde *et al* [56] reported human fasting basal GIP levels fell within the range 12-92 pM, and rose to 35-235 pM postprandially. Generally speaking, most studies report between a 2X and 10X increase in immunoreactive GIP concentrations in response to appropriate stimuli regardless of the antibody employed or study subject. More recent studies have shown that GIP is inactivated by dipeptidyl peptidase IV (DPIV; discussed in Chapter 4), and that GIP_{3-42} represents a significant proportion of circulating IR-GIP, further hindering interpretation of the data [19; 53; 57-61]. Another complication when comparing literature values of GIP release in response to different stimuli are the different methodologies used. Commonly, oral nutrients are given in solid or liquid form, with varied composition (glucose/carbohydrate, fat, protein/amino acids), but it is well documented that meal composition can dramatically affect gastric emptying, and thus nutrient delivery to the site of GIP release. Furthermore, salivary and gastric enzymes may metabolize nutrients prior to reaching the K-cell, or nutrients may stimulate release of secondary agents, such as gastric acid, making it difficult to conclusively determine factors capable of releasing GIP. For these reasons, emphasis is put on studies using intra-duodenal (*ID*) infusion of nutrients for *in vivo* release experiments and *in vitro* models for GIP secretion.

1.4.2 Stimuli for Release

1.4.2.1 Carbohydrates:

It is generally accepted that GIP granule exocytosis from the K-cell is by direct dose-dependent simulation with specific sugars, fats, and amino acids, as well as duodenal acid; hence ingestion of a mixed meal is a potent stimulus for hormone release [62; 63]. Glucose is perhaps the best characterized stimulant for GIP release, as shown by *ID* perfusion studies in rat, dog, pig and human [55; 63-74]. An elegant study by Thomas *et al* [75] using positional perfusion of the

10

human small intestine with proximal occlusion, demonstrated glucose-stimulated GIP secretion was greatest from the duodenum and proximal jejunum, compared to the mid-jejunum or ileum. It was shown that GIP release required intestinal sodium-dependent sugar transport and was specific for *ID* glucose, galactose, maltose or sucrose – fructose, mannose, 6-deoxygalactose, 2-deoxyglucose, myoinositol, sorbitol and lactose were without effect [64; 70; 76; 77].

1.4.2.2 Lipids:

Similarly, *ID* fat has been shown to be a potent GIP secretagogue [55; 67; 74]. Specifically, long chain fatty acids were required to stimulate GIP secretion, whereas medium chain fatty acids had no effect [78; 79]. The differential stimulation by medium versus long chain fatty acids is thought to be linked to chylomicron formation; medium chain fatty acids are directly absorbed, whereas absorption of long chain fatty acids requires formation of chylomicrons. Blockade of chylomicron formation completely ablated the GIP response to intra-duodenal fat and the associated rise in plasma triglycerides [80; 81]. In comparing oral fat and oral glucose in dogs, it was demonstrated that lipids caused a greater and sustained release of GIP compared to glucose, an effect likely due to the slower gastric emptying of fat [82]. Another study comparing isocaloric doses of intra-duodenal glucose or lipid in humans indicated fat to be the more potent stimulus on both weight and molar basis [55]. Results from studies in swine suggested that fat alone was a weak GIP stimulus, but when in administered in combination with glucose, it was able to stimulate greater GIP release than glucose alone [67].

1.4.2.3 Protein and pH:

Intra-gastric peptone (protein hydrolysate) stimulated GIP release in rats [40], but this was likely indirect via stimulation of acid release, as indicated by inhibition with omeprazole; in another study, *ID* lactalbumin hydrolysate was capable of stimulating GIP secretion [74]. Duodenal acidification has been shown to stimulate GIP secretion in rats and humans in most [40; 64; 72], but not in all cases [66]. Contrary to the dose-dependent effect of HCl on GIP

11

release, duodenal alkalinization with NaOH or perfusion with comparable ionic strength salt solutions were unable to change plasma GIP levels [64; 67; 70]. Amino acids alone also appear to stimulate hormone release from the K-cell directly [78; 83-85]. Infusion of a solution containing Arg, His, Ile, Leu, Lys, and Thr to the small intestine of human volunteers increased plasma GIP by about 7-fold, whereas an isotonic solution containing amino acids known to potently stimulate cholecystokinin (CCK) release potently (Met, Phe, Trp, and Val) was only able to cause a 2-fold rise in circulating GIP [83]. Hence, it appears that GIP is differentially released depending on the meal content, such that its biological effects act to maintain plasma nutrient homeostasis under the specific dietary conditions.

1.4.2.4 Feedback Regulation:

Modulation of GIP release from small intestine has been studied with respect to hormonal and nutrient feedback, as well as neural input. Extensive study has been directed at the role of circulating glucose and insulin in attenuating GIP release by luminal nutrients; the close relationship between these parameters make conclusions drawn from these studies difficult to interpret [68; 86; 87]. In a study of insulinopenic type 1 diabetes mellitus patients, both glucose and insulin independently inhibited the GIP response to oral fat but not oral glucose [88]. In one study, Dryburgh *et al* [89] found intravenous infusion of C-peptide ablated GIP release in response to ID Intralipid emulsion, while insulin and glucose levels were unchanged by the fat perfusion, possibly indicating negative hormonal feedback from the endocrine pancreas. GIP is known to stimulate both gastric and pancreatic somatostatin release [50; 90-92]. Immunoneutralization of somatostatin augmented GIP release *in vitro* [48; 50], whereas somatostatin has been shown to inhibit GIP secretion *in vivo* and *in vitro* [50; 71]. A recent study has shown that inhibition of DPIV in dogs, thus increasing the biological half-life of GIP and the related incretin glucagon-like peptide-1 (GLP-1; discussed below), as well as other hormonal substrates of DPIV, resulted in diminished GIP secretion in dogs, implicating possible

autocrine, paracrine or endocrine feedback [93]. However, this may be mediated by enhanced somatostatin and/or insulin and C-peptide release. Other studies have examined the effects of infusion of other hormones *in vivo* [64; 94-96], although the design of these studies prevents dissecting influences from changes in blood glucose, insulin, or exogenous hormones on GIP release. Hence, it is important that studies such as these are duplicated using *in vitro* K-cell models and the vascularly perfused small intestine to establish primary versus secondary effects on GIP release. Most studies agree that there is little if any evidence for modulation of K-cells by the autonomic nervous system [63; 65; 69; 73], although gastrin-releasing peptide (GRP) has been shown to stimulated GIP release *in vitro* [48]. Calcitonin-gene related polypeptide (CGRP) may negatively regulate GIP release via the enteric nervous system [97]. Hence, GIP cells also express receptors for neurotransmitters, although the significance is unclear.

1.4.2.5 GIP Release *in Vitro*:

Very few studies have been undertaken to examine GIP release *in vitro*, stemming from the diffuse distribution of enteroendocrine cells in the gut. Use of elutriation centrifugation of canine intestinal mucosa has been shown to allow enrichment of canine K-cells to a sufficient degree to allow release studies [48]. In this manner, it was possible to demonstrate glucose- and GRP-stimulated GIP secretion, and the inhibitory effects of somatostatin. Furthermore, it was shown that cell depolarization effected GIP exocytosis, and that secretion could be modulated by signal transduction cascades involving intracellular calcium or cyclic AMP [48]. The expense and difficulty of this method prompted the development of an alternative system for studying GIP secretion. Subcloning the intestinal endocrine tumour cell line, STC-1, resulted in a derivative cell line, STC 6-14, that contained ~30% IR-GIP containing cells and a similar percentage of somatostatin containing cells [50]. To date, studies using these models have been limited to those on the effect of glucose on GIP release *in vitro* and the role of somatostatin in control of GIP release. Further studies using these methodologies are necessary to clarify the

13

roles of other nutrients and hormones with respect to GIP secretion, particularly for non-glucose nutrients and hormonal modulation.

1.5 Biological Effects

1.5.1 Gastrointestinal and Pancreatic Effects

1.5.1.1 Enterogastrone Action:

Following Bayliss and Starling's demonstration that the gastrointestinal tract was an endocrine organ [98], many studies were performed in attempts at explaining physiological phenomena with responses to isolated humoural factors from gut extracts. One such study was that of Kosaka and Lim [16], who coined "enterogastrone" as the name of the mucosal hormone secreted from the small intestine in response to fat and resulting in gastric acid inhibition. As mentioned previously, peptide purification techniques allowed isolation, purification and testing of mucosal hormones, and several are candidates for enterogastrone activity; among candidates are peptide YY, secretin, CCK, glicentin/oxyntomodulin, and GIP [3; 99-102]. Recent progress in elucidation of GIP's enterogastrone action has fallen from popularity, primarily due to the question as to the physiological relevance of this function and the shifted emphasis towards the other biological functions of the hormone.

Early studies examining inhibition of acid secretion were conflicting, apparently due to differing methodologies employed. Original studies were performed in denervated Heidenhain gastric pouches [12-15], and when studies were duplicated in models employing intact innervated stomach, the potency of GIP as a physiological enterogastrone was difficult to demonstrate [103-106]. Clarification of these discrepant results came when the role of the vagus nerve was taken into account [107-109], although some studies have been able to show an effect of endogenous GIP immunoneutralization on acid secretion from the innervated stomach [64; 110]. Studies on the mode of action of GIP in the stomach suggest that somatostatin is the final

14

mediator of GIP's inhibitory ability [92; 107], although this pathway can be negatively regulated by acetylcholine and endogenous opioids [90; 111; 112]. GIP is one of the most potent stimuli for gastric somatostatin release, suggesting that the inhibitory activity of GIP on exogenous pentagastrin- and histamine-stimulated acid secretion was via paracrine somatostatin activity at the parietal cell, although GIP may also mediate paracrine regulation of gastrin-producing G-cells, histamine-releasing enterochromaffin cells and possibly chief cells [12-14; 90; 107; 113]. With specific regard to gastrin, some studies have reported GIP to be a stimulant [92; 114; 115], while others report GIP to diminish gastrin release [109; 110; 116; 117]; regardless, the net inhibition of acid secretion indicates that the effect of somatostatin is dominant. Given the strong neural influence of the vagus on somatostatin release from gastric D-cells [90; 107; 109; 115; 118], the inconclusive results regarding the physiological importance of GIP in acid secretion are not surprising. Indeed, inhibition of GIP-stimulated somatostatin by exogenous acetylcholine and vagal stimulation was demonstrated, and it was suggested that in order for GIP to play a role in acid regulation, parasympathetic tone must be reduced, possibly involving a catecholamine mediated enterogastric reflex [107; 109]. Most recently, Rossowski et al [119] developed a potent somatostatin antagonist which, when administered intravenously to rats prepared with gastric fistulae, resulted in a potent blockade of the enterogastrone activity of GIP, confirming earlier studies. In all likelihood, the enterogastrone effect proposed by Kosaka and Lim [16] is mediated by a number of gastrointestinal hormones with overlapping functions, only one of which is GIP.

1.5.1.2 Other GI Effects:

Investigation of other possible actions of GIP on the gastrointestinal system have been extremely limited. Prior to demonstration of expression in the salivary gland [26; 35], GIP was considered to act as a regulator of salivary duct electrolyte transport [120]. Similarly, GIP was shown to be a local regulator of mucosal alkalinization in the proximal duodenum [121] and to

15

control water and electrolyte absorption in the jejunum [122; 123]. Early studies indicating GIP had a stimulatory effect on exocrine pancreatic acinar cells were later suggested to be due to contaminating CCK in natural source preparations of hormone [124; 125]. Later studies employing synthetic or highly purified peptide preparations indicated that GIP was capable of potentiatiating acetylcholine- and CCK-stimulated amylase excretion [126; 127], whereas it inhibited bombesin-stimulated amylase secretion [32]; it is thought that GIP's action on the exocrine pancreas may be a secondary effect mediated via insulin. The well designed studies of Cheeseman and co-workers indicated GIP upregulated phloridzin-insensitive hexose transport, thus augmenting absorption of sugars from the small intestine [128; 129]. GIP appears to have only weak effects on gastrointestinal motility during the digestive [130-132] and interdigestive phases [133; 134]. In some animals (but not humans) high concentrations of GIP stimulated hormone release from intestinal L-cells [45; 135-140]. Additionally, GIP has also been shown to affect blood flow to the mesentery [132; 141-143].

As with biological functions attributed to any hormone, the distinction between physiological and pharmacological effects must be made. While the enterogastrone and incretin effects of GIP are well established, uncorroborated studies must be carefully scrutinized with respect to hormone concentration and experimental design in order to discriminate between physiological and pharmacological effects. Often the tendency is to administer larger hormone doses to convincingly (*i.e.* statistically) demonstrate an effect – this is a two edged sword that must be regarded with caution.

1.5.2 The Enteroinsular Axis & Incretin Concept

The seminal articles demonstrating an augmented insulin response to nutrients when administered orally versus intravenously [144-147] prompted Unger and Eisentraut [148] to propose the "Entero-insular Axis," a concept later expanded by Creutzfeldt [80; 149] to describe

16

all gut derived input – direct substrate, neural and hormonal signals – on release of any hormone (insulin, glucagon, somatostatin, and pancreatic polypeptide) from the Islets of Langerhans on nutrient ingestion. Prior to the discovery of insulin, Moore, Edie and Abram attempted to purify a hormone from duodenal mucosa to treat type 1 diabetes [150]. After Banting and Best [151] succeeded in isolating insulin, the internal secretion of the pancreas, La Barre termed mucosal hormones able to stimulate insulin secretion *"l'incretine"* [152-154]. Currently, two criteria define an incretin: (1) it must be released by luminal nutrients, particularly carbohydrates, and (2) at physiological levels, it must stimulate insulin secretion in the presence of elevated blood glucose levels [80]. Of potential gastrointestinal hormones, GIP may be the only uncontested candidate as a true physiological incretin [155-157]; glucagon-like peptide-1 (GLP-1; discussed below) has potent antihyperglycemic effects, and has also been considered a potential incretin, however, recently it has been suggested that glucose-lowering effects attributed to this peptide may be primarily derived from slowing gastric emptying and/or local activation of afferent neural fibres, rather than incretin activity by definition [158; 159].

The first indication that GIP had insulin stimulating ability came from the research group of Dupré. Impure preparations of CCK-PZ improved glucose tolerance when infused intravenously, however, results could not be duplicated with highly purified CCK-PZ [160; 161], much like the early findings of Brown and Pederson on gastric acid secretion. Hence, Dupré reasoned GIP was responsible for the insulinotropic action in impure CCK-PZ, and when this hypothesis was tested, it was shown to be correct [162]. Further human studies using an intravenous glucose infusion to maintain a hyperglycemic clamp, with a concurrent oral glucose load [163] or GIP infusion [164], unequivocally established GIP as a physiological incretin in man, and suggested that GIP could be responsible for the entire incretin-mediated insulin response. Importantly, the insulinotropic action of GIP was dependent upon prevailing glycemic conditions, such that GIP was unable to stimulate insulin during euglycemia, thus preventing the

17

risk of hypoglycemia [82; 87; 162; 165]. Considering that fat is the most potent GIP secretagogue, the glucose-dependency of its insulinotropic activity is crucial. In the isolated vascularly perfused rat pancreas, in order for GIP to stimulate insulin release, a threshold glucose concentration of 5.5 mM was necessary, and maximum potentiation occurred with 16.7 mM glucose in the perfusate [165]. GIP's actions on the β-cell were also concentration dependent [57; 165]; a linear peptide gradient in the perfused pancreas resulted in significant insulin release at concentrations as low as 70 pM [57], consistent with the physiological postprandial concentrations of GIP. The insulinotropic actions of GIP have been replicated using isolated islets of Langerhans [166-173], purified β-cells [174], and clonal β-cell models [175-182]. Confirmation of the physiological role of GIP as an incretin has been found using methodologies to ablate GIP signalling: immunoneutralization of GIP [64; 183; 184], immunoneutralization of the GIP receptor [185], injection of peptide antagonists of the GIP receptor [186-188], and generation of a transgenic mouse with a null mutation in the GIP receptor gene [189]. These studies generally indicate that 50-70% of the postprandial insulin response results from stimulation by GIP.

The mode of action of GIP is mediated via specific activation of a cell surface receptor present on the β-cell. Receptor activation results in generation of second messengers cyclic AMP, intracellular calcium flux, and arachidonic acid release (discussed below), which ultimately results in greater insulin secretion. The dogma of β-cell activation is that cellular glucose uptake and metabolism increases the cellular ratio of ATP:ADP, resulting in the closure of K^+_{ATP} channels and thus membrane depolarization; the opening of voltage-dependent calcium channels (VDCC) allows influx of Ca^{2+}, a requirement for granule exocytosis. Hence, activation of the GIP receptor must accelerate the stimulus-exocytosis cascade or recruit additional (un)responsive β-cells to potentiate insulin release. While the dependence of GIP's proximal intracellular signals on prevailing glucose conditions is unclear, GIP has been shown to decrease

conductance of ATP-sensitive K^+ channels responsible for β-cell depolarization [190-193]. Although electrophysiological studies were not able to show a direct action of GIP on calcium channels [190], other studies indicate GIP does augment influx of extracellular calcium via these channels [4; 176; 194]. Additionally, studies have shown that GIP is able to further stimulate exocytosis at a level distal to the rise in intracellular calcium [190; 191], as well as via a K^+_{ATP} channel independent pathway [195]. It has been proposed that the "glucose sensor" allowing incretin-induced insulin release only in the presence of elevated glucose may be simply the requirement of PKA-stimulated granule mobilization of a high ATP:ADP ratio [192]; notably, oxidative metabolic intermediates have also been shown to permit the insulinotropic activity of GIP [57; 168].

The β-cell integrates various external stimuli, such that GIP and GLP-1 have additive effects on insulin release [196-199], and GIP potentiates the glucose-dependent insulinotropic action of CCK, acetylcholine and arginine [200-204]. Cholinergic augmentation of GIP-stimulated insulin release has been implicated [200; 204-206], whereas somatostatin, enterostatin, galanin, VIP and islet amyloid polypeptide (IAPP, amylin) were able to inhibit GIP's action on the β-cell [201; 207-210]; pancreastatin may or may not play an inhibitory role [207; 211; 212]. In addition to enhancing insulin release, GIP further acts as an insulinotropic agent by stimulating proinsulin gene transcription and translation [213-216] and up-regulating plasmalemmal glucose transporters and hexokinase in the β-cell [216].

Islet hormone regulation by GIP is not limited to the β-cell. Early studies in the perfused rat and dog pancreas indicated that GIP stimulated release of glucagon, somatostatin, and pancreatic polypeptide [170; 202; 217; 218]. The effect of GIP on glucagon release was only under low glucose conditions and decreased upon increasing glucose concentration in the perfusate, consistent with the physiological release of glucagon [202; 217]. In purified rat α-cells, GIP and GLP-1 were able to promote exocytosis via a cyclic AMP-dependent potentiation of calcium

currents. Using the same preparation, somatostatin was able to restrain the glucagonotropic effects of GIP and GLP-1, whereas insulin was without effect [219]. While the ability of GIP to stimulate glucagon release has been duplicated in isolated perfused human cadaver pancreata [206], in clinical studies, no effect of GIP on serum glucagon is observed [87; 164; 220-222]. Hence, it is likely that the somatostatinotropic activity of GIP in the pancreas is more physiologically relevant, resulting in suppression or no change in glucagon in humans during exogenous GIP infusion.

1.5.3 Effects on Nutrient Storage and Metabolism

1.5.3.1 Liver:

Few studies have been performed regarding the biology of GIP and the hepatocyte. Expression of the known GIP receptor mRNA present in other tissues has not been detected in hepatic tissue [223; 224], nor were GIP binding sites detected [175; 225; 226]. However, some work has indicated GIP does have biological effects on liver. A gut factor was considered to be responsible for a decrease in hepatic extraction of insulin [227-229], however, other studies suggested that GIP was unlikely to be the mediator [230]. Canine experiments using chronically implanted catheters and Doppler-flow probes confirmed that a gut factor reduced insulin extraction by the liver, but comparison of oral versus intraportal glucose administration indicated hepatic glucose uptake was not influenced by gut hormones; indeed, when co-infused with *IV* glucose, GIP had no influence on hepatic glucose uptake [231]. In isolated cultured rat hepatocytes, GIP acted in a catabolic fashion, stimulating glycogenolysis and a slight but significant increase in gluconeogenesis. Somatostatin was able to reduce these glucagon-like effects on the liver cells [232]. In the perfused rat liver, GIP acted anabolically in concert with insulin to potently suppress hepatic glucose production induced by glucagon [233; 234]. Similarly, in dog and human euglycemic clamp experiments, GIP acted to inhibit hepatic glucose

production only in the presence of insulin [235-237]. Studies examining both GIP receptor expression and biological effects in liver are required to clarify the hormone's action on this tissue.

1.5.3.2 Skeletal Muscle:

One research group reported the ability to detect specific binding sites for GIP on striated muscle [226], whereas others have failed [225]. While this tissue was not tested for receptor expression using molecular cloning techniques, muscle has been considered to be a potential target organ for GIP in a limited number of experiments. Preliminary studies aimed at establishing whether the glucose lowering effects of GIP were entirely mediated by insulin or whether GIP had insulin-independent actions were initially negative. GIP was unable to stimulate glucose uptake in the rat hemidiaphragm preparation [238]. In a more recent systematic approach to the subject, O'Harte and co-workers found native GIP alone to be nearly as potent as equimolar insulin in stimulating glucose uptake, glucose oxidation, glycogenesis, and lactate formation in mouse abdominal muscle slices, and effects on these parameters were exerted at physiological concentrations of hormone [239].

1.5.3.3 Adipose Tissue:

As fat is the most potent GIP secretagogue, many studies have been performed examining effects of GIP on fat metabolism. Specific GIP receptors have been demonstrated on adipocytes by a number of techniques [11; 240; 241]. In rats, immunoneutralization of endogenous GIP caused an increase in plasma triglycerides and exogenous GIP resulted in the opposite effect after intra-duodenal fat [234; 242]. However, in studies designed to examine GIP's effect on an intravenous fat tolerance test with a commercial fat emulsion (Intralipid), it was concluded that GIP had no effect on plasma triglycerides in man or dog [243; 244]. In a unique approach, Wasada *et al* [245] collected chyle from thoracic duct fistulae in donor dogs fed a fatty meal. When chyle was infused *IV* with or without exogenous GIP in recipient dogs, the rise in plasma

triglycerides was significantly lower when GIP was co-infused. Thus chylomicron formation may not only be necessary for fat-stimulated GIP release [80; 81], but also for GIP-stimulated triglyceride removal from the circulation. In this regard, GIP has been linked to stimulation of lipoprotein lipase activity and incorporation of fatty acids in 3T3-L1 mouse preadipocytes and rat epididymal fat pad explants, acting in synergy with insulin [246-251]. GIP has also been causally related to *de novo* lipogenesis, acting with insulin to increase glucose uptake in adipocytes and stimulating fatty acid synthesis (incorporation of glucose and acetate into extractable lipids) [251-254]. The role of GIP in lipolysis is currently unclear: it has been reported to exert weak or no lipolytic effects on its own in some reports on isolated rat adipocytes [253; 255], whereas other studies using 3T3-L1 cells have found GIP to exert lipolytic effects via a cyclic AMP mediated pathway similar to adrenergic agonists [241]. Ebert and Creutzfeldt [234] reported that alone, GIP was equally lipolytic as glucagon in isolated rat fat cells, but GIP dose dependently inhibited glucagon-stimulated lipolysis with a concurrent reduction of cellular cAMP; the same study showed similar effects on secretin-stimulated lipolysis, albeit to a lesser degree. In the study by McIntosh et al [241], insulin was shown to block GIP- and isoproterenol-stimulated lipolysis, whereas in earlier studies [253; 255], GIP was found to attenuate the lipolytic effects of glucagon and isoproterenol, but not those of VIP or secretin. The mode of GIP's inhibitory activity is not certain as most of its actions are thought to occur through the cyclic AMP pathway, the same pathway that glucagon, VIP, secretin and isoproterenol also exert their effects on the adipocyte [234; 241; 253; 255]. It was suggested that GIP may directly compete for glucagon binding to fat cells [234; 255], however, the ligand specificity of the cloned glucagon and GIP receptors does not support this contention. It is hypothesized that GIP has a dual action on adipocytes depending on the fed state of the animal: during fasting, GIP is lipolytic and during the fed state, GIP acts to promote nutrient storage via

lipogenesis, both dependent upon ambient circulating insulin levels. In this case, methodological differences may help explain the contradictory results.

1.5.4 Other Attributed Biological Functions

The GIP receptor has been localized to many tissues of the body, for which no characterized function of GIP has yet to be described. This section will be limited to tissues and organs where biological effects have been described. Central injection (*ICV*) of GIP dose- and time-dependently inhibited plasma follicle-stimulating hormone (FSH) concentration while stimulating growth hormone (GH) release in ovariectomized rats (and not affecting luteinizing hormone (LH), prolactin or thyroid stimulating hormone); in the same study, GIP injection *IV* was without effect on any pituitary hormone measured [256]. Peripheral (*SC*) administration of GIP to anesthetized male rats dose-dependently decreased GH levels [257]. In primary dispersed cultured anterior pituitary cells, GIP-stimulated both FSH and LH accumulation in the culture medium [256]. Given the different experimental designs, it is difficult to determine how and where GIP was acting to modify pituitary hormone secretion. The significance of exogenous GIP effects on pituitary hormones is presently unclear; GIP receptors have been well described in brain [11; 225], however, the receptors are localized in areas inaccessible to blood borne hormone, and neither GIP mRNA nor GIP peptide have been found in brain [4]. GIP has been reported to regulate blood flow in gut vascular beds [132; 141-143], and functional receptors have been described in endothelial cells; it has been proposed that GIP's activity on the vasculature may be present to maximize nutrient absorption [11; 258; 259]. GIP stimulated cortisol secretion in a type of food-dependent Cushing's syndrome has been well characterized [260; 261]. The GIP receptor was reported to be expressed in the rat adrenal gland [11], but studies on the human disease found GIP receptor expression limited to the cortical adenoma responsible for the condition, but not in normal adrenal cells [260; 262]. A recent study

examining the corticosterone response to bolus *IP* GIP injection found it to be a stimulant in normal rats [263], possibly indicating species differences. Recently, the unique hypothesis of an 'entero-osseous axis' has been proposed, whereby GIP has been shown to have osteotropic effects on bone osteoblast cells via cyclic AMP and calcium second messenger cascades coupled to the GIP receptor; furthermore, chronic GIP treatment in ovariectomized rats enhanced bone density *in vivo* [259; 264]. Use of GIP receptor knockout mice or receptor antagonists have yet to confirm most extra-intestinopancreatic effects of GIP.

1.6 GIP Binding Sites

1.6.1 GIP Iodination and Binding Studies

The development of an iodination protocol for purified porcine (p)GIP_{1-42}, using the chloramine-T method with subsequent high-pressure liquid chromatography (HPLC) purification, allowed proof of the existence of specific GIP receptors present on the pancreatic β-cell [175; 265; 266]. Fractions collected from two peaks identified on the HPLC chromatogram were found to have similar binding ability to hamster insulinoma membranes and insulin-releasing ability from the perfused rat pancreas, and preliminary evidence suggested both were iodinated on Tyr^{10} [265; 266]. Comparison of porcine and bovine GIP sequences (Table 1, Introduction section 1.3.1) indicate potential iodination of residues Tyr^1 or Tyr^{10} (or possibly His^{38}); iodination of bovine GIP_{4-42} (lacking Tyr^1) resulted in only one biologically active iodinated product, presumably labelled on Tyr^{10} [267]. Later studies confirmed [mono-[^{125}I]iodo-Tyr^{10}]-$pGIP_{1-42}$ to be the preferred biologically active iodinated GIP form to use in experimentation [4; 59; 182]. Iodination of synthetic human GIP using the same protocol results in a more complex HPLC profile – specific peaks are biologically active, but their molecular identities have not been characterized (unpublished observations).

To date, GIP receptor binding sites have been limited to brain and specific *in vitro* cell types (transformed cell models of various tissues) or receptor transfected cells. Although only published in abstract form, Whitcomb *et al* [226] provided evidence for specific binding sites for GIP in pancreas, the glandular portion of the stomach, the duodenum, jejunum, ileum, colon and various muscle groups, using a novel *in vivo* radioreceptor assay for the anesthetized rat described elsewhere in detail [268; 269]. In the same abstract, it was reported that specific receptors were not found in liver, adrenal gland, submandibular gland, spleen, kidney, testis, epididymus, prostate or seminal vesicles. In a later autoradiographic survey of rat tissues it was only possible to detect specific binding in regions of the brain, including cerebral cortex, anterior olfactory nucleus, lateral septal nucleus, subiculum, inferior colliculus, and inferior olive of the medulla oblongata, however, saturable binding sites were not detected in spinal cord, pituitary, stomach, small intestine colon, pancreas, liver, heart or skeletal muscle [225]. Similarly, the first studies employing monocomponent iodinated GIP failed to detect specific binding to various tissue membranes, including kidney cortex, liver, brain, adrenal cortex, adipose tissue and intestinal epithelium, but could measure binding to (transformed) hamster β-cell membranes [175; 266]. A specific analysis of the adrenal gland using autoradiography resulted in the detection of binding in the inner cortical layers [263]. Destruction of receptors during tissue preparation and degradation of iodinated ligand are possible explanations for the mixed success of these studies. Binding experiments have since demonstrated receptors on whole isolated islets and purified β-cells [3; 174], transplantable hamster insulinoma membranes [21; 266; 267; 270; 271], cultured insulinoma/transformed cells: In111 [175; 272], βTC-3 [178], human insulinoma [182], RINm5F cells [198; 273; 274], BRIN-D11 and INS-1 cells [275], differentiated 3T3-L1 preadipocytes [240; 241], and human osteoblast-like cells: SaOS2 and MG63 [264].

Scatchard analysis of binding competition curves on hamster and human insulinoma cells and transformed hamster β-cells indicated a two site model with high-capacity/low-affinity and low-

capacity/high-affinity binding sites; (K_D high affinity: 0.2-7 nM, low affinity: 0.039-8.93 μM; Table 2) [175; 182; 266; 272]. Membrane binding dissociation studies, by dilution with and without added cold GIP, demonstrated disassociation constants (K_{off}) to be 5.3 X 10^{-3} min^{-1} for high affinity sites and 2.3 X 10^{-2} min^{-1} for low affinity sites [272]. Scatchard analysis of autoradiographys of brain slices identified a single high affinity binding site, K_D = 16-62 pM [225]; however, because of the associated inaccuracies with calculating K_D values by Scatchard analysis compared to direct curvilinear regression analysis of saturation binding curves, these data should be interpreted with caution. Saturation binding has been performed on insulinoma cells (βTC-3 and INS-1 cells), differentiated 3T3-L1 mouse adipocyte cells, and osteoblast-like cells to accurately measure binding constants (Table 2).

Optimization of GIP binding study parameters showed an increase in binding capacity with decreasing temperature. This correlation also reduced ligand and membrane receptor degradation, but required a longer incubation time to reach equilibrium. Optimal pH for binding was between 6.5 and 8.0; $CaCl_2$ (5 mM) completely blocked receptor binding, whereas binding was moderately reduced by hypertonic salts (1-2 M NaCl or KCl), but enhanced by inclusion of 5 mM $MgCl_2$ or $MnCl_2$ in the binding buffer. Binding of ^{125}I-GIP was specifically displaced only by GIP, and not glucagon, insulin, VIP, secretin, CCK-8, GHRH, PHI or EGF [266; 272]. Further biochemical analysis of the GIP receptor by covalent cross-linking indicated it was a monomeric glycoprotein with an electrophoretic mobility corresponding to a predicted receptor mass of 59 KDa, however, incubation with dithiothreitol proved that intrachain disulfide bonds existed and resulted in a slower mobility, predicting a receptor mass of 68 KDa; disulfide bonds were not required for binding of ^{125}I-GIP to its receptor, however. Elution of lectin bound membranes from wheat germ agglutinin and concanavalin A suggested glycosylation with oligosaccharide moieties possibly containing N-acetylglucosamine, methyl-α-D-mannopyranoside and/or sialic acid [270; 271].

26

Following the cloning of the rat GIP receptor, hamster and human isoforms were isolated allowing study of the GIP receptor using transfected cell models (described below). Binding analyses were performed to confirm the specificity of GIP binding sites, and compare the binding affinities measured using various GIP labels and/or GIP preparations. In general, all studies identified a single class of specific GIP binding sites, with K_D values (from Scatchard analysis or saturation binding) in the range 180 pM to 19.3 nM (Table 2). Studies have examined transfected rat [276], human [277; 278] and hamster [223] GIP receptors expressed in CHO-K1 [223; 276], COS-7 [276] or CHL [277; 278] cells, using either iodinated synthetic porcine or human GIP label (Table 2). Only two studies employed saturation binding isotherms to measure K_D values more accurately, both using synthetic $pGIP_{1-42}$ monocomponent tracer, but in one case measuring whole cell binding to human GIPR transfected CHL cells [277], and in the other, whole CHO or COS-7 cells, or CHO membrane preparations from rat receptor transfected cells [276] (Table 2).

While methodological differences (time, temperature, receptor isoform, cell type, expression level, label concentration, molecular species of label, competing ligand) certainly must be considered, in properly designed experiments using transfected cells with synthetic human or pork GIP_{1-42}, IC_{50} values should be in the low nM range, and accurate determinations of K_D values to be in the high pM range. The remarkable binding specificity of the transfected GIP receptor was demonstrated in all studies: displacement of GIP label by high concentrations (1 μM) of glucagon, GLP-1, GLP-2, VIP, secretin, PACAP-27, PACAP-38, or PHI could not be detected – only the Gila monster venom peptides exendin-4 and exendin-(9-39) were found to displace significant amounts of specific ^{125}I-GIP binding [223; 276-278]. In an analysis of hybrid GIP/GLP-1 receptor chimeras, it was shown that only the N-terminal 132 amino acids of the GIP receptor (Figure 2, section 1.6.2) were necessary for high affinity ^{125}I-GIP binding, however, this was enhanced if the length was extended to 151 (NT and TM1) or 222 (NT, TM1,

27

IC1, TM2, EC1, and TM3) amino acids [279; 280]. Hence it was concluded that the primary binding determinants were within the extracellular N-terminus of the GIP receptor, however additional contact sites may be present in the "binding pocket" within the transmembrane domains, and possibly in the first extracellular loop. The latter possibility may be supported by the reduced functionality of a naturally occurring mutant human GIP receptor bearing a missense mutation (Gly198Cys) in the first extracellular loop [281].

Table 2: Comparison of binding constants measured using transformed cells and transfected cell models.

Cell Line	Receptor	Iodinated Peptide	Binding Constants	Ref.
Insulinoma	Hamster	$pGIP_{1-42}$	K_D^a 2.05 nM (high), 39 nM (low)	1
In111	Hamster	$pGIP_{1-42}$	K_D^a 7 nM (high), 0.8 μM (low)	2
Insulinoma	Human	$pGIP_{1-42}$	K_D^a 223 pM (high), 8.93 μM (low)	3
Brain slices	Rat	$pGIP_{1-42}$	K_D^a 16-62 pM	4
βTC-3 cells	Mouse	$pGIP_{1-42}$	K_D^b 277 pM	5
INS-1 cells	Rat	$pGIP_{1-42}$	K_D^b 531 pM	5
3T3-L1 cells	Mouse	$pGIP_{1-42}$	K_D^b 46 pM	6
SaOS2 cells	Human	$hGIP_{1-42}$	K_D^b 362 pM	7
MG63 cells	Human	$hGIP_{1-42}$	K_D^b 320 pM	7
CHO-K1 cells[c]	Hamster	$hGIP_{1-42}$	IC_{50} 9.6 nM K_D^a 18.2 nM	8
CHL cells[c]	Human	$pGIP_{1-30}$	K_D^a 11.3 nM (vs. $pGIP_{1-30}$) K_D^a 19.3 nM (vs. $hGIP_{1-42}$)	9
CHL cells[c]	Human (short)[d]	$pGIP_{1-42}$	K_D^b 180 pM	10
CHL cells[c]	Human (long)[d]	$pGIP_{1-42}$	K_D^b 650 pM	10
CHO-K1 cells[c]	Rat Islet	$pGIP_{1-42}$	IC_{50} 7.6 nM (vs. $pGIP_{1-42}$) IC_{50} 8.9 nM (vs. $hGIP_{1-42}$)	11
COS-7 cells[c]	Rat Islet	$pGIP_{1-42}$	IC_{50} 2.6-3.7 nM (vs. several preparations of $hGIP_{1-42}$ and $pGIP_{1-42}$)	11
CHO-K1 cells[c]	Rat Islet	$pGIP_{1-42}$	K_D^b 204 pM (whole cell) K_D^b 334 pM (cell membranes)	11

[a]: K_D values calculated from competitive binding studies by the Scatchard method.
[b]: K_D values accurately measured from saturation binding analysis.
[c]: Transfected cell model
[d]: The short form corresponds to the other published human GIPR sequences, and better aligns with other species isoforms, the long form contains a 27 amino acid C-terminal insertion due to incomplete mRNA splicing.
References: (1) [266], (2) [175], (3) [182], (4) [225], (5) J. Ehses, unpublished, (6) S. Hinke, unpublished, (7) [264], (8) [223], (9) [278], (10) [277], (11) [276].
Cell lines: In111: hamster insulinoma, βTC-3: mouse insulinoma, INS-1, Rat insulinoma, 3T3-L1 cells, mouse adipocyte, SaOS2 and MG63 cells, human osteoblast-like cells, CHO-K1 cells, Chinese hamster ovary cells, CHL cells, Chinese hamster lung cells, COS-7 cells, green monkey kidney fibroblast cells.

1.6.2 Cloning the GIP Receptor, Gene Expression & mRNA Distribution

In 1993, Usdin *et al* described the cloning of the rat GIP receptor from a rat cerebral cortex cDNA library [11]. Initially, they used degenerate primers based on sequences in the third and seventh transmembrane regions of the secretin and PTH receptors to isolate a unique 507 bp PCR fragment that was used as a probe to screen cDNA libraries from rat brain and RINm5F cells. Upon isolation of the complete receptor, sequence analysis revealed a potential 52,223 Da protein made up of 455 amino acids with substantial similarity to cloned receptors from the secretin-VIP family (Figure 2); the likely cleavage of an 18 amino acid signal peptide would result in a protein with a mass of 50,063 Da. However, consensus sequences for N-linked glycosylation were also found at amino acids 59, 69, and 74 of the external N-terminal region, and an additional site in the first extracellular loop, confirming earlier biochemical analyses indicating that the GIPR was a glycoprotein, and suggesting that the molecular weight was likely substantially greater than 50 KDa [11]. Comparison to structurally homologous receptors indicated that greatest sequence similarity was found with the glucagon (~44%) and the GLP-1 (~40%) receptors from rat, and that the GIP receptor belongs to the Family B class of G-protein coupled receptors which contains all GPCRs for small peptide ligands. Not long after Usdin's initial report, papers were published describing the cloned GIP receptors for human pancreatic islet [277], human insulinoma [278], human insulinoma/lung [282], as well as hamster insulinoma [223] and isolated rat islets [276]. Comparison of interspecies sequence differences shows ~86% identity between rat and hamster receptors, and the human to be 79-81% identical to both rodent receptors. Hydropathy plots suggest the presence of seven possible transmembrane domains, characteristic of G-protein coupled receptors (Figure 2).

Use of molecular biology techniques has allowed testing of different tissues for the cloned GIP receptor, particularly those where receptor transcript abundance might be low. Northern (mRNA) blotting revealed receptor transcripts of 5.5, 3.8 and 2.2 Kb in length from RNA

prepared from rat telencephalon and RINm5F cells, but mRNA degradation precluded detection in pancreatic tissue [11]. In the following year, Yasuda *et al* [223] was able to detect a 3.8 Kb transcript in rat islets and HIT-T15 cells, but not other hamster tissues. Volz *et al* was able to detect the 5.5 Kb transcript in human insulinoma, but not stomach carcinoma (HGT-1) or colon mRNA, whereas Moens *et al* detected bands corresponding to GIP receptor mRNA in insulinoma, glucagonoma, isolated islets, as well as purified β-cells and purified non-β-cells consisting of ≥ 80% α-cells, but none in lung, stomach, intestine, liver or brain [224; 278]. Using *in situ* hybridization in rat embryos, GIP receptor expression was detected in pancreas, cardiac endothelium, blood vessel endothelium, lung endothelium, inner adrenal cortex, adipose, stomach and intestine, but not spleen or liver [11]. Using PCR based methodologies, the rat GIP receptor has been detected in pancreas, stomach, duodenum, proximal small intestine, fat, adrenal and pituitary, and brain regions: telencephalon, diencephalon, brain stem and cerebellum, and particularly abundant in the olfactory bulb, however not in liver or spleen [11]. A more recent publication examining human tissues reported GIP receptor in weak amplicon abundance in liver and adrenal cortex, as well as in cultured pancreatic islets and adipose, but not in muscle or pancreatic ductal tissue [283]. While many of these tissues exhibit characterized responses to GIP, several tissues were never considered as targets for GIP, thus allowing other avenues of research on GIP physiology.

The genomic structure of the GIP receptor has been described for both rat and human [282; 284]. The intron/exon pattern is very similar, with the exception of one additional exon for the rat – the human gene spans 13.8 Kb on chromosome 19q (bands 13.2-13.3) comprised of 14 exons, 13 of which encode receptor protein; splicing out intronic sequence yields a 1389 bp open reading frame (ORF) predicting a 466 amino acid protein [277; 282]. The rat receptor gene is only 10.2 Kb in length, but when spliced, yields the 1365 ORF/455 amino acid receptor predicted by the cloned cDNA sequences [11; 276; 284]. Splice variants have been detected in

various tissues, however, most encode non-functional/truncated receptors [277; 278; 283; 284]. Comprehensive functional analysis of the GIP receptor promoter has yet to be published, however, a preliminary report of sequence analysis of the rat GIP receptor gene suggests the presence of three SP-1 sites, and one each of OCT-1, AP-1 and CRE sites, which may regulate GIP receptor expression via transcription factor binding. No TATA box was identified immediately upstream of the transcriptional initiation site, however distal TATA (-1001 bp) and CAAT (-1071 bp) motifs were found, although RNAse protection assays suggested that they may not be used to regulate expression. Driving luciferase enzyme expression by various lengths of GIP receptor 5'upstream promoter sequence showed basal expression in RIN38 cells was primarily conferred by proximal sequences between -100 and +1 bp, relative to the transcriptional start site; in contrast, a sequence upstream of -181 bp resulted in cell specific transgene expression [284]. Recently, functional studies in clonal β-cells (INS-1 and BRIN-D11), Lynn *et al* (In press) were able to show regulation of GIP receptor expression by fat and glucose, and found supportive evidence that expression level was dependent on the transcription factor PPARα.
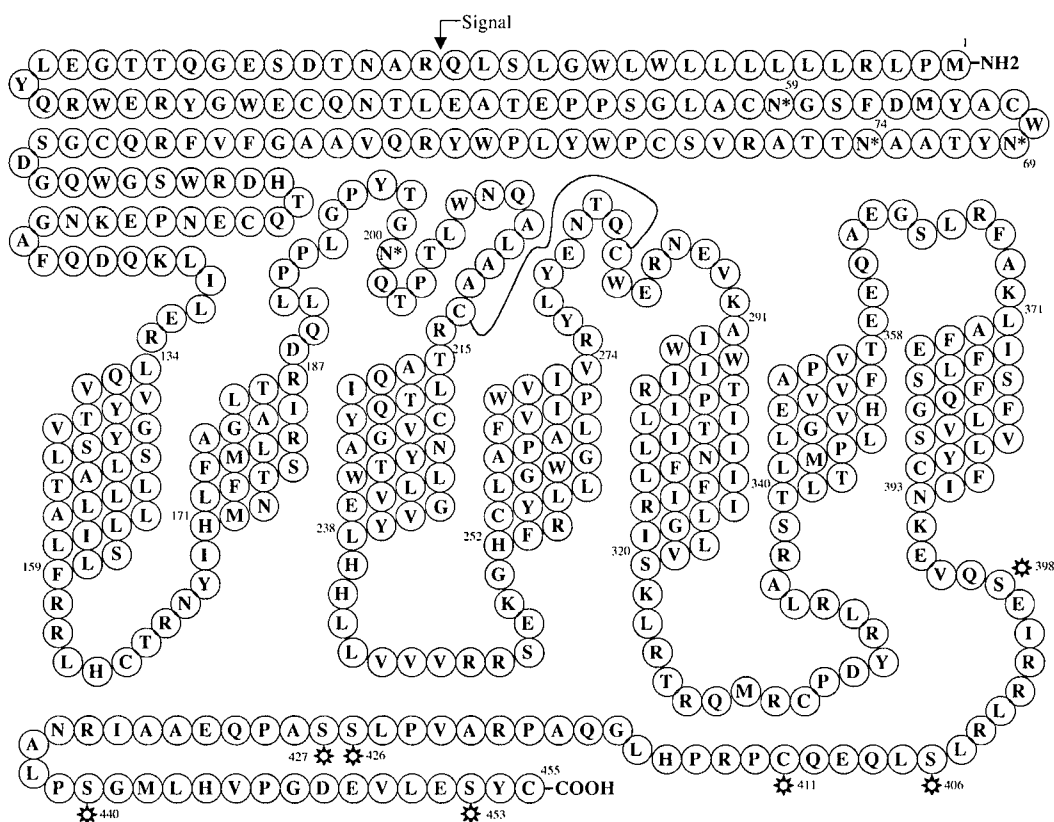
Figure 2: Schematic of the two dimensional topography of the rat GIP receptor
Amino acid numbers of putative transmembrane domain junctions are indicated, as well as potential N-linked glycosylation sites (N*) and disulfide bridge [11; 276]. COOH-terminal residues mutated in the current thesis are indicated by the symbols.

1.7 GIP Receptor Signal Transduction

A preliminary report by Frandsen and Moody [285] demonstrated GIP-stimulated adenylyl cyclcase activity in mouse islet membrane preparations, however, the first complete study to show activation of intracellular messenger cascades in response to GIP was that of Szecówka *et al* [170] using whole isolated rat islets. In this paper, they described the correlation between glucose and GIP with tritiated cyclic AMP accumulation and insulin release. Under elevated glycemic conditions ($\geq$ 6.7 mM), 30 nM GIP produced significant effects on both cAMP and insulin, whereas no effect was observed under low glucose (3.3 mM) conditions [170]. A duplication of this study found that inclusion of the phosphodiesterase inhibitor, IBMX, allowed detection of cAMP responses to GIP at concentrations as low as 200 pM, which falls within the normal physiological range of the hormone [172]. The first report using a homogeneous cell system was the study of Gespach, Emami and Rosselin [286] employing the human gastric cancer cell line, HGT-1. Cyclic AMP stimulation by GIP in these cells was found to be dose- and time-dependent, with plateau cAMP levels achieved within 10-15 min (in the presence of IBMX), and half-maximal stimulation achieved at 8 nM GIP; under these conditions, GIP was able to stimulate a maximal 5-fold stimulation of cAMP levels over basal [286]. As GIP was unable to directly stimulate cyclic AMP production in isolated antral and fundic glands [287], Gespach and colleagues hypothesized that GIP's acid inhibitory effect was mediated by cyclic AMP-dependent stimulation of somatostatin release [286; 288], consistent with the current understanding of the hormone's action. At the same time, researchers from the same institute published a report of GIP-stimulated cyclic AMP formation in the transformed hamster β-cell model, In 111. In these cells, GIP was similarly dose- and time-dependent, with plateau cyclic AMP levels (+ IBMX) achieved after 20 min, and half-maximal cAMP production occurring at 30 nM GIP; a significant rise above basal cAMP levels was detected at 0.3 nM peptide, and

maximal GIP-stimulated cAMP accumulation was 4-times basal [175]. In light of these results, the GIP receptor was proposed to be coupled to the stimulatory "alpha subunit of the guanyl regulatory protein" (GTP-binding protein subunit $G\alpha_s$) to transduce receptor activation upon ligand binding to stimulation of adenylyl cyclase [289], although this hypothesis has not been confirmed directly. GIP receptor mutagenesis studies have suggested that putative G-protein coupling occurs via specific residues in the 3rd intracellular loop (IC3) and the intracellular COOH-terminal tail [290-292].

Cyclic AMP is currently considered to be the primary intracellular signalling pathway through which GIP mediates most of its biological actions [4], and in general, GIP action is mimicked by cAMP raising agents such as forskolin. GIP-stimulation of cyclic AMP production has been detected in many cell models, including isolated β- and α- cells [224], human insulinoma [182], HIT-T15 [176], βTC-3 [214], RIN [198; 214; 273; 274], INS-1 and BRIN-D11 (F. Lynn and J. Ehses, unpublished observations), as well as differentiated 3T3-L1 preadipocytes [240; 241], and SaOS2 osteoblast-like cells [264]. Many of the actions of GIP, including its stimulatory action on exocytosis, may partially or wholly result from activation of cyclic-AMP dependent protein kinase (PKA), as indicated by use of PKA inhibitors Rp-8-Br-cAMPS or H89 [136; 190; 191; 219; 263]. More recently, high concentrations of GIP were shown to affect the cellular distribution of PKA in a specific endothelial cell line [258], and GIP activated the PKA/CREB signalling module in insulin secreting INS-1 cells at physiological levels [293]. Cyclic AMP stimulation by GIP was shown in all cell lines transfected with the cloned GIP receptors from all species [11; 223; 276-278], and with normal EC_{50} values ranging between 0.3 and 0.9 nM [11; 276; 277]. No cAMP production was detected in response to any peptide hormones other than GIP, but the venom peptide exendin-4 produced very small responses at high concentrations [11; 223; 276-278]. It should be noted that there are PKA independent activities of cyclic AMP and GIP is able to activate other signalling cascades, and

34

thus PKA likely does not mediate all actions of GIP. Recently GIP-stimulated increases in cyclic AMP were reported to activate cAMP binding protein GEFII-Rim2 complexes as a means of augmenting β-cell insulin release by a PKA independent mechanism [294].

Early studies on islets indicated that GIP is not involved in phosphoinositol hydrolysis [295], and this finding was later confirmed with the cloned hamster receptor transfected in CHO cells [223]. In more recent work, Ehses *et al* [296] were able to demonstrate dose- and time-dependent GIP-stimulated release of arachidonic acid from βTC-3 and receptor transfected CHO cells, likely via G$\beta\gamma$ subunit activation of Ca^{2+}-independent phospholipase A_2, confirming an earlier hypothesis [297]. Most evidence indicates that cyclic AMP/PKA activation by GIP is not affected by prevailing glucose conditions. However, with ion currents in glucose sensitive excitable cells, elevated glycemia is necessary for closure of K^+_{ATP} channels and subsequent opening of VDCCs, although electrophysiological maneuvers may allow glucose-independent current movement [176; 190; 191; 193; 194; 219]. In the first comprehensive examination of GIP induced intracellular calcium ($[Ca^{2+}]_i$) fluxes, using the calcium sensitive fluorophore fura-2 in HIT-T15 insulinoma cells, glucose alone modulated $[Ca^{2+}]_i$, and, in order to exert a dose-dependent effect ($EC_{50} = 0.2$ nM), GIP required the presence of glucose; addition of extracellular EGTA completely blocked GIP's ability to increase $[Ca^{2+}]_i$ and involvement of the VDCC was confirmed by use of the specific blocker nimodipine. In the presence of nimodipine, AVP was still able to mobilize intracellular stores of calcium, whereas GIP could not [176]. Following cloning of the rat GIP receptor by Usdin *et al*, they showed receptor activation was able to cause an increase in calcium entry, when transfected into reporter HEK-293 cells co-expressing apo-aequorin [11], however, later studies on the human receptor in CHL fibroblasts were unable to detect a calcium signal in response to GIP [277; 278]. Using rat GIP receptors transfected in monkey kidney COS-7 cells, GIP-stimulated $[Ca^{2+}]_i$ was shown to originate primarily from mobilization of intracellular pools, but also via a reversible plasma membrane calcium flux not

mediated by VDCC [276]. It is presently unclear whether differences in calcium signalling are receptor (species isoform) or cell type specific.

One of the frontiers of GIP research is elucidation of pleiotropic signal transduction cascades. GIP has recently been suggested to regulate protein kinase modules other than the prototypical cAMP/PKA pathway. Although results are limited, Straub and Sharp [298] reported inhibition of GIP-stimulated insulin release from HIT-T15 cells by wortmannin, a relatively selective inhibitor of phosphatidylinositol 3-kinase (PI3K). The following year, GIP was shown to time- and dose-dependently activate mitogen activated protein kinase (MAPK; peak at 10 min, EC_{50} = ~590 pM), a key enzyme in the regulation of cell proliferation, differentiation and metabolism, by both wortmannin-sensitive and -insensitive pathways in human receptor transfected CHO cells [299]. Using broad screening approaches, Trümper *et al* [293] and Ehses *et al* [300] have been able to show GIP coupling to pleiotropic signalling modules including cAMP/PKA, MAPK, PI3K/PKB as well as upstream and downstream effectors of these modules. These preliminary findings may have important consequences for GIP's role in β-cell survival, proliferation, and apoptosis [301; 302].

1.8 The Proglucagon Gene Products and Receptors

Upon the first isolation and sequencing of proglucagon mRNA from vertebrates (anglerfish), it was apparent that the transcript encoded additional glucagon-like peptides within the same open reading frame [303-305]. When mammalian proglucagon mRNAs were subsequently sequenced, it was revealed that in addition to glucagon, two glucagon-like peptides, GLP-1 and GLP-2, were also contained in the transcript [306-310]. It was clear from cloning and hybridization studies that the same mRNA transcript gives rise to both pancreatic and gut glucagons. Subsequent work on posttranslational processing revealed that tissue specific cleavage by prohormone convertases results in formation of GLP-1$_{[7-36NH2]/[7-37]}$ and GLP-2, along

with glicentin and/or glucagon-related polypeptide (GRPP) and oxyntomodulin, in intestinal L-cells and brain, whereas in pancreatic α-cells, GRPP, glucagon, and the major proglucagon fragment are generated (Figure 3) [100].

In contrast to glucagon, the primary counter-regulatory hormone responsible for maintaining normoglycemia in the fasted state by promoting gluconeogenesis and glycogenolysis [99; 311], based on sequence homology to GIP, GLP-1 was predicted to have insulin releasing effects as a potential incretin [303; 304]. Now, it is generally accepted that GLP-1 acts as a glucose lowering hormone *in vivo*. Although it has been questioned whether GLP-1 acts as an incretin by definition (see section 1.5.2), it may act to combat glycemic excursions by promoting enteroinsular-neural reflexes, slowing gastric emptying, and acting as a satiety factor in the brain [100; 155; 158; 159; 312]. GLP-2, in contrast, appears not to be involved in regulation of glucose homeostasis, but rather acts as a potent intestinotrophic factor to maintain bowel mass [312]. The G-protein coupled receptors for glucagon, GLP-1 and GLP-2 have all been cloned from various species, and shown to be coupled to cyclic AMP production, inositol-trisphosphate (IP_3) generation and calcium mobilization [8-10; 176; 313-323]. Hence, it appears that biological divergence after gene duplications resulting in the glucagon-like peptides and their receptors, has allowed unique tissue specific effects mediated by common signal transduction cascades.
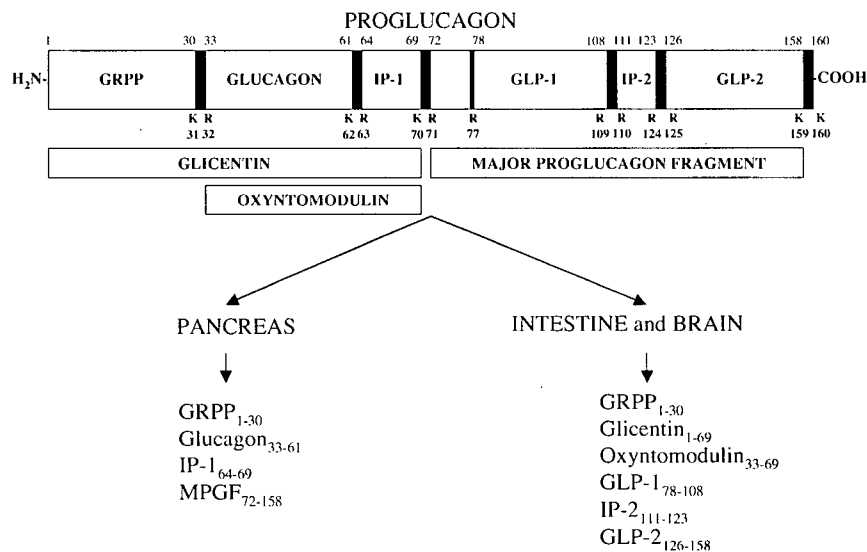
PROGLUCAGON

Figure 3: Post-translational processing of the proglucagon gene products

Prohormone convertase cleavage at specific pairs of basic residues (K, R) results in tissue specific production of bioactive hormones. In the pancreas, glicentin-related pancreatic polypeptide (GRPP), glucagon, intervening peptide-1 (IP-1) and the major proglucagon fragment (MPGF) are generated. In intestine and brain, GRPP, glicentin, oxyntomodulin, glucagon-like peptide-1 (GLP-1$_{7-36NH2/7-37}$), IP-2, and glucagon-like peptide-2 (GLP-2) are produced. Adapted from [100].

1.9 Thesis Investigation

In summary, the peptide GIP is generally considered to be an anabolic hormone, acting to promote nutrient storage and utilization by insulin-dependent and -independent actions, as well as acting as a gut-derived gastric acid inhibitory factor. GIP's role as an integrative hormone regulating the postprandial handling of nutrients is exemplified by the explicit requirements for its release, and the existence of specific receptors on target tissues. The cloning and functional expression of the GIP receptor has provided the opportunity to examine GIP and its receptor at the molecular level in a relatively isolated experimental model. With this means to an end, one of the primary goals of the current work was to compare the cellular regulation of GIP receptor function in clonal β-cells and receptor transfected cells, and to characterize the process of homologous receptor desensitization. The second aim herein was to examine the structural requirements of the ligand necessary for GIP receptor activation. Finally, modulation of GIP, GLP-1 and glucagon bioactivity by the ubiquitous serine protease, dipeptidyl peptidase IV, was probed with the strategy of designing enzyme-resistant peptide analogues, which were examined *in vitro* and *in vivo*.

Hypothesis 1: The GIP receptor undergoes homologous desensitization and internalization in clonal β-cells and/or transfected cell models, and regulation differs from related homologous receptors.

Hypothesis 2: The GIP peptide can be dissected into smaller peptide fragments with either agonist and antagonist properties.

Hypothesis 3: DPIV-degradation of GIP, GLP-1 and glucagon will allow generation of superactive enzyme resistant analogues by N-terminal modification.

Chapter 2: Materials and Methods

2.1 Reagents

All chemicals were of reagent, analytical or higher grade, from Canadian distributors. Common chemicals and salts were from Gibco (Life Technologies Inc., Burlington, ON), Sigma-Aldrich (Oakville, ON), BDH Inc. (Toronto, ON), Fisher Scientific (Nepean, ON), VWR Canlab (Mississauga, ON), Merck (Darmstadt, Germany), Amersham Pharmacia Biotech (Mississauga, ON) and Perkin-Elmer/Mandel Scientific/NEN Life Scientific Co. (Guelph, ON). Specific sources for chemicals are indicated in brackets in the following sections describing experimental methodology.

2.2 Receptor Plasmid Constructs

The rat pancreatic islet GIP receptor was previously isolated by RT-PCR by Dr. R. W. Gelling [276; 324]. This construct was provided in the mammalian expression vector, pcDNA3 (Invitrogen, Carlsbad, CA), subcloned in the *HindIII/XhoI* (Gibco) restriction endonuclease sites, and the plasmid was the template for the creation of mutant GIP receptors, generated in collaboration with Dr. M. B. Wheeler (Dept. of Physiology, University of Toronto). All mutant GIP receptor constructs were made using the QuikChange site-directed mutagenesis kit (Stratagene, La Jolla, CA), with a PCR based methodology and complementary mutant oligonucleotide primers (25 to 32 bp in length) to amplify the entire plasmid. Degradation of methylated and hemi-methylated parental (wild-type) DNA was accomplished by incubation with *DpnI* (Gibco); chemically competent Top10F' *E. coli* cells (initially obtained from Invitrogen; rendered competent in house by the RbCl method) were transformed with resultant DNA, prior to spreading on LB/agar petri dishes with appropriate (100 µg/mL ampicillin or kanamycin) selection agent. Individual colonies were grown overnight in suspension (Luria-Bertani broth with appropriate antibiotic) and plasmid DNA was isolated by "mini-prep" [325].

Introduction of the intended mutation (and not additional PCR errors) to the DNA sequences was confirmed using Big Dye chain terminator sequencing reactions (done primarily in Toronto, and confirmed a second time in some cases at UBC; sequencing kindly performed by Dr. Ivan Sadowski, Dept. of Biochemistry). Large scale (midi- or maxi-preparations) plasmid DNA preparations were then prepared using kits provided by Qiagen (Mississauga, ONT), resulting in sufficiently pure DNA suitable for mammalian cell transfection (spectrophotometry A_{260}/A_{280} ratios between 1.8 and 2.0).

Nine receptor constructs with mutations in the carboxyterminal tail were generated by this method: GIPR-S398A, GIPR-S406A, GIPR-C411A, GIPR-S426A, GIPR-S427A, GIPR-S426/427A, GIPR-S440A, GIPR-S453A, GIPR-S398/406/426/427/440/453A (Figure 2), as well as a GIP receptor chimera with green fluorescent protein (pGIPR-GFP). The latter construct was generated by removal of the stop codon of the GIP receptor and subcloning into the vector pEGFP-N2 (Clontech, Palo Alto, CA), bearing an in-frame 3' ORF for the red-shifted (F64L/S65T) mutant of *A. victoria* jellyfish green fluorescent protein. The resulting pGIPR-GFP plasmid encoded the GIP receptor and GFP intervened by a 14 amino acid sequence (KPNSADGIHRPVAT) derived from the polylinker of the vector used for mutagenesis and pEGFP-N2. Due to extenuating circumstances, the precise sequences of oligonucleotides used for mutagenesis of the GIP receptor cannot be reproduced here, however, mutant constructs will be made available upon request.

2.3 Cell Culture and Transfection

Two cell types were used in experiments contained in this thesis: Chinese hamster ovary (CHO) fibroblast cells (strain K1; American type tissue collection: CCL-61) and βTC-3 cells, a clonal mouse β-cell insulinoma cell line derived from transgenic mice expressing a hybrid insulin/oncogene [326]. Non-transfected CHO-K1 cells were propagated until passage 15.

Transfected cells were discarded after 30-40 passages. βTC-3 cells were tested between passages 20 to 25. Qualitative assesment of cell growth and health was accomplished by observation with an inverted microscope. It is important to maintain low passage number for clonal β-cells, as the age-related decline in glucose-responsiveness and insulin content is well characterized [327], although the βTC-3 cells may be responsive to insulin secretagogues up to passage 39 [178], or even higher [326]. CHO-K1 cells were grown in a 1:1 mixture of Dulbecco's modified Eagle medium (DMEM) and Ham's F12 nutrient solution powder provided containing 25 mM glucose, 2 mM glutamine and 110 mg/L pyruvate (Gibco), 50 U/mL penicillin G (Sigma), 50 µg/mL streptomycin (Sigma), and 10% newborn bovine calf serum (Cansera, Rexdale, ON). Growth medium of stably transfected cells was additionally supplemented with Geneticin (G418, Gibco; 800 µg/mL) to ensure maintenance of the neomycin cassette containing plasmids, present in pcDNA3 and pEGFP-N2. βTC-3 cells were propagated in low glucose (5.5 mM) DMEM with 2 mM glutamine and 110 mg/L pyruvate (Gibco), with antibiotics (as above), 12.5% horse serum and 2.5% fetal bovine calf serum (Cansera). The pH of the medium was adjusted to 7.2-7.3, such that upon vacuum-filter sterilization, physiological pH would be achieved. All tissue culture operations were performed in an aseptic laminar flow biohazard cabinet to minimize the chances of microbe contamination.

Cells were grown at 37°C under a humidified atmosphere of 95% air/5% CO_2. Cells were fed as necessary, until 80-90% confluence was attained and then harvested using 0.25% trypsin/0.3% EDTA solution (w/v) made up in Ca^{2+}- and Mg^{2+}-free Hank's balanced salt solution (HBSS; Gibco). Cells were mixed with an equal volume of growth medium, centrifuged, and the cell pellet vigorously resuspended by repeated passage through a 2 mL serological pipette. One-tenth of the cells was added to 10 mL of fresh growth medium in a new 75 cm^2 T-flask culture vessel (Falcon, Beckton-Dickinson, Mississauga, ON), and the remainder used for experimentation. Cells were counted using a haemocytometer: CHO-K1 cells were seeded at 50-

70,000 cells/well and βTC-3 cells at 500,000 cells/well into 24-well plates (Falcon) in 1 mL growth medium, and maintained for 48 hours before testing.

For stable transfection of CHO-K1 cells, the $CaPO_4$ co-precipitation method was employed. Briefly, this method consisted of plating CHO-K1 cells in 10 cm diameter culture dishes (Falcon), such that they were 60-80% confluent on the day of transfection. Media were replaced with fresh growth media (6 mL) at least 2-4 hours prior to transfection. The co-precipitation reaction was performed in a sterile microcentrifuge tube: 10 μg Qiagen purified plasmid DNA were added to 62.5 μL of 2.5 mM $CaCl_2$, and brought up to a final volume of 500 μL with sterile de-ionized H_2O. To the DNA/Calcium mixture, 500 μL of 2X HBS (for 100 mL: 1.6 g NaCl, 0.074 g KCl, 0.02 g Na_2HPO_4 (anhydrous), 0.2 g dextrose, 1 g HEPES, pH adjusted to precisely 6.95) were added, the solution vortex mixed and the precipitate was allowed to form for 30 minutes at room temperature. The entire 1 mL of DNA/Calcium/HBS solution was added to the cells in 6 mL growth medium and incubated for 4 hours at 37°C. Media were aspirated, and cells subjected to a 90 second glycerol shock by addition of 2 mL 15% glycerol/1X HBS. Glycerol was removed, 6 mL fresh growth medium added, and cells were allowed to recuperate overnight. Cells were split 1:2 into two 10 cm dishes with growth medium supplemented with 800 μg/mL G418; medium was changed as necessary, and after 7-10 days, colonies were visible to the naked eye. In some cases, single colonies were subcloned and expanded for further characterization (where noted), or dishes were simply trypsinized, and pooled clones were used. It was established that pooled subclones of CHO-K1 cells transfected with the GIP receptor showed similar levels of surface expression as the well characterized high-expressing subclone rGIP-15 (also known as wtGIPR or GIPR-455) [276; 280; 290]; in the current report, it was found that such pooled clones did show similar levels of receptor binding, cyclic AMP production, and could be used in many types of experiments. However, the heterogenous nature of these cell populations presented some difficulties for other experiments, and subcloning was

43

performed where feasible. Transfection by the CaPO$_4$ method initially resulted in approximately 10-12% transfection efficiency; following selection with G418, greater than 85% of cells expressed the protein contained in the plasmid (as estimated in experiments with pGIPR-GFP). Subcloning was accomplished by aspirating the media from the 10 cm dishes and using a P20 Pipetman (Gilson Inc., Middleton, WI) with sterile tips to carefully pick clusters of cells from the centers of visible colonies; colonies were transferred to individual wells of 24-well plates (Falcon) to expand. Subclones were then screened for receptor expression by measuring ^{125}I-GIP binding in the presences and absence of unlabelled GIP (see below).

Transient transfection was used in several experiments when it was desired to transfect more than one plasmid into the same cell (*e.g.* the GIP receptor and G-protein receptor kinase 2). This was accomplished using the LipoFectamine 2000 reagent (Gibco) and a modified manufacturer's protocol. Briefly, cells were plated in 10 cm dishes such that 90-95% confluence was achieved on the day of transfection; for CHO-K1 cells, this was achieved by plating ~2 X 10^6 cells in 7 mL growth media, and culturing for 48 hours. In an autoclaved microcentrifuge tube, 10 μg of total DNA (*e.g.* 3 μg pGIPR and 7 μg of pcDNA3 or pGRK-2) were diluted in 250 μL of sterile room-temperature DMEM/F12 (antibiotic and serum-free) and in a second tube, 20 μL of LF2000 reagent were added to 250 μL DMEM/F12. Solutions were vortex mixed, incubated for 5 min at room-temperature, and then combined and mixed. The DNA/liposome complexes were allowed to form for 30 min at room-temperature; the entire 500 μL solution was then added to cells in 3 mL fresh growth media (final volume 3.5 mL), and cells were incubated at 37°C overnight. The following day, cells were harvested and seeded in 24-well plates for experimentation 48 hours later. This protocol resulted in transfection efficiencies between 40 and 45%. While this method was more time-consuming than generating pooled stable clones, it was less labour intensive than subcloning stable cell lines, and allowed control of receptor

44

expression level by keeping total plasmid DNA constant (to maintain transfection efficiency) and varying the proportion of receptor plasmid.

Stable transfected CHO-K1 cell lines expressing the human GLP-1 receptor (hGLP-1R cells) or human glucagon receptor (hGlucR cells) were generated by Dr. R. Gelling, and previously described in the literature [280; 328].

2.4 Peptides

Synthetic human and porcine GIP_{1-42}, $GLP-1_{7-36NH2}$, and $[Glu^9]glucagon_{2-29}$ were purchased from Bachem (Torrance, CA). All other peptides described in the current report were synthesized by Dr. Susanne Manhart, Probiodrug AG, Halle (Saale), Germany; additional batches of GIP_{1-42} and $GLP-1_{7-36NH2}$ were also prepared. These peptides were synthesized using an automated peptide synthesizer, Rainin Symphony, according to published methods [329]. Crude peptides were purified by HPLC using a CH_3CN/H_2O gradient in the presence of 0.1% trifluoroacetic acid (TFA), and subjected to mass spectrometry (MALDI-TOF) and analytical HPLC to confirm identity and purity. A table of peptides is provided in Appendix A, with expected and measured masses. Peptide content of lyophilized peptides was determined to be approximately 70% for all syntheses (including commercially bought peptides), but was not factored in during testing of the peptides described here, as is common practice. Peptide handling was according to standard protocol. Basic peptides were appropriately dissolved in a small volume of 0.1 M CH_3OH, and made up to volume with sterile de-ionized water, whereas 0.1 M NH_4OH was used for acidic peptides; GIP_{1-42}, human and porcine, were the only basic peptides, of all those presented. Peptides were dispensed at 2 nmol or 20 nmol in siliconized tubes, and freeze dried *in vacuo*, using either a lyophilizer or Speed-Vac. Tubes containing dried peptides were sealed with Parafilm, and kept at -20°C until use.

2.5 Peptide Iodination

Radioactive labelling of peptides was accomplished using established techniques developed in our laboratory. Briefly, 1 mCi of carrier-free iodine-125 (Perkin-Elmer) was added to 1 nmol of peptide dissolved in 100 μl of 0.4 M phosphate buffer (pH 7.5), and iodination initiated by addition of 10 μl chloramine-T (14.2 mM in 0.4 M PO_4 buffer; BDH) for 15 seconds and the reaction was quenched with 20 μl sodium metabisulphite (66.3 mM in 0.4 M PO_4 buffer; Fisher). Radiolabelled peptide was separated from free iodine by gel filtration (Sephadex G-10 or G-15; Pharmacia, Uppsala, Sweden) in 0.2 M acetic acid with 0.5% BSA (RIA fraction V) and 2% Trasylol® (aprotinin; Bayer, Etobikoke, Canada). Labelled peptides were then purified by HPLC to yield single molecular species; the $CH_3CN:H_2O$ (+ 0.1% TFA) gradients used depended on the specific peptide, and are shown in Figure 4. Solvents were filtered and degassed on each day of purification. The HPLC apparatus consisted of two Beckman 110B solvent delivery module pumps (flow rate = 1 mL/min) with a programmable Beckman 421A controller, a μBondapak-C18 column (Waters, Milford, MA), and a model 170 in-line Radioisotope Detector connected to a chart recorder. Peaks were manually collected, aliquotted at 3-4 X 10^6 cpm into tubes containing 5 μL of 1% BSA (w/v) and 50% Trasylol (v/v); tubes were freeze-dried, sealed with Parafilm, and stored at -20°C until used.

Peak II of the ^{125}I-GIP$_{1-42}$ chromatogram is known to be [^{125}I-Tyr^{10}]GIP$_{1-42}$ [59], and is a biologically active product [174; 266]. For [D-Ala^2]GIP$_{1-42}$, GLP-1$_{7-36NH2}$, and GIP$_{1-14OH}$, all peaks were empirically tested for receptor binding using appropriate methodologies. For the first two peptides, two biologically active iodinated products were detected for each (Figure 4), but only the first more abundant product was used for experimentation, whereas no biologically active iodinated GIP$_{1-14OH}$ product could be detected. Using the same iodination protocol, but with non-radioactive NaI at the same concentration, mass spectrometric analysis detected only oxidized forms of mono- and di-iodinated GIP$_{1-14OH}$ (data not shown). Use of this method for

46

iodination and purification routinely resulted in specific radioactivities in the range of ~250-350

μCi/μg (~45 to 65 MBq/nmol) [59; 178; 276; 324; 330].

Glucagon label (3-[^{125}I]iodotyrosyl[10]-glucagon) was purchased from Amersham.

A. Purification of ^{125}I-GIP$_{1-42OH}$

B. Purification of ^{125}I-[D-Ala^2]GIP$_{1-42OH}$

C. Purification of ^{125}I-GIP$_{1-14OH}$

D. Purification of ^{125}I-GLP-1$_{7-36NH2}$
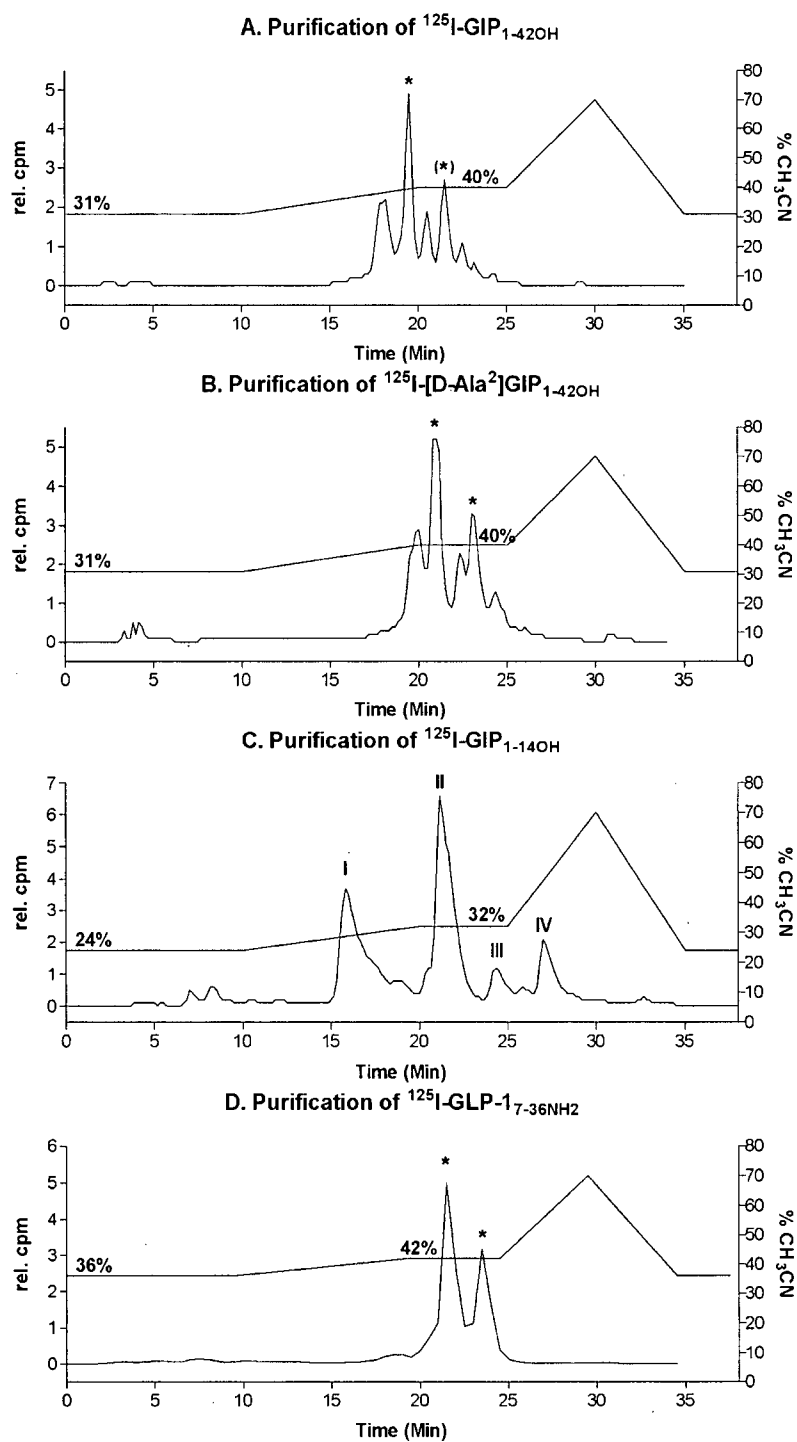
Figure 4: HPLC profiles of iodinated synthetic peptides
Peptides were iodinated by the chloramine-T method (see text) using 1 mCi carrier free iodine and 1 nmole of peptide. Iodinated product was separated from free iodine by gel filtration, and then separated using a $CH_3CN:H_2O$ + 0.1% TFA gradient (right Y axis on graphs) at a flow rate of 1 mL/min on a μBondapak C-18 column. Peaks were empirically tested for specific binding to wtGIPR or hGLP-1R cells, and those producing acceptable specific binding with low non-specific binding are indicated by (*). Two biologically active peaks were identified for each peptide except GIP_{1-14}, which had none and, invariably, the earlier eluting peak was used in all further experiments. The second bioactive peak for $pGIP_{1-42}$ has been previously reported [174; 266]. Mass spectrometric analysis indicated that iodinated GIP_{1-14} consisted only of oxidized forms of mono- and di-iodo peptides (data not shown).

2.6 Binding Studies

All transfected CHO-K1 cells were tested for receptor expression and receptor binding affinity by competition binding studies. Cells were prepared in 24-well plates, and had been grown for 48 hours to approximately 2-5 X 10^5 cells/well (~90% confluent). Cells were washed twice with ice-cold 15 mM HEPES-buffered (pH 7.4) DMEM/F12 supplemented with 0.1% BSA. Cells were then incubated 12-16 hours (overnight) at 4°C in 200 μL of the same buffer additionally supplemented with 1% Trasylol, 50,000 cpm iodinated peptide and concentrations of unlabelled peptides indicated in the figures (1 pM to 1-40 μM, depending on the experiment and peptide tested; triplicate determinations). Medium was then aspirated from the wells, which were washed twice with ice-cold buffer, prior to solubilization of cell-associated radioactivity using 1 mL of 0.1 M NaOH and transfer to borosilicate tubes for counting. Non-specific binding was defined as cpm measured in the presence of 1 μM of native peptide, GIP_{1-42}, $GIP_{1-30NH2}$, GLP-$1_{7-36NH2}$, or glucagon$_{1-29}$, where appropriate. Non-linear regression analysis of competitive-binding curves followed algorithms included with the Prism 3 software package (GraphPad, San Diego, CA). Data were fitted to a single site model:

$$Y = \text{Bottom} + [(\text{Top} - \text{Bottom})/(1 + 10^{(X - \text{Log IC50})})] \qquad \text{Eq. 1}$$

Where Y is the bound label and X is the log value of the concentration of unlabelled competitor, Top and Bottom are high and low measured cpm values (respectively), and IC_{50} is the

concentration of unlabelled competitor that displaces 50% of bound label. Specific binding in the absence of competitor (B_0) is proportional to maximal binding (B_{max}) by the relationship:

$$B_0 = B_{max} \cdot X/(X + K_d) \qquad \text{Eq. 2}$$

Where X is the label concentration (molar), and is constant for a given experiment, and K_d is the equilibrium dissociation constant for the receptor and ligand, also in molar units. Hence B_0 could be used in competitive-binding experiments to estimate B_{max}, and determine relative levels of expression, provided affinity was constant.

Saturation binding isotherm experiments were also performed in some cases to experimentally determine B_{max} values accurately. In these studies, cells in 24-well plates were prepared similar to above, except that serial 1:2 dilutions of 2×10^6 cpm were added to wells in the presence or absence of 1 μM unlabelled peptide (in triplicate). Total label concentrations were calculated using the specific radioactivity of the label and measured cpm values of added label and specific binding. Data were fitted to the relationship:

$$Y = B_{max} \cdot X/(X + K_d) \qquad \text{Eq. 3}$$

Where Y is experimentally measured specific binding in units of cpm/cell and X is the molar concentration of added label, thus allowing calculation of B_{max} (converted to sites/cell) and K_d. Scatchard plots were not used, due to the well documented inaccuracies associated with that method [331].

2.7 Cyclic AMP Measurements

Cyclic AMP studies performed in CHO-K1 cells were performed on cells plated 48 hours prior in 24-well plates, having grown to ~2-5 $\times 10^5$ cells per well. Cells were washed 2X and preincubated for one hour in warm HEPES-buffered DMEM/F12 with 0.1% BSA. Subsequently, cells were stimulated for 30 min in the presence or absence of peptides (at the concentrations shown in figures, in triplicate), in the same buffer additionally supplemented with

1% Trasylol and 0.5 mM isobutyl-methylxanthine (IBMX; Research Biochemicals Intl., Natick, USA). IBMX was dissolved at 0.5 M in dimethylsulfoxide (DMSO; BDH), dispensed into 25 µL aliquots and frozen at -20°C until use. (Gelling [324] reported that maximal cyclic AMP levels varied between experiments; it is thought that a contributing factor to this variability was in part because in the earlier work by Gelling, IBMX was weighed and dissolved in warm isopropanol on the day of each individual experiment). Following stimulation, media was decanted from the wells, and cells were lysed in 1 mL ice-cold 70% ethanol. Cellular debris was removed by centrifugation (5-10 min, 4°C, 12-15,000 rpm), and cell contents were dried by vacuum centrifugation. Samples were reconstituted in an appropriate volume of sodium acetate buffer (0.05 M, pH 6.2) and assayed for cyclic AMP content by radioimmunoassay kit according to the manufacturer's instructions (Biomedical Technologies Inc, Stoughton, USA). Analysed data are presented as pmol cylic AMP/well, femtomol/1000 cells, or as a percentage of maximal GIP-stimulated cAMP production. Modified versions of the protocol above were designed to characterize desensitization of the GIP receptor in transfected cells. The effect of receptor expression level, a cyclic AMP accumulation time-course and a time-course of desensitization were established. Generally, 100 nM GIP with 1% Trasylol was included for various times (in the absence of IBMX) prior to a 10 minute washout period, during which time media were changed twice, and subsequently a 30 min stimulation with GIP in the presence of IBMX was carried out. Concentration and measurement of intracellular cyclic AMP proceded unchanged.

Cyclic AMP measurements in βTC-3 cells were performed essentially as described with minor modifications. Two days after plating, cells were incubated in standard growth media, but with only 1 mM glucose, for 6 hours prior to experimentation. Cells were washed twice with 37°C buffer (DMEM, 25 mM HEPES, 0.1% BSA, pH 7.4, and glucose: 0, 5.5 or 11.0 mM). Cells were then incubated for 1 hour in cAMP buffer of varying glucose concentrations, supplemented with 1% Trasylol, with or without 100 nM GIP. Treated cells were rinsed twice

with appropriate glucose-containing cAMP buffer over a 10 minute washout period. Cells were then stimulated for 30 minutes with a range of GIP concentrations in triplicate, as indicated in the figures, in βTC buffer supplemented with 0.5 mM IBMX. Forskolin (10 μM; Sigma) was used as a positive control. Cyclic AMP content was measured as above (70% ethanol lysis, centrifugation, drying, and cAMP RIA). Further control experiments were performed in Kreb's Ringer Bicarbonate HEPES (KRBH) buffer (120 mM NaCl, 5.7 mM KCl, 1.2 mM NaH_2PO_4, 15.5 mM $NaHCO_3$, 1.2 mM $MgCl_2$, 15 mM HEPES, 0.1% BSA, 2.5 mM $CaCl_2$). Cells were similarly incubated for 1 hour in 0 or 5.5 mM glucose KRBH, prior to a 30 minute test period measuring basal, 100 nM GIP-stimulated or 10 μM forskolin-stimulated cAMP production. The effect of glucose on cAMP production and desensitization were examined in parallel, such that one independent experiment consisted of 6 experimental conditions on cells prepared all at the same time. Cyclic AMP data were expressed as pmol per well or normalized to production of cyclic AMP stimulated by 10 μM forskolin.

Further experiments on βTC-3 cells were conducted on the effect of dipeptidyl peptidase IV (DPIV) inhibition, pertussis toxin, phosphodiesterase inhibition, or protein kinases A and C on desensitization of the cyclic AMP response of βTC-3 cells to GIP. As desensitization could be explained by degradation of extracellular GIP by induction of DPIV or pertussis toxin-sensitive G-proteins, these hypotheses were tested. Cells were prepared as above, pretreated with 100 nM GIP in HEPES-buffered 5.5 mM glucose DMEM, and subsequently stimulated with 10 nM GIP in the presence or absence of 50 μM isoleucine-thiazolidide (Ile-thia, DPIV K_i = 130 nM; Probiodrug, Halle, Germany) or pertussis toxin (100 μg/mL during washout and 500 μg/mL during stimulation; Sigma). The effect of IBMX (phosphodiesterase IC_{50} = 2-50 μM) on GIP desensitization was similarly tested. Cells were pretreated in the presence or absence of 100 nM GIP followed by a 10 minute washout period; during the subsequent stimulation period with 10 nM GIP, IBMX concentration was varied between 0 and 4 mM. Blockade of protein kinases A

51

or C was accomplished using 5 μM H89 (PKA K_i = 48 nM) or 100 nM staurosporine (PKC K_i = 0.7 nM; both from Calbiochem, La Jolla, CA), included 15 minutes prior to and during the 100 nM GIP/60 min desensitization period. Inhibitor concentrations were based on inhibitory constants and commonly used values. The effect of these inhibitors on basal and GIP-stimulated cAMP production was also measured.

2.8 Insulin Release Experiments

βTC-3 cells were washed twice with appropriate glucose containing KRBH and preincubated for 1 hour in the presence or absence of 100 nM GIP (in quadruplicate) in KRBH supplemented with 1% Trasylol at 37°C/5% CO_2. As with the cAMP studies, cells were washed over a 10 minute period and then either stimulated a further 30 minutes in KRBH with glucose (0, 5.5 mM, or 11 mM) with or without 10 nM GIP or 10 μM forskolin. Media were removed for insulin radioimmunoassay (described below) and untreated cells were extracted with 2.0 M acetic acid for determination of total cell insulin content.

2.9 Receptor Internalization

GIP receptor sequestration in transfected CHO-K1 cells was measured using modifications of two methods previously described: the first examined loss of surface binding sites, designed by combining the methods of [332] and [333], and was similar to methods published later [334], and the second was an altered protocol examining internalization of iodinated peptide [335]. The first method measured remaining surface receptor binding following exposure to GIP for set durations. Cells in 24-well plates were washed 2X with 37°C assay buffer (15 mM HEPES-buffered DMEM/F12 + 0.1% BSA), and covered with 180 μL of the same buffer. Cells were held on a shallow stage in a 37°C waterbath, and at designated time-points (counting down from 60 min), 20 μL of peptide were added (in triplicate or quadruplicate) to give a final concentration

52

of 100 nM in the well. At t = 0, cells were rinsed with ice-cold acid stripping buffer (2 X 1 mL; 150 mM NaCl, 50 mM glycine [analytical grade; Merck], brought to pH 3 with glacial acetic acid) and incubated on ice in this buffer for 5 minutes to remove surface bound (non-internalized) unlabelled GIP. Cells were again washed two times with cold assay buffer, resuspended in 200 μL of buffer containing 50,000 cpm ^{125}I-GIP with 1% Trasylol. Remaining surface binding was measured after a 4 hr incubation at 4°C, as per the radioligand binding studies. Non-specific binding was determined by inclusion of excess unlabelled peptide; data were normalized to non-internalized surface binding (t = 0 min). In some experiments, different concentrations of peptide or pharmacological agents were used (0.5 mM IBMX, 10 μM forskolin, 100 μM MDL-12,330A {Calbiochem}, 100 μM 2',5'-Dideoxyadenosine {Calbiochem}, 5 μM H89, 400 nM PMA {4-phorbol-12-myristate-13-acetate; Calbiochem}, 100 nM staurosporine, added 15 min prior to GIP), and compared at a single time-point (*i.e.* 30 min GIP alone, 45 min agent alone versus 30 min GIP + 45 min agent), relative to control untreated cell surface receptor expression.

The second method involved measurment of internalized ^{125}I-GIP, and was only used for wtGIPR cells, and CHO-K1 cells transfected with GIPR/GFP constructs. Briefly, cells in 24 well plates were washed twice in ice-cold assay buffer, and incubated with 50,000 cpm of ^{125}I-GIP at 4°C for 60 min. Plates were heated to 37°C for the indicated times; half of the cells were treated by acid stripping on ice (as above), the other half washed with cold buffer (total binding). Non-specific binding measured in the presence of excess unlabelled GIP was determined separately for acid-stripped and total binding cells. Binding that is resistant to acid stripping is generally accepted as radioligand which has been internalized by receptor mediated endocytosis, and expressed as % acid resistant binding/total binding. Acid-resistant binding at t = 0 (cells not warmed to 37°C) was between 10-15%, and represents the efficiency of the acid stripping

protocol at removing surface bound label – many studies subtract this value, however, it is included as important control data.

2.10 Fluorescence Microscopy

Cells were seeded onto 3-aminopropyl triethoxy silane (APES; Sigma) coated 18 mm glass coverslips (Fisher) in 12 well plates at densities of 12.5, 25, 50 and 100 X 10^5 cells and grown for two days. For GIPR/GFP studies, transfected cells were washed twice with assay buffer, and incubated for 60 min ± 100 nM GIP_{1-42} at 37°C. Cells were washed twice with phosphate-buffered saline (PBS, pH 7.4), and fixed with 4% paraformaldehyde (Merck) freshly prepared in PBS at room temperature. Coverslips were rinsed again with PBS, and mounted on slides in 30% glycerol/PBS and adhered with rubber cement. For [Fluorescein-Trp^{25}]GIP$_{1-30NH2}$ studies, cells were washed twice with Earle's balanced salt solution (140 mM NaCl, 5 mM KCl, 1.8 mM $CaCl_2$, 0.9 mM $MgCl_2$, 25 mM HEPES, 0.09% glucose, 0.2% BSA; adjusted to pH 7.4 with 500 mM trisma base), and incubated with 25, 50 and 100 nM [Fluo-Trp^{25}]GIP for 60 min at either 4°C as a control, or 37°C to study receptor internalization. Cells were washed with PBS and fixed with paraformaldehyde as above. Coverslips were mounted on slides in 30% glycerol/PBS and adhered with nailpolish. Separate sets of coverslips were additionally permeabilized with 0.1% Triton-X 100 (5 min), blocked with 5% BSA (60 min), and then treated with the Alexa-fluor 488 fluorescein amplification protocol (according to the manufacturer's directions: 25 µg/mL AF488 rabbit anti-fluorescein IgG, followed by 15 µg/mL AF488 goat anti-rabbit IgG; Molecular Probes, Eugene, OR). Images were captured using a Zeiss Axiophot microscope (Thornwood, NY) and a FITC filter set (excitation $\lambda = 488$ nm, emission $\lambda = 520$ nm).

2.11 Peptide Degradation Studies and Cell DPIV Activity

The hydrolysis of iodinated peptides by purified DPIV (specific activity = 31.2 U/mg; prepared by Leona Wagner, Probiodrug AG, Halle (Saale), Germany) was studied as previously described [59; 330]. In brief, radiolabelled peptides (750,000 cpm/150 μL) were incubated in HBS (40 mM HEPES, 154 mM NaCl, pH 7.6) with or without DPIV (10 mU) for 16 h. Samples were resolved by HPLC using a CH_3CN/0.1% TFA (v/v) and H_2O/0.1% TFA solvent system at a flow rate of 1 mL/min, according to published methods. Iodinated GIP peptides (approx. 50,000 cpm/20 μL injection) were separated by a protocol consisting of 14 minutes at constant 32% CH_3CN/0.1% TFA and following, a linear gradient to 38% CH_3CN/0.1% TFA over 10 min, followed by a further 5 minutes at 38% CH_3CN/0.1% TFA. Fractions were collected at 15 second intervals between minutes 5 and 27 of this protocol. Data were normalized to the total radioactivity recovered in all of these fractions. Between each sample injection, the C-18 μ-Bondapak HPLC column was rinsed for 20 minutes in 100% CH_3CN/0.1% TFA, and any residual radioactivity was removed with 3 consecutive injections of 300 μl DMSO; the sample port was rinsed with 400 μL of H_2O and the column was allowed to re-equilibrate at 32% CH_3CN/0.1% TFA for 5 min prior to the next injection. Under these conditions, a second peak eluting earlier than intact ^{125}I-GIP$_{1-42}$ has been confirmed to be ^{125}I-GIP$_{3-42}$ by Edman degradation analysis [59].

A single experiment was conducted to establish if *in vitro* cell models display DPIV-like activity. CHO-K1 or βTC-3 cells were harvested in 1 mM EDTA/PBS (pH 7.4) and washed 2X with 0.9% NaCl + 40 mM HEPES + 0.1% BSA. Cells were resuspended in 250 μL buffer ± 100 μM Ile-thia (after substrate addition, 50 μM final) at ~ 2 X 10^6 cells/tube. Substrate (250 μL; Gly-Pro-paranitroaniline; Sigma) in buffer (defined above) was added to cells, for a final [substrate] = 400 μM and cells were rotated slowly at 30°C for 30 min. Cells were centrifuged

(1200 rpm, 5 min, 4C) and 100 µL of the supernatant was added in duplicate to a 96 well plate. Absorbance was read at 405 nM on a MRX plate reader (Dynatech Laboratories, Chantilly, VA). DPIV activity was determined from a standard curve, and normalized for cell number.

2.12 Animals and Peptide Bioassay

Male Wistar rats were purchased from the University of British Columbia Animal Care Facility (Vancouver, Canada); male VDF Zucker rats were obtained from the colony maintained in the Department of Physiology, University of British Columbia (Vancouver, Canada). Animals were held in group housing with free access to rat chow and tap water, with a 12 hour light:dark cycle. Animals were fasted overnight (15-18 hours) prior to experimentation. Anesthesia, where indicated, was achieved with intraperitoneal (*IP*) Somnotol® (65 mg/Kg sodium pentobarbital; MTC Pharmaceuticals, Cambridge, Canada). Animal experiments conformed to the guidelines set forth by the University of British Columbia Committee on Animal Care and the Canadian Council on Animal Care.

Early bioassay experiments were performed using intravenous infusion of peptide and intraperitoneal injection of glucose. Cannulae were inserted into the jugular vein and the carotid artery of anesthetized fasted male Wistar rats (150-250 g). Basal blood samples were withdrawn from the carotid artery (500 µl), and fasted blood glucose was measured via the tail vein using a SureStep® glucose analyser (LifeScan Canada Ltd., Burnaby, B.C.). Intravenous (*IV*) saline or peptide infusion (2.3 mL/hr to deliver 1 pmol/min/100 g bw or 100 pmol/min/100 g bw) was then started (t = -5 min). At t = 0 min, an *IP* glucose injection was given (1 g/Kg body weight, bw). Blood samples were taken at 10, 20, 30 and 60 min, and blood glucose was monitored at 10 minute intervals throughout the experiment. Plasma was separated by centrifugation (10,000 rpm, 20 min, 4°C) and immunoreactive insulin was measured by radioimmunoassay, as described below.

A bioassay was later developed for the conscious unrestrained rat, in order to minimize surgical labour and animal sacrifice. Male Wistar rats (approx. 290 g) were fasted overnight, and then given an oral glucose tolerance test (OGTT; 1 g glucose/Kg body weight) with concurrent subcutaneous (*SC*) saline or peptide (8 nmol/Kg bw in most cases) injection (500 μL). Blood samples were taken at indicated times from the tail vein using heparinized capillary tubes, and the plasma separated by centrifugation for radioimmunoassay. Blood glucose was measured every 10 minutes using a SureStep® glucose analyser (LifeScan Canada Ltd., Burnaby, Canada). Similar experiments were subsequently carried out using age matched 16-20 week old lean and obese VDF Zucker rats (approx. 335 g and 575 g, respectively). Obese Zucker rats have a homozygous recessive defect in their leptin receptor (fa/fa) causing hyperphagia leading to hyperglycemia, hyperlipidemia, hyperinsulinemia, and insulin resistance, similar to human disorders of obesity and diabetes. The dominant genotype (Fa/Fa or Fa/fa) results in a normal lean Zucker rat.

2.13 Hormone Radioimmunoassays

Insulin measurement by RIA was done by incubating samples diluted (usu. 1:3 v/v) in insulin RIA buffer (0.5% charcoal extracted human donor plasma, in 40 mM phosphate buffer, pH 7.5), with insulin antisera (GP01; 1:1,000,000 final dilution) under disequilibrium conditions using rat insulin (Linco Research Inc., St. Charles, USA) as a standard. After 24 h at 4°C, 2000 cpm of chloramine-T iodinated porcine insulin (Sigma) was added to all tubes; subsequent to another 24 h 4°C incubation, antibody bound and free radioactive insulin were separated by centrifugation with dextran-coated charcoal. This protocol has been previously reported [336; 337], and has a lower detection limit of 0.125 ng/ml.

Measurement of GIP by RIA was performed as previously described using a C-terminally directed antibody [336]. Plasma samples were appropriately diluted (usually 1:5 v/v) in GIP

RIA buffer (5% charcoal extracted human donor plasma, 2% Trasylol, 40 mM phosphate buffer, pH 6.5), and incubated with GIP antiserum (RK343F, 1:300,000 final dilution) at 4°C. ^{125}I-GIP (5000 cpm) was added 24 h later and, following a second 24 h incubation, antibody bound and free radiolabelled GIP were separated by PEG-8000 precipitation (12.5% w/v final concentration; BDH) and centrifugation. The lower detection limit for this assay is 7.8 pg/ml.

Measurement of immunoreactive GLP-1 was accomplished using a commercially available kit (Linco) that employed an antibody recognizing C-terminally amidated forms of GLP-1 independent of whether the N-terminus was intact (*i.e.* GLP-1$_{7-36NH2}$, GLP-1$_{9-36NH2}$, GLP-1$_{1-36NH2}$). Non-extracted plasma samples were treated according to the manufacturer's instructions, allowing the assay to measure GLP-1 in samples at concentrations above 10 pg/ml.

2.14 Analytical Methods

For *in vitro* experiments, in all studies, a minimum of three independent experiments were performed. Each independent experiment was conducted on a different day using triplicate or quadruplicate determinations for each condition. Animal experiments were performed with a minimum of 4-6 animals in each group, assigned treatment in a random fashion. No data points were excluded, except in cases where human error was noted. Data shown in figures represents the mean ± standard error of the mean (S.E.M.), and the number of independent experiments is indicated in the figure legends or text. Statistical significance was assessed using Prism data analysis software (GraphPad, San Diego, CA). Student's t test or analysis of variance (ANOVA) were performed where appropriate, followed by the post-hoc tests, Newman-Keuls multiple comparison test, Dunnet's t-test or the Tukey test (where indicated). $P < 0.05$ was considered significant; F tests confirmed variances were equal. Integrated glucose and insulin responses were calculated using the trapezoidal method, with the algorithm included in the Prism software package, and basal levels as a baseline.

Chapter 3: Regulation of GIP Receptor Function

3.1 Introduction

3.1.1 G-Protein Coupled Receptor Regulation

Therapeutically, it may be beneficial in specific disease states to either activate or antagonize/inactivate a given receptor, thus it is useful to characterize the physiological mechanisms of receptor regulation. Exposure of a receptor to high and/or continuous agonist usually leads to dimunition of the cellular response. There are several levels at which the signal can be modulated: (1) extracellular degradation of the ligand, (2) ligand removal by cellular uptake, (3) sterically preventing G-protein coupling by receptor phosphorylation (desensitization), (4) modulation of GTP hydrolysis by G-proteins, (5) modulation of receptor effectors, (6) receptor sequestration, (7) receptor degradation, and (8) down-regulation of receptor gene transcription. Mechanisms of desensitization have been reviewed recently [338-350].

Classically, desensitization refers to the rapid effect of receptor phosphorylation functioning to block heterotrimeric G-proteins from re-coupling to the receptor, thus blocking further signalling. In order to completely block the signal, β-arrestin proteins are recruited to the receptor's intracellular face. The time scale of receptor desensitization by phosphorylation is generally a matter of seconds [338; 340; 341; 343]. Desensitization is further classified into two types: homologous and heterologous desensitization. The first type refers to desensitization of a receptor by its own ligand, and generally occurs by phosphorylation of ligand-bound receptors by G-protein coupled receptor kinases (GRKs), although depending on the signalling pathways used by the receptor, this could also theoretically be mediated by signal transduction kinases, such as PKA and PKC. Heterologous desensitization, however, is not as specific – both ligand-bound and unbound receptors may be phosphorylated by signal transduction kinases activated by alternate receptors. This latter means of desenstization has been less extensively studied than

homologous desensitization [338; 340; 341; 343]. Heterologous desensitization was not examined in the current manuscript, and only homologous desensitization will be considered further.

The discovery of receptor endocytosis stems from work on the adrenergic system whereby, following agonist treatment, binding sites were lost from plasma membranes of erythrocytes [351]; later, binding sites were discriminated by separation of intracellular membrane compartments from the plasma membrane by sucrose gradient centrifugation or by using hydrophilic versus hydrophobic ligands [352; 353]. Subsequent work was able to show internalization of adrenergic receptors using epitope tagged receptors [354] and in real-time using receptor/green-fluorescent protein chimeras [355]. Although there is controversy as to whether phosphorylation is necessary for receptor endocytosis, it does appear to be an antecedant in most cases, and may result in the wide variability observed in kinetics of internalization, when comparing different types of receptors. While phosphorylation may not be an absolute prerequisite for internalization of many receptors, phosphorylation does appear to promote receptor endocytosis. In general, the time-scale of receptor endocytosis is in the order of minutes to hours [338]. Once sequestered into the intracellular compartment known as an "endosome", the ligand is degraded and receptor may undergo dephosphorylation (facilitated by the low intravesicular pH) and be recycled to the cell surface (*i.e.* re-sensitization), or the receptor may also be degraded [345]. Recent studies have indicated that receptor sequestration is a requirement for dephosphorylation, recycling and resensitization [356; 357]. When a receptor agonist persists for hours or days, the reduced number of receptors expressed appears to extend beyond protein degradation [345]. Currently, there is evidence that prolonged stimulation results in down-regulation of steady-state mRNA levels, and can influence mRNA stability [339].

3.1.2 Regulation of Family B G-Protein Coupled Receptors

The β-adrenergic receptor is often considered to be the prototypical GPCR, and thus the paradigm of desensitization and internalization, as characterized using the β-adrenergic system has been broadly applied to all GPCRs. However, in a side-by-side comparison of the $β_2$-adrenergic (family A) and secretin (family B) receptor, it was found that the family B receptor behaved differently from the family A counterpart [358; 359]. While the secretin receptor was a substrate for GRK-2 and -5, and phosphorylation was shown to promote desensitization [359], GRKs and β-arrestin had no influence on receptor internalization, but PKA did [358]. Hence, it is clear that the dogma of receptor desensitization does apply to most G protein-coupled receptors, however, each receptor must be considered individually with respect to the precise mechanisms of desensitization. A review of desensitization of receptors of the secretin/VIP superfamily of receptors is found elsewhere [360], and only desensitization of receptors closely related to the GIP receptor will be considered further, namely the GLP-1 and glucagon receptors.

Desensitization and internalization of the cloned glucagon receptor have been characterized less than these processes for the GLP-1 receptor. Treatment of CHO-K1/glucagon receptor cells with glucagon induced a rapid time- and concentration-dependent phosphorylation of the receptor; phosphorylation was independent of PKA and PKC activity [361]. Phosphorylation of serines in the intracellular C-terminus was correlated with receptor endocytosis [335; 361]. Pretreatment of baby hamster kidney (BHK) cells transfected with the human glucagon receptor with glucagon or carbachol desensitized the calcium response to a subsequent glucagon stimulation, indicating that the receptor undergoes homologous and heterologous desensitization [322], however, the involvement of GRKs or signal transduction kinases has not been proven.

The first report of desensitization of the GLP-1 receptor examined attenuation of cyclic AMP and insulin responses to GLP-1 following preperifusion of HIT-T15 cells with GLP-1, GIP or glucagon [177]. A rapid, reversible desensitization of both cAMP and insulin responses to GLP-

1 were observed; a 10 min desensitization period with 100 nM GLP-1, followed by a 10 minute washout period, and subsequent 30 min stimulation reduced the cAMP response to 49% of control [177]. Further work in insulinoma βTC-3 cells, found evidence for PKA-independent homologous desensitization of GLP-1-stimulated calcium transients, and that PKC activation reduced calcium responses by 75%, but that PKC-independent pathways were also involved [362]. Fehmann et al [363] suggested that GLP-1 receptor responsiveness was determined by surface expression; a reduced GLP-1 binding capacity was observed in RINm5F cells with GLP-1 treatment, and on a longer time-scale, chronic treatment with PKA activators reduced surface receptor expression and mRNA stability. Internalization of ^{125}I-GLP-1 has been shown for insulinoma and transfected cells [364; 365]. GLP-1R homologous desensitization and internalization were correlated with specific phosphorylation of C-terminal tail serine doublets, but differential quantitative impairment of desensitization or internalization in mutant receptors indicated different cellular mechanisms controlling these processes [366]. However, heterologous desensitization of the GLP-1 receptor with phorbol esters similarly involved phosphorylation of serine doublets in the intracellular tail of the receptor [367; 368]. Like the glucagon receptor, involvement of GRKs in desensitization and/or receptor endocytosis is unknown.

On initiating work for the current thesis, only two reports regarding GIP receptor desensitization existed. The first reported a single experiment demonstrating homologous desensitization of GIP-stimulated insulin release from perifused HIT-T15 cells, as part of a larger study of GLP-1 receptor regulation [177]. The other reported chronic desensitization of the GIP receptor in diabetic rats resulting from elevated serum levels of GIP in these animals [369]. Unfortunately, experimental flaws in this latter report prevent the extraction of results it claimed to report. Preliminary work on GIP receptor mutants with C-terminal truncations indicated that the C-terminus played a role in receptor sequestration [290; 324]. During preparation of our own

reports on GIP desensitization in βTC-3 cells [370], internalization of GIP receptor mutants in transfected cells [290], and further studies contained in the present thesis, Tseng and Zhang released a series of publications implicating C-terminal residues (S406 and C411) in desensitization and surface expression [291], and the involvement of regulator of G protein signalling (RGS) proteins [371] and G protein-receptor kinases [372] in the attenuation of GIP receptor activation.

3.1.3 Potential Physiological Relevance of GIP receptor Desensitization

Studies in insulin-resistant type 2 diabetic patients, suggested that there was a reduced incretin effect in the disease [373]. Subsequent results have indicated that alterations in both GIP and GLP-1 are involved: a secretory defect appears to result in diminished GLP-1 secretion, while the responsiveness of the β-cell to GIP is blunted [155; 374]. As such, physiological concentrations of exogenous GLP-1 can still act as a potent antidiabetic agent, whereas GIP is much less potent [220; 375-378]. Poor preparations of early batches of synthetic GIP contributed to the reduced potency of GIP in both normal and type 2 diabetic patients [92; 276]. Regardless, there is little doubt that there is a blunted response to GIP by the β-cell in type 2 diabetes. The root of the problem is difficult to ascertain, considering that GIP levels in diabetics have been reported to be elevated, normal, or low, however, these differences are likely due to complications with radioimmunoassay of GIP [52; 53]. Recently, it was proposed that the blunted responsiveness to GIP in type 2 diabetes patients may be due to decreased expression of the GIP receptor [374]. When testing this hypothesis in an animal model of type 2 diabetes, the Vancouver diabetic fatty (VDF) rat, Lynn and colleagues [379] discovered a reduction in GIP mRNA and protein expression in isolated islets, and correlated the diminished expression to decreased ability to stimulate cyclic AMP and insulin release from islets, and inability of GIP to reduce glycemic excursions *in vivo* when infused at physiological concentrations.

3.1.4 Thesis Objective

In the current study, homologous desensitization and internalization of the GIP receptor were characterized, as it is possible that these two cellular processes are involved in the diminished incretin effect observed in type 2 diabetes. With this goal in mind, βTC-3 cells (Methods 2.3) were employed to examine regulation of GIP-stimulated cyclic AMP by glucose and homologous desensitization of endogenously expressed receptors (Methods 2.7), as well as desensitization of insulin release (Methods 2.8). Wild type and mutant (Methods 2.2) GIP receptor transfected CHO-K1 cells (Methods 2.3) were used to further characterize desensitization (Methods 2.7) and internalization by radioactive (Methods 2.9) or fluorescent means (Methods 2.10). Furthermore, using pharmacological inhibitors of signal transduction molecules, cellular processes involved in desensitization of GIP-stimulated cAMP in βTC-3 cells (Methods 2.7) and internalization in transfected cells was accomplished (Methods 2.9).

3.2 Results

3.2.1 Desensitization of βTC-3 Cells to GIP

Possible mechanisms of desensitization to GIP were studied using βTC-3 cells as a β-cell model. GIP receptors have been demonstrated to be expressed in this cell line, and stimulation of insulin release by GIP is glucose-dependent [178]. Cyclic AMP production in response to GIP was found to increase in a concentration-dependent manner (Figure 5A-D), and was only slightly affected by glycemic conditions. The maximal cyclic AMP produced in response to GIP was moderately blunted with increasing ambient glucose conditions (Table 3), while sensitivity to GIP was not affected (EC_{50} values: 0 glucose: 12.5 ± 4.8 nM; 5.5 mM glucose: 9.5 ± 2.0 nM; 11 mM glucose: 10.9 ± 4.4 nM). At each glucose concentration, however, the desensitized cAMP response was similar following pretreatment of cells with 100 nM GIP for 1 hour (Table 3). Cyclic AMP production stimulated by 10 μM forskolin was neither altered by glycemic

condition nor pretreatment with 100 nM GIP for 1 hour (Table 3). A time-course for desensitization of GIP-stimulated cAMP indicated a mild but significant reduction in cAMP production could be observed with 10 min of 100 nM GIP pretreatment, and the apparent desensitization was more pronounced with increasing duration of pretreatment (Figure 6A).

Table 3: Summary of cyclic AMP production in βTC-3 cells in response to GIP and forskolin

Data represent mean ± S.E.M. of 3 independent experiments. Cells were incubated with GIP (320 pM-1 μM) or 10 μM forskolin for 30 minutes in the presence of 0.5 mM IBMX, and cAMP was measured by RIA (see Figure 5). Refer to Methods section 2.3 and 2.7 for more detail.

	Glucose (mM)	Control (pmol cAMP/well)	100 nM GIP-Pretreated* (pmol cAMP/well)
Maximal GIP Response	0.0	70.5 ± 7.9	52.4 ± 10.3
	5.5	66.3 ± 8.1	55.7 ± 9.1
	11.0	55.2 ± 7.8	44.4 ± 7.6
10 μM Forskolin	0.0	331.0 ± 40.8	347.1 ± 29.1
	5.5	346.3 ± 16.8	328.3 ± 25.8
	11.0	337.3 ± 30.0	342.6 ± 36.6

*: Cells were prestimulated with 100 nM GIP for 1 hour, followed by a 10 min washout period

Previous studies have reported failure of GLP-1 or GIP to stimulate cAMP production in the absence of glucose in rodent insulinoma cell lines when performed in Kreb's Ringer solution [176; 177]. Upon finding that GIP was able to produce a concentration dependent production of cAMP in βTC-3 cells in zero glucose DMEM (Figure 5A,B), experiments were repeated in KRB to rule out the involvement of more complex constituents. GIP (100 nM) and forskolin (10 μM) yielded similar responses in the presence of either 0 mM or 5.5 mM glucose, respectively (P > 0.05), and were similar in magnitude to experiments performed in DMEM (data not shown).

Degradation of extracellular ligand is a well accepted mechanism for attenuation of stimulation. Induction of dipeptidyl peptidase IV, the primary enzyme responsible for incretin inactivation [58; 59; 380], could contribute to the desensitized state observed in βTC-3 cells with static incubations. Thus, the potent reversible non-hydrolysable transition state inhibitor,

isoleucine-thiazolidide [381; 382] was employed to test this hypothesis. Ile-thia did not affect basal, stimulated or desensitized GIP induced cyclic AMP responses (Figure 6B). During the preparation of this thesis, Kesper *et al* [383] found that chronic exposure of INS-1 cells to GIP resulted in induction of $G_{\alpha i}$ G-proteins. An increase of inhibitory G-protein complement could also diminish the cAMP response to GIP. However, pertussis toxin had no effect on basal, stimulated or desensitized GIP-induced cyclic AMP responses in βTC-3 cells (Figure 6C).

Prior work examining desensitization of the glucagon receptor has suggested that alterations in phosphodiesterase (PDE) activity could also lead to an apparent reduction in cAMP production by hormones [384]. It was hypothesized that, if PDE were modulated by pretreatment with GIP, then a change in sensitivity to IBMX would be observed relative to control cells. To test the possibility of modulation of phosphodiesterase activity in the desensitized state, the effect of IBMX concentration was tested in both the control and GIP-pretreated conditions (Figure 6D). Intracellular cyclic AMP levels increased with increasing concentration of IBMX over the range tested, however, maximal inhibition of phosphodiesterase was not achieved. When cAMP was normalized to the maximal value observed in either control or desensitized state, no alteration in sensitivity to IBMX was observed. Higher concentrations of IBMX would probably result in non-specific effects.

Signal transduction kinases PKC and PKA have been shown to contribute to receptor desensitization in other hormone models. These kinases can form a negative feedback loop whereby surface receptors are phosphorylated, thus blunting their response to further stimulation. Broad specificity inhibitors of PKC (staurosporine) and PKA (H89) were used during the pretreatment period to block this feedback, if present (Figure 6E and F). Staurosporine acted to significantly reduce the basal cAMP concentrations in non-stimulated cells ($P < 0.05$) and to enhance GIP-stimulated cAMP production (1.9-fold; $P < 0.01$), but did not inhibit the attenuation

of the cAMP response by pretreatment with GIP. In contrast, H89 had no effect on basal or stimulated cAMP values, or desensitization of the cAMP response to GIP.

The degree of glucose stimulated insulin release from βTC-3 cells in KRB was similar to that previously observed [178], with significant insulin released by 5.5 and 11 mM glucose (163 ± 16 % and 182 ± 21 % basal release in 0 glucose, respectively; $p < 0.05$ and $p < 0.01$ versus basal) (Figure 7A). In the absence of glucose, GIP failed to stimulate insulin release (102 ± 10 % basal), but forskolin stimulated a small but significant release (140 ± 18 % basal; $p < 0.05$). In the presence of elevated glucose, 10 nM GIP potentiated insulin release (5.5 mM glucose: 223 ± 26 % basal; 11 mM glucose: 247 ± 28 % basal; $p < 0.05$), as did 10 μM forskolin (5.5 mM glucose: 397 ± 17 % basal; 11 mM glucose: 472 ± 26 % basal; $p < 0.001$) (Figure 7A). In contrast to the weak effect of GIP pretreatment on cyclic AMP production, pretreatment of cells with 100 nM GIP completely abolished the potentiating effect of GIP on insulin secretion under elevated glucose conditions (5.5 mM glucose: 113 ± 4 % basal; 11 mM glucose: 101 ± 3 % basal; $p < 0.001$ versus euglycemic controls). Furthermore, while GIP pretreatment yielded no effect on forskolin-stimulated cAMP production, the same treatment significantly reduced forskolin-stimulated insulin release to values roughly half the magnitude of euglycemic controls (5.5 mM glucose: 168 ± 17 % basal; 11 mM glucose: 218 ± 14 % basal; $p < 0.001$ versus euglycemic controls).
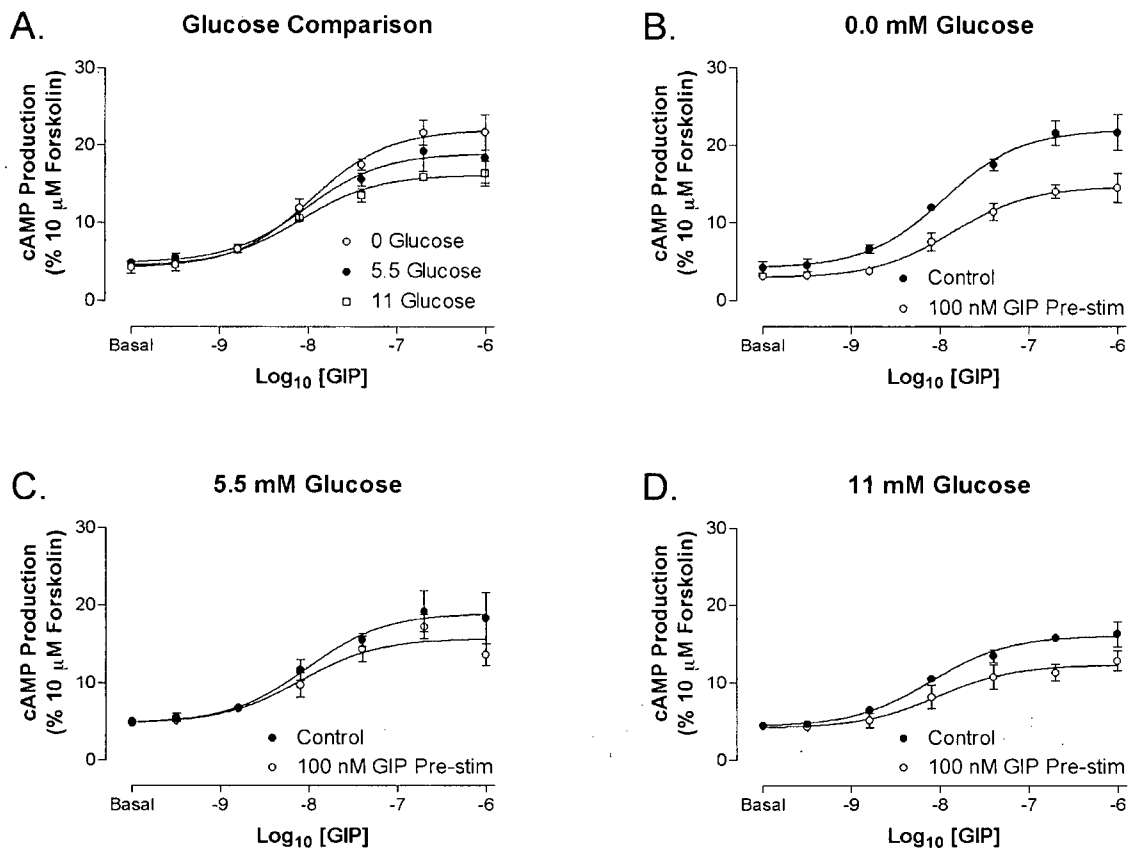
Figure 5: Effect of glycemic conditions on cyclic AMP production in βTC-3 cells
(A) Comparison of GIP-stimulated cAMP production under various glucose conditions. (B-D) Effect of pretreating cells with 100 nM GIP for 60 min prior to performing concentration-response studies. Glucose had no effect on forskolin-stimulated cAMP production. Data represent the mean ± S.E.M. of 3 independent experiments. Refer to Methods sections 2.3 and 2.7 for more detail.

A. GIP Desensitization Timecourse

cAMP Production (% Control)

☐ Basal
■ 10 nM GIP

*

Control   10 Min   30 Min   60 Min
Duration of GIP Pretreatment

B. Effect of DPIV Inhibition

cAMP Production (% Control)

■ Control
▨ Desensitized

| 10 nM GIP | -- | -- | + | + |
| 50 μM Ile-Thia | -- | + | -- | + |

C. Effect of Pertussis Toxin

cAMP Production (% Control)

■ Control
▨ Desensitized

| 10 nM GIP | -- | -- | + | + |
| 500 ng/mL PTX | -- | + | -- | + |

D. Effect of IBMX

cAMP Production (% control)

cAMP Production (pmol/well)

Log_{10} [IBMX]

—●— Control
—○— Desensitized

Log_{10} [IBMX]

E. Effect of Staurosporine

cAMP Production (% Control)

■ Control
▨ Desensitized

b

a

| 10 nM GIP | -- | -- | + | + |
| 100 nM Stauro | -- | + | -- | + |

F. Effect of H89

cAMP Production (% Control)

■ Control
▨ Desensitized

| 10 nM GIP | -- | -- | + | + |
| 5 μM H89 | -- | + | -- | + |

Figure 6: Time-course of homologous desensitization of GIP-stimulated cAMP production and effect of various inhibitors on desensitization in βTC-3 cells

(A) Cells were pretreated with or without 100 nM GIP for indicated times, followed by a 10 min washout period and subsequent stimulation with 10 nM GIP. Subsequent figures show GIP-stimulated cAMP production with or without pretreatment with 100 nM GIP for 60 min, followed by a 10 min washout period and subsequent stimulation with 10 nM GIP. 0.5 mM IBMX was used during the stimulation period, except where indicated. (* = p < 0.05). (B) Effect of isoleucine-thiazolidide (Ile-thia), a potent DPIV inhibitor, administered during the stimulation period. (C) Effect of pertussis toxin (100 ng/mL during washout period and 500 ng/mL during stimulation) on GIP-stimulated cAMP production. (D) Effect of IBMX on apparent desensitization of GIP-stimulated cAMP production. Data were normalized to the response observed in the control or desensitized state at 4 mM IBMX. Inset shows the same data

69

as pmol cAMP/well. N.B. IBMX concentration is plotted using a logarithmic scale. (E and F) Effect of 100 nM staurosporine or 5 µM H89 on homologous desensitization of GIP-stimulated cAMP formation, administered 15 min prior to and during the GIP pretreatment. ($a = p < 0.05$, $b = p < 0.01$). Data represent the mean ± S.E.M. of 4 independent experiments. Experiments shown here were in the presence of 5.5 mM glucose. Refer to sections 2.3 and 2.7 for specific methods.
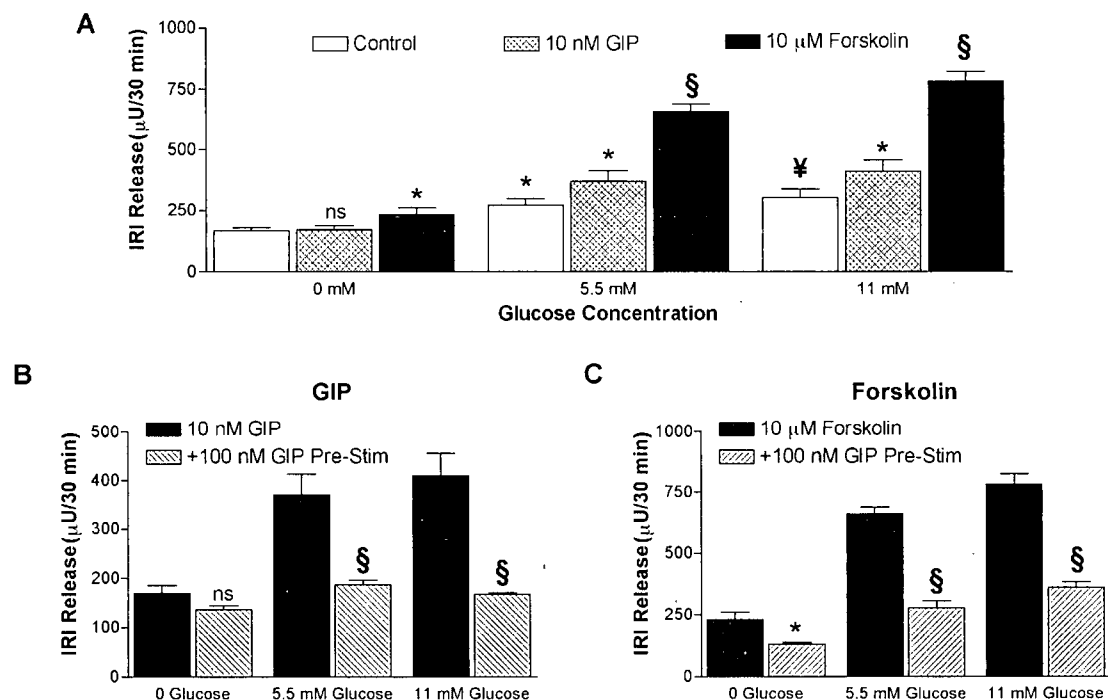
Figure 7: Insulin release from βTC-3 cells
(A) Comparison of glucose, GIP and forskolin-stimulated insulin release. (B) The effect of pretreating cells with 100 nM GIP prior to 10 nM GIP stimulation. (C) The effect of pretreating cells with 100 nM GIP prior to 10 mM Forskolin stimulation. Data represent mean ± S.E.M. of at least 4 independent experiments. (* = $P < 0.05$, ¥ = $P < 0.01$, § = $P < 0.001$). Statistical comparisons of GIP and forskolin-stimulated insulin release versus euglycemic controls were analyzed, whereas glucose-stimulated insulin release was compared to basal release in the absence of glucose. Refer to sections 2.3 and 2.8 for specific methods.

3.2.2 Desensitization of the Transfected GIP Receptor

Experiments designed to examine the regulation of the GIP receptor were continued using a transfected cell model. Unfortunately, transfected cell models are usually over-expression systems, which complicated demonstration of GIPR desensitization. Following work presented by the research group of Thorens on the GLP-1 receptor [366], only low expressing clones of GIP receptor transfected CHO-K1 cells were able to be desensitized. Subcloning a pooled clone of wild type GIP receptor transfected cells yielded two cell lines, rGIPR-L2 and rGIPR-L13, which had sufficiently low receptor expression to allow receptor desensitization studies to be performed. Saturation binding (Figure 8) on transfected cells indicated maximum binding values (Bmax) of 76.5 ± 16.9 cpm/1000 cells (wtGIPR), 18.6 ± 6.7 cpm/1000 cells (rGIPR-L2) and 4.35 ± 2.93 cpm/1000 cells (rGIPR-L13), and K_d values between 208-838 pM. No further studies beyond preliminary desensitization and saturation binding were done on rGIPR-L13 due to the intrinsic variability of responses with this extremely low expressing cell line. Figure 9 shows a concentration-response curve of GIP_{1-42} (with IBMX) on wtGIPR and rGIPR-L2 cells with or without a 60 minute pretreatment with 100 nM GIP in the absence of IBMX. The normal GIP curve for wtGIPR cells displayed an EC_{50} of 22.6 ± 3.8 pM, and maximal cyclic AMP accumulation was 255 ± 54 fmol/1000 cells; it appeared that the 100 nM GIP could not be washed off in 10 min in the case of pretreatment of wtGIPR cells, as a constant high cyclic AMP production level persisted even in the absence of GIP in the medium (Figure 9). In contrast, rGIPR-L2 cells were only able to maximally increase intracellular cyclic AMP to 38.4 ± 5.0 fmol/1000 cells in response to GIP, which was reduced to 25.2 ± 1.6 fmol/1000 cells after GIP pretreatment (P < 0.05). However, a small but significant persistent elevation of basal cyclic AMP was noted in the pretreated cells: 2.85 ± 0.12 fmol/1000 cells (control) versus 8.98 ± 0.55 fmol/1000 cells (pretreated) (P < 0.05), indicating that it was not possible to wash away all of the residual GIP (Figure 9). Half-maximal cyclic AMP stimulation by GIP occurred at 607 ± 57 pM

GIP in the case of the control, whereas the EC_{50} for cells pretreated with 100 nM GIP for 60 min prior to the concentration-response curve was significantly right shifted: 1.27 ± 0.38 nM GIP.

Some investigations have used cyclic AMP accumulation time-course experiments as indicating desensitization, as cyclic AMP levels plateau. Others have argued that the plateau may arise from overcoming the IBMX blockade of cAMP degradation by phosphodiesterase due to such high levels of cyclic nucleotide. With this in mind, a 1 nM GIP-stimulated cyclic AMP time-course experiment was performed in wtGIPR cells with and without 0.5 mM IBMX (Figure 10). In both cases, plateau levels of cyclic AMP were approached by 15 min. Repetitive stimulation experiments were performed on rGIPR-L2 cells. In a similarly designed experiment, a time-course of cAMP accumulation in rGIPR-L2 cells in response to 1 nM GIP (in the presence of 0.5 mM IBMX) was measured, with and without a 60 min 100 nM GIP pretreatment (in the absence of IBMX) (Figure 11A). In control cells, cAMP levels reached a plateau by 30 min, despite the fact that rGIPR-L2 cells displayed much lower maximal GIP-stimulated cAMP production than wtGIPR cells (rGIPR-L2: 38.4 ± 5.0 versus wtGIPR: 255 ± 54 fmol/1000 cells; Figure 9). When rGIPR-L2 cells were pretreated with 100 nM GIP for 60 min (+ 10 min washout), during the subsequent 1 nM GIP stimulation, the plateau was simply reset to a lower level, approximately 63% of the maximal control value (Figure 11A).

To establish the time scale during which receptor desensitization was occurring, rGIPR-L2 cells were prestimulated for various times (60, 25 and 10 min) with 100 nM GIP in the absence of IBMX, followed by a washout period, and a 30 min stimulation in the presence of IBMX with or without 1 nM GIP (Figure 11B). GIP receptor desensitization in transfected CHO-K1 cells was slow and moderate, with a profile similar to that observed in βTC-3 cells (Figure 6). A series of nine GIP receptor mutants was generated (refer to Figure 2) to examine the role of potential phosphorylation sites in receptor sequestration (using high expressing pooled cell lines). At the same time, two mutant lines were selected to subclone for examination of

72

desensitization in low expressing cell lines. In the standard 60 min/100 nM GIP prestimulation

protocol, receptors with a serine doublet mutated to alanines (rGIPR-S426/427A) desensitized to

a similar degree as wild type receptors, ~72% of control, whereas a receptor mutant with all six

C-terminal serines mutated to alanines (rGIPR-S398/406/426/427/440/453A) still displayed 94%

of control cAMP production. These results indicate that specific serines in the C-terminal tail

permit receptor desensitization, likely via phosphorylation, but the residues are unlikely to be

Ser^{426} or Ser^{427}.
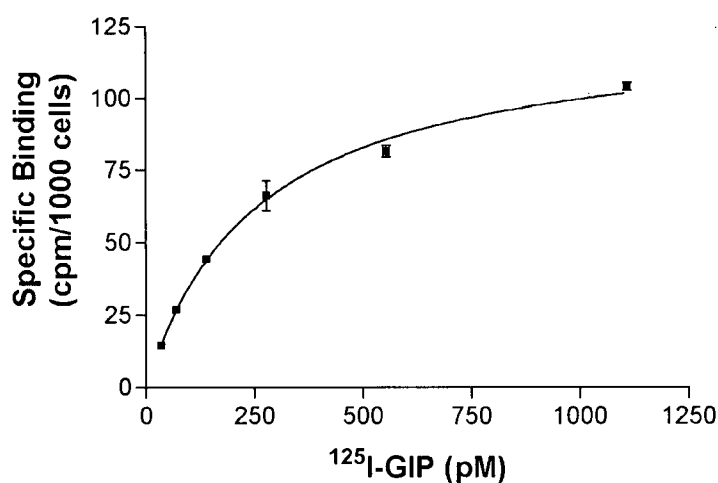
Figure 8: A representative saturation binding curve for wtGIPR cells
Cells were incubated in the presence of ^{125}I-GIP with or without 1 μM GIP at 4°C for 12-16
hours. See Methods sections 2.2 and 2.6 for details.
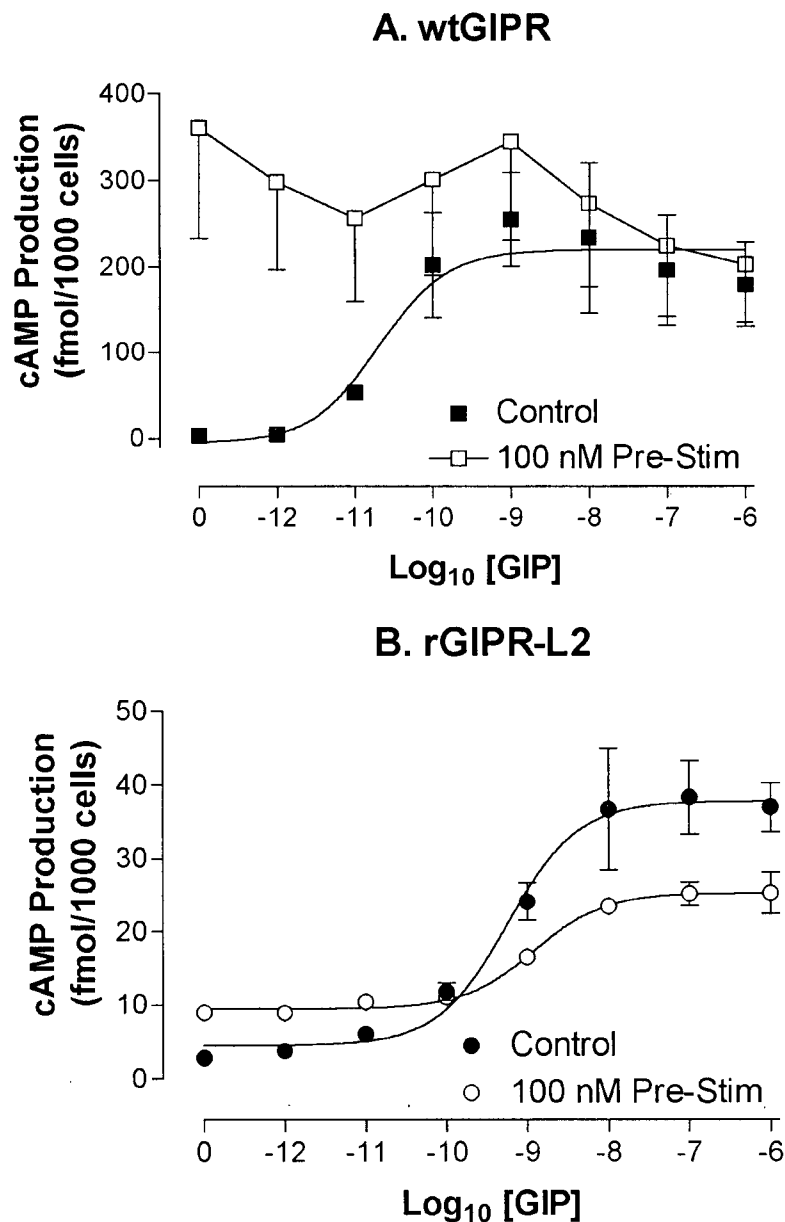
A. wtGIPR

B. rGIPR-L2

Figure 9: Effect of GIP prestimulation on the concentration-response curve of wtGIPR and rGIPR-L2 cells

Cells were pretreated with 100 nM GIP in the absence of IBMX for 60 min in buffer containing 1% Trasylol at 37°C. Cells were washed twice over 10 min with warm buffer, followed by a concentration-response experiment with varied GIP concentrations in the presence of 0.5 mM IBMX. Data represent mean ± S.E.M.; n = 3-4. See sections 2.2, 2.3, and 2.7 for detailed methods.
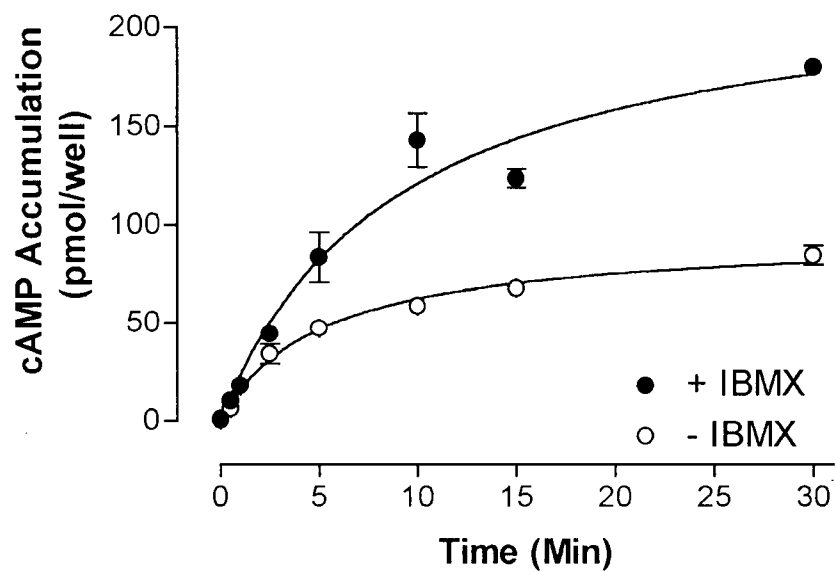
Figure 10: Time-course of cAMP accumulation in wtGIPR cells with and without IBMX
Cells were preincubated in 37°C buffer for 60 min, prior to adding 1 nM GIP to wells with or without 0.5 mM IBMX in buffer containing 1% Trasylol. Data represent mean ± S.E.M.; n = 4. See sections 2.2, 2.3, and 2.7 for detailed methods.
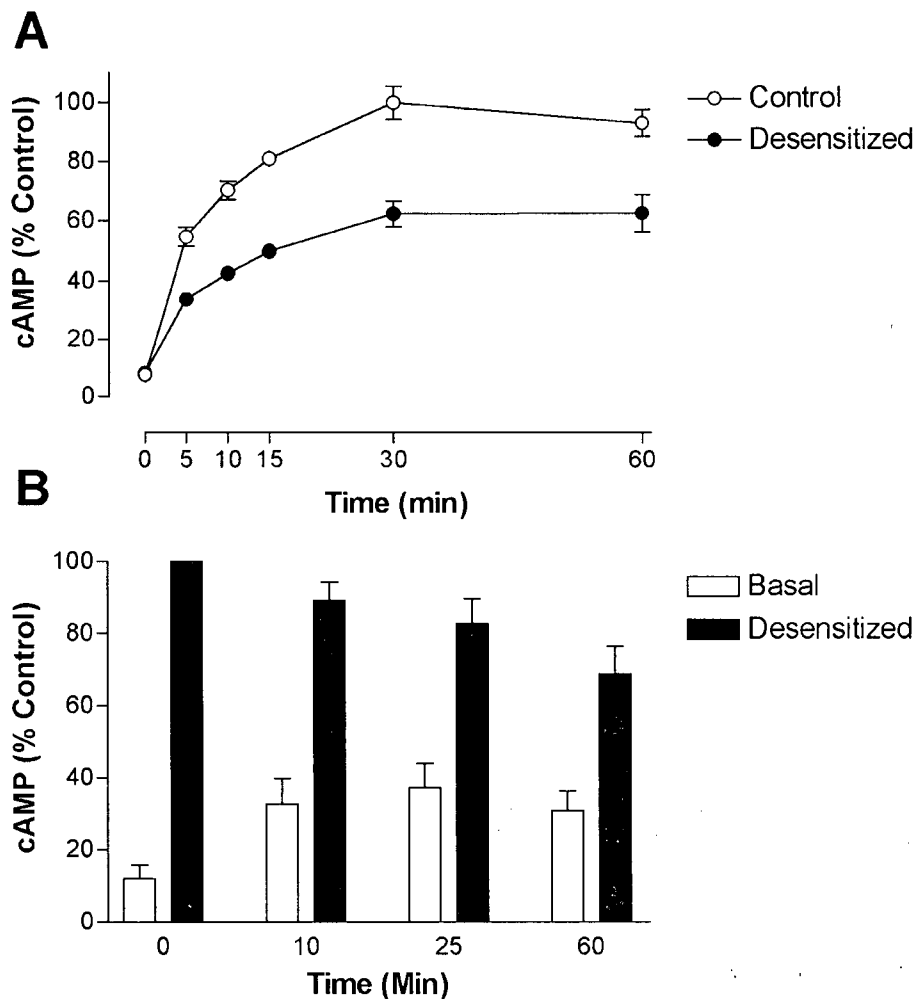
Figure 11: Time-course of desensitization in rGIPR-L2 cells
(A) Cells were preincubated in 37°C buffer (with 1% Trasylol) for 60 min with or without 100 nM GIP, prior to a 10 minute washout period, and adding 1 nM GIP to wells with 0.5 mM IBMX for various times. (B) Cells were preincubated for various times with 100 nM GIP (no IBMX), prior to washout and subsequent stimulation with 1 nM GIP for 30 min; "Basal" refers to cells which were incubated in the absence of GIP during the 30 min stimulation period. Data represent mean ± S.E.M.; n = 4. See sections 2.2, 2.3, and 2.7 for detailed methods.

76
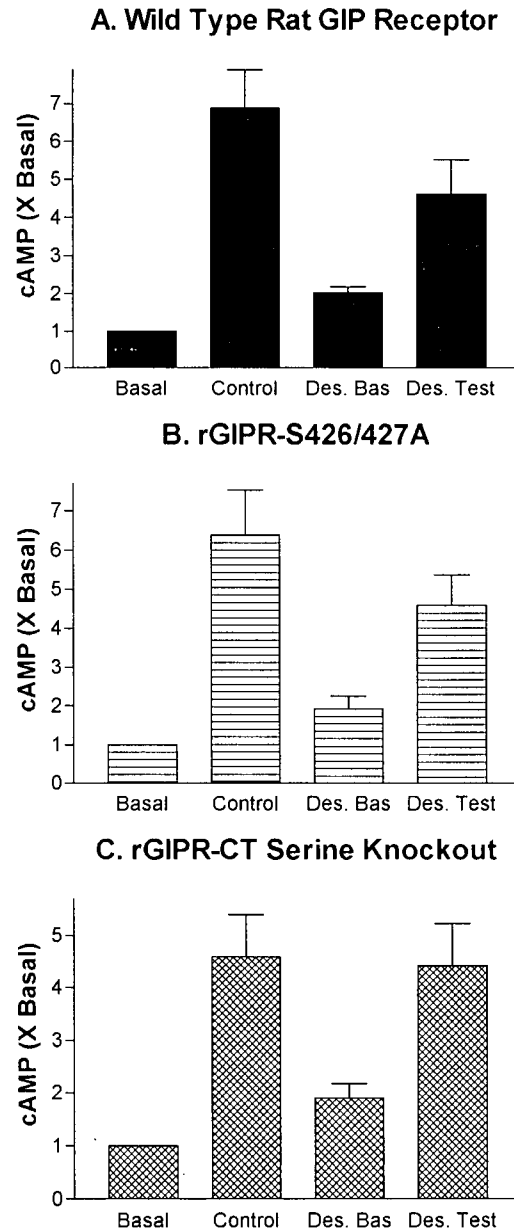
Figure 12: Desensitization of C-terminal mutant GIP receptors

Low expressing subclones of CHO-K1 cells transfected with (B) GIPR-S426/427A or (C) GIPR-S398/406/426/427/440/453A were compared to control low expressing wild type GIPR subclone rGIPR-L2 (A), when treated with 100 nM GIP for 60 min, prior to a 10 min washout and subsequent 30 min stimulation in the absence (Des. Bas.) or presence (Des. Test) of 1 nM GIP in the presence of IBMX. Data represent mean ± S.E.M.; n = 4. See sections 2.2, 2.3, and 2.7 for detailed methods.

3.2.3 Internalization of the Transfected GIP Receptor

3.2.3.1 Development of an Internalization Protocol

Efforts were made to develop a protocol to measure receptor internalization. Of several methods attempted, the one with the most success involved adding 100 nM GIP at various time-points to wtGIPR cells (or mutants), stripping off surface bound peptide with a hypertonic acidic solution, washing with buffer, and then performing a binding experiment to measure the remaining surface receptors (Methods section 2.9). To validate the internalization protocol, it was necessary to ensure that receptor binding affinity was not affected by GIP treatment or the acid stripping protocol. Binding to wtGIPR cells was allowed to proceed for 4 hours at 4°C, as this achieved near equilibrium (Figure 13); acid treatment alone reduced total binding (B_0) to $64.0 \pm 1.6\%$ of control values, and 100 nM GIP for 1 hour, prior to the acid wash resulted in a B_0 of $36.5 \pm 2.7\%$ of control (Figure 14). Binding affinity was not significantly affected by GIP pretreatment or acid stripping procedure (IC_{50} values: 3.64 ± 0.26 nM, control untreated; 5.73 ± 0.55 nM, acid alone; 5.87 ± 1.11 nM, GIP pretreatment and acid wash), validating the use of B_0 as an estimate of B_{max} in these studies (Eq. 2, Methods section 2.6). Non-specific binding was slightly, but not significantly elevated in both acid treated groups (% of total label added: control, 0.85%; acid alone, 1.27%; internalized, 1.09%), and was on the order of 400-600 cpm. Hence, from this control experiment, the estimated internalization caused by 60 min treatment with 100 nM GIP was a ~27.5% loss of surface binding.
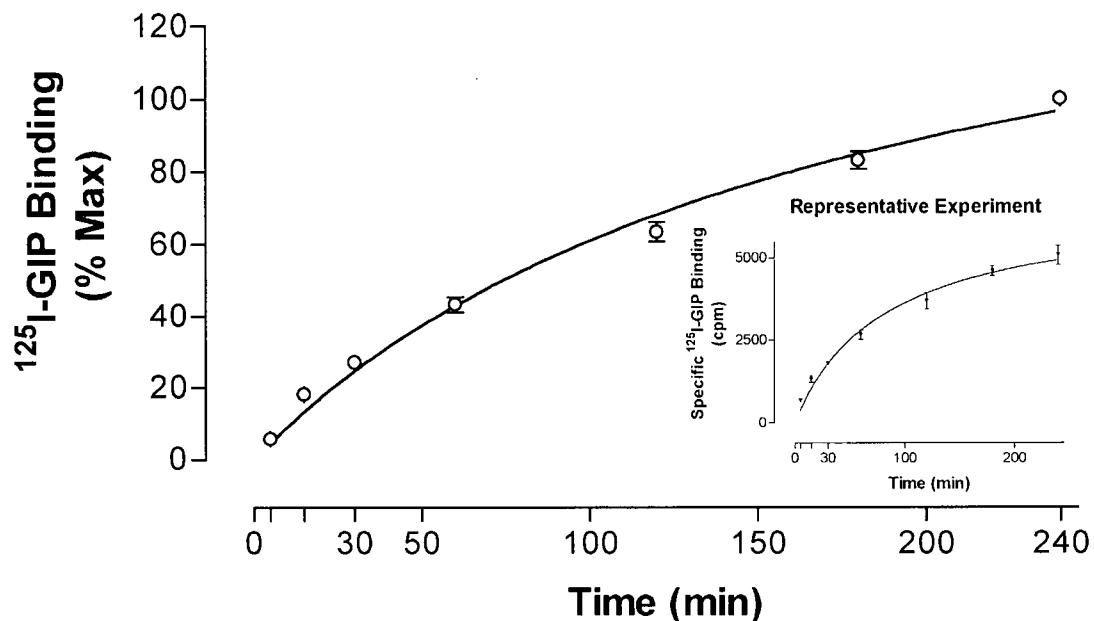
Figure 13: Time-course of ^{125}I-GIP binding to wtGIPR cells

GIP tracer (50,000 cpm/well) was incubated with attached wtGIPR cells in 24 well plates for indicated times at 4°C. Wells were washed twice with cold buffer, prior to solubilization with 0.1 M NaOH and transfer to borosilicate tubes for counting. Non-specific binding was measured at each time-point in wells containing excess unlabelled GIP. Data represent mean ± S.E.M., normalized to the maximal specific binding observed at 4 h; n = 4. Refer to Methods sections 2.3, 2.5 and 2.6.
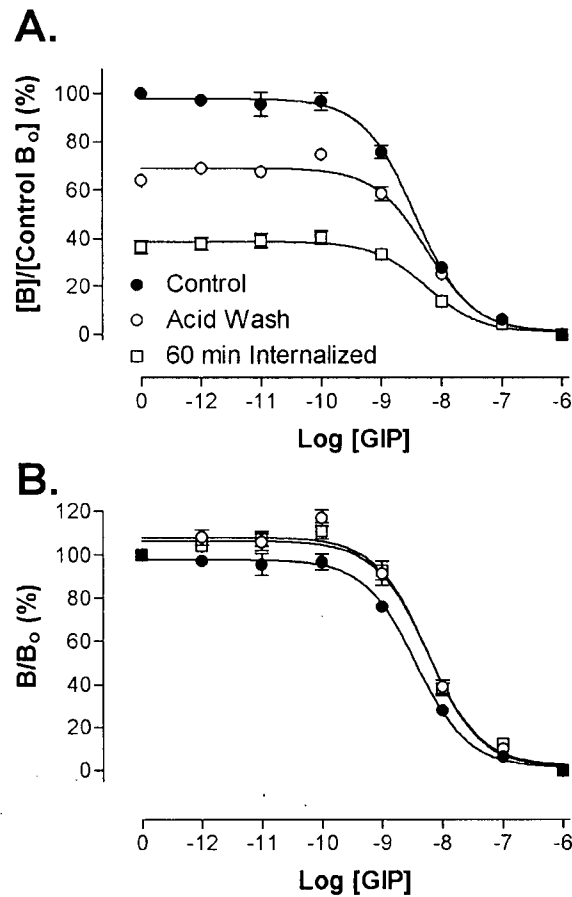
Figure 14: Effect of acid stripping alone or in combination with 60 min 100 nM GIP pretreatment on GIP receptor binding on wtGIPR cells

Acid stripping (5-10 min with 150 mM NaCl/50 mM glycine, pH 3) is commonly performed to remove surface bound non-internalized peptide. This experiment was designed to establish whether acid stripping had any effect on receptor expression or affinity alone. (A) Binding data normalized to B_0 of control untreated cells. (B) Binding data normalized to B_0 of each condition. Data represent mean ± S.E.M.; n = 4. The control is a normal competitive-binding inhibition curve with non-treated cells. Refer to Methods sections 2.3, 2.5, 2.6, and 2.9.

3.2.3.2 Agonist and Antagonist Stimulated Receptor Internalization

Further characterization of GIP receptor internalization continued with a sequestration time-course in response to 100 nM GIP or the GIP receptor antagonist (see Chapter 4, section 4.2.1, cf. Figure 34), 1 μM GIP$_{7-30NH2}$ (Figure 15). Sixty min of GIP$_{1-42}$ treatment resulted in internalization of 38.6 ± 1.1% of the surface receptors, whereas a ten-times greater concentration of GIP$_{7-30NH2}$ resulted in the internalization of 18.8 ± 3.1% (Figure 15A). The threshold for GIP$_{1-42}$ stimulated loss of surface binding was between 10 and 20 nM, and above this concentration, concentration-dependent internalization was observed (Figure 15B). GIP$_{7-30NH2}$ did not stimulate measurable cAMP production at concentrations as high as 10 μM, and exhibited approximately a 10-fold lower binding affinity, when compared to native GIP (Chapter 4, section 4.2.1, cf. Table 7). Significant GIP$_{7-30NH2}$-stimulated loss of surface receptors was observed at a concentration of 1 μM, and at 10 μM, this peptide caused a 72.4 ± 1.3% reduction in surface binding. The concentration at which 50% of surface receptors were lost was between 0.5 and 1 μM for GIP$_{1-42}$, and 5 and 7.5 μM for GIP$_{7-30NH2}$. Hence, it would appear that ligand binding by the receptor is a more important determinant of internalization than receptor activation, with half-maximal internalization potencies correlating well with binding affinities.

A. Agonist and Antagonist Stimulated Receptor Internalization

B. Agonist and Antagonist Internalization Dose Response
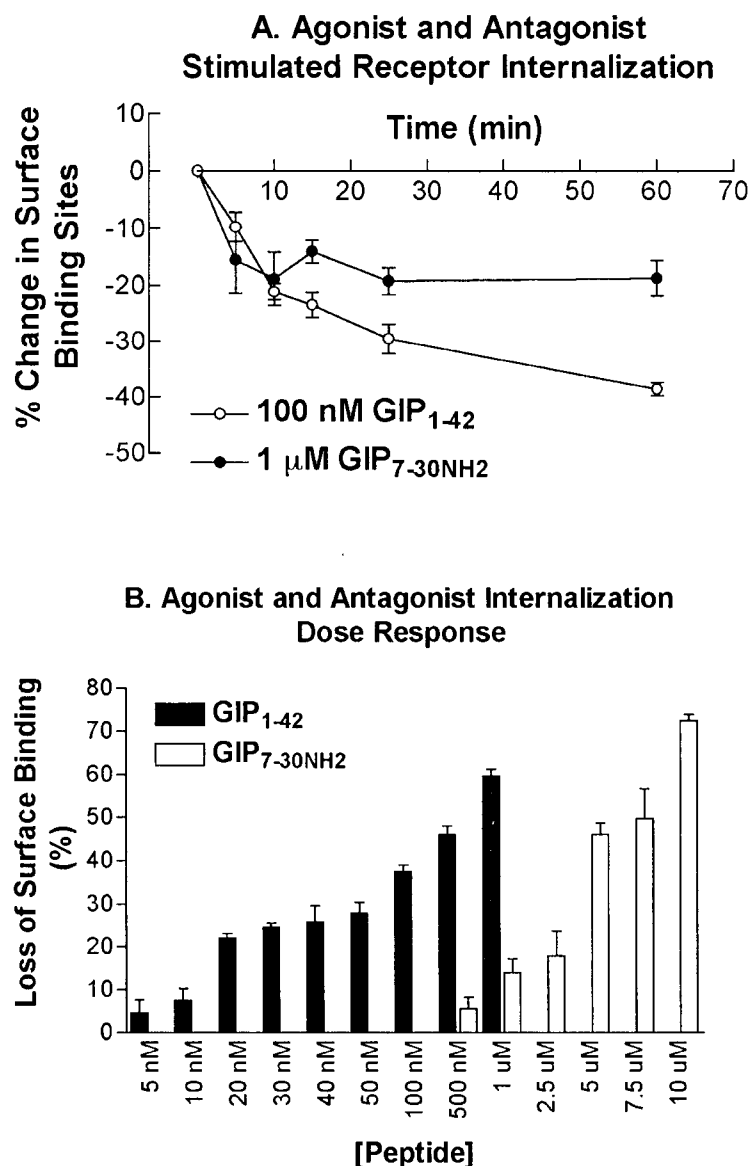
Figure 15: GIP receptor internalization by agonist and antagonist

(A) wtGIPR cells were treated for the indicated times with 100 nM GIP_{1-42} or 1 μM $GIP_{7-30NH2}$, prior to acid stripping and measurement of remaining surface binding as per methods described in the text. (B) wtGIPR cells were treated with increasing concentrations of GIP_{1-42} or $GIP_{7-30NH2}$ for 60 minutes, prior to acid stripping and surface expression determination. Data represent mean $\pm$ S.E.M.; n = 4. Refer to Method section 2.9 for more details.

3.2.3.2 Role of Signal Transduction in GIP Receptor Internalization

Elucidation of the pathways necessary for internalization required various pharmacological inhibitors. Hypertonic sucrose has been used to block clathrin-coated pit-mediated endocytosis, as has concanavalin A (a glycoprotein binding lectin) [385]. Treatment of wtGIPR cells with 0.5 M sucrose and 100 nM GIP time dependently increased surface receptor binding (47.6 ± 7.3% at 60 min); this was not due to sucrose alone, as all cells were treated with sucrose for the duration of the experiment, and GIP was added at the various time-points (Figure 16). It was hypothesized that GIP was stimulating a receptor recycling pathway, hence monensin, an inhibitor of vesicular transport acting to increase intravesicular pH [386; 387], was inlcuded in conjunction with sucrose and GIP, and reversed the increase in surface binding (Figure 16). In contrast, when cells were treated with just monensin and GIP, the degree of receptor internalization was not significantly different from cells treated with GIP alone (60 min GIP treatment: 39.8 ± 2.4% versus GIP/monensin treatment: 34.8 ± 9.5% loss of surface binding), suggesting GIP stimulation of the endosomal recycling pathway is very minor (Figure 16). Preliminary experiments indicated that treatment of cells with concanavalin A also blocked GIP receptor internalization (data not shown).

While both GIP receptor agonists and antagonists were able to cause receptor internalization, the role of receptor signalling was probed using cyclic AMP pathway activators and blockers, as well as phospholipase C/protein kinase C modulators. Table 4 shows the effect of these inhibitors on basal,1 nM and 100 nM GIP-stimulated cAMP production; the 1 nM concentration was chosen to establish if the agents had an effect on the GIP concentration-response curve, and 100 nM to compare to the results of the internalization studies. A 45 minute treatment of cells with adenylyl cyclase inhibitors (MDL-12,330 and 2',5'dideoxyadenosine, DDA), a protein kinase A blocker (H89), or an activator (phorbolmyristic acid) or inhibitor (staurosporine) of protein kinase C, had no measurable effect on basal cAMP levels in wtGIPR cells. Only the

83

adenylyl cyclase activator, forskolin, was able to increase cAMP on its own (Table 4). Protein kinase A and C appeared not to affect GIP-stimulated cAMP greatly, but PMA was able to double the cAMP response to 100 nM GIP. Adenylyl cyclase inhibitors were able to significantly reduce both 1 nM and 100 nM GIP-stimulated cAMP formation, although inhibition ranged between 22 and 60%. 10 µM forskolin is often used as an agent to demonstrate maximal cyclic AMP production. Here, 1 nM or 100 nM GIP combined with 10 µM forskolin, more than doubled the cAMP response to forskolin alone, and the two agents were not acting in an additive manner, but rather synergistically (Table 4).

Table 4: Effect of signal transduction cascade activators/inhibitors on basal and GIP-stimulated cAMP accumulation in wtGIPR cells

Cells were treated with pharmacological agents 15 min prior to addition of GIP. Peptide stimulation for 30 minutes followed; data are expressed as picomoles cyclic AMP/well (* = $P <$ 0.05; $n \geq 3$, shown in brackets).

	Basal	1 nM GIP	100 nM
Control[a]	1.67 ± 0.20 (12)	65.0 ± 10.5 (6)	105.6 ± 5.8 (6)
100 µM MDL-12,330	1.01 ± 0.20 (3)	26.4 ± 2.7* (3)	79.2 ± 7.5* (3)
100 µM 2',5' DDA	1.12 ± 0.13 (3)	50.5 ± 4.7* (3)	76.5 ± 7.7* (3)
10 µM Forskolin	246.0 ± 51.1* (3)	531.9 ± 28.3* (3)	558.4 ± 64.9* (3)
5 µM H89	1.55 ± 0.21 (5)	74.1 ± 5.2 (5)	122.6 ± 8.5 (5)
400 nM PMA	1.73 ± 0.66 (3)	57.4 ± 10.3 (3)	201.4 ± 12.7* (3)
100 nM Staurosporine	1.40 ± 0.21 (3)	70.1 ± 5.2 (3)	117.5 ± 5.1 (3)

All measurements were made in the presence of 0.5 mM IBMX, a concentration that completely blocks phosphodiesterase activity, thus values represent cAMP production over the 30 minute stimulation period.

[a]: For comparison, control values without IBMX were 0.49 ± 0.01 (basal), 20.4 ± 6.9 (1 nM GIP) and 60.5 ± 1.3 (100 nM GIP), n = 3.

Table 5: Effect of signal transduction cascade activators/inhibitors on GIP receptor expression and internalization in wtGIPR cells

Cells were treated with pharmacological agents 15 min prior to addition of GIP. Stimulation for 30 minutes followed; data are expressed as % control receptor expression (* = P < 0.05; n = 4-6). The % loss of surface binding is shown in brackets versus appropriate control.

Agent:	45 min Agent Alone	30 min 100 nM GIP	Agent + GIP
100 μM MDL-12,330	8.2 ± 0.8*	78.9 ± 3.7 (21.1)	15.9 ± 0.6* (84.1[a])
100 μM 2',5' DDA	75.5 ± 2.4*	79.2 ± 3.4 (20.8)	70.6 ± 2.5* (29.4[a])
500 μM IBMX	105.8 ± 2.7	69.9 ± 0.8 (30.1)	78.9 ± 4.3 (26.9)
10 μM Forskolin	103.9 ± 5.4	74.5 ± 3.3 (25.5)	78.6 ± 4.0 (25.3)
5 μM H89	97.4 ± 2.1	73.9 ± 2.5 (26.1)	77.6 ± 1.8 (19.8)
400 nM PMA	74.6 ± 4.9*	71.1 ± 0.8 (28.9)	63.8 ± 2.8* (36.2[a])
100 nM Staurosporine	112.4 ± 1.8*	78.7 ± 1.7 (21.3)	82.3 ± 4.4 (17.7[a])

All measurements were made in the absence of 0.5 mM IBMX, except where noted.

[a]: Agent alone caused changes in receptor expression; internalization difference is versus control without agent.

Effect of pharmacological agents on receptor expression and sequestration followed a similar protocol to that employed for examining effects of agents on basal and GIP-stimulated cAMP production. Briefly, experiments consisted of four study groups: (1) control surface expression (*i.e.* untreated cells), which was used to normalize other data, (2) cells treated with 100 nM GIP for 30 min, *i.e.* "control internalized", (3) cells treated with pharmacogical agent for 45 minutes to see the effect of the agent on receptor expression alone, and (4) cells treated with agent for 45 minutes and with GIP for 30 min (*i.e.* GIP added 15 min after agent), to see the effect of the agent on GIP-stimulated receptor endocytosis. In all four groups, cells were acid stripped and surface receptor binding measured as described in Methods section 2.9. Cyclic AMP raising agents, IBMX and forskolin, alone appeared to slightly (but not significantly) increase cell surface binding but, in combination with GIP, did not affect the degree of receptor internalization after 30 min (~25-30%; Table 5). In contrast, when cells were treated with inhibitors of adenylyl cyclase alone, GIP receptor surface expression was dramatically reduced (MDL-12,330: 91.2 ± 0.8% reduction; 2',5'-DDA: 24.5 ± 2.4% reduction). When GIP was administered in combination with adenylyl cyclase inhibitors, it did not produce a greater effect, however, as the inhibitors had effects of their own, it makes interpretation of these data very difficult (Table 5).

85

These data may suggest that adenylyl cyclase inhibitors may also be able to stimulate sequestration of the enzyme, and that the enzyme is in close proximity with the GIP receptor, so that they are co-internalized, or alternatively, this result may be an artifact of receptor overexpression in these cells. PKA inhibition did not alter surface receptor expression alone, and did not affect GIP-stimulated receptor endocytosis (Table 5). Activation of PKC with phorbol esters alone caused a 25.4 ± 4.9% reduction in surface receptor expression, and in combination with GIP, yielded a 36.2 ± 2.8% loss (P < 0.05; Table 5), indicating PKC is able to stimulate receptor internalization, and is additive with that stimulated by GIP. PKC inhibition with staurosporine, however, did not alter the degree of loss stimulated by GIP (GIP control: 21.3 ± 1.7%; GIP + staurosporine: 17.7 ± 4.4%); staurosporine alone appeared to moderately increase surface receptor expression (12.4 ± 1.8%). Together, these results indicate that PKC can be a negative modulator of GIP receptor expression, and when activated by other pathways, can contribute to GIP-stimulated receptor endocytosis. A short study was undertaken to characterize ligand-independent GIP receptor internalization further. Internalization time-courses and dose-response relationships for MDL-12330 and PMA are shown in Figure 17. MDL treatment resulted in a rapid internalization profile that reached a nadir between 25 and 60 min; the effect of PMA was latent and much less pronounced, and did not significantly reduce surface receptor expression until 45-60 min of treatment. Both drugs appeared to have concentration dependent effects, with PMA causing significant internalization at 4 nM, and MDL at 10 µM (Figure 17).
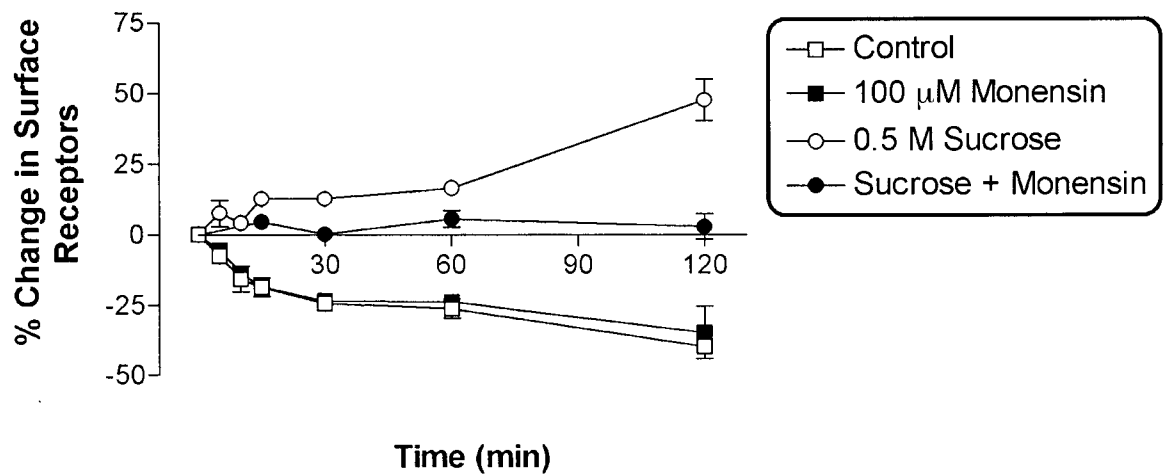
Figure 16: Effect of sucrose and monensin on receptor internalization in wtGIPR cells

Cells were pretreated with 0.5 M sucrose or 100 µM monensin 15 minutes prior to addition of GIP. The experiment was designed such that sucrose and/or monensin were present with the cells for the duration of the experiment, and the only variable was time exposed to GIP; control cells are treated with GIP alone (in the absence of sucrose or monensin). Cells were acid stripped and cell surface receptor expression was estimated by radioligand binding (see Methods 2.9). Data represent mean ± S.E.M.; n = 3-4.
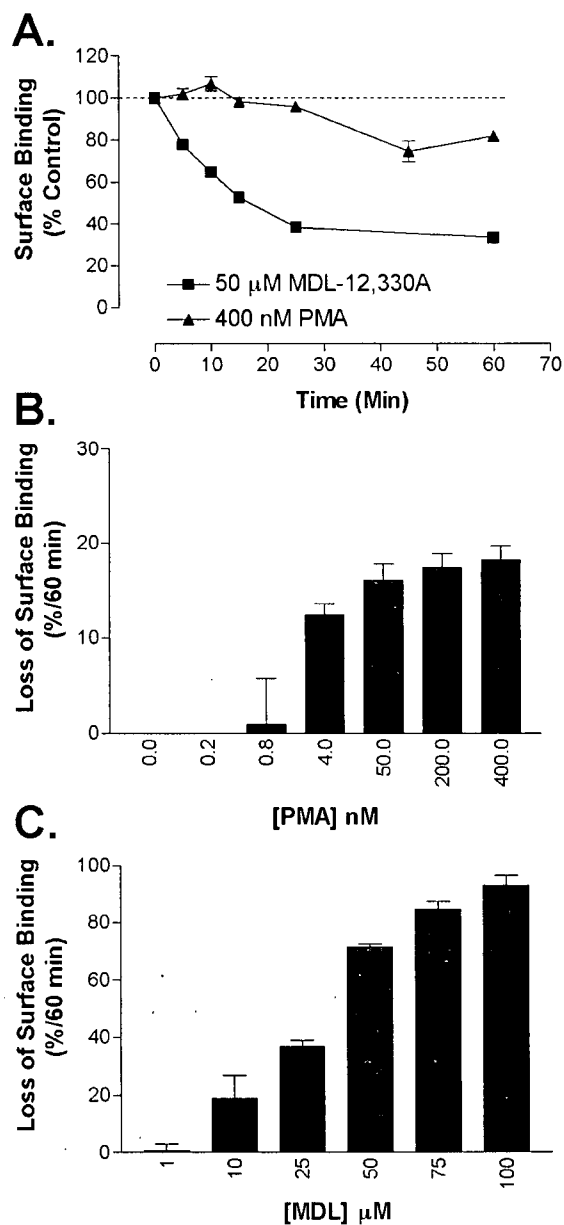
Figure 17: Ligand-independent GIP receptor internalization
Wild type GIPR cells were treated with adenylyl cyclase inhibitor (MDL-12,330A) or protein kinase C activator (PMA) for various times (A), or with increasing concentrations of MDL-12,330 (B) or PMA (C) for 60 min. Cells were acid stripped and cell surface receptor expression was estimated by radioligand binding (for more detail see Methods section 2.9). Data represent mean ± S.E.M.; n = 3-4.

3.2.3.3 Role of GRK-2 in GIP Receptor Expression, Signalling and Internalization

One of the initial goals of this thesis was to establish the role of G-protein receptor kinases in receptor desensitization and internalization. However, before work was fully initiated, Tseng and Zhang [372] published a report of GRK-2, -5 and -6 effects on the GIP receptor. As constructs for all GRKs had already been kindly provided by Dr. R. J. Lefkowitz (Duke University, North Carolina), we sought to independently retest the role of GRK-2 in modulation of the GIP receptor. Transient transfection of CHO-K1 cells with 3 μg pGIPR with 7 μg "empty vector" pcDNA3 (*i.e.* 10 μg total plasmid DNA) resulted in a similar expression level to that observed in wtGIPR cells, however, co-transfection of 3 μg pGIPR with 7 μg pGRK-2 (*i.e.* 10 μg total plasmid DNA) resulted in only 55.7 $\pm$ 2.6% of the expression level seen in control cells ($P < 0.05$; Figure 18A), but did not change receptor binding affinity. Cells transfected with 10 μg pGIPR/pcNDA3 or 10 μg pGIPR/pGRK-2 had identical transfection efficiencies (~40-45%). Examination of cAMP concentration-response curves in the same cells similarly indicated maximal GIP-stimulated cAMP production was only 58.6 $\pm$ 2.4% that observed in controls ($P < 0.05$), without affecting the EC_{50} value (~260 pM; Figure 18B). As cyclic AMP is proportional to receptor expression level (cf. Figures 9 and 23), it is difficult to convincingly state that GRK-2 affected GIP receptor signalling independently, although it may have reduced receptor signalling by causing a reduction in receptor expression. When GRK-2 was co-transfected with the GIP receptor, it appeared to augment the internalization stimulated by GIP in control cells (Figure 18C). Control experiments indicated that receptor expression level did not affect internalization kinetics if B_0 was between 2 and 10 Kcpm (data not shown), suggesting that the effect of GRK-2 on GIP receptor internalization was not an artifact of the reduced surface expression observed in co-transfected cells. At 60 min of 100 nM GIP treatment, in control cells there was a 30.6 $\pm$ 1.4% loss in surface binding, whereas in GIPR/GRK-2 transfected cells, 49.4 $\pm$ 2.8% of surface binding was lost at the same time-point ($P < 0.05$).
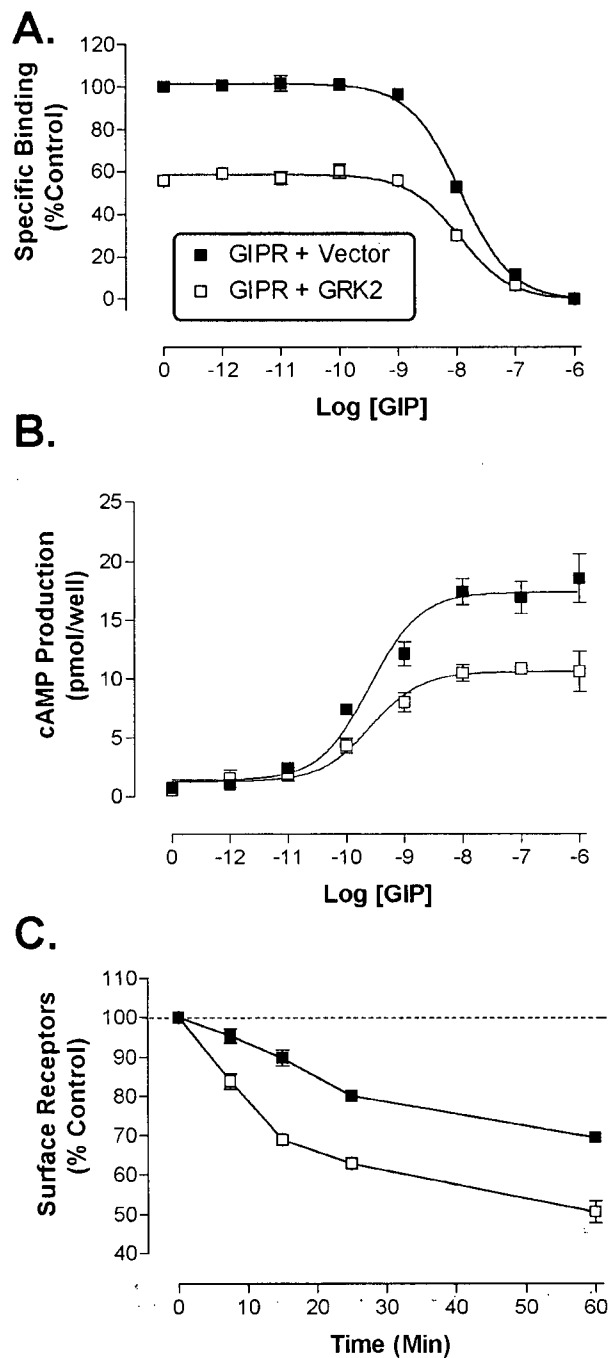
Figure 18: Effect of co-transfection of the GIP receptor with GRK-2

CHO-K1 cells were transiently transfected with 3 µg pGIPR and 7 µg empty vector or 7 µg pGRK-2. (A) Competitive-binding displacement curves. (B) Cyclic AMP concentration-response curves. (C) Receptor internalization time-course. Data represent mean ± S.E.M.; n = 3-4. Refer to methods sections 2.2, 2.3, 2.6, 2.7 and 2.9.

3.2.3.4 Effect of C-Terminal Serine Mutation on GIP Receptor Binding, Signalling and

Internalization

A series of 8 receptor mutants were generated with point mutations in the intracellular carboxyl terminal tail of the GIPR (cf. Figure 2 and Methods section 2.2); most mutations were single serine to alanine substitution (S398A; S406A; S426A; S427A; S440A; S453A). During preparation of our manuscript [290], describing these mutants, as well as a double mutant (S426/427A) and a complete serine knockout (S398/406/426/427/440/453A), Tseng and Zhang [291] also reported a receptor mutant with a S406A substitution, and additionally GIP receptor mutants C411G and C411A. Thus we also generated a receptor construct with a C411A mutation, as this mutant was reported to affect receptor desensitization and down-regulation. Screening of all mutant receptors for cyclic AMP production indicated that the C-terminal mutations had no overt effects on GIP receptor signalling, when stably transfected in CHO-K1 cells (Figure 19) or transiently transfected in COS-7 cells [290]. Results were corroborated by the similar binding affinities and expression levels for all mutant receptors in CHO-K1 stable lines (Figure 20, Table 6). When examining receptor internalization time-course experiments, the receptor mutants could be divided into two groups: those that showed no difference in sequestration kinetics (Figure 21A: S398A, S406A, C411A, S453A), and those that showed significant reductions in internalization rate and/or maximum internalization (Figure 21B: S426A, S427A, S440A, S426/427A, S398/406/426/427/440/453A). Quantitative analysis of receptor internalization is reported in Table 6.

Table 6: Binding and internalization characteristics of CHO-K1 cells stably transfected with GIP receptor C-terminal serine mutants

Construct:	IC_{50} (nM)	Bmax (%wt)	Initial Internalization Rate (%/15 min)	Maximum Internalization (%)
wtGIPR-455	2.88 ± 0.26	100	1.64 ± 0.17	36.4 ± 1.4
GIPR-S398A	2.75 ± 0.22	102 ± 10	1.60 ± 0.05	34.6 ± 2.3
GIPR-S406A	3.75 ± 0.37	89 ± 41	1.63 ± 0.06	36.5 ± 0.3
GIPR-C411A	2.41 ± 0.26	70 ± 16	1.70 ± 0.14	36.7 ± 3.0
GIPR-S426A	3.88 ± 0.67	106 ± 39	1.14 ± 0.09**	27.8 ± 1.0**
GIPR-S427A	4.21 ± 0.84	89 ± 45	1.22 ± 0.06*	30.7 ± 0.5*
GIPR-S440A	4.30 ± 0.92	80 ± 31	1.32 ± 0.06	30.0 ± 0.8*
GIPR-S453A	2.96 ± 0.30	73 ± 10	1.55 ± 0.12	34.6 ± 1.9
GIPR-S426/427A	4.25 ± 0.23	116 ± 7	1.19 ± 0.10*	30.1 ± 1.6*
GIPR-S398-453A	3.35 ± 0.20	164 ± 16	0.75 ± 0.08**	28.3 ± 1.0**

Data represent mean ± S.E.M. (n = 3-10). IC50 and Bmax values were not significantly different from wild type GIPR by ANOVA or Dunnet's t test. * and **, significant differences from wtGIPR, $p < 0.05$ and 0.01, respectively.
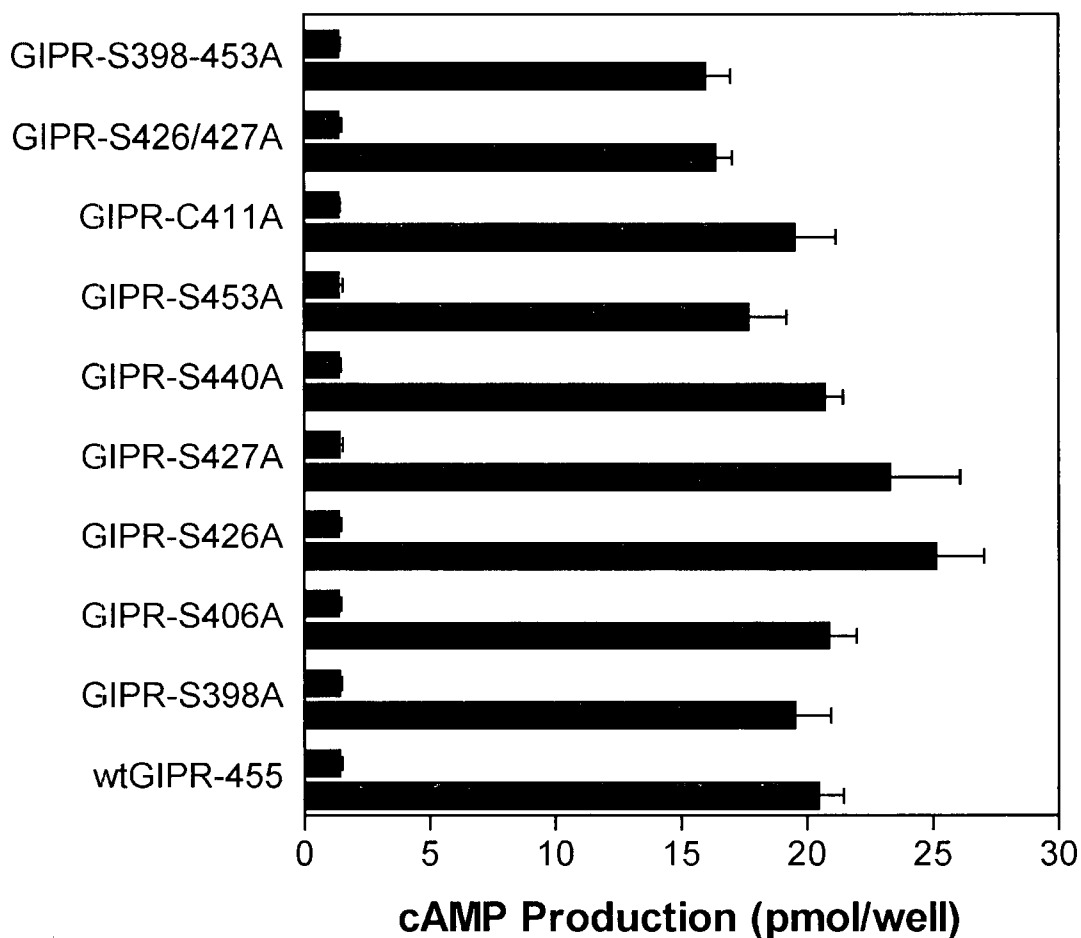
Figure 19: GIP-stimulated cAMP production in CT Ser to Ala substitution mutant receptors expressed in CHO-K1 cells

Basal and 10 nM GIP-stimulated cAMP accumulation was measured as per materials and methods. Data represent mean ± S.E.M.; n = 3-4; no significant differences could be measured. Refer to Methods sections 2.2, 2.3, and 2.7 for more details.
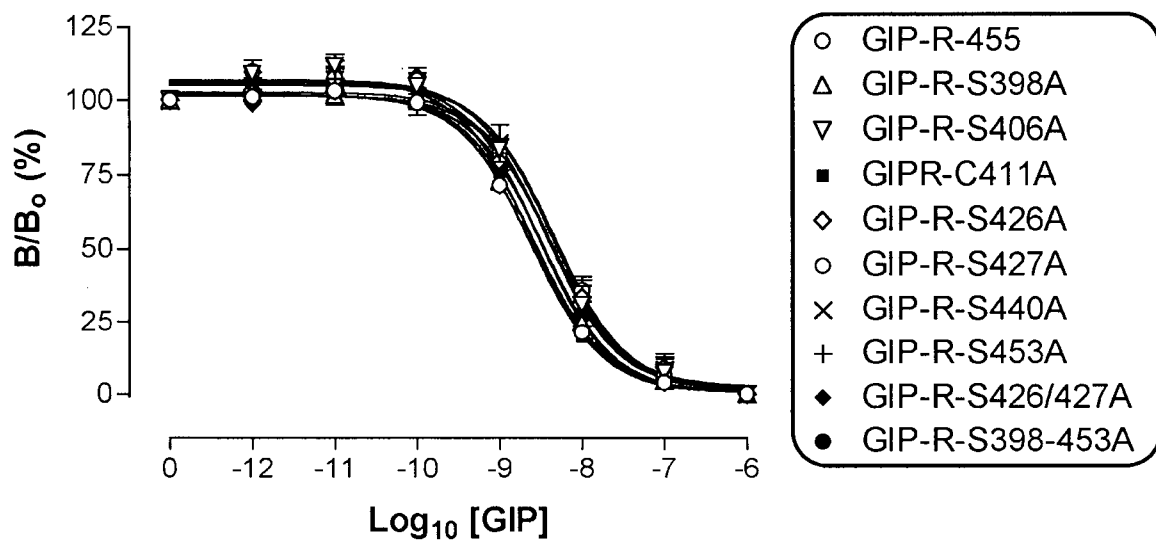
Figure 20: Competitive-binding studies on CHO-K1 cells stably transfected with C-terminal Ser to Ala mutant GIP receptors

Data represent mean ± S.E.M.; n = 3-10. Summary statistics are shown in Table 5. Refer to Methods sections 2.2, 2.3, and 2.6 for more details.
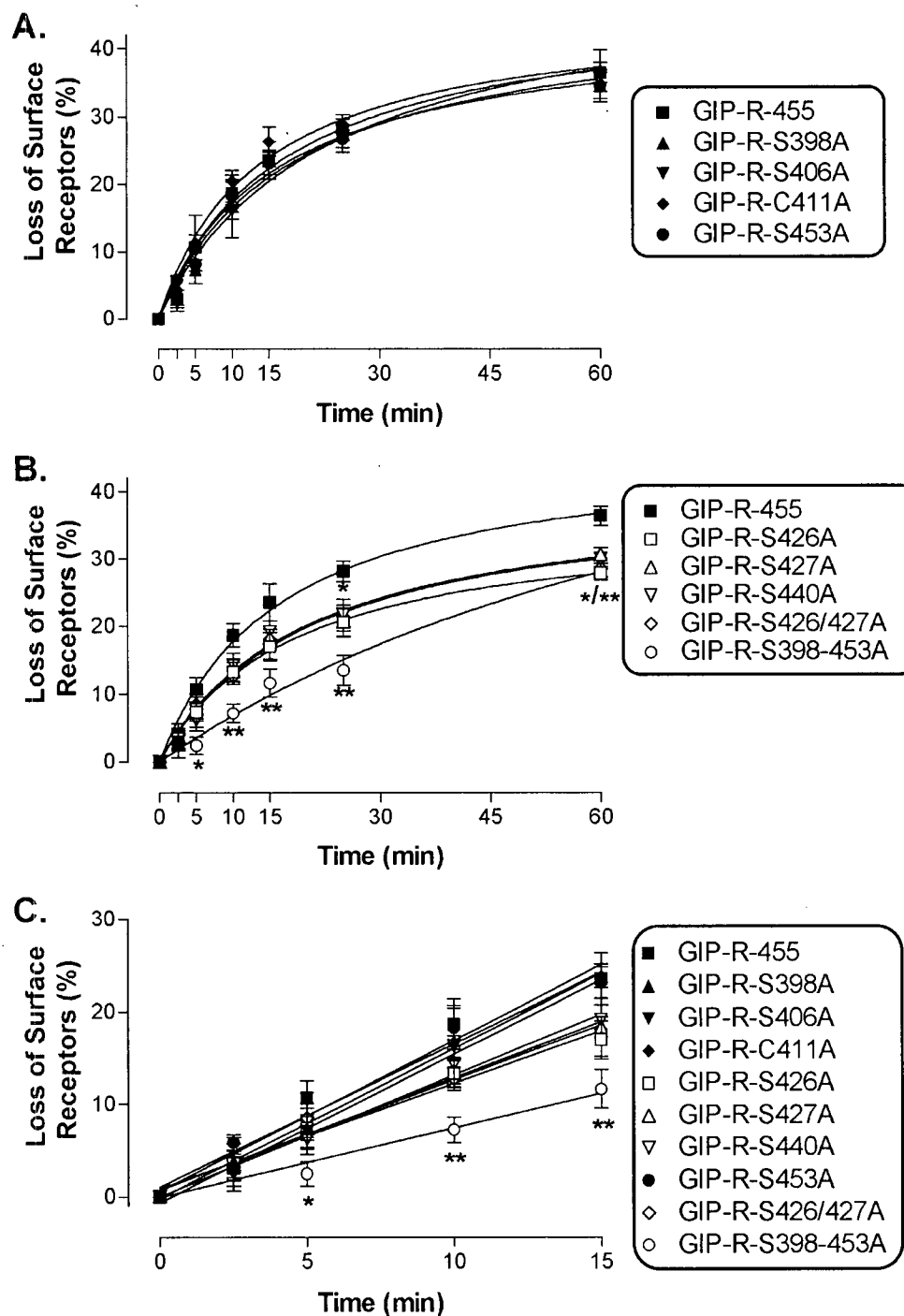
Figure 21: Internalization kinetics of C-terminal serine to alanine mutant receptors in transfected CHO-K1 cells

(A) Mutants not differing from the wild type GIP receptor. (B) Mutants showing altered internalization kinetics. (C) Examination of the first 15 min of internalization. Data represent mean ± S.E.M.; n = 3-10; * = $P < 0.05$, ** = $P < 0.01$. Refer to Methods sections 2.2, 2.3, and 2.8 for more details.

3.2.3.5 Internalization of GFP-tagged GIP Receptor

In an attempt to validate results obtained from radiometric analysis of GIP receptor internalization, a plasmid construct encoding a GIPR/GFP chimera was generated to allow internalization to be studied by fluorescent microscopy (refer to Methods section 2.2). Four stable transfected cell lines were used in the current set of experiments. Wild type GIP receptor expressing CHO-K1 cells (wtGIPR) were used for control purposes, in order to establish effects of adding GFP to the carboxyl terminus of the receptor on receptor expression, binding affinity, and signal transduction. Upon killing non-transfected cells with G418, isolated colonies of GIPR-GFP expressing cells arose, and were transferred to culture vessels for further characterization. One hundred lines were screened, and three were selected based on their expression level relative to wtGIPR cells: GIPR/GFP-1 (rGIPR/GFP-23S: 0.49 ± 0.12), GIPR/GFP-2 (rGIPR/GFP-8L: 0.68 ± 0.09) and GIPR/GFP-3 (rGIPR/GFP-20G: 2.41 ± 0.24). Hence, the GIPR/GFP chimera was still able to be expressed at comparable levels to the native receptor, and C-terminal extension did not prevent correct intracellular sorting of the receptor to the cell surface. Binding competition experiments similarly showed that binding affinity was not adversely affected by the large C-terminal addition (IC_{50} values: 3.21 ± 0.83 nM [wtGIPR], 4.21 ± 0.90 nM [GIPR-GFP-1], 3.79 ± 0.64 nM [GIPR-GFP-2], and 5.54 ± 1.30 nM [GIPR-GFP-3]) ($P > 0.05$; Figure 22).

Concentration-response curves of GIP_{1-42} on transfected cells, measuring cyclic AMP production over 30 minutes, indicated major differences between wild type and tagged receptors (Figure 23). Only GIPR-GFP-3 displayed similar sensitivity to GIP as the native receptor (EC_{50} values: 446 ± 80 pM versus 174 ± 45 pM, respectively; $P > 0.05$), however there was a proportional association between maximal cAMP production and expression level: wtGIPR (338.1 ± 39.1 fmol/1000 cells), GIPR-GFP-1 (43.0 ± 3.2 fmol/1000 cells), GIPR-GFP-2 (115.7 ± 6.7 fmol/1000 cells), GIPR-GFP-3 (288.7 ± 39.6 fmol/1000 cells); GIPR-GFP-1 and GIPR-GFP-

2 were significantly different from wtGIPR, P < 0.05. The sensitivities of the lower expressing tagged receptors was significantly right shifted (EC_{50} values: GIPR-GFP-1, 8.86 ± 1.88 nM, GIPR-GFP-2, 1.52 ± 0.20 nM; P < 0.05). Thus it appears that the GFP tag may have interfered with G-protein coupling to a degree, but this could be somewhat overcome by overexpression.

For GIPR-GFP cells, it was possible to examine receptor sequestration by two validated independent methods. The first method employed involved measurement of remaining surface binding following treatment with 100 nM GIP for various times, and a hypertonic acid wash. Using this method, it was readily apparent from the two higher expressing GIPR-GFP cell lines that receptor internalization kinetics were blunted (Figure 24A). At t=60 min, there was a 31.8 ± 0.8% reduction in wild type receptor surface binding, whereas GIPR-GFP-2 and GIPR-GFP-3 displayed reductions of 10.3 ± 2.6% and 11.1 ± 1.5%, respectively. The expression level of GIPR-GFP-1 was too low to permit measurement of internalization by this method with any sensitivity, and it appeared to not internalize at all (Figure 24A). The second method used to examine receptor endocytosis measured internalization of ^{125}I-GIP (acid resistant cell associated radioactivity). This method indicated that the acid stripping protocol used in all internalization studies was approximately 85-90% effective at removing surface bound ligand. As with the first method, GIPR-GFP transfected cells showed reduced sequestration kinetics. Acid resistant binding of wild-type receptors was 43.3 ± 1.6% (accounting for efficiency of the acid stripping protocol) after warming to 37°C for 60 min (Figure 24B). In contrast, the acid resistant binding of the three clones of GIPR-GFP cells at 60 min ranged between 26.7 and 29.0% (P < 0.05).

Despite the fact that alterations in signalling and sequestration were observed with GFP tagged receptors, studies were continued using fluorescence microscopy. In the non-stimulated state, all three cell lines transfected with GFP-tagged receptor showed diffuse apparent surface fluorescence, with micropili-like projections (Figure 25A); thus receptors were appropriately processed and sorted to the cell surface. Most cells appeared to have normal morphology to non-

97

transfected CHO-K1 cells (≥ 95% fibroblast-like). Upon stimulation for 60 min with 100 nM GIP, the fluorescence appeared to redistribute: surface fluorescence was less intense, and punctate peri-nuclear fluorescence was observed, characteristic of the endosomal degradation pathway (Figure 25B). In a small proportion of the cells (≤ 15%), changes in cell morphology were observed following treatment with GIP in addition to the redistribution of fluorescence.
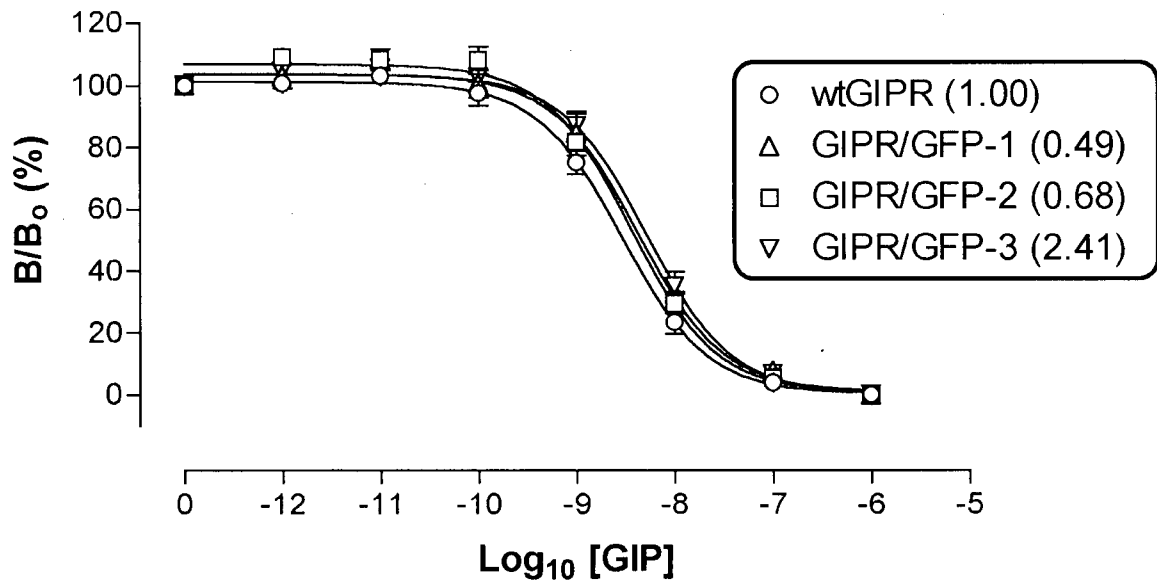
Figure 22: Binding competition experiments with C-terminal green fluorescent protein (GFP) tagged GIP receptors in transfected CHO-K1 cells
Three stable subclone cell lines were selected based on their surface expression level (in brackets) relative to wtGIPR cells. No significant difference was observed in IC_{50} values. Data are mean ± S.E.M. of 4-6 experiments. Refer to Methods sections 2.2, 2.3, and 2.6 for more details.
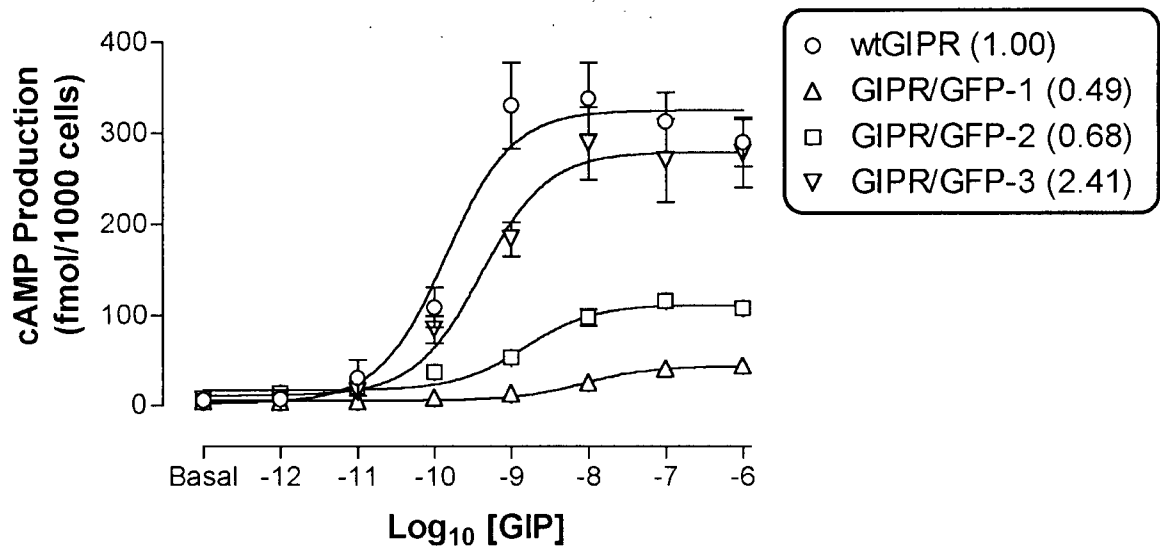
Figure 23: Cyclic AMP production by subclones of GIPR-GFP cell lines

Both GIPR-GFP-1 and GIPR-GFP-2 showed significant differences in maximal cAMP production and half-maximal activation statistics ($P < 0.05$). GIPR-GFP-3 showed slightly reduced maximal cAMP and right shifted receptor sensitivity to GIP, but these were not significantly changed from wtGIPR cells ($P > 0.05$). Data represent mean ± S.E.M.; $n \geq 3$. Refer to Methods sections 2.2, 2.3, and 2.7 for more details.

A.

Loss of Surface Receptors

B.

Internalized ^{125}I-GIP
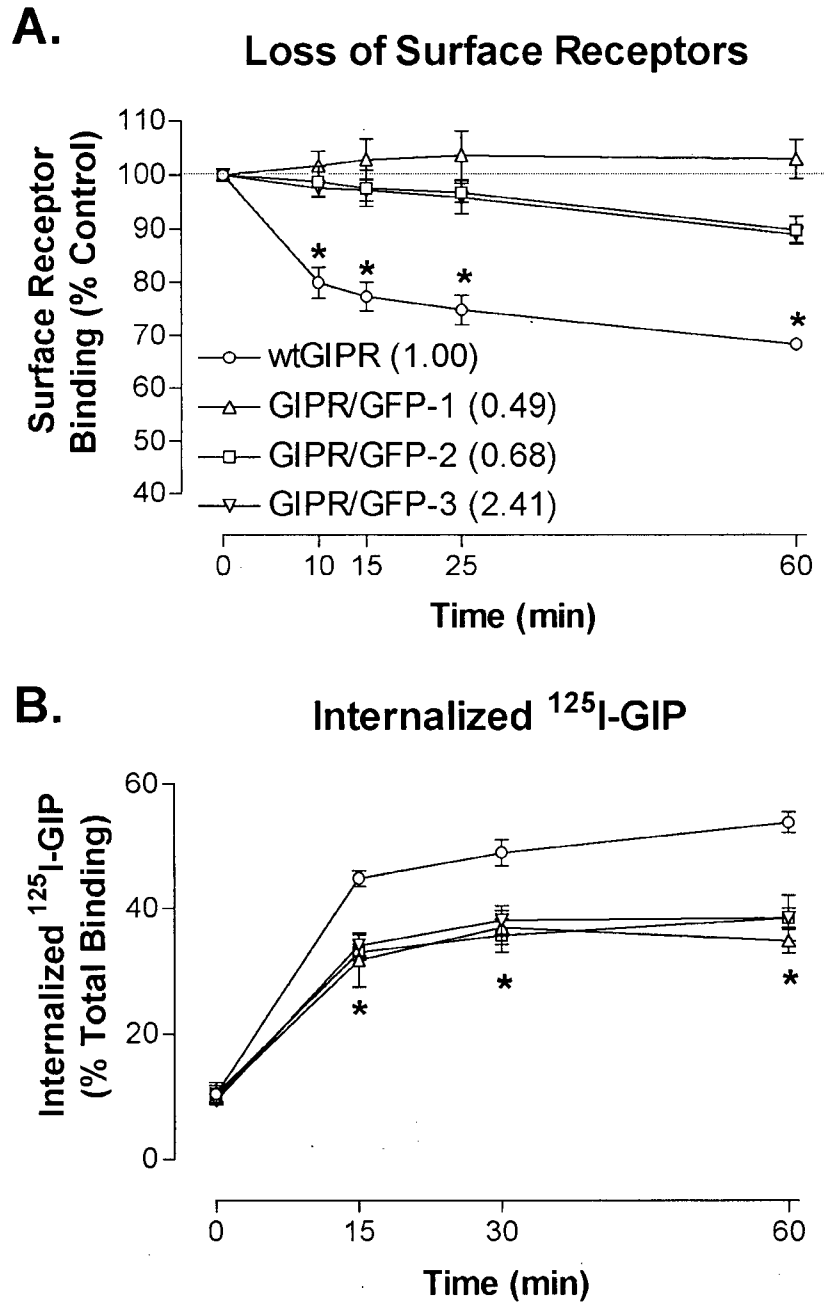
Figure 24: Internalization of GIPR-GFP in transfected CHO-K1 cells
(A) Loss of surface receptor expression on treatment with 100 nM GIP. (B) Internalization of ^{125}I-GIP versus time. Data represent mean ± S.E.M.; n = 4-8; * = P < 0.05. Refer to Methods sections 2.2, 2.3, and 2.8 for more details.
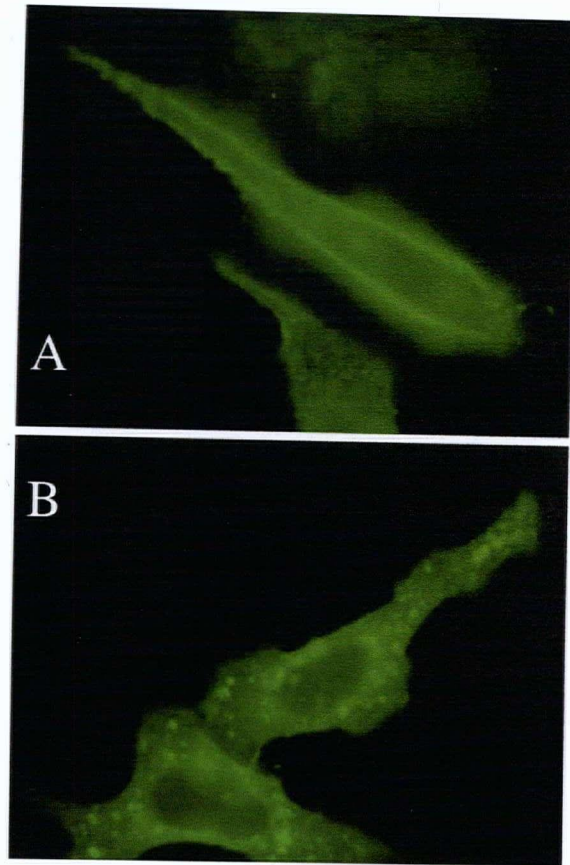
Figure 25: Fluorescence microscopy of GIPR-GFP distribution in transfected CHO-K1 cells

(A) Fixed control GIPR-GFP-3 cells in the unstimulated state. (B) GIPR-GFP-3 cells, fixed following 60 min with 100 nM GIP at 37°C. wtGIPR cells did not show specific fluorescence above autofluorescence level of non-transfected CHO-K1 cells. Figures are representative images of the entire cell populations observed in each case. Refer to Methods sections 2.2, 2.3, and 2.9 for more details.

3.2.3.6 Internalization of [Fluorescein-Trp[25]]GIP$_{1-30NH2}$ in wtGIPR cells

Although useful for fluorescence imaging, tagging the GIP receptor resulted in retarded internalization kinetics, thus an alternative approach was made to examine internalization by fluorescence, namely, conjugating fluorescein to tryptophane[25] of GIP. Competitive-binding inhibition experiments with GIP$_{1-30NH2}$ [n] and [Fluo-Trp[25]]GIP$_{1-30NH2}$ [f] versus ^{125}I-GIP$_{1-42}$ on wtGIPR cells showed similar IC$_{50}$ values (Figure 26A), with the fluorescent conjugate having slightly greater affinity: 1.68 ± 0.07 nM [n] and 1.14 ± 0.08 nM [f] ($P < 0.05$). Similarly, [Fluo-Trp[25]]GIP was slightly more potent than native GIP when examining maximal cAMP production (430.6 ± 52.5 and 390.4 ± 54.2 fmol/1000 cells, respectively; $P > 0.05$; Figure 26B), however, receptor sensitivity to these peptides was not different (EC$_{50}$ values: 101 ± 33 pM [n] and 104 ± 18 pM [f]). When measuring loss of GIP surface binding sites on wtGIPR cells on exposure to 100 nM GIP$_{1-30NH2}$ or fluorescein-conjugated peptide, the latter peptide caused significantly greater receptor internalization at all time-points used (Figure 27). At t = 60 min, wtGIPR cells exposed to [Fluo-Trp[25]]GIP had ~10% fewer binding sites remaining than those exposed to native GIP. Thus, it appears that [Fluo-Trp[25]]GIP suffers from the opposite problem to that observed with GIP-GFP receptors. Study of cells using [Fluo-Trp[25]]GIP by fluorescence microscopy was somewhat more difficult than anticipated. Photobleaching and weak fluorescence prevented the production of usable images with cells fixed after incubating for 60 min with 25-100 nM peptide either on ice or at 37°C (data not shown). However, use of a fluorescein amplification kit consisting of an anti-fluorescein antibody, an Alexafluor-488 conjugated secondary antibody, and permeabilized cells produced satisfactory images (Figure 28), although the signal-to-noise ratio appeared to be lower than that observed with GIPR-GFP cells. Incubation of cells with 25-100 nM [Fluo-Trp[25]]GIP at 37°C indicated primarily intracellular fluorescence in the area around the nucleus (Figure 28B), whereas fluorescence of control cells with the same procedure at 4°C appeared to be mainly on the cell surface (Figure

28A). As with studies using GIPR/GFP, to definitively establish the location cellular

fluorescence, confocal microscopy would have to be performed.
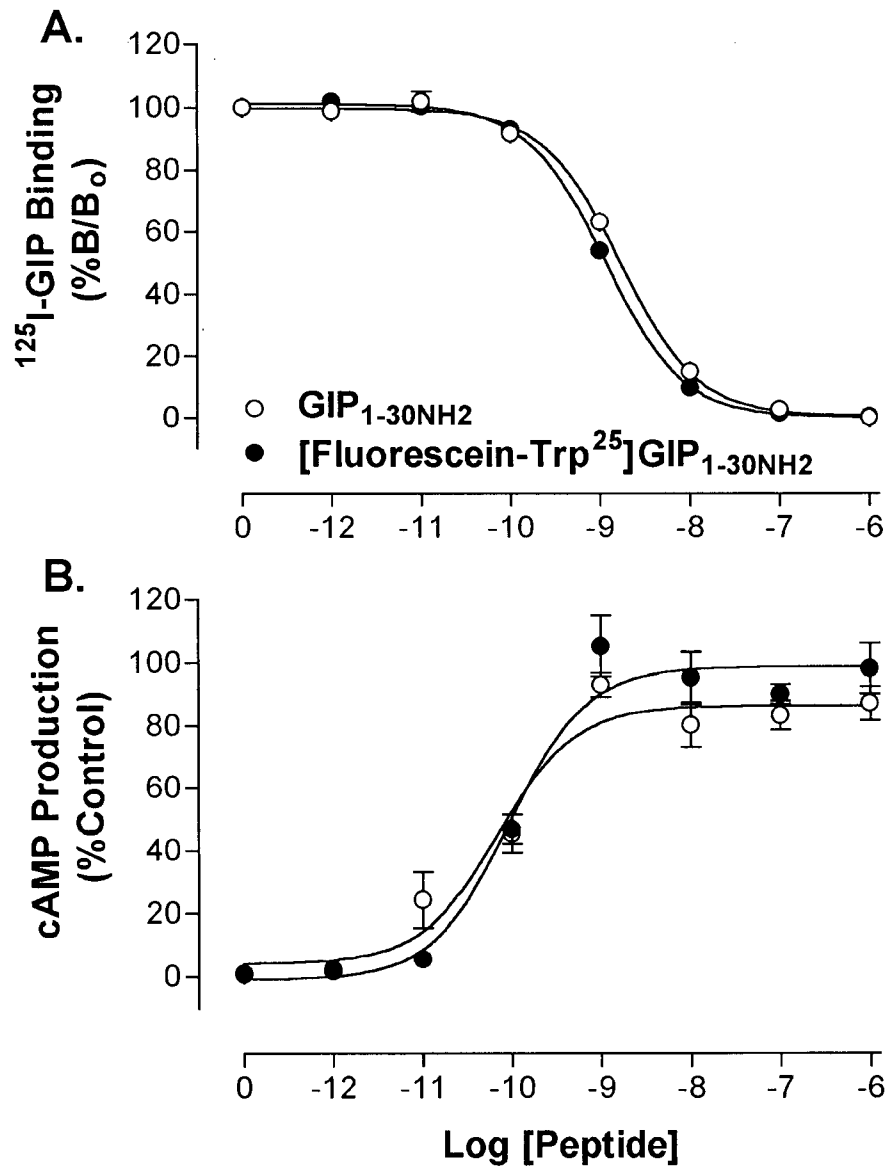
Figure 26: Binding and cAMP production of fluorescein-conjugated GIP
(A) Competitive-binding inhibition of ^{125}I-GIP$_{1-42}$ on wtGIPR cells incubated with increasing concentrations of GIP$_{1-30NH2}$ or [Fluo-Trp^{25}]GIP$_{1-30NH2}$. (B) Cyclic AMP accumulation in wtGIPR cells incubated with GIP$_{1-30NH2}$ or [Fluo-Trp^{25}]GIP$_{1-30NH2}$. Data represent mean ± S.E.M. of 4-6 experiments. Refer to Methods sections 2.2, 2.3, 2.4, 2.6 and 2.7 for more details.
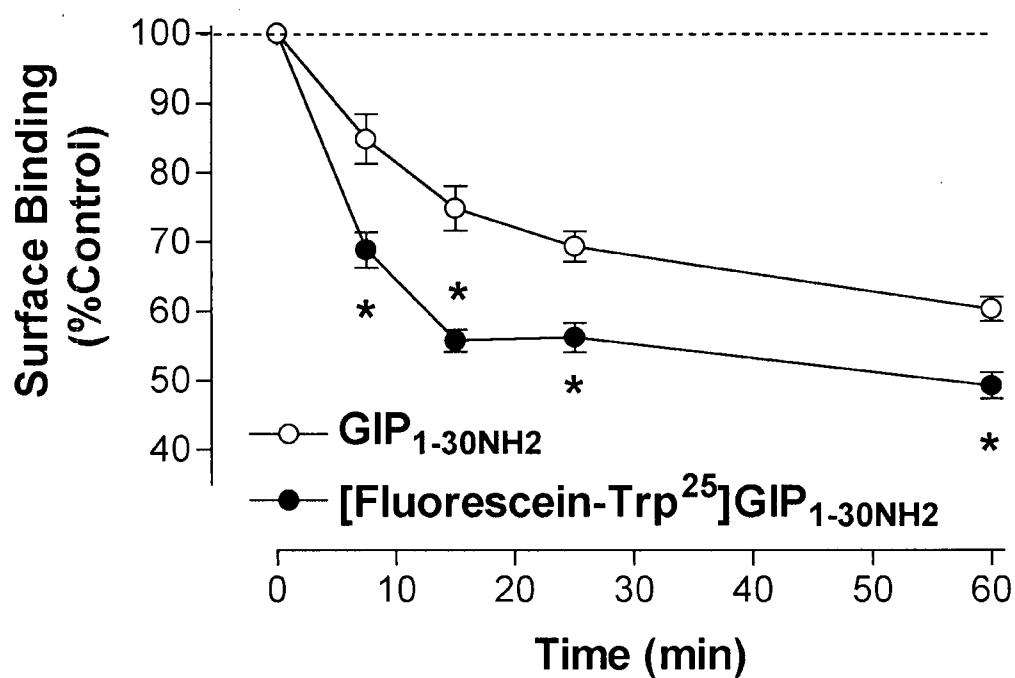
Figure 27: Loss of wtGIPR binding sites on incubation with [Fluo-Trp^{25}]GIP

Cells were incubated with 100 nM GIP$_{1\text{-}30NH2}$ or fluorescein-conjugated equivalent for various times at 37°C. Non-internalized surface bound peptide was stripped with low pH hypertonic saline, and remaining surface receptors estimated by radioligand binding. Data represent mean ± S.E.M. of 6 experiments. Refer to Method section 2.8 for more details.
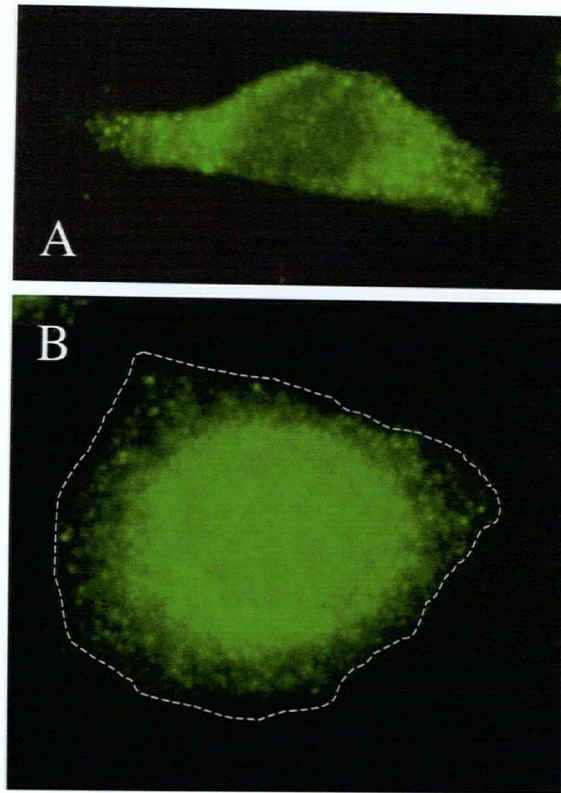
Figure 28: Fluorescence microscopy of wtGIPR cells incubated with [Fluo-Trp^{25}]GIP
(A) Cells incubated with 25-100 nM peptide on ice for 60 min, prior to washing, fixing, and treatment with fluorescein amplification kit, as per text. (B) The same protocol as in (A), but performed at 37°C. The dashed line indicates the cell perimeter. Figures are representative images of the entire cell populations observed in each case. Refer to Method section 2.9 for more details.

3.3 Discussion

3.3.1 Insulinoma Cell Desensitization

In order to understand the basis of desensitization more clearly at the level of intracellular signalling cascades, the βTC-3 insulinoma cell line was employed. The effect of glucose on homologous desensitization of β-cells to GIP was studied with respect to cyclic AMP production, and the subsequent effect, insulin release. In contrast to previous work on transformed β-cells [176; 177], βTC-3 cells exhibited GIP-concentration dependent effects on cAMP production in the absence of glucose, as well as at physiological glycemic levels (Figure 5). Glucose alone appeared to have very mild effects on cyclic AMP production, slightly reducing cellular responsiveness to GIP with increasing glucose. Prior work on glucose dependence of incretin-stimulated cAMP in transformed cells found that neither GLP-1 nor GIP could elevate intracellular cAMP in the absence of glucose, while forskolin stimulated cAMP production was unaffected [176; 177]. The apparent conflict between the glucose dependence of the cyclic AMP data from HIT, RIN and βTC beta cell models may be species dependent and will likely be clarified by similar experiments on alternative insulinoma cells [327] or purified β-cells [224], although previously glucose-independent GIP-stimulated cAMP has been shown to occur in human insulinoma tissue [182]. Regardless, the necessity for the presence of glucose for GIP to potentiate insulin release was observed in βTC-3 cells (Figure 7), indicating that the glucose-dependency of GIP was intact.

Homologous desensitization of GIP mediated effects was first described by Fehmann and Habener [177]. In their study, only effects of GIP pretreatment on insulin release from HIT cells were examined, not second messenger cascades. Desensitization of GIP-stimulated cAMP production in βTC-3 cells resulting from GIP pretreatment was at best moderate (Figure 5). The magnitude of the desensitized response was similar under all glycemic conditions although, due to the slight inhibitory effect of glucose on GIP-stimulated cAMP formation, the desensitization

appears to be greater in the absence of glucose. Using an identical protocol, the degree of desensitization observed in the absence of glucose corresponds well with that observed in non-glucose sensitive CHO-K1 cells transfected with the pancreatic GIP receptor (cf. Figures 5 and 9, and Figures 6A and 11B). However, the time-course of GIP receptor desensitization (Figures 6A and 11B) does not match the rapid potent desensitization that the GLP-1 receptor underwent in HIT-T15 cells, using a very similar protocol [177].

In order to elucidate the point in the signal transduction cascade at which desensitization of the cAMP response to GIP was occurring, various inhibitors were used (Figure 6). The apparent reduction in cAMP produced after GIP pretreatment could be explained by degradation of extracellular ligand, activation of pertussis-sensitive G-proteins, modulation of adenylyl cyclase or phosphodiesterase (PDE) activity, or negative feedback by signal transduction kinases (PKC and PKA). Inhibition of DPIV, the primary enzyme responsible for degradation of GIP *in vivo* [59], had no effect on GIP-stimulated cAMP levels or desensitization; neither did pertussis toxin. GIP pretreatment reduced only GIP-stimulated cAMP production, not forskolin-stimulated cAMP production, suggesting that adenylyl cyclase activity was unaffected by GIP pretreatment. Furthermore, PDE sensitivity to IBMX was unchanged in the desensitized state, ruling out an increase in PDE activity resulting in a reduction of intracellular cAMP. Staurosporine did affect basal and GIP-stimulated cAMP accumulation in control cells, indicating that PKC probably has a role in regulating normal β-cell responsiveness to GIP, but did not affect homologous desensitization to GIP. PKA inhibition affected neither responsiveness nor desensitization of βTC-3 cells to GIP. These results, taken together, suggest that homologous desensitization of GIP-stimulated cAMP formation occurs at the receptor level, and may involve mechanisms such as RGS (regulators of G protein signalling) proteins [371], GRK-2 [372], receptor sequestration [290], or unidentified processes.

Both glucose and GIP produced similar changes in insulin release from βTC-3 cells to those previously published [178]. Parallel experiments on desensitization of insulin release showed that the same protocol used for the cAMP studies yielded a significant reduction in insulin release. Pretreatment of cells with GIP dramatically returned 10 nM GIP-stimulated insulin to basal levels in either 5.5 and 11 mM glucose conditions. It would be difficult to attribute the dramatic alteration in insulin release to the mild attenuation of GIP-stimulated cAMP by GIP pretreatment, possibly implicating desensitization of distal steps in the stimulus-exocytosis coupling cascade. This hypothesis is supported by similar experiments utilizing forskolin. Forskolin potentiates glucose-induced insulin release via direct activation of adenylyl cyclase and cyclic AMP production. In contrast to GIP-stimulated cAMP production, pretreatment with GIP had no effect on forskolin-stimulated cAMP accumulation (Table 3). Nevertheless, GIP pretreatment significantly blunted forskolin-mediated insulin release to near basal levels (Figure 7). GIP has been found to augment depolarization-induced exocytosis from individual mouse β-cells via a protein kinase A (PKA)-dependent mechanism [190]. Consistent with results using cyclic AMP analogues and forskolin, GIP exerts its action on exocytosis at a level distal to elevation in intracellular calcium via PKA [190; 388]. Evidence also exists that cyclic AMP interacts directly with the secretory machinery, sensitizing it to $[Ca^{2+}]_i$ [388; 389]. Modulation of kinases activated by GIP [293; 298-300] or any element of the stimulus-secretion machinery by these kinases, or other uncharacterized mediators of GIP effects could account for the profound effect of GIP prestimulation on both GIP and forskolin-stimulated insulin responses. Indeed, the related incretin hormone, GLP-1, has been implicated in the tyrosine phosphorylation of several proteins, one of which was identified as the synaptic-associated protein of 25 kDa (SNAP-25) [390], supporting the notion of direct modulation of the exocytotic machinery. Further support of this hypothesis is the recent finding that chronic 9 hour pretreatment of INS-1 cells with GIP also blunted glucose induced insulin release [383].

Insulin release from βTC-3 cells was reported to be reduced by 42-55% by a 10 min exposure to 100 nM GIP preincubation, followed by a 10 min washout period [371]. While desensitization of GIP-stimulated cAMP production in βTC-3 cells was not demonstrated in this report, it was shown that GIP induced an increase in the steady-state level of RGS2 mRNA and that transfection of βTC-3 cells with RGS2 attenuated GIP-stimulated but not glucose-stimulated insulin release [371]; further, Tseng and Zhang presented evidence that RGS2 was capable of co-precipitating with $G\alpha_s$ from transfected cells *in vitro*. In a separate report, they also found evidence for expression of GRK-2 and β-arrestin-1 in βTC-3 cells, and that transfection of these proteins diminished GIP-stimulated insulin release [372]. The insulin data from those reports do not compare well with previous data on the same cells [178] or that presented here, likely because Tseng and Zhang used βTC-3 cells over the high passage range 62-70 [371; 372], for which insulin content and cell response to secretagogues have not been characterized. Lower passage ranges are generally preferable due to the well characterized decline in insulin content and glucose responsiveness over time in transformed β-cells [327]. RGS2 is ubiquitously expressed [391], and thus does represent a potential mechanism for βTC-3 desensitization to GIP, however, the increased rate of GTP hydrolysis by RGS proteins should in theory also affect cyclic AMP levels. As stated previously, the dramatic desensitization of the insulin response in βTC-3 cells (Figure 7) did not correlate well with homologous desensitization of cAMP responses to GIP in these cells (Figure 5 and 6). This is particularly important considering the 10 minute time-point of the cAMP desensitization time-course (Figure 6A), and the 10 min desensitization period reported by Tseng and Zhang [371] with respect to insulin. Another question is raised considering that RGS proteins were identified 20 years ago, and exhibit interactions with $G\alpha_i$ and $G\alpha_q$ strong enough to facilitate G-protein-RGS complex crystallography structure determinations, yet all attempts by those who have focused their

research on RGS proteins have failed to show any interaction with $G\alpha_s$ [349; 350; 391]. Nevertheless, reports have shown that specific $G\alpha_s$ RGS proteins exist [392], and also that RGS proteins may inhibit cAMP formation via direct interaction with adenylyl cyclase [393], rather than by accelerating G-protein GTP hydrolysis. Hence, GRK-2 and RGS2 attenuation of GIP signalling may be a feasible desensitization mechanism, however, given the points raised, independent duplication by other researchers should be done to validate these findings. It is likely that desensitization to GIP occurs at both proximal (receptor-effector) and distal (exocytotic machinery) stages of the stimulus secretion cascade.

3.3.2 Desensitization of Transfected Cells

Difficulties in development of a desensitization protocol for the transfected rat GIP receptor hampered early work on this subject. Once it was found that overexpression of the receptor artefactually prevented measurement of desensitization (Figure 9), specific studies could be performed. Some studies have used cyclic AMP accumulation time-course experiments as indicating desensitization, as cyclic AMP levels plateau (*e.g.* [358; 359]). Others have argued that the plateau may arise from overcoming the IBMX blockade of cAMP degradation by phosphodiesterase due to such high levels of cyclic nucleotide [394]. In the absence of IBMX a plateau was achieved, and cyclic AMP levels did not begin to return to basal values (Figure 10). Hence an equilibrium between GIP-stimulated cAMP production and PDE-mediated cAMP degradation was achieved, indicating that the GIP receptor is fairly resistant to desensitization (or the plateau would have declined towards basal levels), and this is not simply an artifact of overexpression. In the low expressing rGIPR-L2 cell line, which produces much lower maximal GIP-stimulated cAMP levels (Figure 9), time-course experiments on cAMP production also revealed a steady state cAMP level with time in the presence of IBMX (Figure 11A); as the cAMP content of these cells is much lower than wtGIPR cells, it is unlikely that the plateau

results from overcoming inhibition of PDE by IBMX. In cells pretreated with 100 nM GIP for 60 min prior to a cAMP accumulation time-course, a plateau was also achieved, except this time it was set at a lower level (Figure 11A). Thus it was shown that plateau steady-state cyclic AMP levels are not simply due to an equilibrium being achieved between phosphodiesterase, cAMP and IBMX, and that prolonged (chronic) stimulation induces a functionally distinct mode of desensitization from repetitive stimulation (Figures 10 and 11A). Notably, the desensitization observed in all experiments in transfected CHO-K1 cells (Figures 10 and 11) also indicated that the GIP receptor is relatively resistant to desensitization, and data compares well with the desensitization observed in βTC-3 cells (Figures 5 and 6).

The first study of GIP receptor desensitization in transfected cells was published in 1996 [369]. In this report, a reporter cell line driving expression of β-galactosidase with a cyclic AMP response element (CRE) containing promoter, transfected with the GIP receptor (LGIPR2) was used. Cells were cultured in the presence of 2 nM GIP for periods between 0 and 24 hours, and it was shown that cAMP-dependent β-galactosidase activity peaked with 4 hours of incubation, but then returned to near baseline within 16 to 24 hours [369]. Hence it was concluded that this represented a chronic desensitization of the receptor. As experiments in which cells were incubated with GIP were performed in the presence of 5% fetal bovine serum, it is likely that degradation of the ligand by serum proteases contributed a large degree towards the attenuation of the signal; cell culture medium and radioimmunoassay buffers containing serum products were shown to degrade GIP by DPIV-like activity *in vitro* [330]. Furthermore, enzyme protein turnover and stability were not considered. Given that cAMP accumulation time-courses presented here and elsewhere (cf. Introduction section 1.7) produce rapid peak responses, reaching a plateau between 15 and 30 min (Figures 10 and 11), the time-course of β-galactosidase activity as a reporter indicates that this method is invalid for examining desensitization.

In the current thesis, strong evidence is presented indicating receptor expression level is critical for demonstration of desensitization. In two prior papers reporting GIP receptor desensitization [291; 371], the authors reported a constant 45% transfection efficiency using 0.75 μg receptor plasmid with 4 μL Lipofectamine and cells in 12-well plates. Given the current results, and the fact that they were able to show desensitization, this transfection protocol must have yielded low level receptor expression. Binding studies were performed, which should have allowed comparison, however, the first step of the binding protocol they used involved detaching cells from culture vessels with trypsin, likely explaining the 10-fold right-shift in binding affinities published in the same report, as many trypsin consensus sites are present in the GIP receptor sequence [291]. Regardless, two desensitization protocols were used: a 24 hour 100 nM GIP preincubation [291] or a 10 min 100 nM GIP preincubtion [371], and in either case followed by a 10 min exposure to a range of GIP concentrations. Apparently, in both cases, this produced approximately a 90-95% reduction in GIP-stimulated cAMP formation in the pretreated cells. The cause of the disparate results from those reports, compared to the current thesis are unclear. While cell specific and/or methodological differences may be the root, GIP receptor desensitization in CHO-K1 cells (Figures 9 and 11) and HEK-293 cells (data not shown), was nearly identical to that observed in βTC-3 cells (Figures 5 and 6).

No studies of the mechanisms of desensitization were pursued in transfected cells in the current report (these were limited to βTC-3 cells), however, it was shown that removal of all potential phosphorylation sites in the C-terminal tail by site-directed mutagenesis completely blocked the desensitization of GIP-stimulated cAMP production in low-expressing cell lines with this construct (Figure 12). In the same set of experiments, the role of the serine doublet at amino acids 426 and 427 in homologous desensitization was assessed, as serine doublet phosphorylation is a well characterized regulatory mechanism for the GLP-1 receptor [366-368]. However, cells transfected with the GIPR-S426/427A mutant receptor desensitized identically to

112

control receptors (Figure 12). Taken together, the results implicate phosphorylation of specific C-terminal serine residues during homologous desensitization, however, apparently S426 and S427 are not involved. Tseng and Zhang [291] found that rat GIP receptors bearing a S406 mutations were slightly protected from chronic desensitization (~20% mutant response compared to ~5% wild type response when preincubated for 24 hours with 100 nM GIP). However, the prolonged treatment with GIP resulted in profound receptor downregulation – 30-32% of mutant receptor binding sites remained following the preincubation, compared to 13% for wild type receptors, so signalling was proportional to these values. These chronic experiments cannot really be compared to the acute signalling data presented here; thus phosphorylation of S406 alone or in combination of other residues (possibly not including S426 and S427) may mediate acute desensitization.

Co-transfection of GRK-2 or RGS2 blunted steady-state GIP-stimulated cyclic AMP in transfected cells [291; 372]. This is corroborated by a similar experiment shown for GRK-2 in Figure 18. It was reported that RGS co-transfection did not affect receptor expression [291], whereas GRK constructs were transfected into stable LGIPR2 cells with approximately 40% efficiency [372], but effects on receptor expression were not measured. As co-transfection with two plasmids theoretically gives proportional DNA:liposome complexes with a given transfection efficiency, all cells successfully transfected will contain both plasmids. When transfecting a stable cell line, where during the original transfection all non-transfected cells were killed by the selection agent, the second transient transfection can only co-express in the percentage of cells determined by transfection efficiency; the majority of cells secondarily transfected by this method will express only the first stably transfected plasmid. In preliminary experiments, transient transfection of wtGIPR cells with 10 µg GRK-2 produced only a minor effect (data not shown), relative to that observed when 3 µg of pGIPR was co-transfected with 7 µg pGRK-2 (Figure 18). Given that co-transfection of GIPR and GRK-2 resulted in diminished

113

surface expression, but with unchanged transfection efficiency, the reduced signalling observed here (Figure 18) and elsewhere [372], probably results from enhanced internalization (Figure 18) mediated by GRK-2 phosphorylation of the GIP receptor [372].

3.3.3 GIP Receptor Internalization in Transfected Cells

Receptor sequestration in response to acute treatment with GIP likely occurs via a clathrin-coated pit mediated pathway, as hypertonic sucrose blocks this pathway (Figure 16) [395]. Receptor signalling appeared not to be a requirement for receptor internalization, as $GIP_{7\text{-}30NH2}$, a receptor antagonist was also able to promote receptor internalization in a time- and dose-dependent manner (Figure 15). Adenylyl cyclase inhibitors were also able to stimulate the loss of specific GIP surface binding sites, independently of GIP (Table 5, Figure 17). However, the specificity of adenylyl cyclase inhibitors to internalize the GIP receptor was possibly non-specific, as the opposite effect was not observed with cAMP raising agents forskolin or IBMX; perhaps the inhibitors caused cyclase endocytosis, and due to close proximity, the GIP receptor was also sequestered. Both PKA activation and inhibition affected GIP receptor sequestration in the presence or absence of GIP, and likely represents a modulator of this process (Table 5, Figure 17).

A role for phosphorylation in the process of receptor sequestration is implied by the altered internalization kinetics of GIPR-S426A, GIPR-S427A, GIPR-S440A, GIPR-S426/427A and GIPR-S398-453A (Figure 21). Signalling and expression of these constructs was not different from wild type (Table 6, Figure 19 and 20). The complete removal of all C-terminal serines (GIPR-S398-453A) resulted in slower internalization kinetics than all other mutants (Figure 21B). Single mutation of S426, S427 and S440 produced a moderate reduction in internalization rate, but not different from the double mutant, GIPR-S426/427A (Figure 21B). Thus, at least for S426 and S427, the reduction in internalization was not additive. As the complete serine

114

knockout had slower kinetics, then perhaps phosphorylation of S440 in combination with S426 or S427 may be additive, but it cannot be ruled out that additive effects from phosphorylation of residues having no effect alone (S398, S406, or S453) may contribute to the slowed internalization of the GIPR-S398-453A mutant. Notably, mutant receptor GIPR-S426/427A was shown not to resist homologous desensitization (Figure 12), but did display reduced internalization kinetics (Figure 21). In contrast, GIPR-S398-453A was both resistant to desensitization (Figure 12) and had a slowed sequestration time-course (Figure 21). These results suggest that the residues required for desensitization and internalization may bear some overlap, but are functionally distinct processes.

The chronic downregulation observed by Tseng and Zhang [291], likely represents a different process than receptor sequestration, as identical mutants GIPR-C411A and GIPR-S406A showed identical internalization kinetics compared to wild type receptors (Figure 21, Table 6), but during chronic 24 hour GIP treatments, both of these mutant receptors were resistant to downregulation [291]. Direct phosphorylation of the GIP receptor has been demonstrated, although the precise residues phosphorylated were not identified [372]. Further, it was reported that GRK-2 and β-arrestin had no effect on receptor sequestration [372]. Only a single time-point of acid resistant binding was presented, and dose- or time-dependent internalization has never been shown by this group. The most plausible explanation for the lack of effect is that Tseng and Zhang transiently transfected stable LGIPR2 cells with GRKs and or β-arrestin, and the 40% transfection efficiency did not allow demonstration of an effect, as previously discussed; co-transfection of the GIPR with GRK-2 clearly showed an increased kinetics of internalization (Figure 18C).

Fluorescent tracking of G protein coupled receptors has been reported by many different groups for different receptors. Use of fluorescently labelled ligands is limited, primarily due to the cost of synthesis, and resulting low yields. The discovery of jellyfish green fluorescent

protein provides a unique opportunity to use fluorescent microscopy to track intracellular receptor trafficking using receptor chimeras [396; 397]. The primary limitation of this approach is the large size of GFP (27 KDa); effects of GFP tagging on surface expression, binding affinity, and receptor activation must be carefully performed prior to extensive use of such a construct. Adrenergic, THRH, CCK and PTH receptors were reported to be unaltered by C-terminal tagging with GFP [332; 355; 398-401]. However, subsequent use of GFP-tagged GLP-1 receptors and secretin receptors, omitted receptor activation control experiments with receptor-GFP chimeras [358; 402]. In our hands, GLP-1R-GFP (the same construct used by Salapatek *et al.* [402]) showed dramatically reduced GLP-1 stimulated cAMP production relative to wild type receptors (data not shown). Similarly, a GIPR-GFP chimera also showed reduced ability to activate adenylyl cyclase (Figure 23), but normal cell surface expression (Figure 22). Unfortunately, GFP-tagging also slowed receptor internalization kinetics (Figure 24), possibly by preventing GRK phosphorylation and/or β-arrestin binding by steric hindrance. Although qualitative, GFP-tagged GIP receptor internalization appeared normal when examined by fluorescence microscopy (Figure 25), and appeared to be similar to that observed for other receptors [332; 355; 398; 399]. Hence, the GIPR/GFP chimeric protein has severe limitations, but may prove useful in select applications, such as showing cell surface expression or marking the endosomal degradation pathway. It is possible that introduction of a more flexible linker or a longer linker between the GIP receptor and GFP may improve the signalling characteristics of this chimera, facilitating further applications.

Because of the drawbacks of GFP-tagged GIP receptors, a fluorescein-conjugated peptide ligand of the GIP receptor was synthesized. Fluorescent peptide ligands have been reported for many peptide hormones, and have proven useful for monitoring receptor sequestration indirectly, via internalization of the ligand [398; 403; 404]. Binding, signalling and receptor sequestration kinetics were favourable for $[Fluo\text{-}Trp^{25}]GIP_{1\text{-}30NH2}$, with only small, but significant, differences

from native peptide (Figures 26 and 27). While signalling was unaltered, [Fluo-Trp^{25}]GIP$_{1-30NH2}$ displaced ^{125}I-GIP binding slightly more efficiently, and was somewhat more potent at stimulating receptor internalization, monitored by radioligand assays. These changes likely would not affect the utility of this compound as a tracking molecule during receptor endocytosis. The real drawback was not discovered until fluorescent microscopy images were obtained. Only low fluorescence could be observed with [Fluo-Trp^{25}]GIP$_{1-30NH2}$ alone – photobleaching and limited shelf life of fluorescent compounds are likely responsible. However, despite this setback, use of a Alexafluor-488 fluorescein amplification kit permitted satisfactory images to be obtained (Figure 28). Hence, perhaps directly conjugating GIP to an alternate, more stable fluorophore may produce better results when examining receptor sequestration by fluorescent microscopy, however, binding, signalling and internalization controls will need to be repeated, and may not match those for [Fluo-Trp^{25}]GIP$_{1-30NH2}$.

3.3.4 Conclusion

In summary, homologous desensitization to GIP has been demonstrated in βTC-3 cells and CHO-K1 cells stably expressing the GIP receptor at low levels. Desensitization of GIP-stimulated cyclic AMP production appeared to be relatively slow, and paralleled GIP receptor sequestration kinetics. Desensitization was shown to not involve extracellular ligand degradation, induction of inhibitory G proteins, modulation of adenylyl cyclase or phosphodiesterase activity, or via signal transduction kinases A or C. In transfected cells, homologous desensitization could be dissected into repetitive versus continuous stimulation, as well as acute and chronic desensitization. Receptor internalization was found to be mediated by a clathrin-coated pit pathway, and did not require receptor activation *per se*. Modulation of internalization was not greatly affected by activators or inhibitors of signal transduction cascades, however inhibition of adenylyl cyclase or activation of protein kinase C was able to

117

sequester surface receptors independently of ligand binding. Phosphorylation was implicated in both receptor desensitization and internalization, however, the specific sites were not fully identified. Evidence indicated that phosphorylation sites for desensitization and internalization may overlap, but are not necessarily identical for both processes. Use of fluorescent methods to track internalization was accomplished by creating a GIP receptor/green fluorescent protein chimera and by conjugating fluorescein to GIP, however, both methods had some drawbacks. The further characterization of GIP receptor desensitization, internalization and downregulation may provide insight into the diminished responsiveness of type 2 diabetic patients to GIP.

Chapter 4: Analogues of Insulinotropic Hormones

4.1 Introduction

4.1.1 Structure-Activity Relationships of GIP

Use of cyanogen bromide to chemically cleave GIP_{1-42} into GIP_{1-14} and GIP_{15-42} [405] for use in peptide sequencing [17; 18] ultimately resulted in the first structure-activity study of the newly discovered hormone [165]. Peptide purification methods had not advanced to the widespread use of HPLC, and as such, early studies must be considered with caution due to the possibility of peptide contamination (for example, later HPLC assessment of the purity of "pure" natural porcine GIP preparations found as much as 32% GIP_{3-42} as well as CCK contamination [19; 166]). Nevertheless, Pederson and Brown [165] demonstrated that pig GIP_{15-42} retained partial insulinotropic activity in the perfused rat pancreas, whereas [Homoserinelactone^{14}]GIP_{1-14} did not. These findings were supported by the finding that bovine GIP_{17-42} [21] also retained 32% insulin releasing ability compared to native hormone using the same experimental model [267]. Use of enterokinase, trypsin and *S. aureus* V8 protease allowed isolation of GIP fragments corresponding to amino acids 1-3, 1-16, 4-42, 17-42 and 19-30 [21; 267]. On transplantable hamster insulinoma membranes, only GIP_{4-42} and GIP_{17-42} were able to significantly displace ^{125}I-GIP binding when tested up to 10 μM. Pancreas perfusions with GIP_{4-42} indicated that this molecule had little, if any, insulinotropic activity, and it was suggested that it may act as a GIP antagonist, while GIP_{1-16} was not tested based on prior results with GIP_{1-14} [165; 267]. Conflicting data were obtained, however, when GIP_{17-42} was tested on RINm5F insulinoma cells: native GIP was able to stimulate cyclic AMP production, whereas 10 μM GIP_{17-42} could not [198]. Neither GIP_{1-18}, nor GIP_{19-42} were able to potentiate glucose-induced insulin release from isolated islets [406].

Another development arose during testing of synthetic GIP preparations. Yanaihara *et al* [407] synthesized a 43 amino acid peptide, based on the original reported structure of GIP [17;

18], and found that a partially purified preparation contained ~30% insulin releasing ability from the perfused rat pancreas. However, purified synthetic GIP_{1-38} was equally insulinotropic to the natural source GIP, but lacked potency when examining acid inhibitory action [408]; the insulinotropic properties of GIP_{1-39} have been independently confirmed [409]. Three possibilities were proposed to explain the discrepancy: (1) the last 5 amino acids (of the 43 a.a. sequence) are important for acid inhibitory activity (*i.e.* there are two separable bioactive domains for acid inhibition and insulin stimulation), (2) the original peptide sequence contained an error, or (3) acid inhibitory activity of natural source peptide was due to contamination with another molecule. Support has been found for the first two suggestions. Upon reassessment of GIP's primary sequence, Jörnvall *et al* [19] found that GIP was only 42 amino acids long, and an extra Gln residue was included at position 30. Synthetic GIP_{1-31} was found to be an equally potent stimulant of cyclic AMP production in human insulinoma compared to natural GIP_{1-42} [182]; the potency of GIP_{1-30} has been confirmed with transformed insulinoma and transfected cell models [198; 276; 278]. Similarly, in the perfused rat pancreas, synthetic porcine (sp) $GIP_{1-30NH2}$ and GIP_{1-42} exhibited equipotent activation of insulin release, but in the perfused stomach, $spGIP_{1-30NH2}$ lacked somatostatinotropic activity [337; 410]. Bioassay of $spGIP_{1-30NH2}$ in isolated perfused organs in rats showed it lacked gastric acid inhibitory activity, but retained inhibitory action on exocrine secretions, likely mediated via insulin [32]. Taken together, fragment analysis suggested the insulinotropic domain resided between the overlap of $GIP_{1-30NH2}$ and GIP_{15-42} or GIP_{17-42}; when tested, GIP_{15-30}, GIP_{17-30} and GIP_{19-30} did possess weak insulin stimulating ability in the perfused pancreas [337]. Residues 27-30 may be important for biological activity, as GIP_{1-27} and GIP_{1-28} lost insulinotropic potency [198; 411; 412]. Antagonism of the GIP receptor has been demonstrated with N-terminally truncated peptides, $GIP_{6-30NH2}$, $GIP_{7-30NH2}$, and $GIP_{10-30NH2}$, and the complete high affinity binding domain of GIP resides between residues 6 and 30 [186; 413].

4.1.2 Metabolism of GIP

4.1.2.1 Enzymatic Inactivation

When the sequence of GIP was reassessed, during HPLC purification of natural porcine GIP, an additional peptide corresponding to GIP_{3-42} was identified as a major component of the preparation, and it was suggested that enzymatic cleavage may have resulted in the N-terminally truncated molecule [19]. Preliminary reports using the perfused rat pancreas model suggested that the peptide was devoid of insulin releasing ability [414; 415]; complete examination in the perfused stomach and pancreas indicated that GIP_{3-42} was not effective in stimulating somatostatin or insulin release [57]. Subsequent studies on isolated rat islets confirmed that GIP_{3-42} was not insulinotropic, and further, that it likely was not an antagonist of the GIP receptor [166; 416]. The seminal paper of Mentlein *et al* [58] on degradation of GIP_{1-42} by purified dipeptidyl peptidase IV (DPIV) and serum confirmed that GIP inactivation by cleavage of a dipeptide from the N-terminus was enzymatic in nature. Using HPLC, it was possible to identify the released Tyr^1-Ala^2 molecule, as well as separate GIP_{3-42} from GIP_{1-42} on chromatograms, facilitating kinetic enzymology studies. Use of the DPIV inhibitor, Lys-Pyrrolidide, in serum, indicated that DPIV was the major degrading enzyme present, and kinetic constants supported a physiological role for cleavage [58]. *In vivo* relevance was demonstrated independently, where ^{125}I-GIP_{1-42} was shown to be degraded to ^{125}I-GIP_{3-42} by purified DPIV, serum, and during *IV* injection at physiological concentrations into anesthetized rats [59; 330].

Subsequent studies have shown that GIP_{3-42} is actually a weak antagonist of the cloned GIP receptor; as such, GIP_{3-42} was unable to stimulate cAMP accumulation in transfected cells and retained high affinity receptor binding [324]. Kinetics of GIP degradation by purified DPIV and serum were reassessed by mass spectrometry, and confirmed GIP_{3-42} as the primary degradation product in both cases [380]. Specific inhibition of DPIV *in vivo* was able to increase the proportion of N-terminally intact bioactive peptide when exogenous GIP_{1-42} was infused [417].

Development of N-terminally specific immunoassay techniques has been critical in showing clinical relevance of DPIV-mediated degradation of GIP in humans [60; 61]. Because of its primary role in inactivating incretin hormones, specific DPIV inhibition has been proposed as a therapeutic approach for type 2 diabetes, to improve glucose tolerance by increasing the biological half-life of endogenously secreted incretins [381; 382; 418; 419].

GIP has been reported to be degraded by neutral endopeptidase (NEP), however, it was a poor substrate for the enzyme [420]. Furthermore, GIP fragments corresponding to amino acids 7-42, 10-42, 11-42, 17-42 and 1-39 have been isolated from natural sources [20; 409; 421], indicating that further cleavage of the peptide is possible, although the enzymes responsible and the physiological relevance have not been established.

4.1.2.2 Pharmacokinetics

Early studies on GIP pharmacokinetics in humans were performed with a C-terminally directed GIP antibody, and resulted in an estimated a $t_{1/2}$ value in the order of 20 min [60; 82; 164; 221; 422]. The similarity between metabolic clearance rate (MCR, man 2.6-8.7 mL/Kg/min; pig 8.3 mL/Kg/min) and the glomerular filtration rate suggests that GIP is likely freely filtered, and implicates the kidneys for extraction of GIP, as measured with C-terminal specific assays [60; 221; 422]. This is consistent with elevated total IR-GIP levels in uremia, renal failure, and experimental nephrectomy, as well as renal arteriovenous differences in man, dog and rat [423-426]. As it was realized that C-terminally directed immunoassays were overestimating bioactive GIP, upon development of an N-terminally specific assay, pharmacokinetic parameters of GIP were reassessed in swine and man [60; 417]. When measuring intact GIP_{1-42}, the $t_{1/2}$ disappearance rate for exogenously infused GIP ranged from 3.3 (pig) to 7.3 min (human) [60; 417], corresponding well to $t_{1/2}$ values for physiological conversion of $^{125}I\text{-}GIP_{1-42}$ to $^{125}I\text{-}GIP_{3-42}$ in rats [59]. When tissue extraction was reassessed using N- and C-

122

terminally directed GIP radioimmunoassays, extraction of C-terminal immunoreactivity was only affected in the kidney by DPIV inhibition [417]. While the renal brush borders are rich in DPIV [427], in order to extract C-terminal immunoreactivity, either secondary degradation of the epitope must occur, or the peptide is removed in urine; as DPIV inhibition reduced C-terminal clearance of GIP [417], these events likely take place after dipeptide cleavage. Further, from these studies was the finding that liver and muscle contribute to the DPIV-mediated N-terminal degradation of GIP [417], whereas prior examination of total IR-GIP extraction by the liver suggested that it was not a major site of GIP removal [230; 428]. Notably, DPIV is present as a soluble isoform in plasma and on the surface of lymphocytes; as such, the bloodstream is likely a major site of GIP cleavage [380].

4.1.3 Metabolism of GLP-1 and Glucagon

In contrast to the long clearance half time for C-terminal GIP immunoreactivity (GIP_{1-42} + GIP_{3-42}), use of side-viewing antibodies to GLP-1 (recognizing N-terminally extended and truncated forms) suggest the molecule is rapidly removed from plasma. In all species tested (rat, pig, dog and human), the $t_{1/2}$ for clearance of total GLP-1 immunoreactivity is approximately 5 min [58; 429-435]. Correspondingly, the metabolic clearance rate in man is on the order of 10 mL/Kg/min [429-432]. Study of tissue specific degradation of GLP-1 in anesthetized pigs showed, like GIP, renal catabolism is the main site of removal of total GLP-1 immunoreactivity, but also lungs, liver and hindleg were implicated for N-terminal truncation [433]. Earlier experimental surgery procedures to rats indicated the kidneys as the major site of GLP-1 clearance; total GLP-1 levels were elevated during nephrectomy and ureteral ligation, whereas GLP-1 was extracted from the perfusate of isolated kidney [435]. Similarly, uremia increases plasma concentrations of GLP-1 in humans [426].

The circulating half-life of glucagon has been reported to be in the range of 5 to 6 min in dogs and humans [436; 437]. Degradation of glucagon by the liver is controversial. It has been reported that glucagon is metabolized by the liver by the cytosolic enzyme dipeptidyl peptidase I (DPI/Cathepsin C) [438-440]. In reviewing the contribution of the liver to glucagon degradation, Holst [441] concluded that in dogs as well as humans, there is low hepatic extraction. This conclusion is supported by findings that glucagon was not degraded by passage through the perfused rat liver [442]. Consensus exists that the kidney plays a major role in the metabolic clearance and degradation of glucagon [441]. Studies by several groups indicated that after glomerular filtration in the kidney, glucagon is hydrolyzed by brush border enzymes in the proximal tubule [443-445].

Like GIP, there was preliminary evidence showing N-terminal truncation in serum [446], prior to establishment of DPIV as the enzyme responsible for GLP-1 degradation by purified enzyme and serum incubations *in vitro* [58]. $GLP-1_{9-36NH2}$ was formed by *in vitro* plasma $GLP-1_{7-36NH2}$ incubation and found to be a primary metabolite in humans [447]; exogenously infused $GLP-1_{7-36NH2}$ was rapidly converted to this truncated form [448]. In the anesthetized rat, *IV* injections of physiological concentrations of iodinated $GLP-1_{7-36NH2}$ were converted to ^{125}I-$GLP-1_{9-36NH2}$ with a half time less than two minutes [59]. Administration of specific DPIV inhibitors has further shown a primary role for DPIV-mediated hydrolysis, as inhibition results in preservation of N-terminally intact GLP-1 whether it is endogenous GLP-1 measured [381; 382; 418], or exogenously infused [449]. *In vitro* studies have indicated that $GLP-1_{9-36NH2}$ may also act as a weak antagonist of the GLP-1 receptor, however, given the proportions of endogenous levels of N-terminally intact to N-terminally degraded peptide, physiological antagonism is unlikely [450; 451]. In pigs, it was reported that the majority of GLP-1 released is degraded by DPIV in capillaries before it reaches target tissues [452], questioning the role of GLP-1 as a physiological incretin. Recently, we have published reports that DPIV is also capable of

124

degrading glucagon by purified enzyme and serum incubations *in vitro* [328; 453]. As such, previous reports indicating the remarkable stability of glucagon incubated in serum [437; 454] were likely flawed in that antibodies cross-reacted with N-terminally truncated glucagon. Further studies are required to establish the physiological role of DPIV in inactivation of glucagon, although kinetic constants compare well with those for GIP and GLP-1, *i.e.* physiological substrates, and thus it is likely that DPIV does normally play a role [453]. Hence, studies on the pharmacokinetics of glucagon and GLP-1 must also consider soluble DPIV present in serum and DPIV expressed on the surface of lymphocytes as sites of peptide metabolism.

4.1.4 Thesis Objective

In the current study, two main goals were established: (1) domains of GIP responsible for receptor activation and binding were delineated, and (2) the modulation of GIP, GLP-1 and glucagon bioactivity by DPIV cleavage was examined, with a specific aim of generating superactive DPIV resistant peptide analogues for use *in vivo*. Hence, studies required the use of CHO-K1 cells stably transfected with the GIPR, GLP-1R or glucagon receptor (Methods sections 2.2 and 2.3), coupled with synthetic peptides (Methods section 2.4). Analogues were tested for cyclic AMP stimulating ability (Methods section 2.7) and receptor binding affinity (Methods sections 2.5 and 2.6). For some peptides, degradation studies (Methods section 2.11) and/or *in vivo* bioassay in rats (Methods sections 2.13 and 2.14) were performed. The rationale for these studies was the potential use of small molecular weight peptides and/or superactive analogues for the treatment of human type 2 diabetes, or other therapeutic applications for these hormones.

4.2 Results

4.2.1 GIP Fragment Analysis

4.2.1.1 Competitive-binding Studies

Binding affinities of synthetic peptides were determined by binding displacement assays on CHO-K1 cells transfected with the wild type rat pancreatic GIP receptor (Figure 29). A summary of statistics is shown in Table 7. Of the peptides tested, only GIP_{1-42}, $GIP_{1-30NH2}$ and $GIP_{7-30NH2}$ were able to fully displace ^{125}I-GIP binding (IC_{50} values: 3.17 ± 0.3 nM, 2.04 ± 0.73 nM and 23.7 ± 3.7 nM, respectively; n = 4). Truncation of the amino-terminus by 14, 15 and 16 amino acids resulted in C-terminal fragments ($GIP_{15-30NH2}$, $GIP_{16-30NH2}$, and $GIPR_{17-30NH2}$) that produced half-maximal displacement values in the low micromolar range (Table 7); further truncation at the amino-terminus resulted in IC_{50} values greater than 10 μM, and thus cannot be determined from the range of peptides tested. Short amino-terminal peptides were less potent at displacing specific ^{125}I-GIP binding: $GIP_{1-42} \geq GIP_{1-30NH2} >>> GIP_{1-14OH} > GIP_{1-14NH2} > GIP_{1-13NH2} = GIP_{1-15NH2}$ (Figure 29, Table 7). Peptides GIP_{1-6NH2}, GIP_{1-7NH2}, GIP_{1-13OH} and GIP_{1-15OH} failed to displace significant ^{125}I-GIP under the given assay conditions (Table 7).

In order to elucidate key residues contained within amino acids 1-14 of GIP conferring biological activity, an alanine scan was performed. Also because DPIV degradation inactivates GIP, and likely GIP_{1-14}, three predicted DPIV-resistant analogues as well as a molecule with a synthetic β-turn induced in the peptide backbone (BTD) were generated. Binding displacement curves were performed for all peptides, and full curves are presented for selected peptides in Figure 30. Substitution of any residue of the 1-14 primary sequence resulted in significantly reduced binding affinity/ability to displace ^{125}I-GIP_{1-42}, with the notable exception of $[Tyr^{13}]GIP_{1-14OH}$ (Figure 30); GIP normally has alanines in position 2 and 13, thus these residues were replaced with those found in glucagon. Residues which may be particularly important for favouring structure for binding or forming contacts with residues of the GIP receptor are

126

suggested by the complete loss of binding potency for $GIP_{1\text{-}14OH}$ analogues with Ala^1, Ala^3, Ala^4 or Ala^5 substitutions (Figure 30B). [$D\text{-}Ala^2$] substitution of $GIP_{1\text{-}14OH}$ was not well tolerated, whereas reduction of the scissile bond between residues 2 and 3 ([$Tyr^1\text{-}Ala^2\psi(CH_2NH)$]$GIP_{1\text{-}14OH}$ gave a similar degree of displacement compared to native sequence, and [$L\text{-}Pro^3$]$GIP_{1\text{-}14OH}$ and $GIP_{1\text{-}11(BTD)12\text{-}14OH}$ were somewhat less potent (Figure 30).

Table 7: Summary statistics for studies on synthetic GIP fragments using wtGIPR cells
Data represent mean ± S.E.M. of at least 3 independent experiments.

Synthetic Peptide:	cAMP Production (Fold Basal[a])		Receptor Binding	
	10 μM	20 μM	% Displacement at 10 μM	IC_{50} (nM)
GIP(1-42OH)	119 ± 11*[b]	-[b]	100[b]	3.2 ± 0.3
1-6NH2	1.27 ± 0.18	1.08 ± 0.03	-3.6 ± 7.8	-
1-7NH2	0.92 ± 0.05	1.06 ± 0.06	-6.1 ± 3.4	-
1-13OH	1.03 ± 0.06	1.15 ± 0.07	-0.2 ± 3.4	-
1-13NH2	6.51 ± 1.33*	15.7 ± 3.0*	5.0 ± 1.1*	-
1-14OH	88.9 ± 9.5*	85.2 ± 7.6*	51.3 ± 1.2*	-
1-14NH2	75.4 ± 10.7*	88.3 ± 5.9*	27.9 ± 2.8*	-
1-15OH	0.97 ± 0.06	0.91 ± 0.05	-3.1 ± 4.3	-
1-15NH2	2.26 ± 0.32*	4.37 ± 0.51*	4.2 ± 1.7*	-
1-30NH2	108 ± 12*[b]	-[b]	99.8 ± 1.2*	2.0 ± 0.7
7-30NH2	0.89 ± 0.06	0.85 ± 0.03	99.3 ± 1.0*	23.7 ± 3.7
15-42OH	1.02 ± 0.10	1.01 ± 0.03	83.3 ± 0.7*	1270 ± 150
15-30NH2	1.24 ± 0.28	1.01 ± 0.11	82.7 ± 1.0*	1400 ± 310
16-30NH2	1.04 ± 0.06	0.80 ± 0.02	82.1 ± 1.9*	2530 ± 450
17-30NH2	1.13 ± 0.09	1.12 ± 0.05	81.9 ± 2.1*	1540 ± 550
19-30NH2	20.1 ± 1.3*	45.0 ± 1.6*	52.3 ± 0.6*	-

[a]: Basal cyclic AMP = 2.96 ± 0.03 fmol/1000 cells.
[b]: cAMP and Binding experiments with $GIP_{1\text{-}42}$ and $GIP_{1\text{-}30NH2}$ were only tested at concentrations as high as 1 μM.
*: p < 0.05 versus control conditions, denoting significant increase in cyclic AMP over basal levels or significant displacement of ^{125}I-GIP.
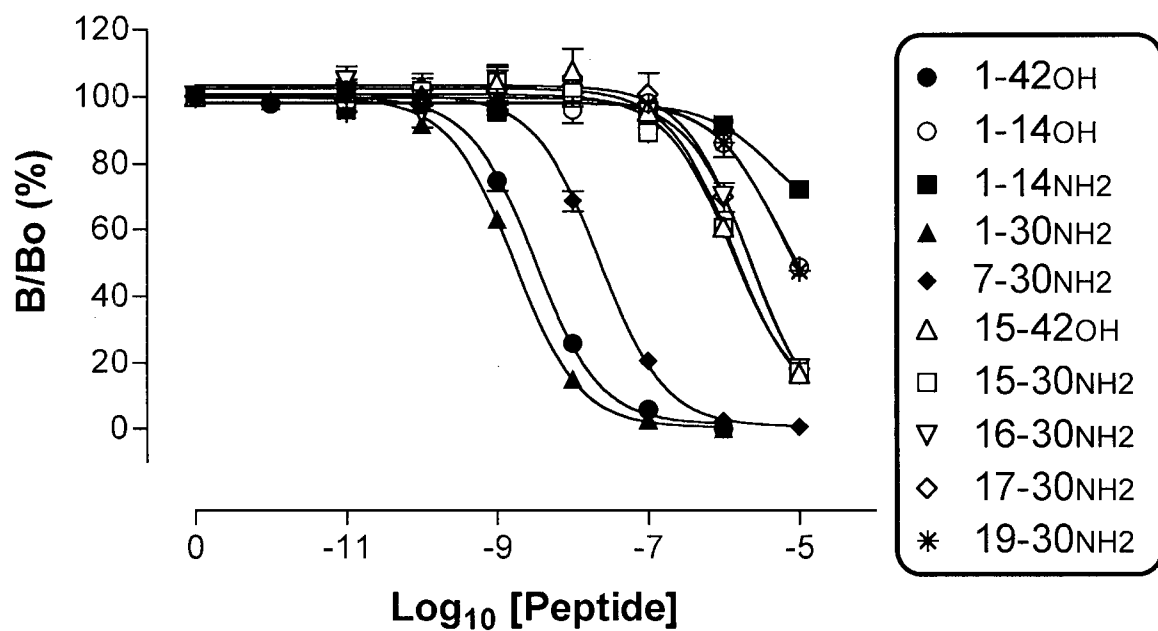
Figure 29: Competition-binding displacement curves of synthetic GIP fragments on wtGIPR cells

Data represent the mean ± S.E.M. of 3-8 independent experiments. Refer to Table 7 for binding statistics. Refer to sections 2.4, 2.5 and 2.6 of the Methods section for more detail.
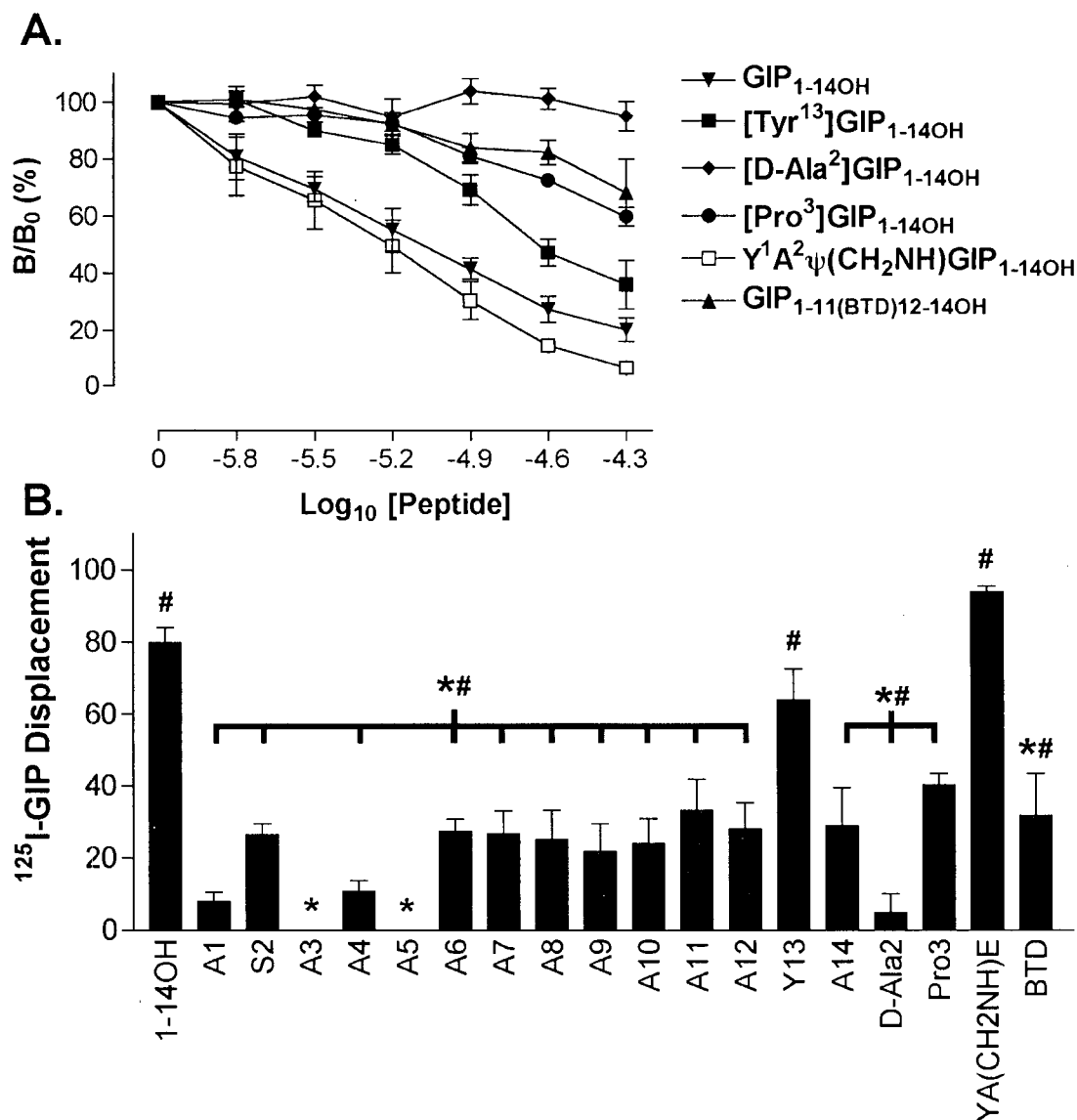
Figure 30: Competition-binding of modified GIP$_{1-14}$ analogues on wtGIPR cells

(A) Concentration-dependent displacement of ^{125}I-GIP$_{1-42}$ binding by GIP$_{1-14OH}$ and substituted peptides. (B) Displacement of GIP tracer by 50 µM peptide. Peptides are a series of GIP analogues based on amino acids 1-14 of the primary sequence with single amino acid substitutions (to Ala, Ser or Tyr, where indicated), modified N-terminal amino acids (D-Ala^2, Pro^3), a reduced scissile bond between amino acids 2 and 3, or introduction of a synthetic β-turn mimetic (BTD) beween residues 11 and 12. Data represent the mean ± S.E.M. of ≥ 3 experiments (# = significantly non-zero, * = significantly different from GIP$_{1-14OH}$; P < 0.05). Refer to sections 2.4, 2.5 and 2.6 of the Methods section for more detail.

4.2.1.2 Cyclic AMP studies

All peptides were screened on wtGIPR cells initially with a concentration-response curve over the range of 1 pM to 20 μM. Table 7 shows the summary of peptides tested for the 10 and 20 μM responses for non-substituted GIP fragments; peptides showing no cyclic AMP stimulation at high concentration did not demonstrate any activity at lower concentrations (data not shown). The basal cyclic AMP level in wtGIPR cells was 2.96 ± 0.03 fmol/1000 cells (n > 30). Of peptides tested, only GIP_{1-14} (amidated or free acid) and GIP_{19-30} produced large cyclic AMP responses. $GIP_{1-13NH2}$ and $GIP_{1-15NH2}$ also showed significant increases in cyclic AMP from basal levels, however, responses were weak compared to GIP_{1-14}. Full concentration-response curves for bioactive GIP fragments are shown in Figure 31. GIP_{1-42} had an EC_{50} of 377 ± 25 pM for cyclic AMP production, and maximal cyclic AMP generation was 358 ± 46 fmol/1000 cells (n = 6); similarly, $GIP_{1-30NH2}$ had an EC_{50} of 139 ± 77 pM for cyclic AMP production, and maximal cyclic AMP generation was 326 ± 35 fmol/1000 cells (n = 3). GIP_{1-14} and GIP_{19-30} did not stimulate maximal cyclic AMP levels over the concentration range tested, and thus it is difficult to estimate EC_{50} values. However, given the maximal cAMP production by GIP_{1-42}, the EC_{50} of GIP_{1-14} (C-terminal amide or free acid) was in the micromolar range, and both amidated and hydroxylated forms of GIP_{1-14} appear to be full agonists of the receptor (Figure 31). Bioactive GIP fragments had no effect on non-transfected CHO-K1 cells (data not shown).

During bioactivity testing of alanine substituted GIP_{1-14OH} analogues, a broader concentration range of peptides was used (Figure 32). Thus it was shown that GIP_{1-14OH} was indeed a full agonist of the GIP receptor ($EC_{50} = 780 \pm 190$ nM) although significantly lower potency than full length GIP ($EC_{50} = 239 \pm 13$ pM), but still producing similar maximal cAMP accumulation in wtGIPR cells (GIP_{1-42}: 312 ± 18 fmol/1000 cells; GIP_{1-14OH}: 323 ± 50 fmol/1000 cells; Figure 33). DPIV-resistant GIP_{1-14OH} analogues, $[Pro^3]GIP_{1-14OH}$ and $[Tyr^1-Ala^2\psi(CH_2NH)]GIP_{1-14OH}$ were also

able to stimulate maximal cAMP production, the former being less potent and the latter more potent compared to GIP_{1-14OH} (Figure 33). Reversing chirality of position 2 or inducing a β-turn completely ablated ability to activate the GIP receptor. A concentration of 20 μM was the highest tested for alanine scanning mutants of GIP_{1-14OH} (Figure 32). At this concentration, almost all residues appeared to be important for signalling, although this may partially reflect the reductions in binding displacement, which were weak for many peptides tested at 50 μM (Figure 30). Only Ala^1, Ser^2, Ala^3, Ala^4 and Tyr^{13} substituted peptides were able to increase cAMP levels above basal ($P < 0.05$), although Ala^1 and Ala^3 were extremely weak. 20 μM native GIP_{1-14OH}, as well as Ser^2 and Tyr^{13} substituted analogues were more potent than 1 nM GIP_{1-42} when examining cAMP production in wtGIPR cells (Figure 33).

GIP fragments truncated at the amino terminus have previously been shown to act as potent receptor antagonists [413], and thus the shorter C-terminal fragments were similarly tested for inhibition of GIP-stimulated cAMP production (Figure 34A). The potency of GIP fragments as antagonists paralleled their binding affinities (Table 7). Peptides $GIP_{15-42OH}$, $GIP_{15-30NH2}$, $GIP_{16-30NH2}$ and $GIP_{17-30NH2}$ acted as weak antagonists of the GIP receptor; $GIP_{7-30NH2}$ was included as a positive control [413]. To further delineate structure-activity relationships of GIP, and as an important control, the ability of $GIP_{17-30NH2}$ to antagonize GIP_{1-14OH} and $GIP_{19-30NH2}$ was examined. It was hypothesized that the non-overlapping C-terminal $GIP_{17-30NH2}$ fragment would not antagonize GIP_{1-14OH}, whereas it should antagonize $GIP_{19-30NH2}$. The results of these experiments are found in Figures 34B and 34C (N.B. data were normalized to 20 μM concentrations of agonist for better comparison, as GIP_{1-14OH} is more potent than $GIP_{19-30NH2}$; see Figure 31). In confirmation of the proposed hypothesis, 20 μM $GIP_{17-30NH2}$ was not able to significantly reduce cyclic AMP production stimulated by 20 μM GIP_{1-14OH}, whereas 1 μM $GIP_{7-30NH2}$ reduced

production by $76.6 \pm 1.9\%$ ($p < 0.05$). Furthermore, 20 μM $GIP_{17-30NH2}$ reduced 20 μM $GIP_{19-30NH2}$-stimulated cAMP by $48.9 \pm 4.7\%$ and 1 μM $GIP_{7-30NH2}$ by $89.0 \pm 1.1\%$ ($p < 0.05$).
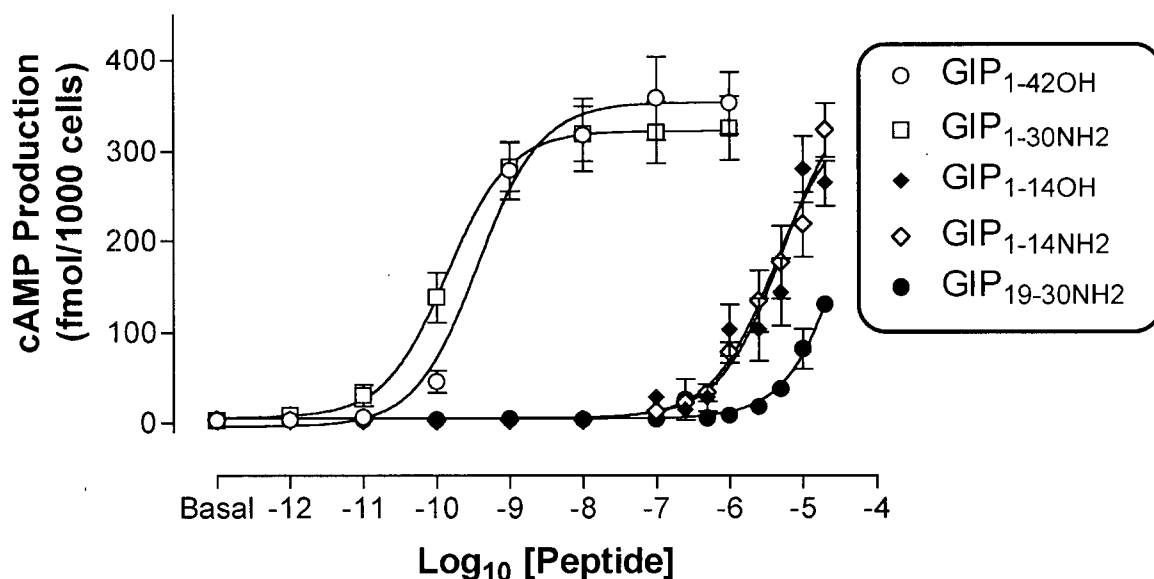
Figure 31: Cyclic AMP production in wtGIPR cells by selected bioactive truncated peptides
Data represent mean $\pm$ S.E.M. of at least 3 independent experiments. Refer to Table 7 for cAMP data for all GIP peptides tested. Refer to sections 2.4 and 2.7 of the Methods section for more detail.
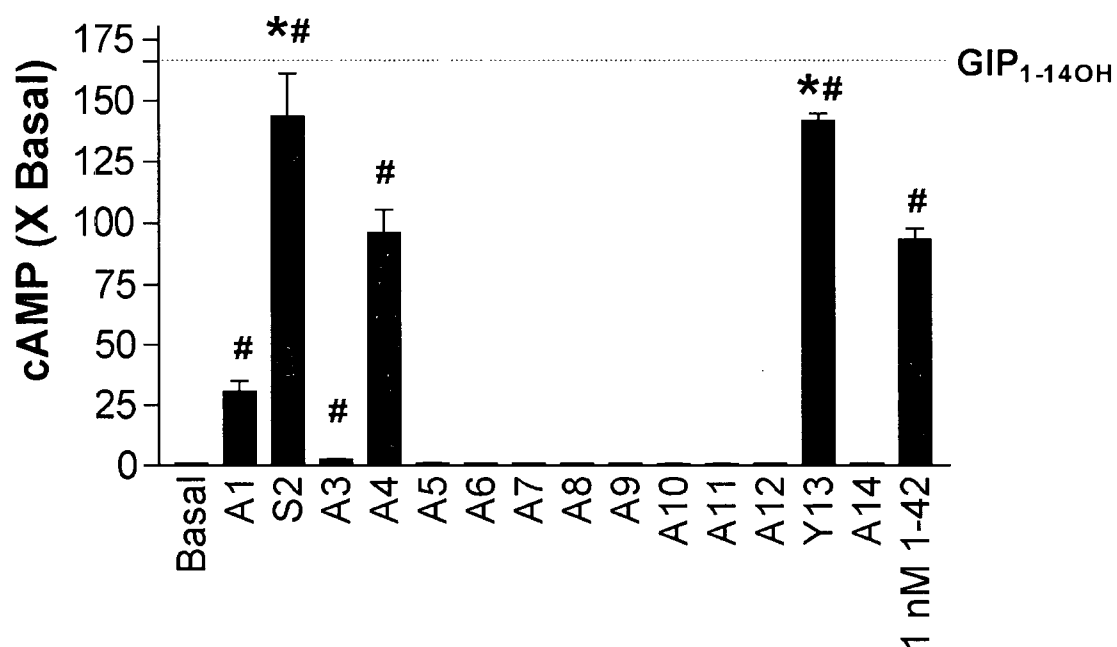
Figure 32: Cyclic AMP production by 20 μM of substituted GIP$_{1-14}$ peptides

An alanine scan of GIP$_{1-14OH}$ was performed (where endogenous Alanines were found, they were substituted with residues found at the corresponding positions of glucagon). Peptides were tested over a concentration range between 0 and 20 μM. Only the highest concentration is shown. (# = significantly greater than basal, * = significantly greater than 1 nM GIP$_{1-42}$, P < 0.05). Refer to sections 2.4 and 2.7 of the Methods section for more detail.

A.

Cyclic AMP (fmol/1000 cells)

500 —
400 —
300 —
200 —
100 —
0 —

Basal   -11   -9   -7   -5

Log_{10} [Peptide]

Legend:
- ■ GIP_{1-42OH}
- ▲ GIP_{1-14OH}
- ▼ $[D-Ala^2]GIP_{1-14OH}$
- ◆ $[Pro^3]GIP_{1-14OH}$
- ● $Y^1A^2\psi(CH_2NH)GIP_{1-14OH}$
- □ $GIP_{1-11-BTD-12-14OH}$

B.

Cyclic AMP (XBasal)

Peptide	
1 nM GIP1-42	#
GIP1-11-BTD-12-14OH	*
YA(CH2NH)GIP1-14OH	#
Pro3-GIP1-14OH	#
D-Ala2-GIP1-14OH	*#
GIP1-14OH	*#
Basal	

0   50   100   150   200
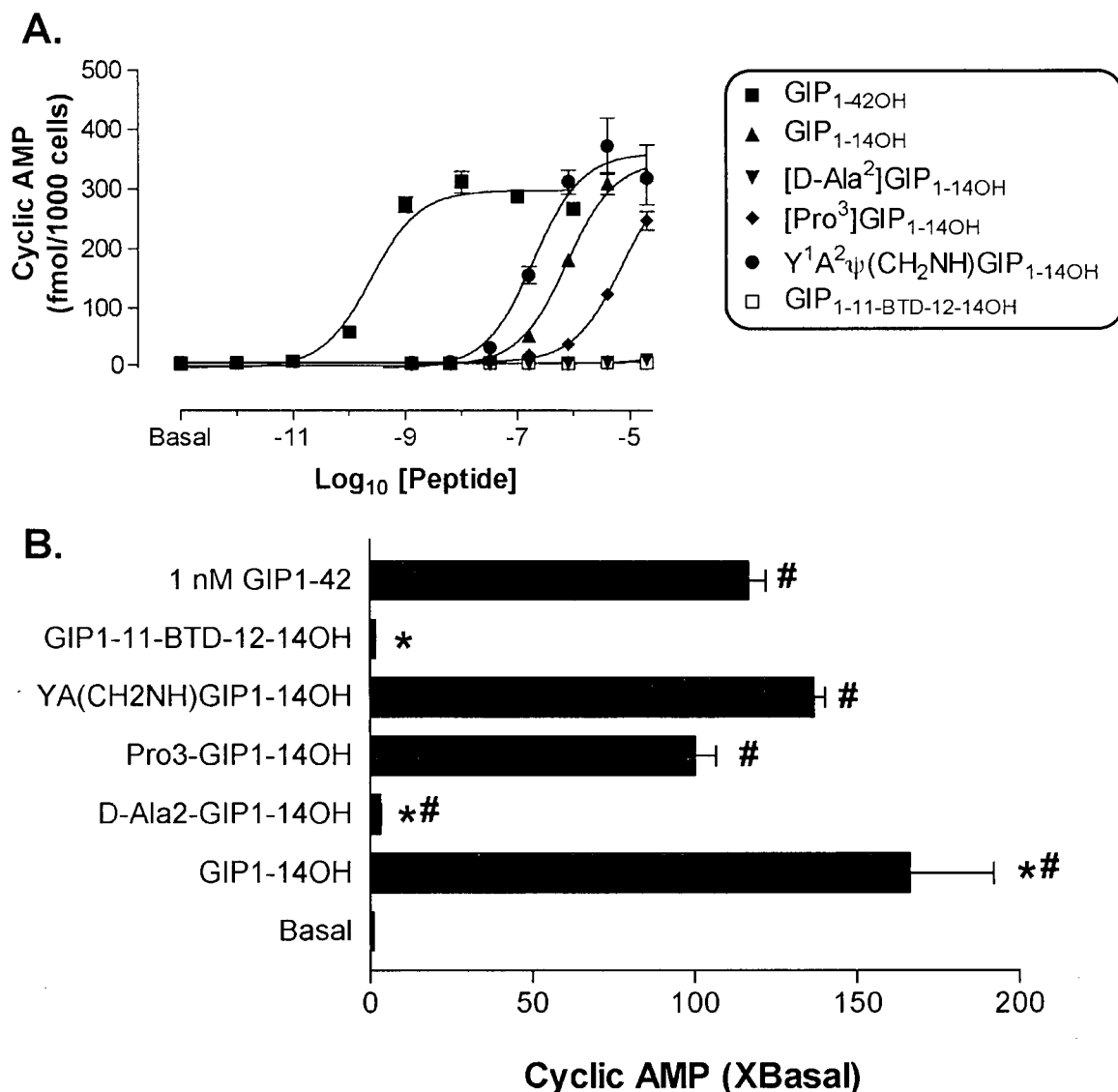
Figure 33: Concentration-response curves of intracellular cyclic AMP production in wtGIPR cells by N-terminally modified GIP_{1-14} peptides

(A) Full concentration-response curve for N-terminally modified analogues. (B) Fold-basal responses for maximal cAMP production values measured. Data represent mean ± S.E.M. of at least 3 independent experiments (# = significantly greater than basal, * = significantly different than 1 nM GIP_{1-42}, $P < 0.05$). Refer to sections 2.4 and 2.7 of the Methods section for more detail.

134
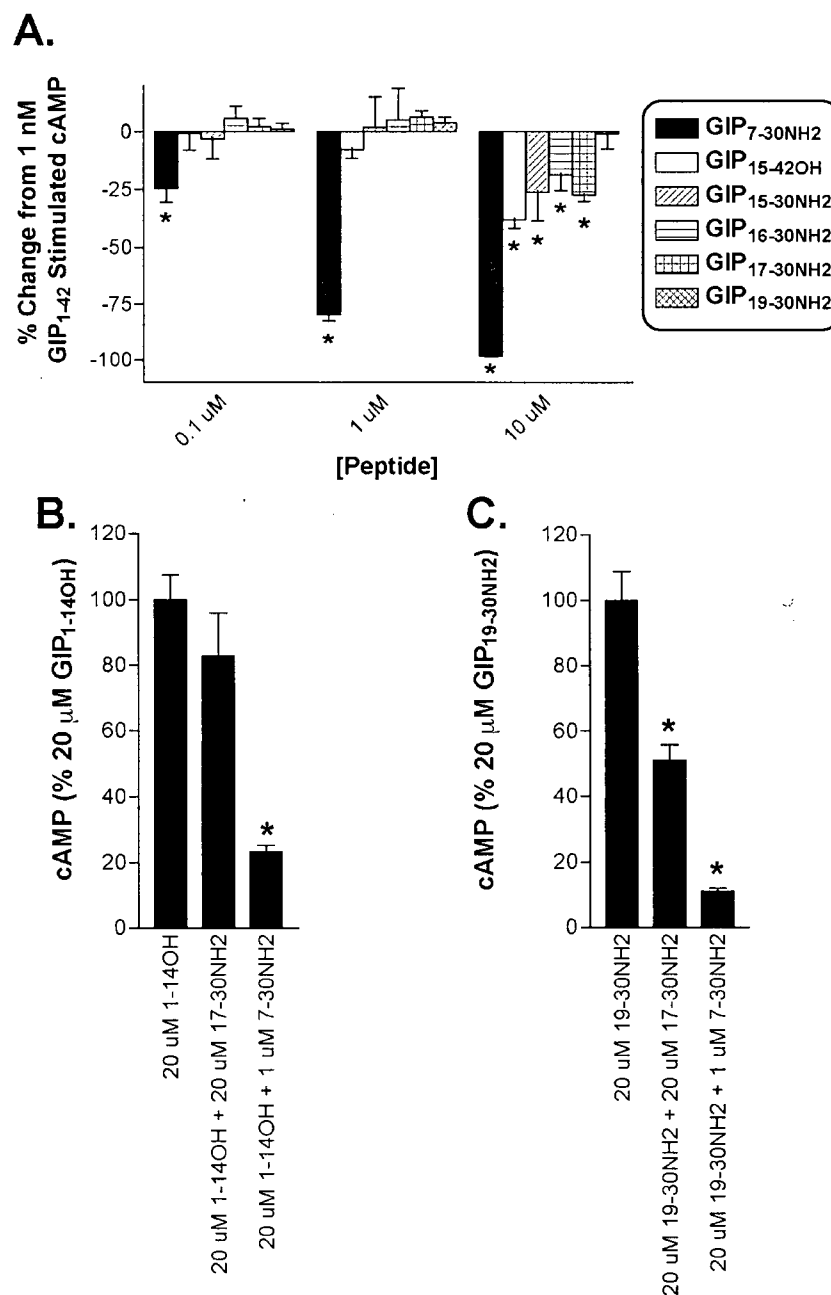
Figure 34: Antagonism of native GIP by C-terminal GIP fragments

(A) Antagonism of 1 nM GIP_{1-42} stimulated cAMP production in wtGIPR cells by N- and C-terminally truncated GIP fragments. On average, 1 nM GIP_{1-42} produced 278 ± 32 femtomoles of cyclic AMP/1000 cells (cf. Figure 31). Antagonism of (B) 20 μM GIP_{1-14OH} or (C) 20 μM $GIP_{19-30NH2}$ by 20 μM $GIP_{17-30NH2}$ or 1 μM $GIP_{7-30NH2}$. Data represent mean ± S.E.M. of >3 independent experiments; * = $P < 0.05$ versus control (1 nM GIP_{1-42} or 20 μM GIP_{1-14OH} or $GIP_{19-30NH2}$). Refer to sections 2.4 and 2.7 of the Methods section for more detail.

4.2.1.3 Perfused Rat Pancreas and in Vivo Bioassay

Given the ability to stimulate cyclic AMP production, GIP_{1-14} was selected for testing in the perfused rat pancreas. The effect of GIP_{19-30} on insulin secretion in the perfused pancreas has already been reported; this peptide exhibited a small but significant response from the endocrine pancreas [337], consistent with its ability to weakly activate the GIP receptor (Figure 31). A peptide gradient from 0-5 nM under high glucose conditions (16.7 mM) was perfused over 40 min. Immunoreactive insulin release profiles are shown for $GIP_{1-30NH2}$ and $GIP_{1-14NH2}$ as well as the glucose control (Figure 35). GIP_{1-14} was found to induce a small, but significant, increase in insulin release ($p < 0.05$). Integrated responses for insulin release from the perfused pancreas were: $GIP_{1-30NH2}$: 167.5 ± 62.7 mU, $GIP_{1-14NH2}$: 43.0 ± 8.5 mU, glucose control: 17.1 ± 9.3 mU, over the 40 minute perfusion period (n = 3-4).

A bioassay was developed based on the principal that GIP acts to lower blood glucose mainly through an insulin-dependent mechanism (Methods section 2.12). Hence, blood glucose was monitored during intravenous peptide infusion following an *IP* glucose tolerance test. Infusion of 1 pmol/min/100 g bw of GIP_{1-42OH} significantly reduced circulating glucose levels relative to control animals (Figure 36A). Concurrent insulin measurements revealed that GIP_{1-42OH} infusion induced a rapid peak in circulating insulin within 10 minutes of glucose injection, followed by a return to baseline at 60 min. In contrast, saline control animals demonstrated a slow rise in insulin, peaking at 30 minutes, and similarly returning to baseline at 60 min (Figure 36B). Because of the sampling times used, it was not possible to determine if GIP treatment enhanced phase-I versus phase-II insulin release, or both; however, recently it was demonstrated that GIP primarily reduces postprandial glucose excursions via augmenting the early phase of insulin release [185]. Synthetic GIP peptides shown to have biological activity on transfected cells and in the perfused pancreas were tested, monitoring only blood glucose. GIP_{1-42OH} and $GIP_{1-30NH2}$ were equally effective in reducing excursions in glycemia, relative to saline controls (Figure 37;

136

p < 0.05 at all time-points). A much greater dose of $GIP_{1-14NH2}$ (100 pmol/min/100 g bw) was required to achieve the same effect (p < 0.05 relative to controls at all time-points), whereas the same dose of $GIP_{19-30NH2}$ only slightly reduced the glucose response after *IP* glucose (Figure 37; p < 0.05 at 20 and 30 minute time-points).
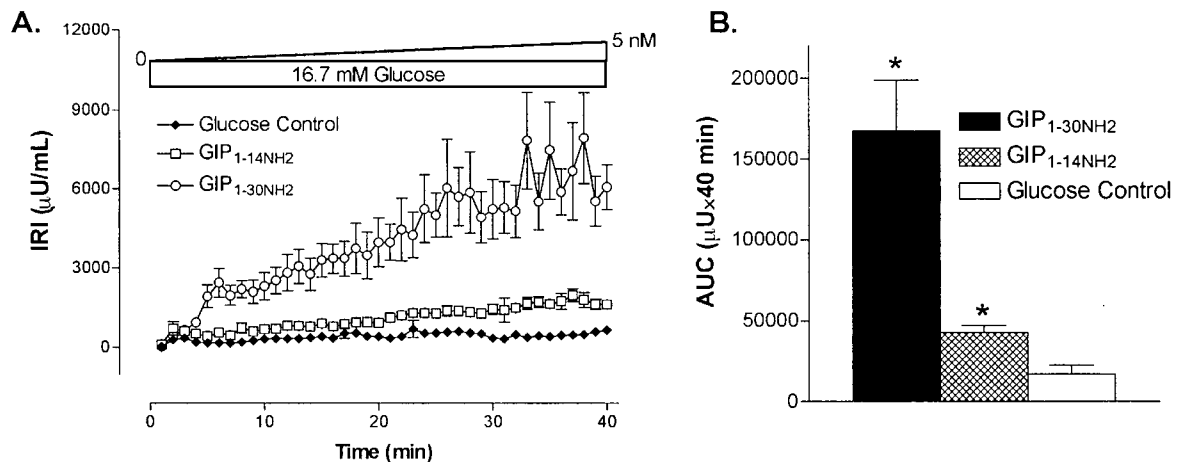
Figure 35: Pancreatic perfusion of GIP fragments in rats
(A) Immunoreactive insulin release from the perfused rat pancreas in response to 16.7 mM glucose, with or without linear peptide gradients of $GIP_{1-30NH2}$ or $GIP_{1-14NH2}$ (0 to 5 nM). (B) Integrated insulin responses for the data shown in (A). Data represent mean ± S.E.M. of 4 experiments; * = P < 0.05 versus glucose control. Perfusions were kindly performed by Nathalie Pamir (M.Sc.) and published in [455]; used with permission.
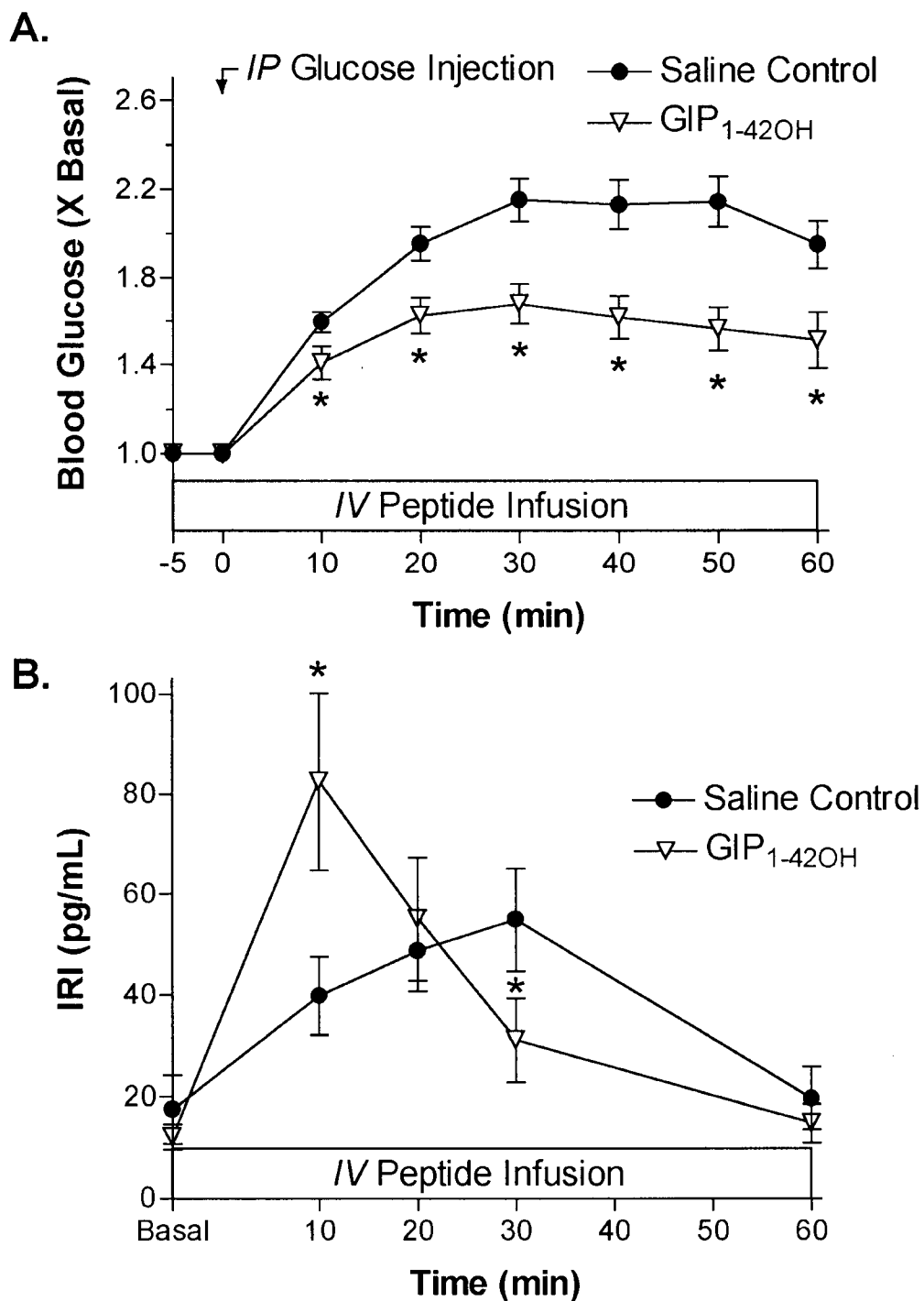
Figure 36: Bioassay of GIP$_{1-42}$ in anesthetized male Wistar rats

Glucose (A) and immunoreactive plasma insulin (B) in anesthetized male Wistar rats on intravenous infusion of saline or GIP$_{1-42}$, with concurrent intraperitoneal glucose challenge (1 g/Kg). Data represent mean ± S.E.M. of 4 animals; * = P < 0.05 versus saline control. Refer to section 2.12 of the Methods for more details.
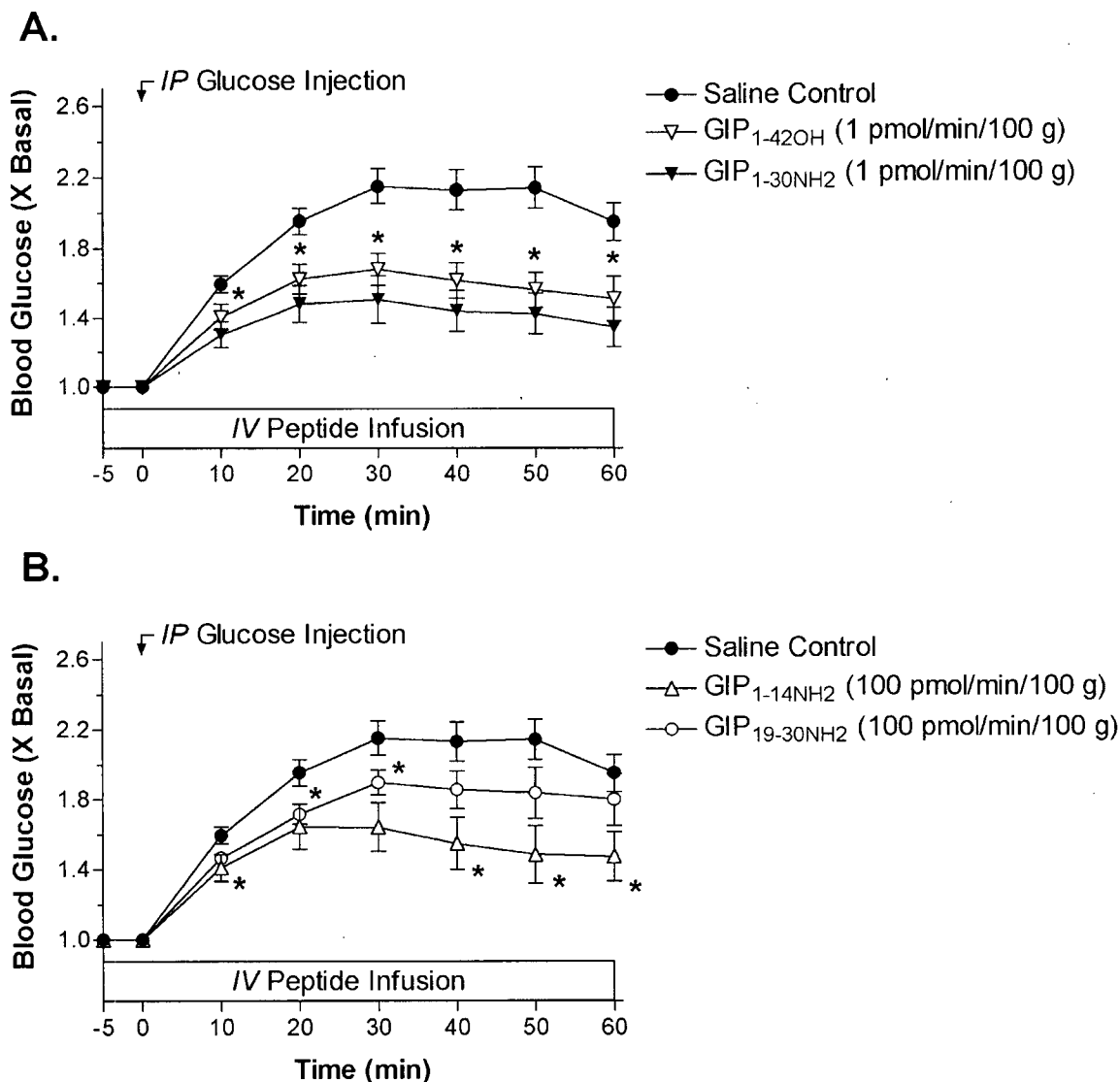
Figure 37: Glucose lowering effects of GIP fragments in anesthetized Wistar rats

(A) Peptides infused at a dosage of 1 pmol/min/100 g bw versus saline control. (B) Peptides infused at a dosage of 100 pmol/min/100 g bw versus saline control. Peptides in phosphate-buffered saline were infused intravenously, while glucose was administered by intraperitoneal injection. Glucose was monitored by tail vein measurements using a SureStep blood glucose analyzer. Data represent mean ± S.E.M. of 4 animals; * = P < 0.05 versus saline control. Refer to section 2.12 of the Methods for more details.

4.2.2 GIP_{3-42} and Studies on Cellular DPIV *in vitro*

Several experiments were performed to examine the activity of N-terminally truncated GIP_{3-42}, the peptide resulting from DPIV hydrolysis of native GIP. Synthetic GIP_{3-42} was able to completely displace ^{125}I-GIP_{1-42} binding, with an IC_{50} value of 58.4 ± 18.8 nM, significantly right-shifted from the half maximal binding displacement observed for native GIP_{1-42} at 3.56 ± 0.81 nM ($P < 0.05$). Cyclic AMP-stimulation by GIP_{3-42} was absent at concentrations as high as 10 μM (Figure 38A). When preincubated for 15 min at various concentrations, followed by addition of 1 nM GIP_{1-42} for a 30 min stimulation period, GIP_{3-42} was able to concentration-dependently antagonize native GIP-stimulated cAMP production by greater than 90% at 10 μM (Figure 38A). Furthermore, when 10 μM GIP_{3-42} was included with varied concentrations of GIP_{1-42} in a cAMP dose-response curve, the EC_{50} value was right shifted 9-fold, but did not affect maximal cAMP production (Figure 38). Taken together, results indicate that GIP_{3-42} behaves as a pure antagonist (over the concentration ranges tested), and acts in a competitive-reversible fashion (with an irreversible antagonist, a reduction in the maximal agonist stimulated cAMP level would be expected). Addition of dipeptides H_2N-Tyr-Ala-OH, H_2N-His-Ala-OH or H_2N-His-Ser-OH (corresponding to N-terminal dipeptides cleaved from GIP, GLP-1 and glucagon, respectively) in conjunction with GIP_{3-42} did not produce measurable cAMP production (Figure 38B). In this experiment, the basal cAMP level was $1.2 \pm 0.1\%$ of that stimulated by 1 nM GIP_{1-42}, whereas 10 μM GIP_{3-42} and the dipeptides (10 or 100 μM), alone or in combination produced cAMP levels between 1.2 and 1.6% of 1 nM GIP_{1-42} cAMP production in wtGIPR cells. Hence, simply the presence of the correct dipeptide is insufficient to restore biological activity to the truncated peptide. The importance of this N-terminal dipeptide was also demonstrated by the complete lack of biological activity of $[Ala^1$-$Tyr^2]GIP_{1-42}$, a full length peptide with only the first two residues switched [324; 456].

In order to quantitate any DPIV activity that may be present on CHO-K1 cells or βTC-3 cells commonly used for testing GIP bioactivity, a DPIV activity assay was performed. Figure 39A shows a DPIV standard curve using purified porcine DPIV with or without 50 μM isoleucine-thiazolidide; inclusion of the DPIV inhibitor completely blocked production of the chromogenic nitroaniline from Gly-Pro-para-nitroaniline to background levels. Cells were incubated with DPIV substrate in HEPES-buffered physiological saline with or without Ile-thia, βTC-3 cells were also additionally tested in the presence of depolarizing concentrations of KCl (30 mM) to test if DPIV activity was present within the secretory granules. When DPIV was inhibited, a non-specific level of substrate hydrolysis was observed in all cases, corresponding to approximately 8-13 $\mu U/10^6$ cells (Figure 39B). In CHO-K1 cells, specific DPIV activity was 56.5 ± 7.4 $\mu U/10^6$ cells (transfected and non-transfected cells showed no difference), and βTC-3 cells varied between 44.7 and 51.9 $\mu U/10^6$ cells, irrespective of extracellular KCl. Thence, to evaluate the importance of this specific DPIV activity during GIP bioactivity analysis, a concentration-response curve of GIP_{1-42} was performed on wtGIPR cells with or without 50 μM Ile-thia; no significant difference was observed with complete DPIV inhibition (Figure 39C), suggesting that this degree of activity is extremely low and can be considered negligible during experimentation.

A.

Legend:
- GIP$_{1-42}$
- GIP$_{3-42}$
- 1 nM GIP$_{1-42}$ + GIP$_{3-42}$
- GIP$_{1-42}$ + 10 μM GIP$_{3-42}$

Y-axis: cAMP Production (% 1 nM GIP)
X-axis: Log$_{10}$ [Peptide]

B.

Y-axis: cAMP Production (% 1 nM GIP)

1 μM GIP$_{3-42}$	−	+	−	−	−	+	+	+	+	+	+
10 μM Tyr-Ala	−	−	+	−	−	+	−	−	−	−	−
10 μM His-Ala	−	−	−	+	−	−	+	−	−	−	−
10 μM His-Ser	−	−	−	−	+	−	−	+	−	−	−
100 μM Tyr-Ala	−	−	−	−	−	−	−	−	+	−	−
100 μM His-Ala	−	−	−	−	−	−	−	−	−	+	−
100 μM Ser-Ala	−	−	−	−	−	−	−	−	−	−	+
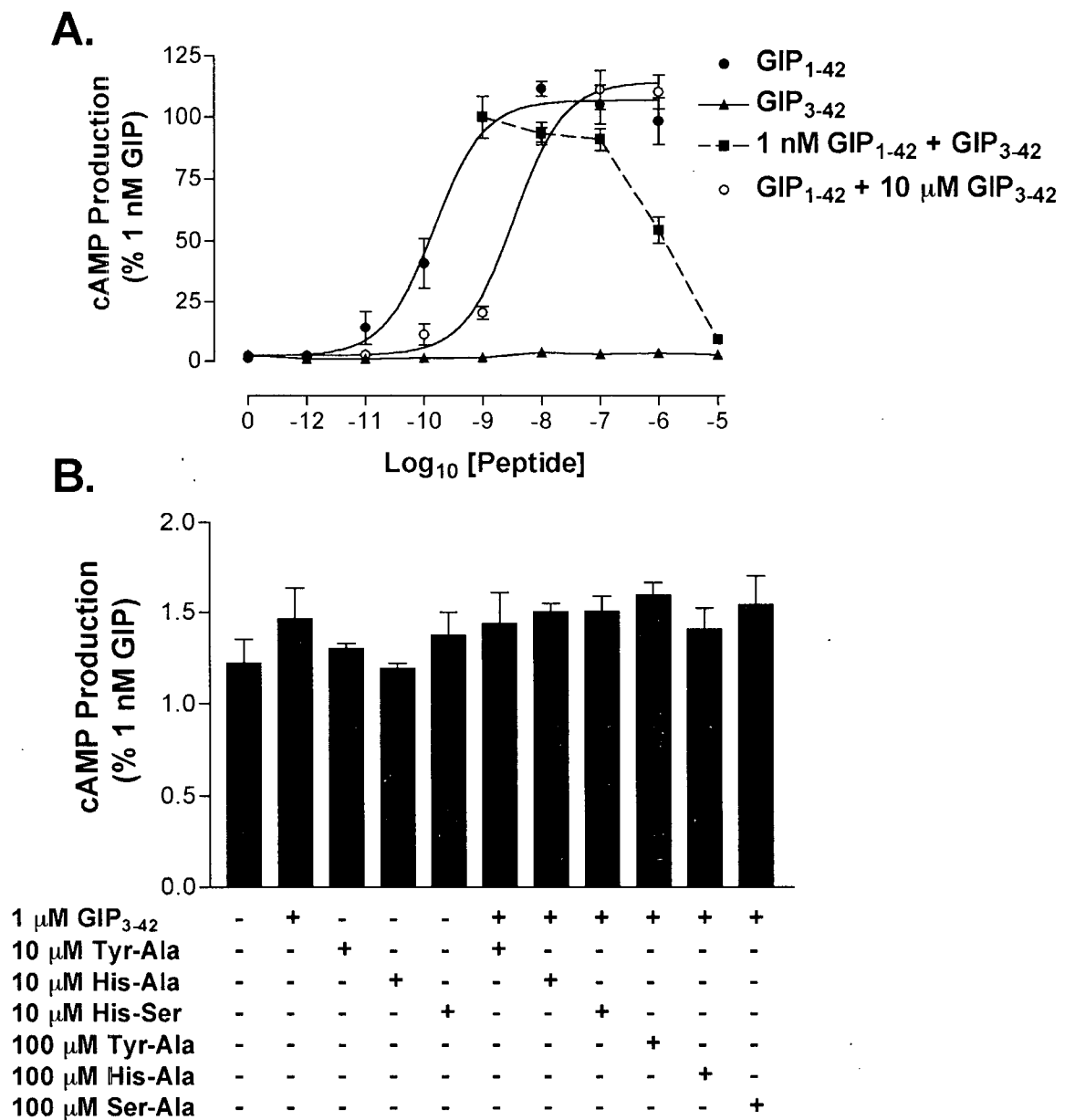
Figure 38: Competitive inhibition of GIP$_{1-42}$ by GIP$_{3-42}$

(A) Inhibition of 1 nM GIP-stimulated cAMP production by varied concentrations of GIP$_{3-42}$ (dashed line) and effect of 10 μM GIP$_{3-42}$ on GIP$_{1-42}$'s concentration-response curve. Antagonists were added 15 minutes prior to the 30 min stimulation with GIP$_{1-42}$. Stimulation of cells with 30 min of GIP$_{3-42}$ alone is also indicated. (B) Effect of 30 min co-incubation of GIP$_{3-42}$ with N-terminal dipeptides. Each data point represents the mean ± S.E.M. of 3-7 independent experiments, normalized to the cAMP level stimulated by 1 nM GIP$_{1-42}$. Refer to Methods sections 2.4 and 2.7 for more details.

A. DP IV Standard Curve

B. Whole Cell DP IV Activity

C. Cyclic AMP Production
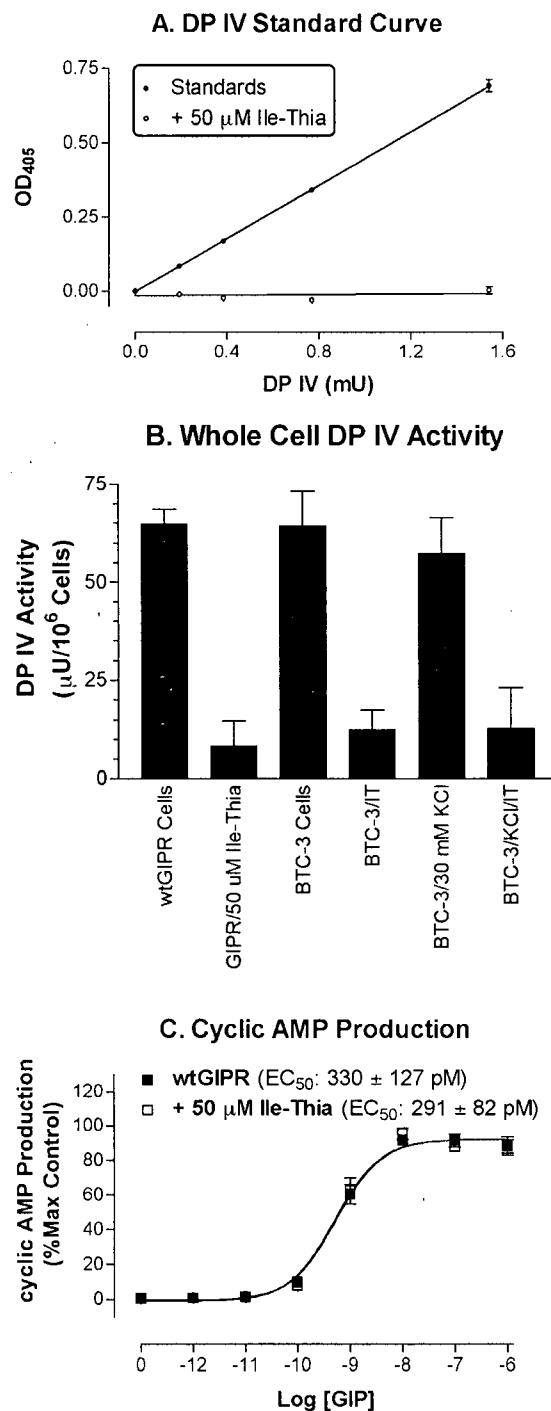
Figure 39: Cell associated DPIV activity

(A) A DPIV standard curve with and without 50 μM isoleucine-thiazolidide. (B) Hydrolysis of Gly-Pro-paranitroaniline substrate by cells in the presence or absence of Ile-thia. (C) A concentration-response curve of GIP_{1-42} on wtGIPR cells in the presence or absence of Ile-thia. Each data point represents the mean ± S.E.M. of 3 independent experiments. Refer to sections 2.7 and 2.11 of the Methods for more detail.

4.2.3 Design of DPIV-resistant GIP Analogues

Nine modified peptides were designed based on the human $GIP_{1\text{-}30NH2}$ sequence. Peptides were designed to not conform to the substrate specificity requirements of DPIV. Modified peptides include $[D\text{-}Ala^2]GIP_{1\text{-}30NH2}$, $[Tyr^1\text{-}Ala^2\psi(CH_2NH)]GIP_{1\text{-}30NH2}$ (*i.e.* a reduced peptide bond between Ala^2 and Glu^3), $[(P)Ser^2]GIP_{1\text{-}30NH2}$ (phosphoserine modified), $[N\text{-}MeGlu^3]GIP_{1\text{-}30NH2}$ (N-methylated), and a cyclized peptide, $[cyclo(Lys^{16}, Asp^{21})]GIP_{1\text{-}30NH2}$, with a 6 amino acid ring. Substituted analogues were also generated with glycine, serine or valine in position two, or proline in position 3. All peptides were tested for DPIV-resistance by MALDI-TOF mass spectrometry (K. Kühn-Wache, Probiodrug AG, Halle, Germany) [329]. Peptides could be divided into three categories: (1) those with degradation kinetics similar to native $GIP_{1\text{-}30NH2}$, which included only $[cyclo(Lys^{16},Asp^{21})]GIP_{1\text{-}30NH2}$ ($t_{1/2}$ = ~2 min with purified enzyme), (2) moderately resistant analogues, $[Gly^2]GIP_{1\text{-}30NH2}$, $[Ser^2]GIP_{1\text{-}30NH2}$, and $[Val^2]GIP_{1\text{-}30NH2}$ ($t_{1/2}$ = 137-298 min with purified enzyme), and (3) stable peptides completely resisting degradation by purified enzyme, $[D\text{-}Ala^2]GIP_{1\text{-}30NH2}$, $[Tyr^1\text{-}Ala^2\psi(CH_2NH)]GIP_{1\text{-}30NH2}$, $[(P)Ser^2]GIP_{1\text{-}30NH2}$, $[Pro^3]GIP_{1\text{-}30NH2}$ and $[N\text{-}MeGlu^3]GIP_{1\text{-}30NH2}$. Binding competition and cyclic AMP stimulation studies were performed on wtGIPR cells with all 1-30NH2 based peptides (Figure 40, Table 8). In general, all peptides were able to displace 100% of bound GIP tracer, and showed rank IC_{50} values: $GIP_{1\text{-}30NH2}$ < $[Ser^2]GIP_{1\text{-}30NH2}$ < $[Tyr^1\text{-}Ala^2\psi(CH_2NH)]GIP_{1\text{-}30NH2}$ < $[D\text{-}Ala^2]GIP_{1\text{-}30NH2}$ < $[Gly^2]GIP_{1\text{-}30NH2}$ < $[Val^2]GIP_{1\text{-}30NH2}$ < $[N\text{-}MeGlu^3]GIP_{1\text{-}30NH2}$ < $[Pro^3]GIP_{1\text{-}30NH2}$ < $[(P)Ser^2]GIP_{1\text{-}30NH2}$ < $[cyclo(Lys^{16},Asp^{21})]GIP_{1\text{-}30NH2}$ (Figure 40A). However, signalling ability did not correlate well with binding affinity (Figure 40B). $[Tyr^1\text{-}Ala^2(CH_2NH)]GIP_{1\text{-}30NH2}$, $[Pro^3]GIP_{1\text{-}30NH2}$, and $[N\text{-}MeGlu^3]GIP_{1\text{-}30NH2}$ were all unable to stimulate maximal cyclic AMP production in wtGIPR cells (Figure 40B, Table 8). Most peptides showed variable reductions in cAMP-stimulating potency, whereas only $[D\text{-}Ala^2]$ or $[Ser^2]$ substituted analogues were not significantly different from native GIP.

Table 8: Binding and cAMP statistics for modified $GIP_{1-30NH2}$ analogues

Analogue	IC_{50} (nM)	EC_{50} (nM)	cAMP (%Max)
$GIP_{1-30NH2}$	3.75 ± 0.55	0.230 ± 0.039	100
$[D-Ala^2]GIP_{1-30NH2}$	8.52 ± 2.3	0.680 ± 0.021	94.5 ± 3.7
$[Y^1A^2\psi(CH_2NH)]GIP_{1-30NH2}$	12.7 ± 1.9	ND	$17.6 \pm 2.0*$
$[Gly^2]GIP_{1-30NH2}$	11.8 ± 1.6	$3.18 \pm 0.8*$	96.2 ± 2.5
$[Ser^2]GIP_{1-30NH2}$	4.59 ± 0.34	0.289 ± 0.042	91.8 ± 5.1
$[(P)Ser^2]GIP_{1-30NH2}$	$93.1 \pm 8.6*$	$106 \pm 7*$	92.5 ± 8.4
$[Val^2]GIP_{1-30NH2}$	$17.4 \pm 1.8*$	$11.2 \pm 1.3*$	91.4 ± 3.6
$[L-Pro^3]GIP_{1-30NH2}$	$25.1 \pm 3.6*$	ND	$36.0 \pm 6.4*$
$[L-(N-Me)Glu^3]GIP_{1-30NH2}$	$23.6 \pm 2.8*$	ND	$10.5 \pm 0.4*$
$Cyclo[Lys^{16},Asp^{21}]GIP_{1-30NH2}$	$94.9 \pm 7.9*$	$3.11 \pm 1.43*$	112.7 ± 14.7

IC_{50} and EC_{50} values were determined by nonlinear regression analysis of curves shown in Figure 40 (n = 3-7).

ND = Not determined (half maximal stimulation was not achieved).

* = differ from responses to $GIP_{1-30NH2}$ by at least $P < 0.05$ as determined by one way ANOVA.
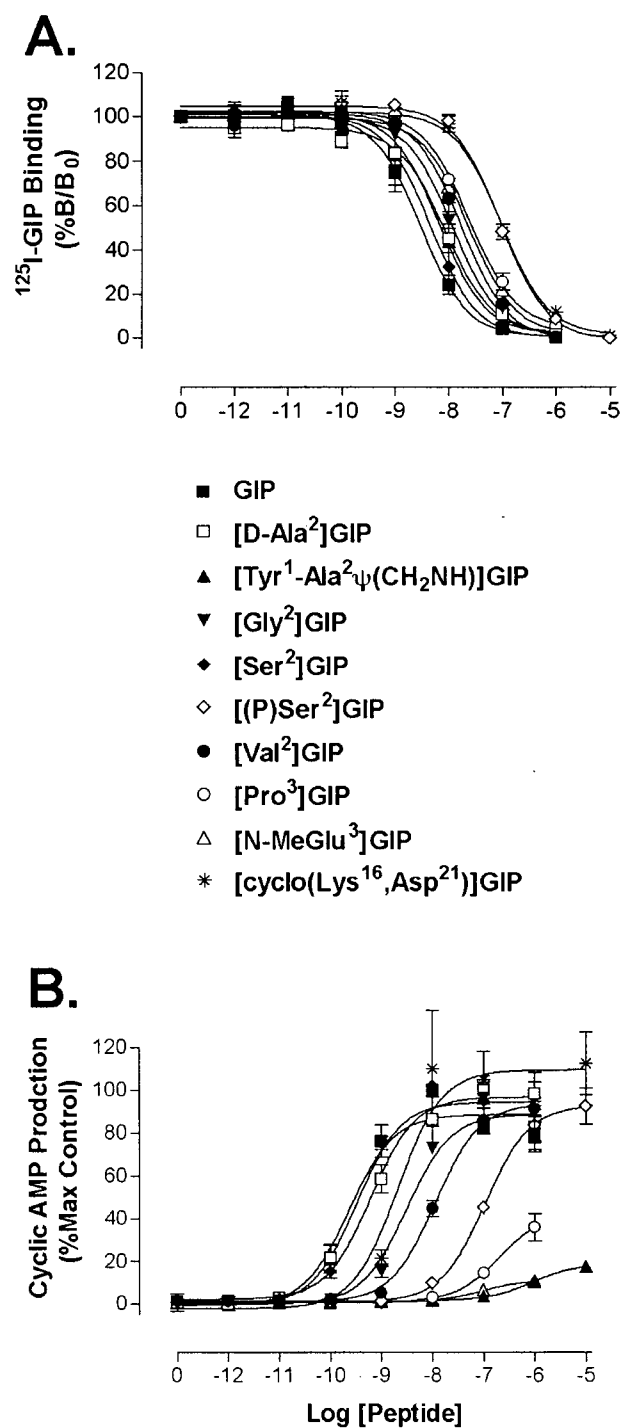
Figure 40: Binding affinity and cAMP-stimulating ability of modified GIP$_{1-30NH2}$ analogues
(A) Competitive displacement of ^{125}I-GIP binding from wtGIPR cells. (B) Concentration-response curves on wtGIPR cells. Each data point represents the mean ± S.E.M. of 3-7 independent experiments. Refer to Methods sections 2.4, 2.6 and 2.7 for more details.

4.2.4 Characterization of [D-Ala^2]GIP$_{1-42}$ *in Vitro* and *in Vivo*

4.2.4.1 In Vitro Characterization

Given the strong DPIV resistance of [D-Ala^2]GIP$_{1-30NH2}$, and minimal changes in receptor potency, this N-terminally modified analogue was resynthesized as a full length peptide. Initial studies were designed to reassess the DPIV resistance of this molecule and examine its effects on the transfected GIP receptor. Following the procedure for iodination of synthetic porcine GIP$_{1-42}$, it was possible to label [D-Ala^2]GIP$_{1-42}$ radioactively and identify peaks with intrinsic binding ability (Figure 4). Using the methodology of Kieffer *et al* [59], it was possible to separate ^{125}I-GIP$_{1-42}$ from ^{125}I-GIP$_{3-42}$ by HPLC (Figure 41). When incubated with purified porcine DPIV, ^{125}I-GIP$_{1-42}$ (R$_T$ = 14.3 ± 0.3 min) was completely degraded to ^{125}I-GIP$_{3-42}$ (R$_T$ = 10.3 ± 0.1 min), as resolved by HPLC (Figure 41A). Similar studies using monocomponent ^{125}I-[D-Ala^2]GIP$_{1-42}$ (R$_T$ = 16.4 ± 0.2 min) indicated that it was not a substrate of DPIV (Figure 41B), as no peak corresponding to ^{125}I-GIP$_{3-42}$ eluted.

Receptor binding and biological activity of GIP$_{1-42}$ and [D-Ala^2]GIP$_{1-42}$ *in vitro* were not significantly different. In binding competition assays, regardless of whether the radioligand used was ^{125}I-GIP$_{1-42}$ or ^{125}I-[D-Ala^2]GIP$_{1-42}$, IC$_{50}$ values were equivalent (Figure 42). [D-Ala^2]GIP$_{1-42}$ showed nearly equal cyclic AMP stimulating potency as native GIP on wtGIPR cells (EC$_{50}$ values: GIP$_{1-42}$, 183 ± 18 pM, [D-Ala^2]GIP$_{1-42}$, 630 ± 119 pM, p < 0.05; Figure 43). Given the *in vitro* data, we hypothesized that [D-Ala^2]GIP$_{1-42}$ may have enhanced bioactivity *in vivo* relative to native GIP, resulting from its DPIV resistance.
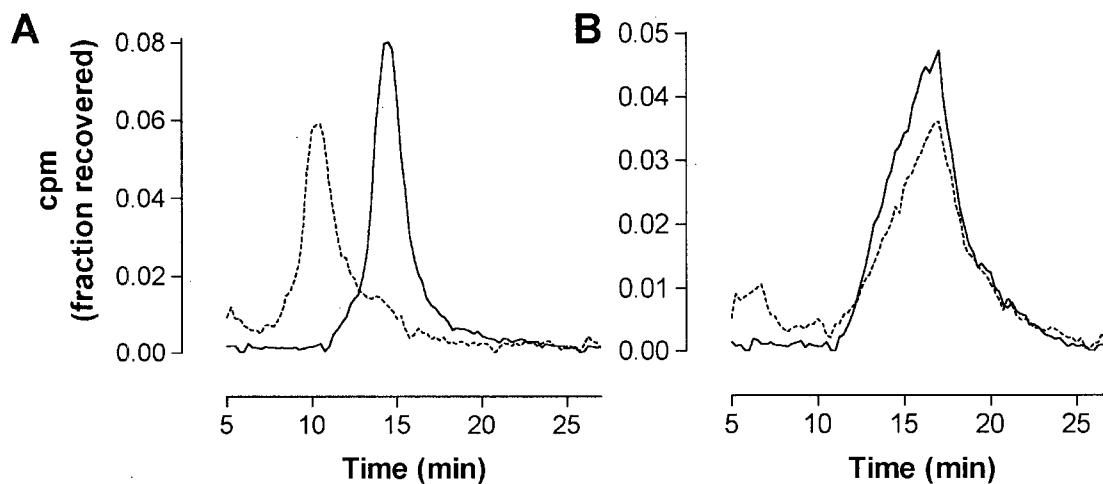
Figure 41: Incubation of ^{125}I-GIP$_{1-42}$ or ^{125}I-[D-Ala^2]GIP$_{1-42}$ with DPIV

HPLC separation of ^{125}I-GIP$_{3-42}$ from (A) ^{125}I-GIP$_{1-42}$ or (B) ^{125}I-[D-Ala^2]GIP$_{1-42}$ incubated with (dashed lines) or without (solid lines) 10 mU of dipeptidyl peptidase IV for 16 h. Iodinated peptides were separated by a protocol consisting of 14 minutes at 32% CH$_3$CN/0.1% TFA and a linear gradient to 38% CH$_3$CN/0.1% TFA over 10 min, followed by a further 5 minutes at 38% CH$_3$CN/0.1% TFA. Each trace represents the compiled results from 3-4 chromatograms. Refer to sections 2.5 and 2.11 of the Methods for more details.
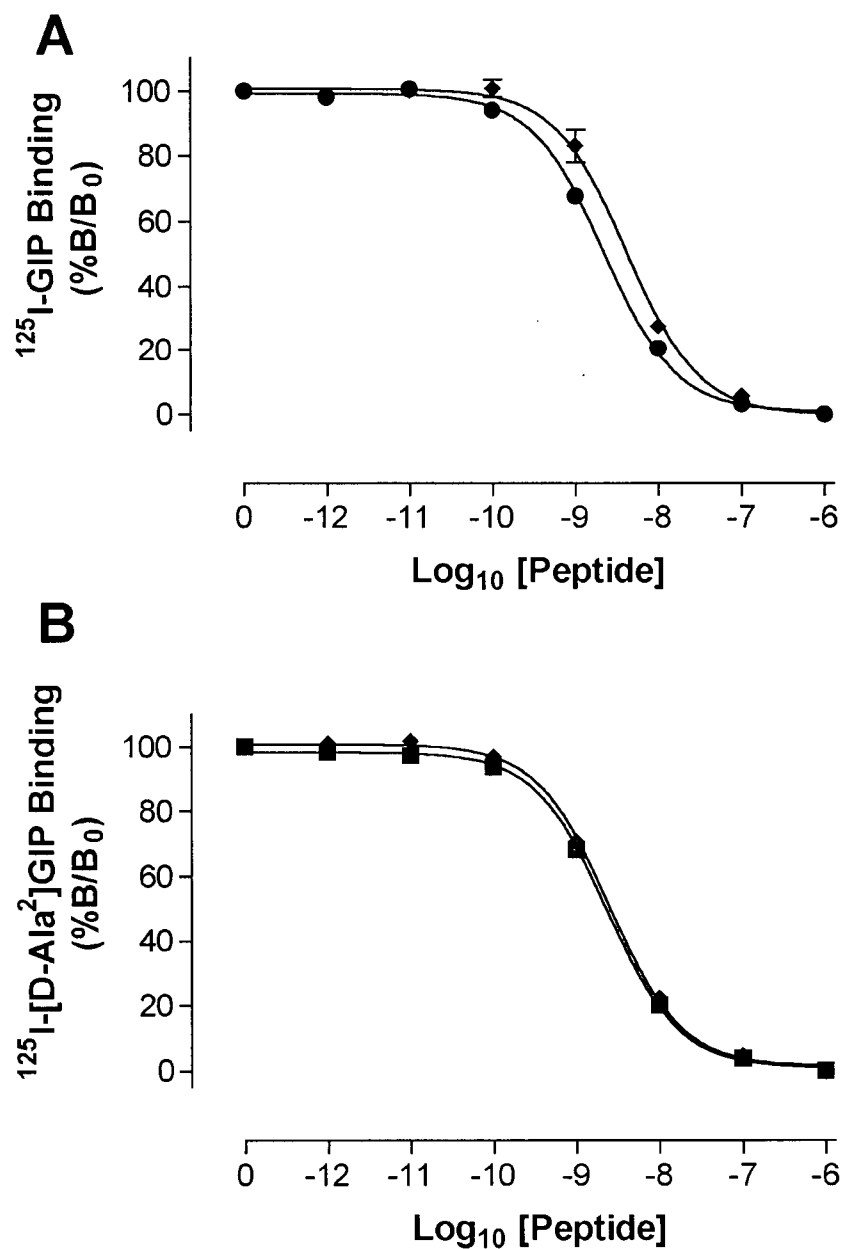
Figure 42: Binding studies using ^{125}I-GIP$_{1-42}$ or ^{125}I-[D-Ala^2]GIP$_{1-42}$ as tracer
Competitive radioligand binding studies on wtGIPR cells using (A) ^{125}I-GIP$_{1-42}$ or (B) ^{125}I-[D-Ala^2]GIP$_{1-42}$ as tracer. (A) solid circles, GIP$_{1-42}$ (IC$_{50}$ = 2.23 ± 0.18 nM), solid diamonds, [D-Ala^2]GIP$_{1-42}$ (IC$_{50}$ = 3.48 ± 0.20 nM). (B) solid circles, GIP$_{1-42}$ (IC$_{50}$ = 2.33 ± 0.18 nM), solid diamonds, [D-Ala^2]GIP$_{1-42}$ (IC$_{50}$ = 2.45 ± 0.24 nM). Each data point represents the mean ± S.E.M. of 4-5 independent experiments. Refer to Methods sections 2.4, 2.5 and 2.6 for details.
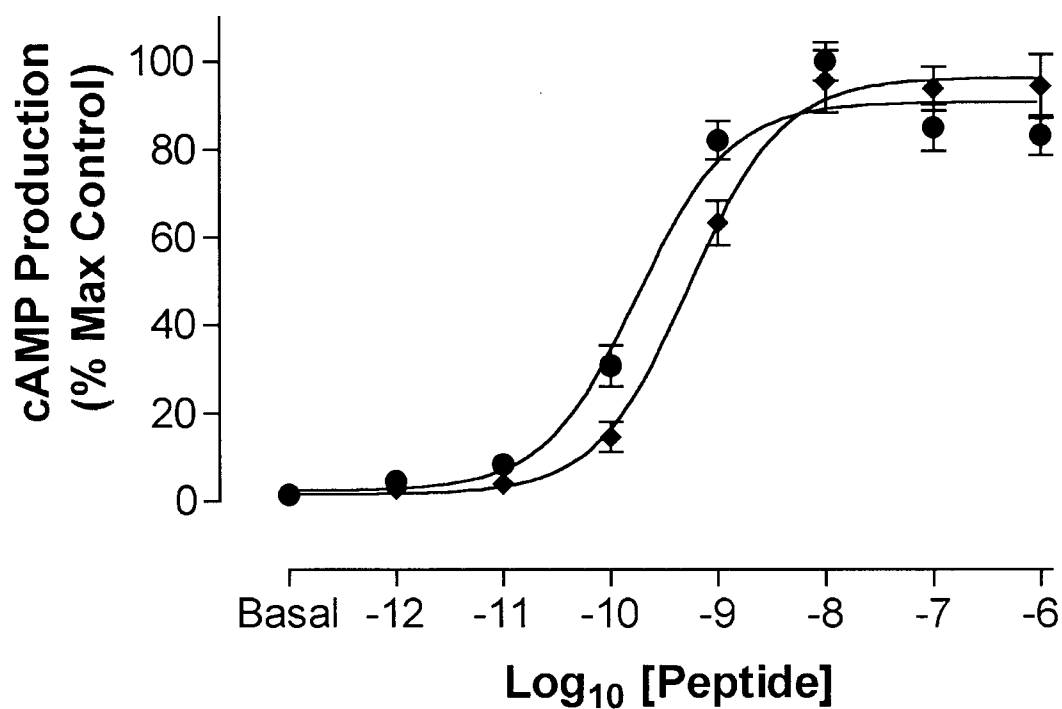
Figure 43: Bioactivity of [D-Ala^2]GIP$_{1-42}$ *in vitro*

Cyclic AMP production in wtGIPR cells by GIP$_{1-42}$ (solid circles) and [D-Ala^2]GIP$_{1-42}$ (solid diamonds). EC$_{50}$s: GIP$_{1-42}$, 183 ± 18 pM, [D-Ala^2]GIP$_{1-42}$, EC$_{50}$ = 630 ± 119 pM (p < 0.05). Each data point represents the mean ± S.E.M. of 6-8 independent experiments. Refer to Methods sections 2.4 and 2.7 for details.

4.2.4.2 In Vivo Bioassay of GIP and [D-Ala^2]GIP in Lean and Obese Rats.

Initial experiments were performed with conscious Wistar rats (287 ± 6.5 g bw, fasting glycemia = 4.7 ± 0.1 mM, fasting insulin = 87.6 ± 11.6 pM, fasting GIP = 606 ± 82 pg/mL; n ≥ 20). Subcutaneous injection of 8 nmol/Kg bw GIP$_{1-42}$ with a concurrent oral glucose tolerance test significantly reduced the glycemic profile relative to the saline control, and this was associated with increased circulating insulin levels (Figure 44). Measurement of GIP levels by RIA indicated that this dose of GIP resulted in a 10-fold greater peak GIP level (control: 1.68 ± 0.17 ng/mL, treated: 16.6 ± 3.0 ng/mL) during the OGTT. The exogenous GIP appeared to be rapidly absorbed and to follow a similar elimination profile to the endogenous GIP in control animals (Figure 44C). In contrast, the same dosage of GIP$_{3-42}$ had no effect on postprandial glycemia or insulin release (Figure 45). Subcutaneous injection of [D-Ala^2]GIP$_{1-42}$ resulted in a more pronounced reduction in the glycemic profile and an enhanced insulin time-course than native GIP during an oral glucose tolerance test (Figure 44). Notably, both GIP and D-Ala^2-modified GIP appeared to exert their glucose lowering effects by significant enhancement of the early phase of insulin release, while the latter peptide displayed more protracted bioactivity. Integrated glucose and insulin profiles can be found in Table 9.

Studies in humans with type 2 diabetes and rodent disease models have suggested that the GIP effect on insulin release and glycemia is blunted when infused at physiological concentrations [220; 375-379]. However, these studies did not address the possible therapeutic application of GIP in diabetes when administered at higher concentrations. Thus, comparison of GIP and [D-Ala^2]GIP was subsequently studied in the VDF Zucker animal model of type 2 diabetes [379]. Age matched obese animals (fa/fa; 576.1 ± 9.1 g bw) displayed significantly higher fasting glycemia than their lean (Fa/?; 335.6 ± 14.9 g bw) littermates (7.3 ± 0.3 mM versus 4.8 ± 0.1 mM) and, similarly, a fasting hyperinsulinemia (979 ± 109 pM versus 8.5 ± 2.4 pM), typical of this animal model (p < 0.05, n ≥ 20). Fasting GIP levels in these animals were

151

not significantly different (lean: 954 ± 72 pg/mL, obese: 926 ± 110 pg/mL; n ≥ 13), whereas following an OGTT in control animals, postprandial GIP levels (the mean of samples taken at t = 10, 20 and 30 min) in obese rats (1730 ± 170 pg/mL, n = 15) were significantly greater (p < 0.05) than levels in lean animals (1150 ± 120 pg/mL, n = 19). Injection of 8 nmol/Kg bw GIP_{1-42} resulted in 15.4-fold (lean) and 9.6-fold (obese) greater peak GIP levels *in vivo* after the OGTT, relative to peak values in saline control animals. In lean animals, GIP injection produced moderate reductions in postprandial glycemic levels (16.8% reduction, compared to saline control at t = 40 min using fold-basal values), whereas $[D-Ala^2]GIP_{1-42}$ was more potent (46.8% reduction at the same time-point) (Figure 46A). Similarly, in obese animals, comparison at the t = 40 min time-point indicated that GIP reduced glycemia by 18.7% and $[D-Ala^2]GIP$ by 41.5%, relative to the saline control (Figure 47A). In lean VDF Zucker rats, both peptides appeared to augment insulin release similarly, with $[D-Ala^2]GIP$ resulting in more elevated insulin levels at the first time-point (3.5 min) (Figure 46B). However, in obese rats, differences in the potencies of GIP and DPIV-resistant GIP were more evident, with insulin levels remaining at near peak values at the 60 min time-point for the $[D-Ala^2]GIP$ treated group, while insulin levels approached control values for the GIP treated group after one hour (Figure 47B). Integrated glucose and insulin profiles for bioassay data can be found in Table 9.
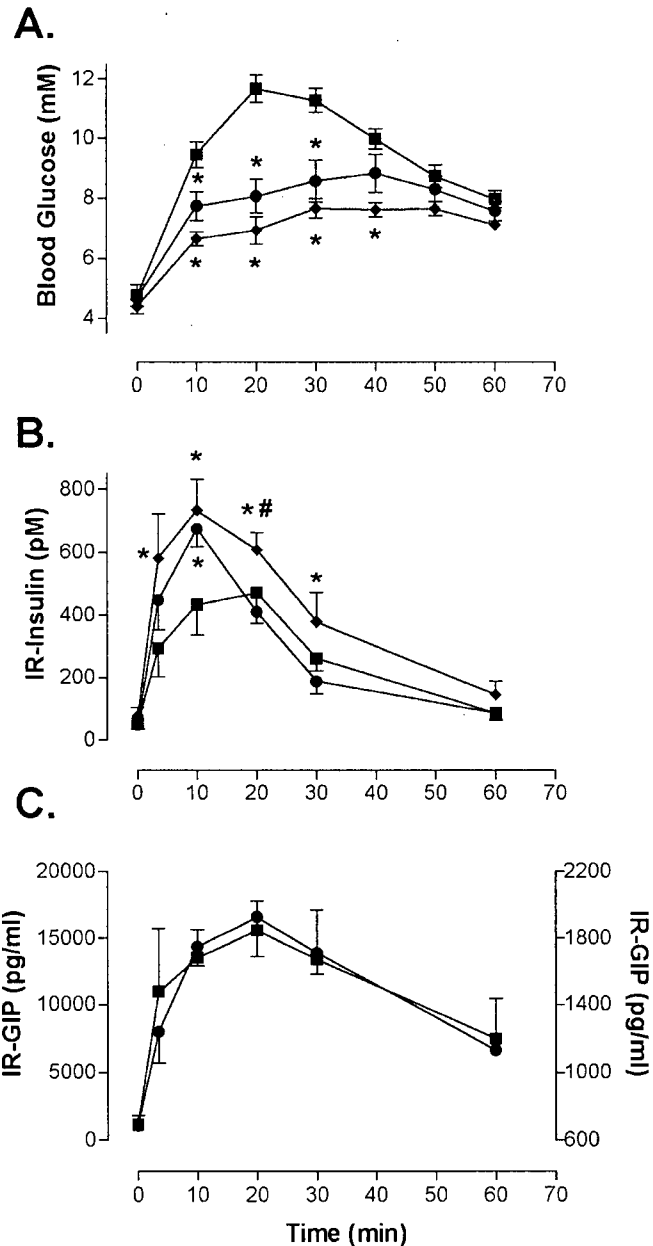
Figure 44: Bioassay of GIP$_{1-42}$ and [D-Ala^2]GIP$_{1-42}$ in Wistar rats
Bioassay of GIP$_{1-42}$ (solid circles) and [D-Ala^2]GIP$_{1-42}$ (solid diamonds) in conscious unrestrained male Wistar rats, compared to a saline control (solid squares). (A) Whole blood glycemia measured from tail vein samples. (B) Immunoreactive plasma insulin levels from tail vein samples. (C) Comparison of immunoreactive GIP profiles in control animals (endogenous GIP, solid squares, right axis) and those receiving SC GIP injection (endogenous + exogenous GIP, solid circles, left axis). Peptides (8 nmol/Kg bw in 500 μL saline) were injected SC at time 0, immediately following an OGTT (1 g/Kg bw). Each data point represents the mean ± S.E.M. of 8 animals; * = $p < 0.05$ versus saline control, # = $p < 0.05$ between peptides. Refer to sections 2.12 and 2.13 for details.

153
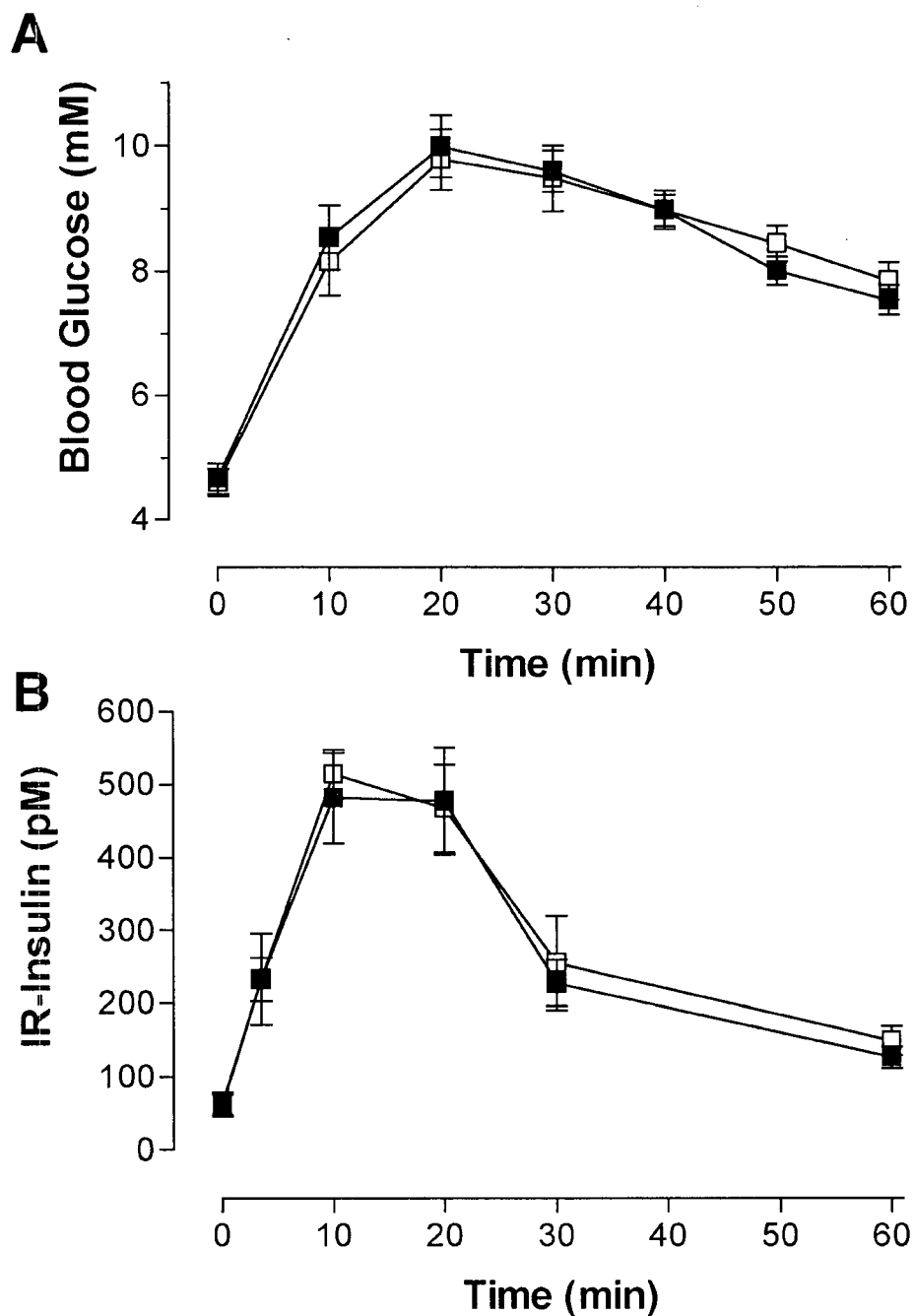
Figure 45: Bioassay of GIP$_{3-42}$ in conscious Wistar rats
(A) Whole blood glycemia measured from tail vein samples. (B) Immunoreactive plasma insulin levels from tail vein samples. GIP$_{3-42}$ (open squares, 8 nmol/Kg bw in 500 μL saline) or saline (solid squares) was injected *SC* at time 0, immediately following an OGTT (1 g/Kg bw). Each data point represents the mean ± S.E.M. of ≥5 animals. Refer to sections 2.12 and 2.13 of the Methods section for details.
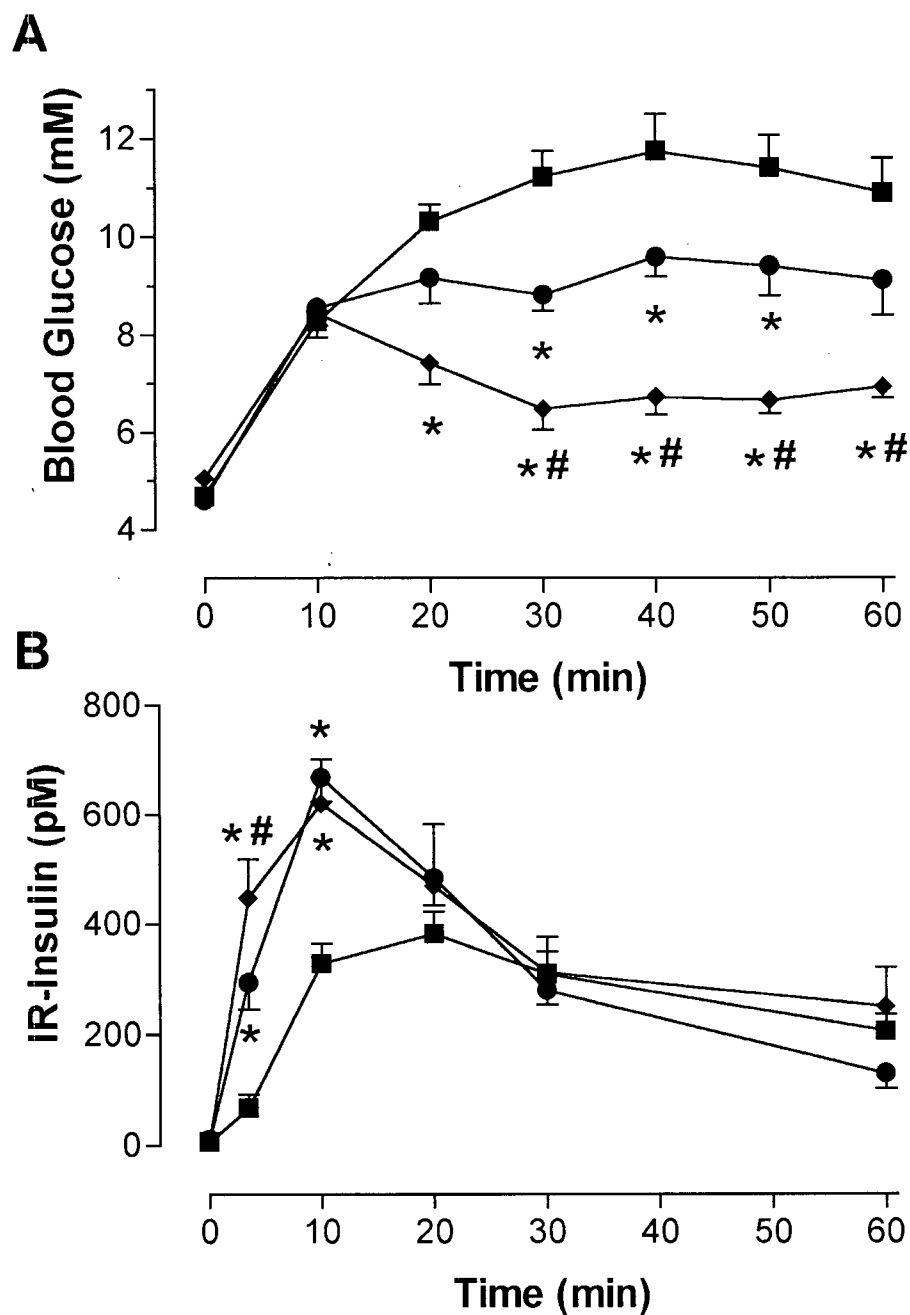
Figure 46: Bioassay of [D-Ala²]GIP$_{1-42}$ in conscious lean VDF Zucker rats

Bioassay of GIP$_{1-42}$ (solid circles) and [D-Ala²]GIP$_{1-42}$ (solid diamonds) in conscious lean (Fa/?) VDF Zucker rats versus injection of saline (solid squares). (A) Whole blood glycemia measured from tail vein samples. (B) Immunoreactive plasma insulin levels from tail vein samples. Peptides (8 nmol/Kg bw in 500 μL saline) were injected *SC* at time 0, immediately following an OGTT (1 g/Kg bw). Each data point represents the mean ± S.E.M. of 6-8 animals; * = p < 0.05 versus saline control, # = p < 0.05 between peptides. Refer to sections 2.12 and 2.13 of the Methods section for details.
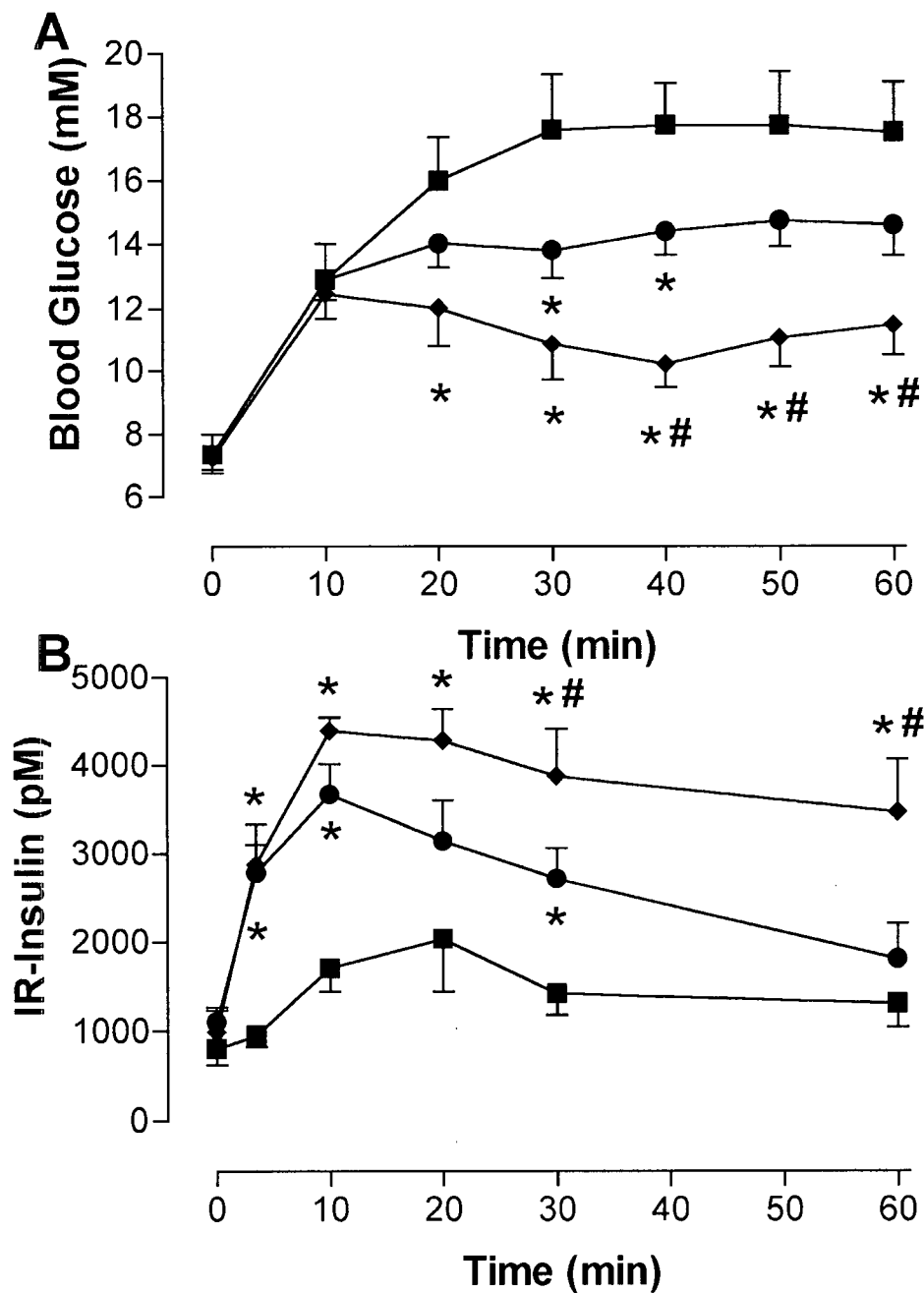
Figure 47: Bioassay of [D-Ala²]GIP₁₋₄₂ in conscious obese VDF Zucker rats

Bioassay of GIP_{1-42} (solid circles) and [D-Ala²]GIP_{1-42} (solid diamonds) in conscious obese (fa/fa) VDF Zucker rats versus saline injection (solid squares). (A) Whole blood glycemia measured from tail vein samples. (B) Immunoreactive plasma insulin levels from tail vein samples. Peptides (8 nmol/Kg bw in 500 μL saline) were injected *SC* at time 0, immediately following an OGTT (1 g/Kg bw). Each data point represents the mean ± S.E.M. of 6-8 animals; * = $p < 0.05$ versus saline control, # = $p < 0.05$ between peptides. Refer to sections 2.12 and 2.13 of the Methods section for details.

Table 9: Integrated glucose and insulin profiles for GIP and [D-Ala^2]GIP *in vivo*

Animal Model	Test	Glucose Profile (mM X 60 min)	Early Insulin Response (pM X 10 min)	Complete Insulin Profile (pM X 60 min)
Wistar Rat	Saline	289 ± 21	2538 ± 545	13258 ± 2305
	GIP	195 ± 26†	4271 ± 493†	14385 ± 1225
	[D-Ala^2]GIP	145 ± 17†	4979 ± 848†	20589 ± 2936
Lean Zucker Rat	Saline	315 ± 21	1433 ± 202	15984 ± 1512
	GIP	258 ± 15†	3225 ± 532†	18570 ± 1094
	[D-Ala^2]GIP	113 ± 13†‡	4168 ± 553†	21178 ± 3759
Fat Zucker Rat	Saline	503 ± 68	4463 ± 1584	44912 ± 15378
	GIP	368 ± 43†	16763 ± 2641†	93488 ± 15674†
	[D-Ala^2]GIP	226 ± 32†‡	20467 ± 1177†	165573 ± 14792†‡

*Data represent the area under the curve (AUC) of data shown in Figures 44, 46, and 47.
†: $p < 0.05$ compared to saline control.
‡: $p < 0.05$ compared to GIP test.

4.2.5 Parallel Comparison of [Ser^2] and [(P)Ser^2] Substituted GIP and GLP-1

Although [Ser^2]GIP$_{1-30NH2}$ was only moderately resistant to DPIV degradation [329], it had favourable binding and signalling characteristics at the cloned GIP receptor (Figure 40, Table 8). [Ser^2]GLP-1$_{7-36NH2}$ has been previously reported to display enhanced antidiabetogenic activity owing to its reduced degradation by DPIV [457-459]. In our examination of degradation of glucagon, which normally has a serine in position 2, we found that modification of serine with a phosphate group, [(P)Ser^2], resulted in complete resistance to purified DPIV, and this molecule was time-dependently dephosphorylated in serum (see next section). Hence, a study was designed to examine GIP, GLP-1, along with [Ser^2] and [(P)Ser^2] substituted analogues in parallel. Analogues were tested *in vitro* for DPIV resistance (K. Kühn-Wache; $t_{1/2}$ values: native peptides, ~2 min; [Ser^2]incretins, ~137-686 min; [(P)Ser^2]incretins, completely resistant), and potency on cells transfected with the GIP or GLP-1 receptors. *In vivo* studies followed the conscious unrestrained male Wistar rat bioassay protocol with respect to glycemic excursions and insulin profiles (Methods section 2.12).

4.2.5.1 In Vitro Binding and Bioactivity

Initial studies were directed at characterizing peptide analogues *in vitro*. Using CHO-K1 cells transfected with the GIP or GLP-1 receptor (GIPR and GLP-1R cells, respectively), it was possible to compare [Ser^2] and [(P)Ser^2]-substituted incretin analogues, with respect to receptor binding affinity and ability to activate the adenylyl cyclase/cyclic AMP cascade. Native GIP$_{1-42}$ was able to displace 50% of ^{125}I-GIP binding to GIPR cells at a concentration of ~4.5 nM (Figure 48A). The IC$_{50}$ of [Ser^2]GIP was slightly greater (1.4X; P > 0.05), and the affinity of [(P)Ser^2]GIP was significantly reduced 21X (P < 0.05; Figure 48A). All three peptides were able to fully displace specific ^{125}I-GIP binding. When examining GIP receptor activation by these peptides, a similar pattern was observed. GIP and [Ser^2]GIP displayed EC$_{50}$ values ranging between 245-289 pM (P > 0.05), but the concentration-response curve for [(P)Ser^2]GIP was significantly right shifted (433X; P < 0.05; Figure 48B). However, the GIP analogues were able to produce maximal cyclic AMP stimulation in GIPR cells similar to that of native hormone (Figure 48B).

Receptor binding of GLP-1 and analogues to the transfected GLP-1 receptor are shown in Figure 49A. The binding affinity of GLP-1 for the GLP-1 receptor was similar to that of GIP for the GIP receptor, having an IC$_{50}$ on the order of ~4.3 nM. The concentration of [Ser^2]GLP-1 required to displace 50% of ^{125}I-GLP-1 binding was ~8.1 nM, or 1.9X lower affinity than native hormone (P > 0.05; Figure 49A). As was the case with [(P)Ser^2]GIP peptide, [(P)Ser^2]GLP-1 showed significantly lower affinity for its respective receptor, with an IC$_{50}$ value right shifted by 284X (P < 0.05). GLP-1, [Ser^2]GLP-1 and [(P)Ser^2]GLP-1 were all able to fully compete with ^{125}I-GLP-1 binding to the GLP-1 receptor (Figure 49A). The cyclic AMP EC$_{50}$ values parallel results for binding affinity, with rank potency being: GLP-1 > [Ser^2]GLP-1 > [(P)Ser^2]GLP-1. While the potency of [Ser^2]GLP-1 was found to be 3.3-fold lower than native GLP-1, statistical

significance was not reached (P > 0.05), however, the EC_{50} value of [(P)Ser^2]GLP-1 was significantly reduced by three orders of magnitude (P < 0.05; Figure 49B).

A.

B.
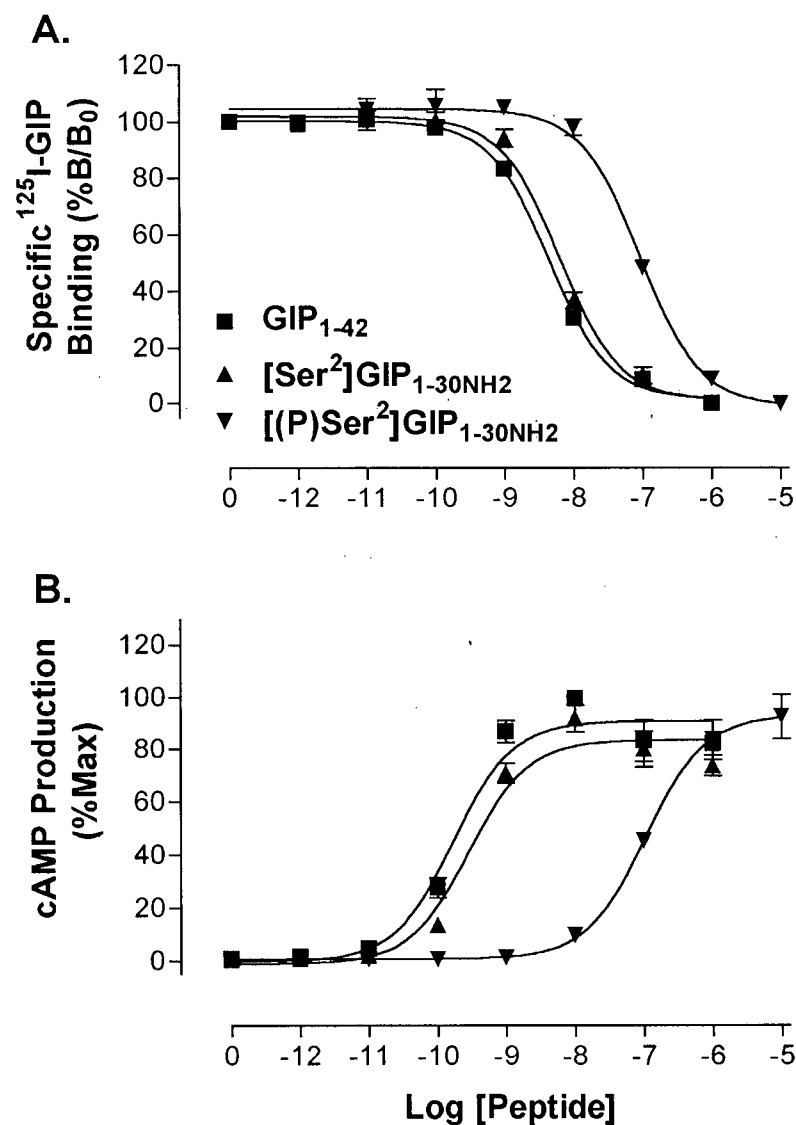
Figure 48: Binding and cAMP stimulation in wtGIPR cells by GIP$_{1-42}$, [Ser^2]GIP$_{1-30NH2}$ and [(P)Ser^2]GIP$_{1-30NH2}$

(A) Competitive-binding inhibition of ^{125}I-GIP$_{1-42}$. IC_{50} values (nM): GIP$_{1-42}$, 4.49 ± 0.55; [Ser^2]GIP$_{1-30NH2}$, 6.40 ± 0.73; [(P)Ser^2]GIP$_{1-30NH2}$, 93.1 ± 8.6. (B) Cyclic AMP stimulation in wtGIPR cells. EC_{50} values (nM): GIP$_{1-42}$, 0.245 ± 0.063; [Ser^2]GIP$_{1-30NH2}$, 0.289 ± 0.042; [(P)Ser^2]GIP$_{1-30NH2}$, 106 ± 7. Each data point represents the mean ± S.E.M. of ≥ 4 independent experiments. Refer to sections 2.4, 2.5, 2.6 and 2.7 of the Methods for details.
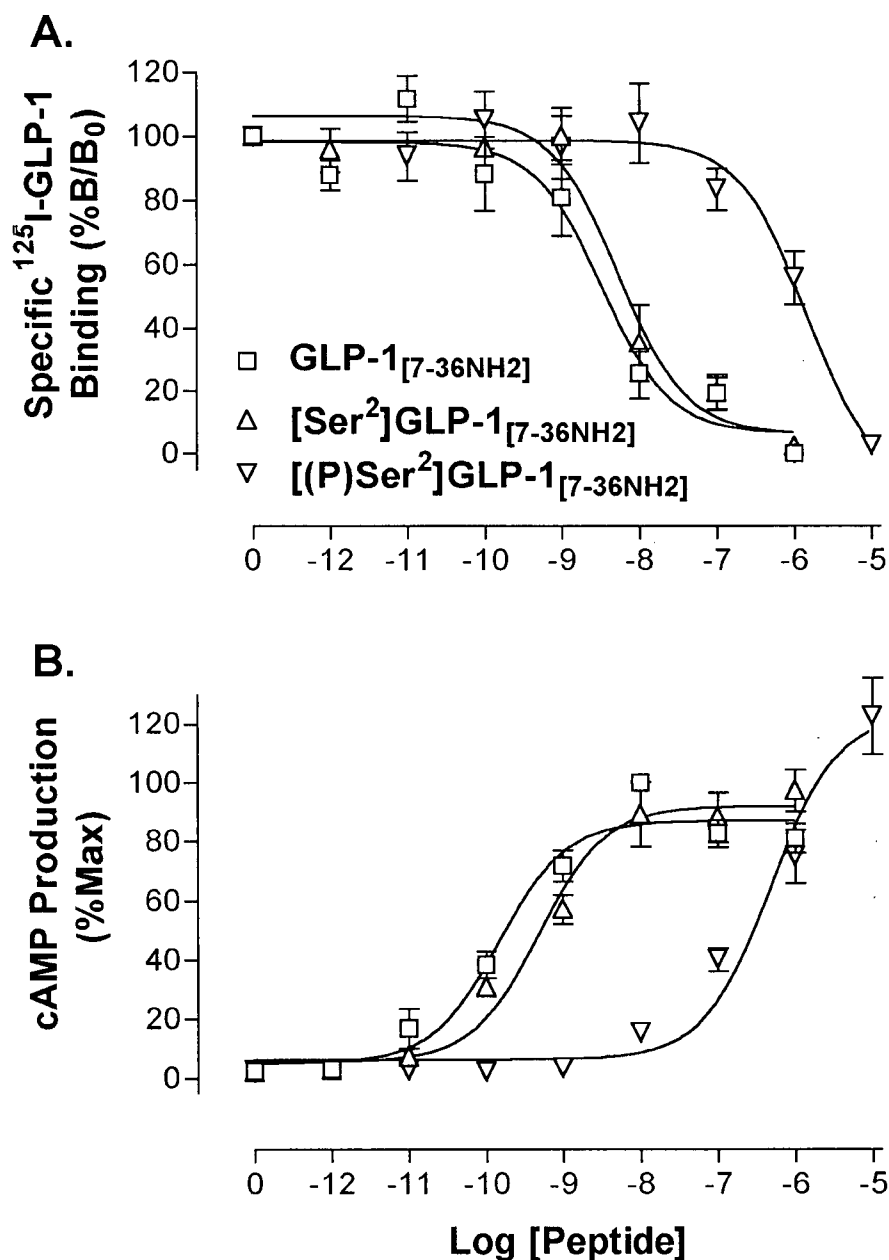
Figure 49: Binding and cAMP stimulation in wtGLP-1R cells by GLP-1$_{7-36NH2}$, [Ser^2]GLP-1$_{7-36NH2}$ and [(P)Ser^2]GLP-1$_{7-36NH2}$

(A) Competitive-binding inhibition of ^{125}I-GLP-1$_{7-36NH2}$. IC$_{50}$ values (nM): GLP-1$_{7-36NH2}$, 4.26 ± 1.19; [Ser^2]GLP-1$_{7-36NH2}$, 8.08 ± 3.11; [(P)Ser^2]GLP-1$_{7-36NH2}$, 1210 ± 430. (B) Cyclic AMP stimulation in wtGLP-1R cells. EC$_{50}$ values (nM): GLP-1$_{7-36NH2}$, 0.155 ± 0.042; [Ser^2]GLP-1$_{7-36NH2}$, 0.509 ± 0.119; [(P)Ser^2]GLP-1$_{7-36NH2}$, 513 ± 107. Each data point represents the mean ± S.E.M. of ≥ 4 independent experiments. Refer to sections 2.4, 2.5, 2.6 and 2.7 of the Methods for details.

4.2.5.2 In Vivo Bioassay

Initial experiments were performed with conscious Wistar rats (312 ± 20 g bw, fasting glycemia = 4.3 ± 0.1 mM, fasting insulin = 72.2 ± 7.5 pM, n = 54; fasting GIP = 897 ± 49 pg/mL, fasting GLP-1 = 13.4 ± 1.2 pg/mL; $n \geq 9$). Subcutaneous injection of 8 nmol/Kg bw GIP_{1-42} or $GLP-1_{7-36NH2}$ with a concurrent oral glucose tolerance test significantly reduced the glycemic profile relative to the saline control, and this was associated with increased "early phase" circulating insulin levels (Figure 50); GIP reduced the integrated glycemic excursion by 27.7% and GLP-1 was slightly more effective, reducing the area under the curve by 33.9% ($P > 0.05$, n = 6; Table 10). Measurement of hormone levels by RIA indicated that this dose of peptide resulted in a 9-fold greater peak GIP level (control: 1.60 ± 0.10 ng/mL, treated: 14.3 ± 0.4 ng/mL) and a 2-fold greater peak GLP-1 level (control: 24.0 ± 5.7 pg/mL, treated: 48.4 ± 6.0 pg/mL) during the OGTT. The difference in the values for GIP and GLP-1, despite identical dosages likely reflects the differing pharmacokinetics of the two hormones. Given that their insulinotropic potency was similar, it can be inferred that the mode of action of GIP and GLP-1 is rapid, as is their inactivation by N-terminal dipeptide cleavage, such that peptide pharmacokinetics do not noticeably affect their biological activity in this assay system. Subcutaneous injection of $[Ser^2]GIP_{1-30NH2}$ resulted in a slightly more pronounced reduction in the glycemic profile and an enhanced insulin time-course during an oral glucose tolerance test, as did $[Ser^2]GLP-1$ (Figure 50, Table 10), however, insulin profiles were not remarkably different from those observed during native hormone administration. Equivalent doses (8 nmol/Kg) of $[(P)Ser^2]$ substituted incretin analogues reduced the blood glucose profile between 31 and 44%, with $[(P)Ser^2]GIP_{1-30NH2}$ being more potent than $[(P)Ser^2]GLP-1_{7-36NH2}$, however, insulin responses at the first time-point sampled (3.5 min) were greatly reduced compared to other peptides tested, and were not significantly different from the control values. Increasing the dosage of phosphoserine[2] incretin analogues to 80 nmol/Kg replaced this deficit, allowing greater reduction

161

in the glycemic profile, and significantly enhanced insulin responses (Figure 51, Table 10).

Differences between GIP and GLP-1 analogues with [(P)Ser^2] substitution were less pronounced

than for native or [Ser^2] substituted peptides. Despite the difference in shape of the glycemic

profile for GIP and GLP-1, the overall antidiabetic potency of the peptides appeared to be very

similar.

Table 10: Integrated glucose and insulin profiles for GIP, GLP-1, [Ser^2]- and [(P)Ser^2]-substituted analogues *in vivo*

Test	Glucose Profile (mM X 60 min)	Early Insulin Response (nM X 10 min)	Complete Insulin Profile (nM X 60 min)
Saline	292 ± 16	1.91 ± 0.35	13.5 ± 2.0
GIP$_{1-42}$	211 ± 18*	3.35 ± 0.38*	15.7 ± 3.4
[Ser^2]GIP$_{1-30}$	188 ± 24*	3.31 ± 0.55*	16.9 ± 2.4
[(P)Ser^2]GIP$_{1-30}$	163 ± 29*	2.21 ± 0.50	15.2 ± 1.2
10X [(P)Ser^2]GIP$_{1-30}$	138 ± 30*	3.35 ± 0.75*	19.5 ± 3.9*
GLP-1$_{17-36NH2}$	193 ± 26*	2.73 ± 0.60	14.0 ± 2.4
[Ser^2]GLP-1$_{17-36NH2}$	156 ± 27*	2.99 ± 0.39*	17.2 ± 4.3
[(P)Ser^2]GLP-1$_{17-36NH2}$	202 ± 30*	2.29 ± 0.45	14.6 ± 2.4
10X [(P)Ser^2]GLP-1$_{17-36NH2}$	123 ± 16*	3.65 ± 0.69*	16.7 ± 5.5

Data represent the area under the curve (AUC) of data shown in Figures 50 and 51.
* = P < 0.05 compared to saline control

A.

B.

Time (min)
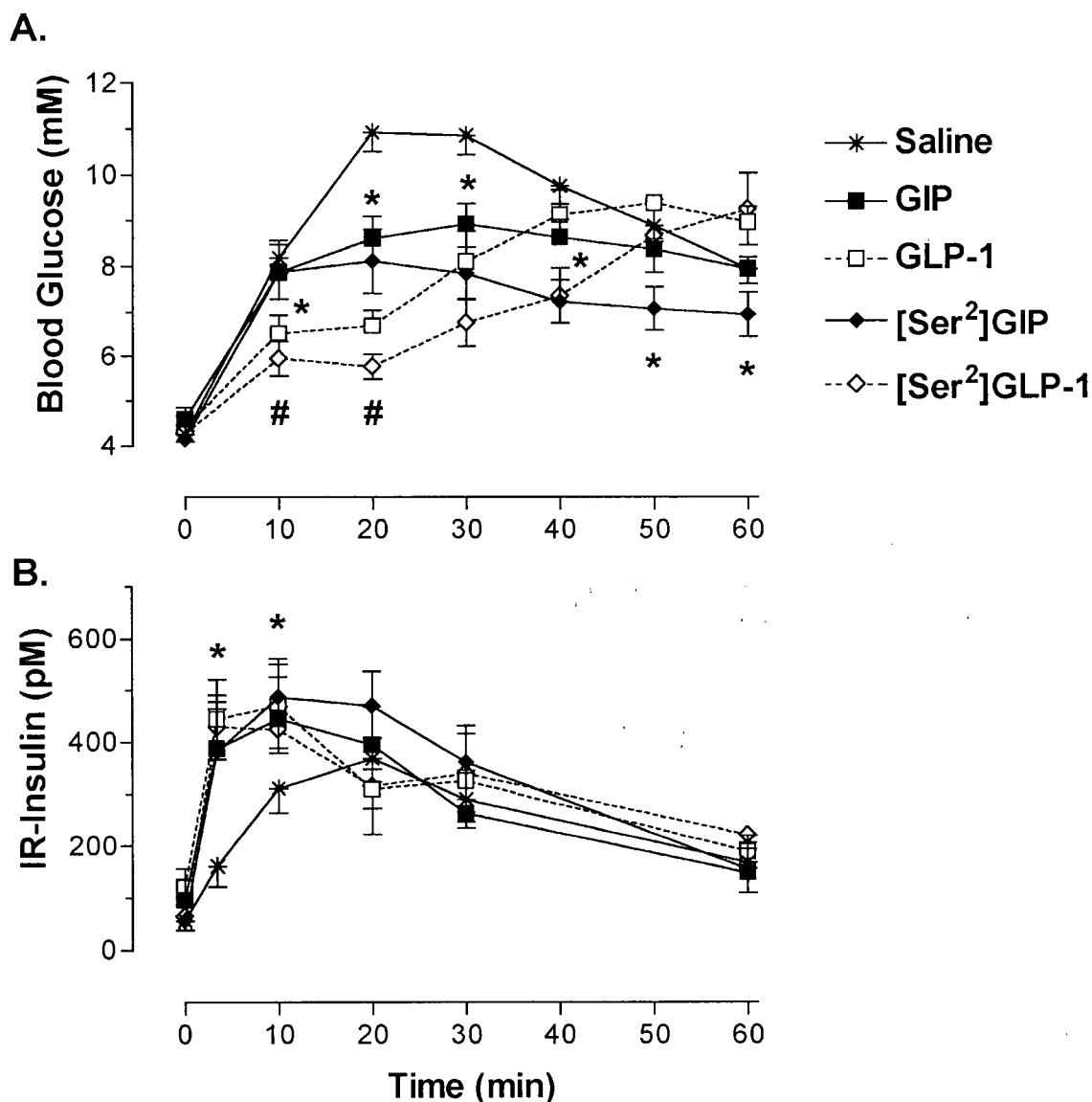
Figure 50: Bioassay of native and Ser²-substituted incretin analogues in Wistar rats
Bioassay of GIP_{1-42}, $[Ser^2]GIP_{1-30NH2}$, $GLP-1_{7-36NH2}$ and $[Ser^2]GLP-1_{7-36NH2}$ in conscious unrestrained male Wistar rats, compared to a saline control. (A) Whole blood glycemia measured from tail vein samples. (B) Immunoreactive plasma insulin levels from tail vein samples. Peptides (8 nmol/Kg bw in 500 μL saline) were injected *SC* at time 0, immediately following an OGTT (1 g/Kg bw). Each data point represents the mean ± S.E.M. of 6 animals; * = p < 0.05 versus saline control, # = p < 0.05 between peptides. Refer to sections 2.12 and 2.13 of the Methods for details.

163
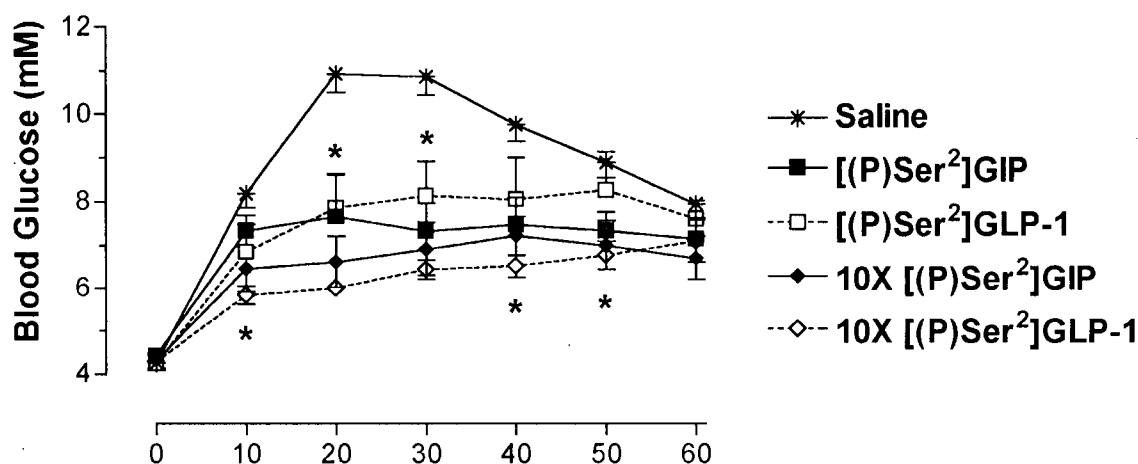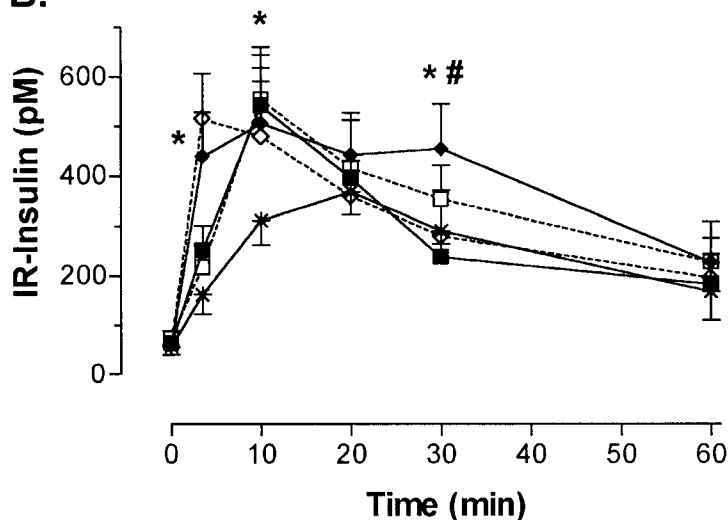
Figure 51: Bioassay of Phosphoser²-substituted incretin analogues in Wistar rats

Bioassay of $[(P)Ser^2]GIP_{1-30NH2}$ and $[(P)Ser^2]GLP-1_{7-36NH2}$ in conscious unrestrained male Wistar rats, compared to a saline control. (A) Whole blood glycemia measured from tail vein samples. (B) Immunoreactive plasma insulin levels from tail vein samples. Peptides (8 or 80 nmol/Kg bw in 500 μL saline) were injected *SC* at time 0, immediately following an OGTT (1 g/Kg bw). Each data point represents the mean ± S.E.M. of 6 animals; * = $p < 0.05$ versus saline control, # = $p < 0.05$ between peptides. Refer to sections 2.12 and 2.13 of the Methods for details.

4.2.6 DPIV Degradation of Glucagon and DPIV-resistant Glucagon Analogues

Mass spectrometry studies with serum and purified DPIV suggested that glucagon$_{1-29}$ was also a substrate for DPIV [328; 453]. Purified pork kidney DPIV hydrolyzed glucagon$_{1-29}$ to glucagon$_{3-29}$ and glucagon$_{5-29}$ *in vitro* and, in human serum, it was converted first to glucagon$_{3-29}$, and subsequently its amino terminus is cyclized by a serum enzyme (possibly to pyroglutamyl-glucagon$_{3-29}$ {[pGlu^3]glucagon$_{3-29}$}), thus preventing further DPIV degradation. Thus, in order to characterize further the potential role these N-terminally truncated peptides might have, they were bioassayed *in vivo* and tested for binding and stimulatory action at the cloned transfected human glucagon receptor. Furthermore, a series of N-terminally modified glucagon analogues was generated to test if DPIV resistance may confer enhanced *in vivo* bioactivity.

4.2.6.1 DPIV Cleavage Inactivates Glucagon

In an initial study into the effects of purified porcine DPIV on glucagon, 2 nmol of glucagon$_{1-29}$ dissolved in 1 mL PBS, was incubated with purified DPIV (0.31 Units) with or without 50 μM Isoleucine-thiazolidide at 37°C for 3.25 hours. When injected *IV* (~7.1 nmol/Kg) into anesthetized male Wistar rats (225-275 g; not fasted), glycemic profiles for control glucagon injection (incubation in saline alone) and that observed for injection of glucagon incubated with DPIV and Ile-thia were superimposable (Figure 52). In contrast, injection of peptide incubated with DPIV alone showed little effect on the blood glucose profile. Mass spectrometry identified glucagon$_{3-29}$ and glucagon$_{5-29}$ as degradation products with purified enzyme, and glucagon$_{3-29}$ and [pGlu^3]glucagon$_{3-29}$ were identified in serum incubations [328; 453]. Bioassay of these peptides by subcutaneous injection (71 nmol/Kg) produced no significant alteration from basal glycemia, while glucagon$_{1-29}$ (7.1 nmol/Kg) caused mobilization of glycogen stores to potently raise blood sugar levels (Figure 53). Incubation of monocomponent ^{125}I-glucagon$_{1-29}$ with purified DPIV without Ile-thia in PBS for 2 hours at 37°C prior to separation by HPLC allowed identification of

a single peak with a slightly longer retention time to that of control tracer incubation or incubation in the presence of Ile-thia (Figure 54). It is likely that the gradient conditions were not suitable for the separation of glucagon$_{3-29}$ and glucagon$_{5-29}$.
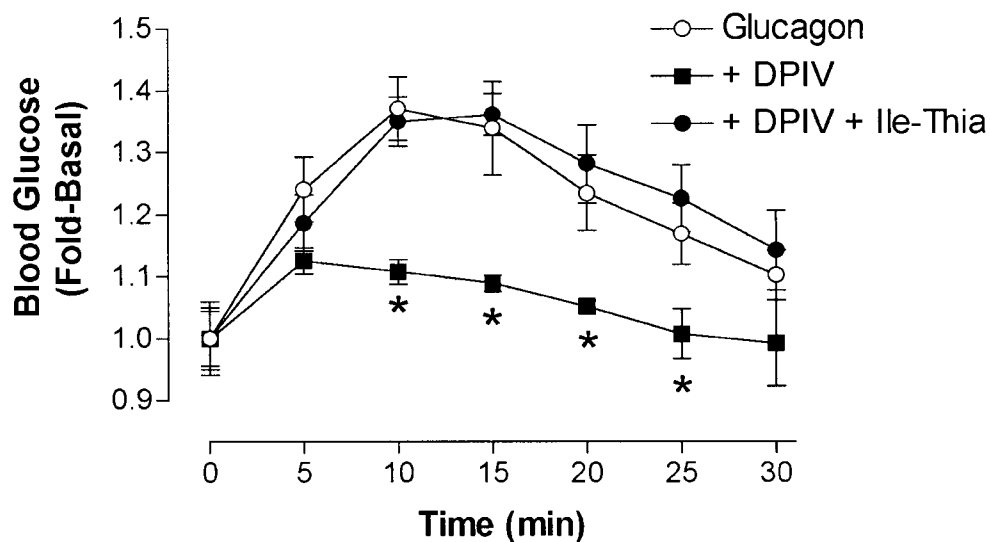
Figure 52: Inhibition of DPIV degradation of glucagon by Ile-thia monitored by bioassay
Glucagon (2 nmol) was incubated (37°C, 3.25 h) in saline with purified DPIV in the presence or absence of Ile-thia (50 µM), prior to intravenous injection in anesthetized male Wistar rats. Data are mean ± S.E.M. (n = 4); * p < 0.05. Refer to section 2.12 of the methods for more details.
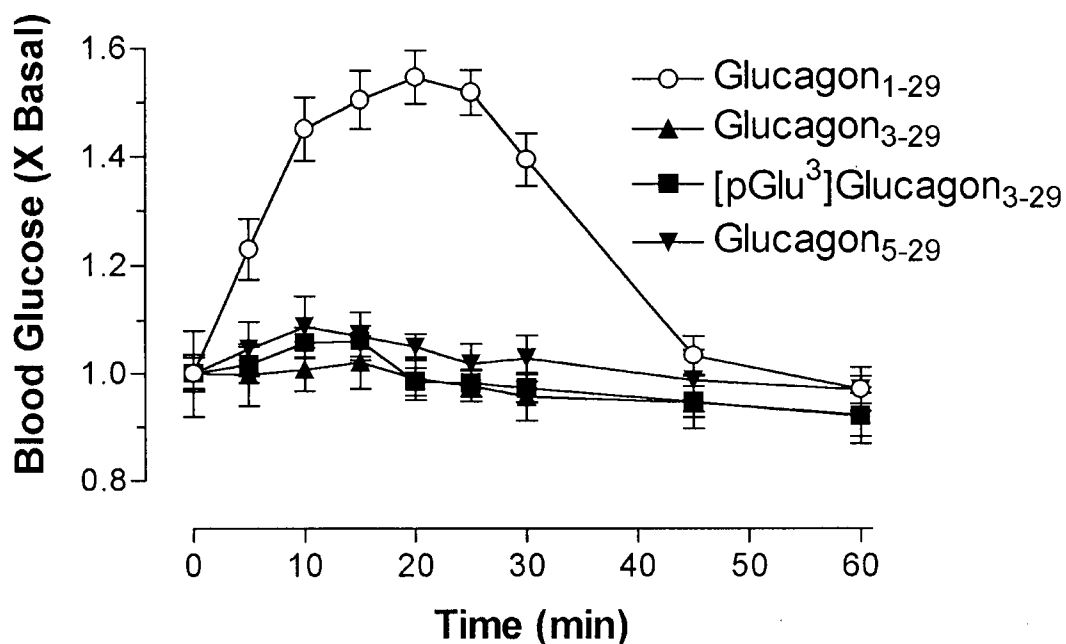
Figure 53: Bioactivity of glucagon and N-terminally truncated analogues *in vivo*
Glucagon (7.1 nmol/Kg) or N-terminally truncated glucagon analogues (71 nmol/Kg) were injected *SC* into conscious unrestrained (fed, not-fasted) male Wistar rats. Blood glucose was monitored via the tail vein and a hand-held glucometer. Data are mean ± S.E.M. (n = 6). Experimental work for this figure was performed by J. Andrew Pospisilik (B.Sc.) and published in [453]; used with permission.

HPLC Profile of pure ^{125}I-Glucagon

HPLC Profile ^{125}I-Glucagon Incubated With Purified Porcine DPIV
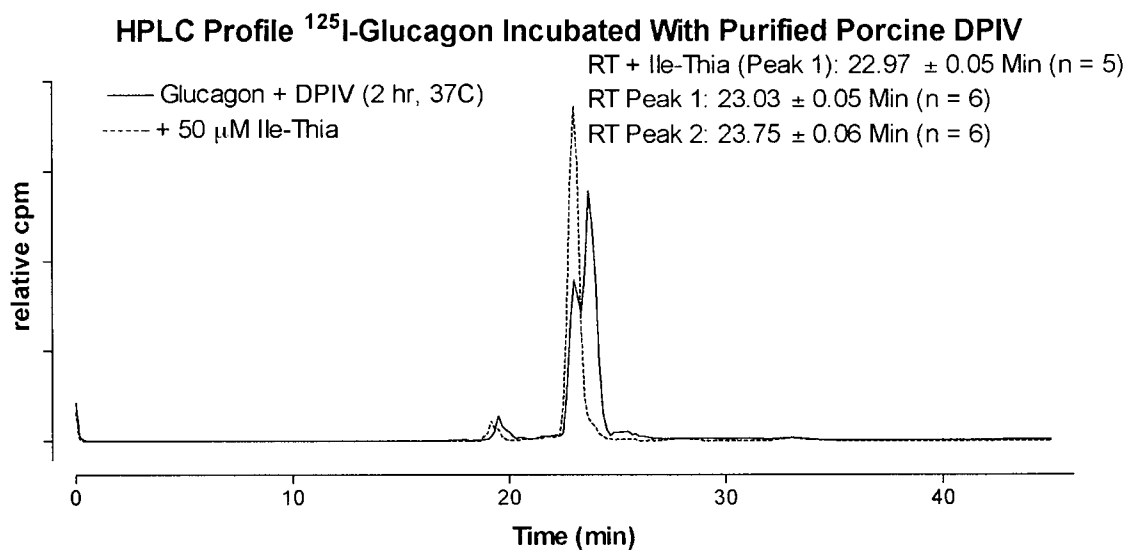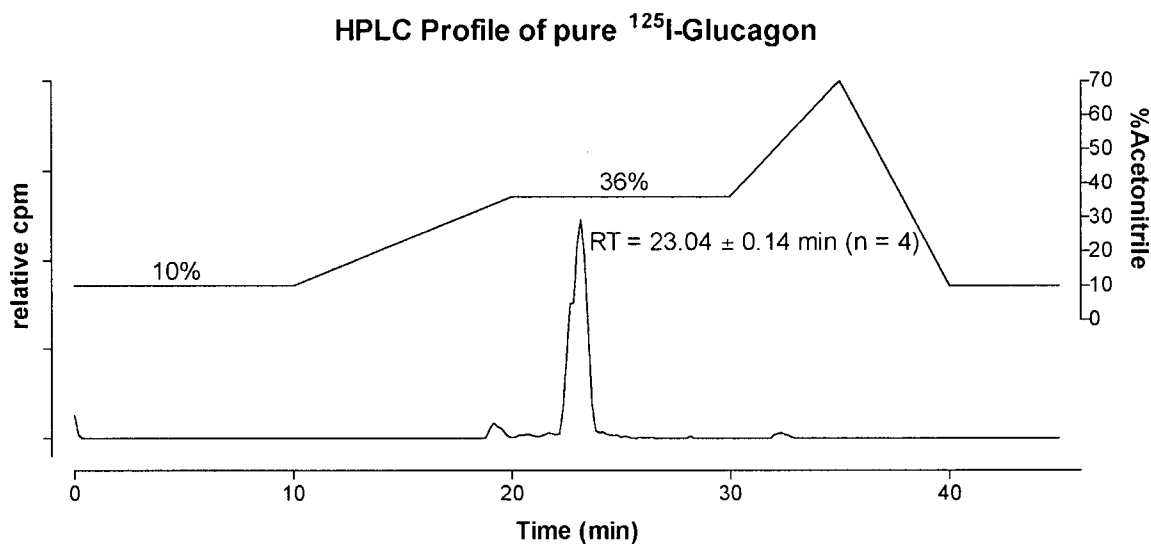
Figure 54: HPLC separation of ^{125}I-glucagon incubated with porcine DPIV

HPLC separation of ^{125}I-glucagon incubated with DPIV in the presence or absence of 50 µM Ile-thia was performed as described in the text. Traces are representative chromatograms of 5-6 HPLC runs; compiled (mean ± S.E.M.) retention times (R_T) are indicated on the figure. Methodology was similar to that used for separation of GIP fragments by HPLC (Methods section 2.11).

4.2.6.2 In Vitro Characterization of N-terminally Truncated Glucagon Fragments

Stimulation of cyclic AMP production in CHO-K1 cells transfected with the human glucagon receptor (hGlucR cells) by glucagon$_{1-29}$, glucagon$_{3-29}$, [pGlu^3]glucagon$_{3-29}$ and glucagon$_{5-29}$ is shown in Figure 55. A summary of the statistical analysis is shown in Table 11. Fragments were all partial agonists of the glucagon receptor, with the rank of potency being: [pGlu^3]glucagon$_{3-29}$ > glucagon$_{3-29}$ > glucagon$_{5-29}$. [Glu^9]glucagon$_{2-29}$ was included in antagonism experiments as a positive control since it is a well characterized antagonist [460]; [Glu^9]glucagon$_{2-29}$ exhibited a small but significant concentration-dependent increase in intracellular cyclic AMP content of hGlucR cells (2.7 times basal). Since the glucagon fragments were only partial agonists, they were also tested for possible antagonist activity (Figure 56). Glucagon$_{5-29}$ was found to antagonize cAMP stimulation by 1 nM glucagon$_{1-29}$ (2 µM: $p < 0.05$; 10 µM: $p < 0.01$), although, to a lesser degree than [Glu^9]glucagon$_{2-29}$. Glucagon$_{5-29}$ was an approximately 11-fold weaker antagonist. Neither glucagon$_{3-29}$ nor [pGlu^3]glucagon$_{3-29}$ were found to antagonize glucagon$_{1-29}$ activity.

Competition binding experiments on hGlucR cells are shown in Figure 57 and affinity statistics in Table 11. Glucagon$_{1-29}$ and [Glu^9]glucagon$_{2-29}$ exhibited approximately equal affinity for the glucagon receptor. All other truncated peptides showed significantly lower affinity for the human glucagon receptor than glucagon$_{1-29}$ under the given assay conditions. [pGlu^3]glucagon$_{3-29}$ and glucagon$_{5-29}$ both had approximately 5-fold lower affinity in binding competition experiments, whereas glucagon$_{3-29}$ had 18-fold lower affinity for the receptor.
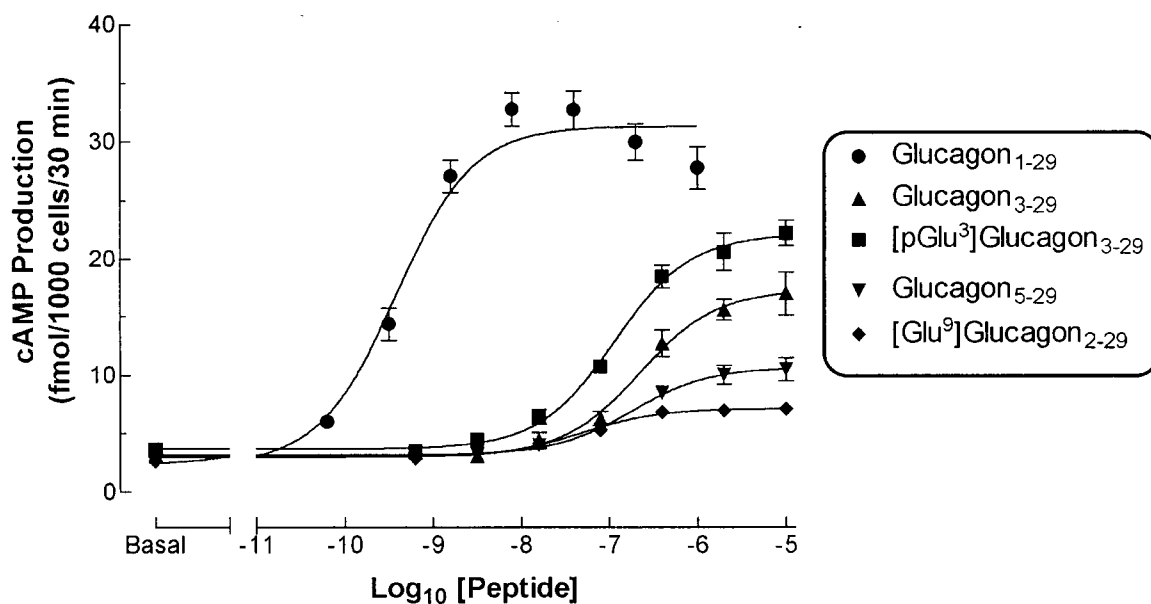
Figure 55: Concentration-dependent stimulation of cAMP production in hGlucR cells by glucagon and synthetic fragments

CHO-K1 cells stably transfected with the human glucagon receptor were incubated in the presence or absence of varying concentrations of peptides with 0.5 mM IBMX for 30 min at 37°C. Intracellular cAMP content was measured by radioimmunoassay. Data are the mean $\pm$ S.E.M. of 3-4 independent experiments. Refer to Table 11 for statistics. See Methods section 2.7 for details.
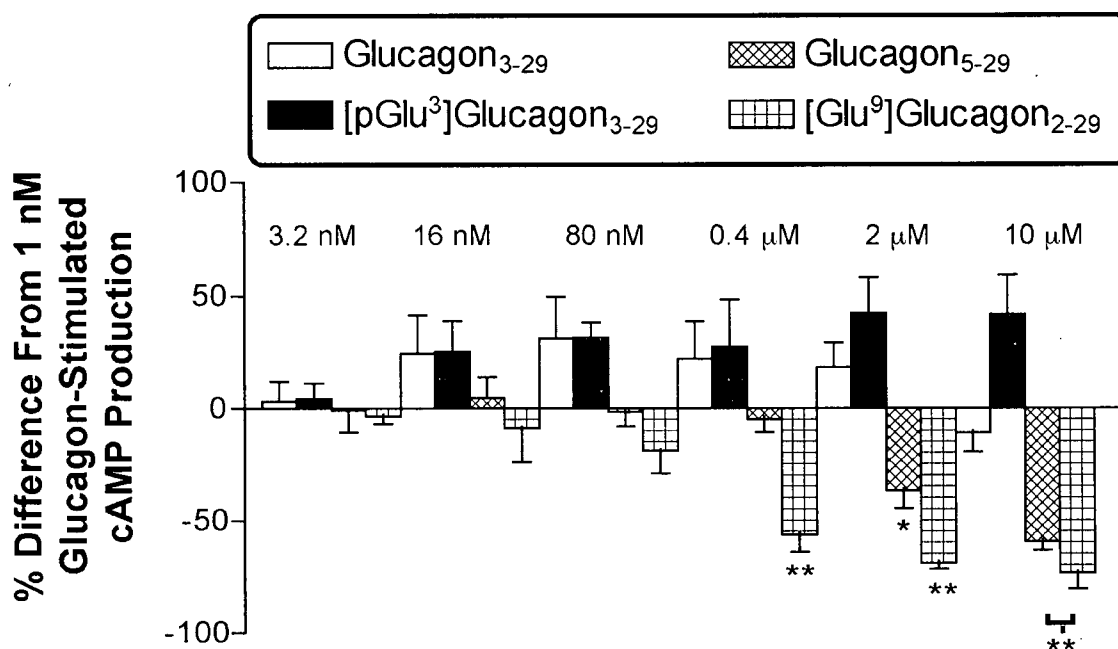
Figure 56: Antagonist properties of N-terminally truncated forms of glucagon

Bars represent the mean ± S.E.M. of the percentage of difference above or below the cyclic AMP stimulated by 1 nM glucagon$_{1-29}$ (n = 4). hGlucR cells were preincubated with synthetic glucagon analogues at the concentrations shown for 15 min prior to challenge with 1 nM glucagon, as described in Methods section 2.7.
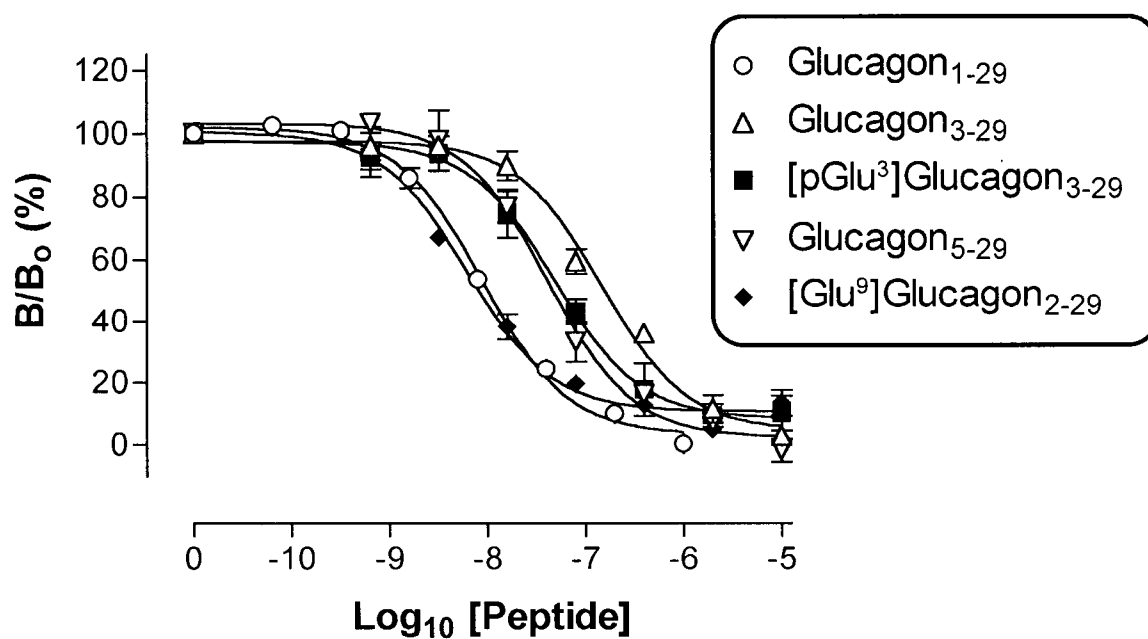
Figure 57: Competitive-binding of synthetic glucagon fragments on hGlucR cells
Data are the mean ± S.E.M. of 3-4 independent experiments. Refer to Table 11 for statistics.
See Methods section 2.6 for more details.

4.2.6.3 *In Vitro Characterization of N-Terminally Modified Glucagon Analogues*

Substitution or modification of amino acids 2 or 3 was used to generate DPIV-resistant glucagon analogues, given the substrate specificity of the enzyme. DPIV-resistance was monitored using MALDI-TOF spectrometry of peptides incubated with purified porcine DPIV; measurements were made by Dr. K. Kühn-Wache (Probiodrug, Halle, Germany) and have been published elsewhere [328]. Substitution of the second amino acid of glucagon (L-serine) with its D-isomer resulted in a completely stable peptide resistant to DPIV, whereas a peptide with the same modification to the third residue ([D-Gln^3]glucagon) was only moderately resistant to DPIV (relative to native glucagon). Altering the chirality of residue 3 also prevented further degradation of the analogue to glucagon$_{5-29}$ by purified DPIV. In contrast, substitution of glycine for serine at position 2 did not render the peptide resistant to DPIV degradation. [D-Gln^3]glucagon was similarly resistant to degradation in human serum – only a slight degradation was observed [328]. [D-Ser^2]glucagon showed an increased susceptibility to trypsin-like hydrolysis compared to native glucagon, indicated by generation of a glucagon fragment corresponding to amino acids 1-17 (cleavage between Arg^{17} and Arg^{18}), followed by a carboxypeptidase-mediated release of Arg^{17}. Modification of serine^2 with a phosphate group rendered the peptide resistant to purified DPIV and, in human serum, [(P)Ser^2]glucagon showed retarded degradation, since the velocity of degradation was limited by the de-phosphorylation of (P)Ser^2.

In vitro characterization of N-terminally modified glucagon analogues on hGlucR cells is shown in Figure 58, and summarized in Table 11. [D-Ser^2] and [Gly^2] substitutions were the best tolerated, giving only slight reductions in receptor binding affinity (2 to 3-fold reduced) and cyclic AMP stimulating potency (approximately a 4-fold right shift in the concentration-response curves) relative to native glucagon. Modifying the chirality of position 3, resulted in a peptide which had 19-fold lower binding affinity and 40-fold lower potency (EC$_{50}$), but an elevated

173

maximal cyclic AMP production at high peptide concentrations (Figure 58, Table 11).

Phosphoserine at position 2 was not well tolerated, giving only an 8-fold reduction in binding

affinity, yet a 76-fold greater EC_{50}.

A.

Legend:
- ○ Glucagon$_{1-29}$
- △ [D-Ser^2]Glucagon$_{1-29}$
- ▲ [(P)Ser^2]Glucagon$_{1-29}$
- □ [Gly^2]Glucagon$_{1-29}$
- ◆ [D-Gln^3]Glucagon$_{1-29}$

B.
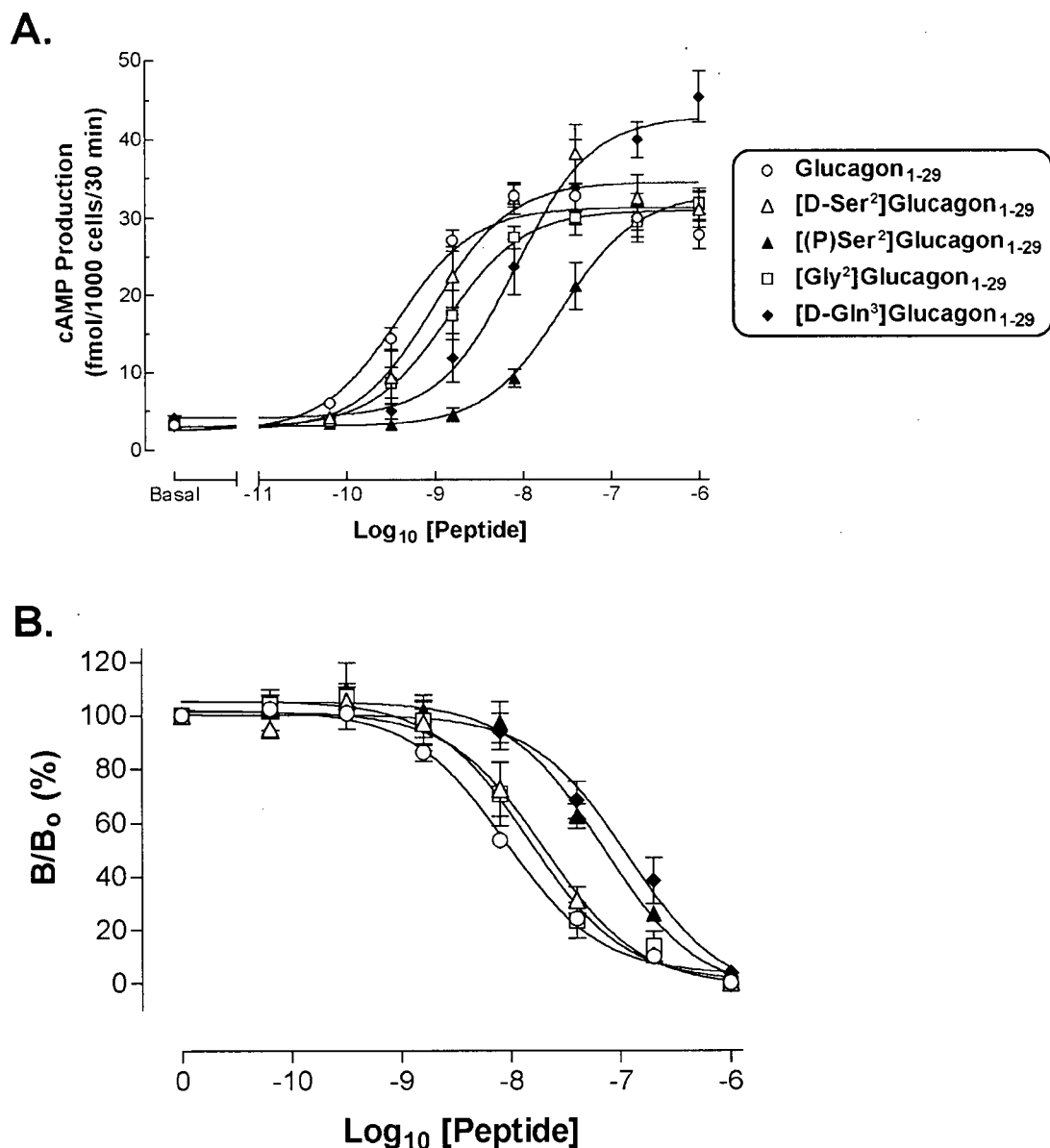
Figure 58: *In vitro* **characterization of N-terminally modified glucagon analogues**
(A) Competitive-binding displacement curves. (B) Concentration-dependent stimulation of cAMP. Data are the mean ± S.E.M. of at least 4 independent experiments. Refer to Table 11 for statistics. See Methods 2.6 and 2.7 for more information.

Table 11: Summary of glucagon receptor binding and activation by synthetic peptides

	Adenylyl Cyclase Activity		Receptor Binding
	EC_{50} (nM)	Max. cAMP (fmol/1000 cells)	IC_{50} (nM)
Glucagon$_{1-29}$	0.398 ± 0.058	32.8 ± 1.4	8.83 ± 0.60
Glucagon$_{3-29}$	239 ± 20 (*)	17.0 ± 1.9 (*)	155 ± 29 (*)
[pGlu^3]Glucagon$_{3-29}$	131 ± 34 (*)	22.3 ± 1.1 (*)	48.7 ± 4.1 (*)
Glucagon$_{5-29}$	182 ± 33 (*)	10.5 ± 1.0 (*)	45.3 ± 9.4 (*)
[Glu^9]Glucagon$_{2-29}$	59.8 ± 19.2 (*)	7.2 ± 0.5 (*)	6.37 ± 0.74
[D-Ser^2]Glucagon	1.41 ± 0.41	38.1 ± 3.8	23.6 ± 6.4 (*)
[(P)Ser^2]Glucagon	30.3 ± 7.2 (*)	31.8 ± 2.0	69.1 ± 5.7 (*)
[Gly^2]Glucagon	1.70 ± 0.67	31.9 ± 1.3	16.6 ± 5.5
[D-Gln^3]Glucagon	15.9 ± 10.1 (*)	45.5 ± 3.2 (*)	164 ± 79 (*)

*: $P < 0.05$ relative to glucagon$_{1-29}$

4.2.6.4 Bioassay of N-Terminally Modified Glucagon Analogues

The basal fed blood glucose concentrations of rats from each test group did not significantly differ from one another, and the mean fed glycemia was 7.5 ± 0.2 mM (n = 60). The characteristic glucagon$_{1-29}$ effect on glycemia over the course of an hour showed a rapid rise in circulating glucose over the first 20 minutes, to a maximum of 11.7 ± 0.4 mM (n = 8), followed by a return to preinjection levels within 60 minutes after injection. N-terminal glucagon modification generated analogues with either enhanced bioactivity ([D-Ser^2]glucagon) or reduced bioactivity ([(P)Ser^2], [Gly^2] and [D-Gln^3] substituted glucagon analogues) *in vivo*, relative to equimolar doses of native glucagon (Figure 59).
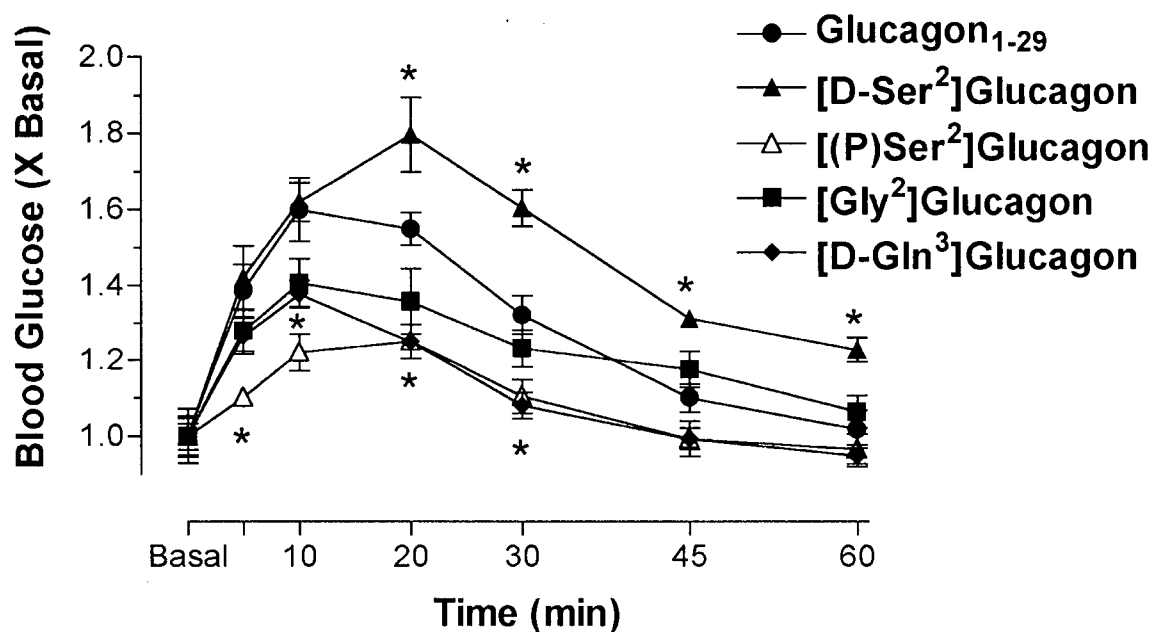
Figure 59: Bioactivity of glucagon analogues *in vivo*

Equimolar doses (7.1 nmol/Kg) of glucagon or analogue were injected subcutaneously into unrestrained conscious rats. Whole blood glucose was measured from the tail vein using a SureStep glucose analyzer. Data are the mean $\pm$ S.E.M. of a minimum of 4 animals (* = P < 0.05). Experimental work for this figure was performed by J. Andrew Pospisilik (B.Sc.) and published in [328]; used with permission.

4.3 Discussion

4.3.1 GIP Fragments

The explicit prerequisite for incretin-induced insulin release is the need for hyperglycemic conditions. Thus, unlike other non-endogenous insulinotropic agents used in the treatment of type 2 diabetes, the incretins are unable to act inappropriately to stimulate insulin release during euglycemia. It is this unique feature which has led to recent interest in the incretins as a novel therapy for diabetes. Clinical trials have been restricted to GLP-1 [461], but administration of peptide analogues of both GLP-1 [457-459] and GIP [462; 463] with prolonged circulating half-lives, as well as inhibition of dipeptidyl peptidase IV [381; 382; 417-419; 449], a physiological regulator of incretin activity, have both been shown to produce improved glucose tolerance in experimental models. Although some populations of type 2 diabetic patients have been reported to show decreased responsiveness to GIP, while responses to GLP-1 were greater [220; 373; 375; 376; 378], β-cell sensitivity to GIP improved with glyburide treatment [464]. Even though GIP and GLP-1 are proposed to improve glucose tolerance via insulin release, recently there has been some interest in use of these peptides in treatment of type 1 diabetes. The enteroinsular axis was preserved in type 1 diabetes [465], and exogenous GIP [378] or GLP-1 [466; 467] improved glucose tolerance to a degree, presumably via enhancing glucose uptake, delaying gastric emptying and/or inhibiting glucagon release. Therefore, GIP analogues may be useful in treatment of diabetes, and it is important to develop a full understanding of the mode of action of GIP.

In the last three decades, considerable effort has been targeted at structural determinations of small peptide hormones. Because short peptides are in general flexible, conformation depends on peptide concentration, solvent composition and other molecules present in solution [468]. X-ray diffraction studies have been limited to glucagon, although these studies compare well with solution structure determinations [468]. Solution structure determination techniques, circular

dichroism (CD) and nuclear magnetic resonance (NMR), have been performed on most members of the glucagon/secretin/VIP family [468-474], with the exception of GIP and PHI (peptide histidine isoleucine). In order to stabilize secondary structure, all studies have been performed in the presence of organic solvents or micelles, as there was little evidence of stable structure in water alone [468; 470]. The general structural features of the glucagon superfamily appear to be a disordered N-terminal region of 6 to 8 amino acids, followed by a helical region of 18 ± 2 amino acids, that can be a continuous helix, or broken into two segments by a hinge region of 2 amino acids [468; 470-474]. The exendin peptides from *Helodermatidae* venom represent a family of peptides structurally related to the glucagon superfamily [475]. Structural determination has been completed for helodermin (exendin-2), which acts as an agonist at VIP and secretin receptors, indicating that it retains significant secondary structure in water, and this is enhanced by organic solvents [476]; helodermin has a core α-helix of 15 amino acids in water, and this extends to 21 amino acids with the addition of trifluoroethanol (TFE). It is thought that helical structure is the preferred conformation for receptor binding, since changing the experimental conditions from aqueous to organic approximately mimics the situation *in vivo* for a blood borne hormone going from solution to a membrane bound receptor-hormone complex [476]. Notably, related *Helodermatidae* venom peptide exendin-4 (a GLP-1 receptor agonist) and exendin-4$_{(9-39)NH2}$ act as weak GIP receptor antagonists [276-278]. A long-term goal of structural studies is to compare NMR solution structures and effects of peptide deletions and substitutions on hormone bioactivity to determine whether there are common or specific structural features relevant to the modes of peptide action [476]. In a unique study, Inooka *et al* [477] were able to use NMR spectroscopy to determine the structure of PACAP in the receptor bound state; from their results, they hypothesized a two-step ligand transportation model whereby the α-helix is induced by non-specific binding to cell membranes, followed by two-dimensional diffusion leading to specific binding to its receptor. To date, GIP structural analysis

has been limited to structure-function relationships using enzyme or chemically cleaved peptides or synthetic peptides and rudimentary computational methods (Figure 60, chapter 4 introduction and described below).

The current body of experimental evidence indicates that there are four dissociable domains in GIP_{1-42}. The high affinity binding domain, $GIP_{6-30NH2}$, is a potent GIP receptor antagonist [413]. Initially, two bioactive domains in GIP were indicated. Truncation of 12 amino acids from the carboxyl terminus of GIP_{1-42} resulted in a peptide with equivalent insulinotropic activity, but lacking somatostatinotropic activity [32; 337; 410]. Part of the GIP molecule in the carboxyl-terminus is therefore critical for its acid inhibitory (enterogastrone) activity [337; 405; 410], although it is unclear whether this is due to the existence of a second GIP receptor, an alternatively spliced receptor, or differential ligand recognition or coupling of the existing receptor in gastric cells. The insulinotropic domain of GIP was initially hypothesized to be contained between residues 19 to 30, consistent with partial retention of insulinotropic activity of GIP_{19-30}, GIP_{15-42} and GIP_{17-42} [165; 267; 337]. However, this was inconsistent with the importance of the amino-terminus in GIP signal transduction and regulation of GIP activity by DPIV [57-59; 166] (Figure 38). In following this hypothesis, evidence presented in the current studies suggests a third bioactive domain of GIP, residing in residues 1-14 (Figures 31, 35, 37, and Table 7).
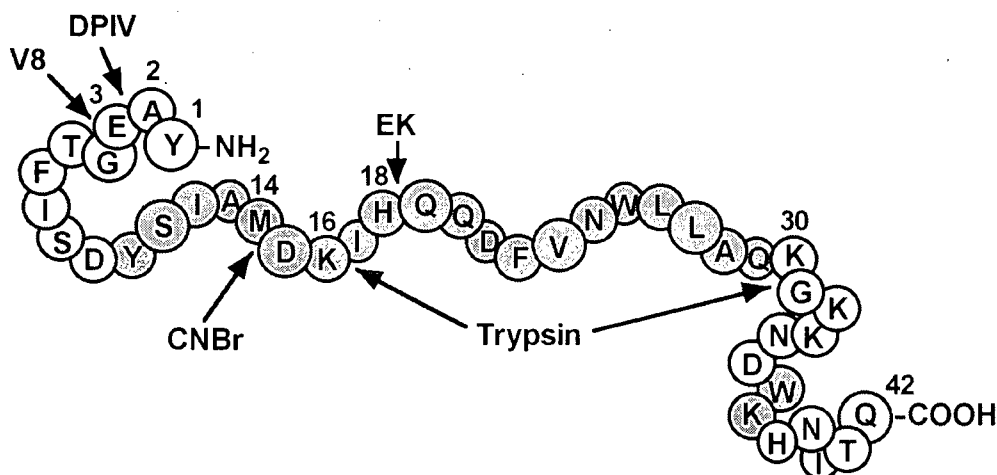
Figure 60: Predicted secondary structure of GIP
Primary structure of GIP_{1-42} with predicted α-helical regions (grey; Gascuel and Golmard Basic Statistical Method) and enzymatic cleavage sites used for structure-function relationships. Amino acid positions are indicated above the residues prior to cleavage sites. Abbreviations: DPIV, dipeptidyl peptidase IV, V8, *Staphylococcus* V8 Protease, CNBr, cyanogen bromide, Trypsin, EK, enterokinase.

Computer assisted secondary structure analysis of GIP predicts an alpha helical region between residues 10 and 29 (Figure 60; PCGENE, IntelliGenetics; GGBSM Method [478]). Bioactivity of N-terminal GIP fragments was limited to GIP_{1-14} (amide or free acid) and amidated forms of GIP_{1-13} and GIP_{1-15}. Hence, it is possible that, along with an intact amino terminus (Tyr^1-Ala^2), preservation of this helical structure is also important for biological activity. In the absence of Met^{14} the helix may be unable to form, but the charged residue Asp^{15} destabilizes it. Amidation of the carboxyl-terminus appears to have minor effects on bioactivity, only noticeable for $GIP_{1-13NH2}$ and $GIP_{1-15NH2}$, where it may partially stabilize the secondary structure (Table 8). Contrary to data in the current report, GIP_{1-14} created by cyanogen bromide cleavage was not insulinotropic in the perfused rat pancreas [165]. However, conversion of Met^{14} to homoserine lactone by this cleavage method, when this region appears particularly sensitive to structural perturbations, likely generates a biologically inactive N-terminal peptide (or alternatively, the sensitivity of the perfused pancreas may have been too low to detect bioactivity of this fragment).

180

Study of the bioactivity of amino terminal peptide fragments of the secretin-glucagon family is not limited to GIP. Data now exists for parathyroid hormone (PTH), secretin, glucagon and GLP-1 and vasoactive intestinal polypeptide (VIP), and PACAP; however, bioactivity of these fragments appears to be largely dependent on the peptides examined. In a recently published report, micromolar concentrations of PTH_{1-14} were able to stimulate cyclic AMP production in cells transfected with the human or rat PTH-1 receptors [479]. While it was not possible to demonstrate $^{125}I-PTH_{1-34}$ displacement by PTH_{1-14} using radioligand binding assays [479], photoaffinity cross-linking experiments have indicated that the amino terminal region of PTH interacts with the PTH receptor in the area of the junction of the extracellular tail and the first transmembrane domain [480-482]. Further work of Gardella and colleagues found that $secretin_{1-13}$ activated the transfected secretin receptor [479]. In the course of our experiments, we have also tested $glucagon_{1-14OH}$ and $GLP-1_{[7-20OH]}$ on CHO-K1 cells transfected with human isoforms of their respective receptors, but neither peptide showed any stimulation of cAMP production at concentrations as high as 20 µM (data not shown). $GLP-1_{[7-20]}$ was previously tested in the perfused rat and canine pancreas, and had little or no effect [483; 484]. Carboxyl-terminal truncation of glucagon dramatically reduced bioactivity [485], and the shortest glucagon fragment reported to retain receptor binding and activation has been $glucagon_{1-17}$ [486]. $PACAP_{1-21}$ was found to be a full agonist of its receptor [477]. Synthetic VIP_{1-14} has also been reported to be inactive [487], as was GIP_{1-18} [406]. Thus, it appears that structural similarities of amino-termini across all members of the secretin/vasoactive intestinal polypeptide/glucagon superfamily of hormones do not necessarily confer biological activity.

Sequential alanine substitution of the GIP_{1-14} amino acid sequence confirmed the sensitivity of this peptide to structural perturbations (Figures 30 and 32). Only replacement of amino acids 2 (Ala^2Ser) and 13 ($Ala^{13}Tyr$) with those found in glucagon failed to produce dramatic reductions in receptor binding and activation; this said, given the explicit selectivity of glucagon receptors

181

for glucagon, and GIP receptors for GIP, the results indicate that either residues 2 and 13 are not important ligand-receptor contacts or the domain responsible for receptor selectivity resides in the C-termini of the peptide hormones. The latter postulate is unlikely, as GIP_{1-14} was not able to activate transfected glucagon or GLP-1 receptors (data not shown). There is some evidence allowing separation of residues important for receptor binding and activation. $[Tyr^{13}]GIP_{1-14}$ potently bound and activated the GIP receptor, however, $[Ser^2]GIP_{1-14}$ displayed comparatively lower displacement of ^{125}I-GIP, with similar receptor activation. Similarly, the only two other peptides from the alanine scanning experiment to show significant cAMP stimulation were those substituted in position 1 and 3, however, these peptides also showed little radioligand displacement, compared to peptides which were unable to activate the receptor (Figures 30 and 32). Alanine scanning of the bioactive PTH_{1-14} N-terminus identified residues 3, 10, 11, 12, 13 and 14 as being tolerant to substitution (*i.e.* identity not important for receptor activation) [479]. Furthermore, alanine scanning of the entire primary sequence of GLP-1 revealed positions 1, 4, 6, 7, 9, 22 and 23 as being particularly important either for maintenance of secondary structure or ligand-receptor interactions [488; 489]. Comparison of Figure 32 to the data of Luck *et al* [479], clearly indicates that although both GIP_{1-14} and PTH_{1-14} are bioactive, important residues for the two ligands differ, and those of GIP apparently are also dissimilar from key residues of GLP-1. Due to the structural sensitivity of GIP_{1-14}, in order to conclusively determine important residues, alanine scanning must be performed for the entire sequence of GIP_{1-42} or at least GIP_{1-30}. Extensive molecular characterization of PTH_{1-14} by multisite substitution and modification suggested it was possible to produce small peptide fragments with improved potency [490-493]. Only four modified GIP_{1-14} peptides were generated (Figures 30 and 33). Introduction of a reduced peptide bond between Ala^2 and Glu^3 resulted in a peptide with improved receptor potency compared to GIP_{1-14}, while at the same time this modification conferred DPIV resistance.

Hence, systematic screening of modified GIP_{1-14} peptides will likely produce potent peptide ligands that may be applied to *in vivo* experimentation.

While structural data for GIP are lacking, it is possible to propose a mechanistic model for ligand binding and receptor activation. A large body of evidence has accumulated regarding receptor ligand interactions for small ligands, including small peptides [494], however, the types of analyses performed on small ligands, such as thyrotropin (TRH; pyroGlu-His-ProNH$_2$) are not possible for larger polypeptide ligands due to their complexity. Use of chimeric ligands and receptors has made it somewhat possible to dissect the molecular domains of peptide hormones necessary for binding and activation. Based on some of this work, Hjorth and Schwartz proposed production of a pseudo-tethered intermediate involving the large extracellular amino-terminus of the cognate receptors for polypeptide ligands, prior to a conformational change drawing the peptide toward the transmembrane helices [495]. Gelling *et al* demonstrated the importance of the N-terminus of the GIP receptor for ligand binding and activation [280]. Given that GIP_{1-14} and GIP_{19-30} both demonstrate receptor binding ability (Figure 29 and Table 7), and that the high affinity binding domain of GIP resides within residues 6 to 30 [413], it is likely that multiple contact residues contribute to high affinity receptor binding. Furthermore, the body of evidence demonstrating the importance of the two N-terminal residues of GIP [57-59; 166] combined with the bioactivity of GIP_{19-30} suggest an interaction or close proximity of the amino terminus of GIP and its core region (possibly indicating the presence of a functional hinge in the alpha helices), resulting in receptor activation. Until the solution structure for GIP is known and/or the contact residues are established by photoaffinity cross-linking, it is not possible to extend this mechanistic hypothesis without extensive testing of further GIP analogues.

4.3.2 DPIV-resistant Incretin Analogues

Recognition of the importance of the structure of the N-terminus for biological activity of peptides in the secretin-glucagon superfamily has resulted in the development of numerous analogues with reduced *in vivo* catabolism and increased biological activity. Substitution of L-Tyr[1] with the D-isomer in growth hormone releasing hormone (GRH) [496-498], L-His[1] with D-His[1] in glucagon [499] and GLP-1 [458], or D-amino acids in P_2 of glucagon (see below) or GLP-1 [500-502] resulted in peptides with increased *in vivo* potency. Although conformational changes in the molecules may play a role in increasing biological activity [499], a more prolonged biological half-life as a result of their resistance to enzymatic degradation is probably the more important factor. Frohman *et al* [496; 503] first showed the importance of DPIV in the physiological degradation of members of the secretin-glucagon superfamily, by demonstrating that GRH is metabolized to biologically inactive GRH_{3-44} by DPIV both *in vitro* and *in vivo*. Additionally, it was shown that amino-terminal substituted analogues, including des-amino-Tyr[1]-, D-Tyr[1]-, and D-Ala[2]-GRH, were resistant to DPIV cleavage [496]. More recently, studies on GLP-1 have shown a similar resistance to DPIV degradation with analogues containing D-amino acids in the P_2 N-terminal position [500-502]. The current study was targeted at developing long-acting analogues of the second important incretin, GIP. Flatt and colleagues have reported that [Tyr[1]-Glucitol]GIP, a peptide analogue modified post-synthesis, displays both DPIV-resistance and improvement of glucose tolerance in a diabetic mouse model [181; 239; 462; 463].

Removal of the first two amino-terminal residues of GIP (GIP_{3-42}) resulted in a peptide which displayed reduced receptor affinity in competition binding studies and that was devoid of the ability to stimulate cAMP production in wtGIPR cells at concentrations as high as 10 μM (Figure 38). This supports the early claim that GIP_{3-42} isolated from porcine intestinal extracts lacked insulinotropic activity in the perfused rat pancreas [57]. GIP_{3-42} was an antagonist of GIP_{1-42}–induced cyclic AMP production in the μM range, inhibiting cAMP production by over 90%

(Figure 38). Schmidt *et al* tested GIP_{3-42} for antagonism of GIP_{1-42} action on isolated rat islets and found that it was unable to reduce GIP-stimulated insulin release when administered in equal or 10-fold greater concentrations [166]; Figure 38 indicates at least a 1000-fold greater concentration of GIP_{3-42} is necessary to reduce native GIP action on the cloned receptor. The claim that GIP_{3-42} lacks insulinotropic activity is further supported by lack of effect on glucose excursions and insulin profile when bioassayed in conscious Wistar rats (Figure 45). In this bioassay, excess exogenous GIP_{3-42} injected subcutaneously, was unable to block or even shift the insulinotropic effect of endogenously released GIP_{1-42} resulting from the oral glucose load; thus it is extremely unlikely that GIP_{3-42} plays an antagonistic role *in vivo*.

Given the sensitivity of the N-terminus of GIP to inactivation by DPIV we sought to generate peptide analogues resistant to this enzyme for use *in vivo*. Initial *in vitro* studies looked at modification or substitution of amino acids in positions 2 and 3 of GIP, using peptides based on the shorter 30 amino acid bioactive core of the hormone (1-30). In general, the amino-terminus of GIP was fairly tolerant of amino acid substitution or modification, when examining binding affinity only, however, when examining bioactivity at the GIP receptor, modification of the N-terminus can have dramatic effects (Figure 40). The data presented here compares well to the earlier limited structure-function analysis of the GIP N-terminus, testing 1-30NH2 analogues [desamino-Tyr^1(phenylproprionic acid)]GIP, [D-Tyr^1]GIP, [D-Ala^2]GIP, [D-Glu^3]GIP and [D-Ala^4]GIP [324] – modifications caused little (less than 10-fold reduced binding for most peptides) or no change in ligand affinity, but specific analogues showed significantly reduced bioactivity. Thus, [D-Ala^2]GIP, [$Y^1A^2\psi(CH_2NH)$]GIP, [Gly^2]GIP, and [Ser^2]GIP were well tolerated with respect to binding affinity, and [Val^2]GIP, [Pro^3]GIP and [N-$MeGlu^3$]GIP were only modestly reduced. However when looking at cyclic AMP production, [$Y^1A^2\psi(CH_2NH)$]GIP, [Pro^3]GIP and [N-$MeGlu^3$]GIP were not even able to stimulate maximal levels such that EC_{50} values could not even be calculated; other analogues showed minor or

185

moderate alterations in receptor activation. [(P)Ser^2]GIP showed both dramatically reduced binding affinity and cAMP production (Table 8, Figure 40).

Cyclic analogues of small peptide hormones generated by lactam bridge formation between endogenous or substituted Lys and Asp or Glu residues have been reported in the literature [504-507]. The current study, to our knowledge, is the first report of a cyclic GIP analogue; this peptide has allowed testing of the effects of further structural constraints on the molecule. By creating a lactam bridge between Lys^{16} and Asp^{21}, a derivative of GIP was generated with a six amino acid ring, spanning the predicted hinge-domain within the alpha-helical binding core. Remarkably, this peptide was able to stimulate maximal cyclic AMP production, with an increase in EC$_{50}$ of one order of magnitude relative to native hormone (Figure 40, Table 8). In contrast, the binding affinity of cyclo[Lys^{16},Asp^{21}]GIP was disproportionately reduced, resulting in an IC$_{50}$ value for cyclized GIP that was 25.3-times greater than the unmodified peptide. Results from cyclo[Lys^{16},Asp^{21}]GIP have shown the feasibility of using cyclic incretin analogues, as well as confirming hypotheses generated from previous structure-activity relationship studies of GIP. It was shown earlier that the high affinity binding domain resided in the predicted core α-helical domain between residues 6 and 30 of GIP [413]; however, two dissociable bioactive domains were discovered: GIP$_{1-14}$ and GIP$_{19-30}$, both of which also possessed weak binding ability (Figures 29 and 31). Solution structure data for related hormones has shown the presence of a common 16-20 amino acid helical core, either as a continuous helix or with a two amino acid hinge region. Hence, the lactam bridge in cyclo[Lys^{16},Asp^{21}]GIP may interfere with receptor binding (Figure 40, Table 8) either by disrupting helix formation or interfering with the flexibility of the hinge domain, without causing proportional reductions in bioactivity.

From these data, substitution with D-Ala in position 2 was shown to have the greatest potential for further development; preliminary trials found that this molecule was completely

resistant to DPIV degradation for over 24 hours, and had minimal changes in receptor activity (Figure 40, Table 8). Unfortunately, all other peptides exhibiting complete DPIV resistance displayed dramatically reduced cyclic AMP stimulating ability at the GIP receptor (Figure 40, Table 8). When testing full length [D-Ala^2]GIP$_{1-42}$, these results were corroborated and studies continued in animal models. While DPIV-resistance did little to the effectiveness of the analogue *in vitro* (consistent with the negligible DPIV activity in CHO and βTC-3 cells; Figure 39), when tested *in vivo*, [D-Ala^2]GIP reduced glycemic excursions in all animal models to a greater extent than native GIP. This was associated with enhanced early phase insulin release in lean animals (Figures 44 and 46, Table 9), and in diabetic rats, where the first phase of insulin release is compromised, an augmentation of the entire insulin time-course was observed (Figure 47). The latter finding is of particular interest, as GIP's effectiveness in type 2 diabetes mellitus and animal models of the disease has been questioned, and remains controversial. Lean Zucker rats showed significant differences in glycemic profiles between GIP and [D-Ala^2]GIP, while both peptides appeared equally insulinotropic except for the first time-point (t = 3.5 min) (Figure 46). These data are consistent with either an increased insulin sensitivity in these animals, as noted by Pederson *et al* [381], and/or enhanced ability of this compound to stimulate glucose uptake in peripheral tissues [239; 251].

Although GIP$_{1-42}$ has been shown to exhibit equivalent insulinotropic activity to GLP-1 [336] there have been no previous reports targeted at developing long acting analogues with therapeutic potential in diabetes until very recently, and these have been limited. The reason for the lack of such studies probably originates in the report of Nauck *et al* [220], in which they observed that human GIP was almost devoid of insulinotropic activity in diabetic patients. It had been shown earlier that there was a reduced incretin response in type 2 diabetes, characterized by a reduction in the component of β-cell secretion resulting from oral glucose relative to that obtained with intravenous glucose [377]. Additionally, the responsiveness of insulin resistant

diabetic patients to exogenous porcine GIP, at concentrations resulting in physiological [376], or near physiological [378] circulating levels, was blunted. It was also observed that porcine GIP_{1-42} stimulated insulin secretion under fasting conditions [508; 509] whereas normal controls did not respond, presumably due to the fact that circulating fasting glucose levels in type 2 diabetes mellitus patients reach the required threshold for the insulinotropic activity of GIP. Therefore, there appears to be little doubt that insulin responses to exogenous GIP are reduced in diabetic patients. Nevertheless, the pancreas still retains some GIP sensitivity. The reason for the almost complete lack of response to human GIP observed in the study of Nauck *et al* [220] may lie elsewhere. In their study, responses of normal controls to the human peptide were also extremely weak, unlike those described by the same group in an earlier study with GIP from a different commercial source [221], suggesting that the synthetic human peptide used in the diabetic study exhibited only weak biological activity. It has recently been shown that some [336], but not all [276], commercial preparations of human GIP exhibit very low biological activity, and it is therefore critical that further clinical trials with human GIP and GIP analogues, are performed with peptide of established biological activity.

It is also important to define the origin of the resistance to GIP. One possibility is increased receptor desensitization/down-regulation or altered signal-transduction pathways (see Chapter 3). Alternative explanations include antagonism of GIP_{1-42} action by GIP_{3-42}, as suggested for GLP-1 [448], or a genetic defect resulting in reduced receptor expression [374]. Antagonism by GIP_{3-42} appears unlikely in view of its low binding affinity for the receptor and strength as an antagonist, with at least 1000-fold higher concentrations being required to show a significant effect. However, some support for the latter hypothesis has been obtained recently, with the finding that obese VDF Zucker rats have compromised GIP receptor expression, both at the mRNA and protein level in isolated islets of Langerhans [379]. During an *IP* glucose tolerance test, when GIP was infused at minimum threshold levels necessary to obtain a biological response in lean

188

animals (4 pmol·min⁻¹·Kg⁻¹), obese animals were unable to respond to the same dose. This was linked to a defect in ability to stimulate cyclic AMP in isolated islets, and quantitative PCR and immunoblotting suggested a reduction in GIP receptor expression [379]. The etiology of the diminished expression, however, has not been elucidated, and may result from elevated postprandial GIP levels and subsequent desensitization/internalization/down-regulation of the receptor. In the current study, fasting GIP levels in lean and obese VDF Zucker rats were not significantly different, confirming the result of Lynn and colleagues [379], however, elevated levels of GIP were detected in obese animals following an OGTT, lending support for the down-regulation hypothesis.

In order to directly compare the potency of DPIV-resistant GIP and GLP-1 analogues, several peptides were tested in parallel *in vitro* and *in vivo*. For this study, [Ser²] substituted peptides were chosen, as this substitution produced no alteration in receptor binding or activation (Figure 40, Table 8), and [Ser²]GLP-1 has been reported to show enhanced *in vivo* bioactivity owing to its DPIV resistance [457-459]. Both Ser² substituted incretins showed relatively normal receptor binding and activation parameters (Figures 48 and 49), and moderate, but not complete DPIV resistance to purified enzyme. Accordingly, bioassay of these peptides demonstrated that they were slightly more effective than native peptides *in vivo* (Figure 50, Table 10). Comparison of native peptides (*i.e.* GIP versus GLP-1) or Ser² substituted peptides showed very similar potencies, particularly when considering the integrated responses, which were not significantly different (Table 10). The glucagonostatic property of GLP-1 has been an often touted benefit of GLP-1 over GIP as a therapeutic possibility [374; 510]. However, both GIP and GLP-1 are glucagonotropic *in vitro* [190; 219], but GIP produces no alteration in glucagon release in humans [164; 220]. To date, no experimental study has been performed demonstrating that GLP-1's glucagon lowering effects actually contribute to its glucose lowering effects independently of its insulinotropic action in normal humans or patients with type 2

diabetes mellitus (although in insulinopenic type 1 diabetes, it was proposed that inhibition of glucagon secretion contributed to the antihyperglycemic effect of exogenous GLP-1 in these individuals [466]). In fact, counter-intuitively, transgenic overexpression of the glucagon receptor in mice actually improved glucose tolerance (Dr. R. Gelling, personal communication) and glucagon confers β-cell glucose competence [283]. Furthermore, GLP-1 is a well characterized inhibitor of gastric emptying, whereas the effect of GIP on gastric emptying is not well characterized [511]. Thus, despite the potential differences in their modes of action, their antidiabetic action is quite similar, consistent with their equal insulin-releasing ability [336].

Phospho-Serine[2] modification was found to render glucagon completely resistant to purified DPIV, but this peptide was time-dependently dephosphorylated in serum. We reasoned that [(P)Ser[2]] modification of incretins would provide an extra degree of protection from enzymatic degradation during absorption after *SC* injection, as these peptides were also completely resistant to purified DPIV, and would likely also be dephosphorylated *in vivo* to the moderately resistant [Ser[2]] incretin analogues. One potential problem was their dramatically reduced potency at their respective receptors (Figures 48 and 49). However, on subcutaneous injection into rats, with a concurrent glucose challenge, these peptides produced equivalent or more potent antidiabetic effects than their non-phosphorylated counterparts, at the same dosage (Figure 51, Table 10). It was noted, however, that phosphoserine[2] substitution ablated incretin effects on the early phase of insulin release, but this could be overcome by administration of a greater dosage (Figure 51, Table 10). Hence, [(P)Ser[2]] incretin analogues represent the first generation of "pro-drug" forms of long acting metabolically stable peptides.

4.3.3 DPIV Degradation of Glucagon and DPIV-resistant Analogues

Several lines of evidence have resulted in the necessity for re-assessment of glucagon degradation *in vivo*. Controversy in the past regarding glucagon degradation, with respect to specific enzymes and organs involved needs to be clarified. Evidence presented indicate that dipeptidyl peptidase IV is a prime candidate for enzymatic inactivation of glucagon [328; 453]. The recent finding demonstrating DPIV in the secretory granules of the pancreatic islet α-cell compels one to question how much of the pancreatic glucagon enters the circulation intact [512]. Grondin and colleagues further argue that the low pH of the secretory granule would not permit activity of DPIV, and thus DPIV would not be active until granule contents are secreted. The discovery that glucagon is successively hydrolyzed by dipeptidyl peptidase IV into N-terminally truncated peptides raises a number of questions. The first question is the role of the hydrolyzed peptides – are they simply degradation products, or do they have a physiological role? The emergence of the "mini-glucagon" story in the pancreas suggests the hypothesis of a local action of N-terminally truncated glucagon. Processing of glucagon by MGE (miniglucagon-generating endopeptidase) to glucagon$_{19-29}$, results in a peptide having differential effects on cardiac myocytes [513], and with the ability to inhibit insulin release in the picomolar range [514]. This report forms the foundation for further work on glucagon degradation products and their possible function *in vivo*.

Preliminary studies using an *in vivo* bioassay suggested that DPIV inactivates glucagon. Incubation of glucagon with purified DPIV abolished its hyperglycemic effects, but not if a specific DPIV inhibitor was included (Figure 52). Similarly, injection of large doses of cleavage products, that were identified by mass spectrometry, demonstrated no biological activity (Figure 53). It is likely that glucagon degradation fragments are present *in vivo*, and thus measurements of glucagon immunoreactivity by "side-viewing" or C-terminally directed antibodies [99] would likely cross-react with these peptides. Studies using antibodies for the measurement of glucagon

191

may therefore be misleading and this is likely the reason that glucagon was previously reported to be stable in plasma [437; 454]. Frandsen *et al* [515] found that glucagon$_{5-29}$ cross-reacted with at least two antisera tested, and it is likely that antibodies also cross react with glucagon$_{3-29}$ and [pGlu^3]glucagon$_{3-29}$. Thus, as for GIP and GLP-1 [60; 448], measurements of glucagon in serum overestimate biologically active peptide.

Fragments similar to those described here have been tested for agonism and antagonism in other biological systems. Glucagon$_{5-29}$ was found to have <0.001% of the potency of native glucagon in the rat hepatocyte membrane adenylyl cyclase activity assay [515], and it was found that this fragment also acted as an antagonist in this tissue. In the current study, using cells over-expressing the human glucagon receptor, it was found that glucagon$_{5-29}$ has 28.5% of the potency of glucagon$_{1-29}$ (Figure 55, Table 11), and indeed, it does act as a weak antagonist on these cells (Figure 56). Similar glucagon analogues to those tested here, [Glu^9]glucagon$_{3-29}$ and [Glu^9]glucagon$_{5-29}$, have also been previously characterized [460]. The binding affinities reported for the Glu^9 substituted analogues [460] are consistent with the trend observed with native fragments on transfected cells (Figure 57), however, the amino acid substitution at position 9 alone ([Glu^9]glucagon$_{1-29}$) was also shown to have dramatic effects on binding affinity [460]. Similarly, [Glu^9]glucagon$_{1-29}$ had significantly reduced potency, and N-terminally truncated (desHis^1) peptides showed negligible adenylyl cyclase stimulating activity [460]. In light of the finding that only glucagon$_{5-29}$ showed antagonism on hGlucR cells, it is likely that the Glu^9 substitution was responsible for the antagonism observed for [Glu^9]glucagon$_{3-29}$, and resulted in antagonism potencies similar to [Glu^9]glucagon$_{2-29}$, as was also the case for [Glu^9]glucagon$_{5-29}$ [460]. Native glucagon$_{5-29}$ showed only weak antagonism compared to [Glu^9]glucagon$_{2-29}$ (Figure 56). The activities of the fragments tested support the importance of the amino terminus in glucagon signal transduction. Cyclization of the side chain of Gln^3 to form [pGlu^3]glucagon$_{3-29}$ both increased binding affinity and potency as compared to glucagon$_{3-29}$

(Figures 55 and 57). Glucagon$_{5\text{-}29}$ also retained high affinity binding (greater than glucagon$_{3\text{-}29}$), but showed lower potency when compared to either [pGlu^3]glucagon$_{3\text{-}29}$ or glucagon$_{3\text{-}29}$.

Characterization of DPIV-resistant, N-terminally modified glucagon analogues is consistent with published literature. The general conclusion from random molecular mutagenesis screening was that modification of the amino terminus of glucagon reduces biological activity, implicating it as an important domain necessary for receptor activation [516]. Robberecht and colleagues found that altering the chirality at positions 2 and 3 of glucagon had minor effects on potency in the hepatocyte adenylyl cyclase assay; [D-Ser^2]glucagon was equivalent to native glucagon in terms of cAMP formation and binding affinity, whereas reversing the chirality of position 3 had significant effects on both parameters [517]. Unson and Merrifield [518] also substituted the D-isomer of serine in position 2, however, they found it dramatically reduced affinity and potency of this analogue *in vitro*. Our work using cells transfected with the human glucagon receptor are consistent with the earlier studies using hepatocyte membranes [517]. The [D-Ser^2] substitution was better tolerated than [D-Gln^3], when looking at *in vitro* cAMP stimulatory activity and receptor binding affinity (Figures 58, Table 11).

Previous studies on [D-Ser^2] and [D-Gln^3] were limited to *in vitro* structure-function studies. With the objective of generating DPIV resistant glucagon analogues, to support the hypothesis of DPIV degradation of glucagon, an *in vivo* assay system was necessary. The [D-Ser^2] substitution was the only analogue which possessed enhanced ability to increase circulating glucose levels relative to native glucagon. The greater potency *in vivo* can be attributed to the lack of degradation by DPIV, as the *in vitro* potency was found to be moderately reduced (Figure 58). However, this substitution rendered the peptide more susceptible to degradation by trypsin-like enzymes [328]. Other N-terminally modified glucagon analogues were not suitable for demonstrating the contribution of DPIV to the degradation of glucagon, as they possessed reduced biological activity *in vitro*, and *in vivo*, or were susceptible to DPIV degradation.

193

4.3.4 Conclusion

The current work has verified the importance of the amino-terminus of GIP for bioactivity. GIP_{1-14} is a unique GIP fragment that displays specific GIP receptor binding, and cyclic AMP production in transfected cells, in addition to insulinotropic activity in the perfused pancreas and improvement of glucose tolerance *in vivo*. Consistent with prior studies in the perfused pancreas, synthetic GIP_{19-30} was able to stimulate cAMP production weakly and had intrinsic receptor binding ability. Hence, it appears that the two insulinotropic domains exhibit secondary structure within GIP_{1-14} and GIP_{19-30}, while a putative enterogastrone/somatostatinotropic domain lies in the C-terminus of the molecule.

The significance of GIP as a physiological incretin has been emphasized in studies using specific GIP antagonists in rat [186] and inhibition of DPIV activity in GLP-1 receptor knockout mice [519]. With the important findings that sulfonylureas improve β-cell sensitivity to GIP [464], that smaller fragments of GIP are bioactive, and in the present report, that even in animals with compromised GIP receptor expression, bolus injections of GIP and analogues with improved plasma stability are still capable of improving glucose tolerance, the pharmacological potential of GIP in treatment of human diabetic states is preserved. In order to truly recognize the potential of GIP and degradation resistant analogues, the extent of the reduced sensitivity to GIP in diabetic patients needs to be quantitatively assessed using a wide range of peptide concentrations, as has been done for GLP-1 [510], rather than single low dosage protocols, biased to show a lack of effectiveness. No matter what underlying cause is ultimately determined to be responsible for the reduced responsiveness to GIP in human diabetes, analogues based on the DPIV-resistant forms of GIP and GLP-1 described here may be useful in stimulating insulin secretion through the residual islet capacity to respond to incretins.

Several structure-activity relationships of glucagon have been assessed *in vitro* and *in vivo*, with specific reference to degradation of glucagon by dipeptidyl peptidase IV. N-terminally

194

truncated glucagon fragments were all weak partial agonists of the human glucagon receptor, and showed no glycemic effect *in vivo*. The role of DPIV degradation in glucagon metabolism was also studied using amino-terminally modified glucagon analogues. DPIV-resistant [D-Ser^2] exhibited enhanced biological activity relative to native glucagon in a bioassay. Thus further evidence that DPIV is likely a primary enzyme involved in glucagon degradation has been provided.

Chapter 5: Summary and Future Directions

Results have been presented regarding the potential regulatory mechanisms modulating insulinotropic peptide hormone bioactivities, namely receptor desensitization and enzymatic inactivation, with a focus on glucose-dependent insulinotropic/gastric inhibitory polypeptide. Studies on insulinotropic hormones glucagon and GLP-1 were limited to design of synthetic analogues. On the one hand, GIP receptor desensitization, sequestration, degradation and down-regulation were considered as a potential mechanism for the attenuated responsiveness of the β-cell to GIP in type 2 diabetes and animal models of the disease [290; 370; 374; 379]. Results indicated that the GIP receptor was fairly resistant to desensitization compared to other receptor models, including the GLP-1 and glucagon receptors (Chapter 3). Thus it is likely that if receptor desensitization/down-regulation is the culprit for the ablated GIP effect in diabetes, it is likely a chronic effect involving degradation of receptors and/or transcriptional down-regulation of GIP receptor expression. Furthermore, the relative resistance of the receptor to rapid desensitization is a favourable characteristic, if GIP receptor agonists are to be used as potential therapies.

Enzymatic inactivation of GIP, GLP-1 and glucagon by dipeptidyl peptidase IV has been reported [328; 427; 453]. The development of specific inhibitors of DPIV and enzyme resistant incretin analogues have been well documented as potential therapies for type 2 diabetes mellitus [456; 461; 511; 520; 521]. Presented here was the first report of systematic design of DPIV-resistant GIP analogues [329; 456], 3 of which were selected for *in vivo* studies (Chapter 4). Although responsiveness to GIP in diabetes is reduced, this does not necessarily preclude the pharmaceutical potential of analogues alone or in combination with traditional oral therapy. Sulphonylureas improve β-cell responsiveness to GIP [464], lending support for combination therapy, while simply raising the dosage will likely overcome the diminished effect of GIP alone. The finding that DPIV also degrades the counter-regulatory hormone, glucagon [328; 453],

raises some interesting issues. While DPIV-resistant analogues were employed in the current report in order to support the hypothesis that DPIV-hydrolysis of glucagon may be a normal physiological process, therapeutic potential of hyperglycemic agents is limited. Glucagon is currently used clinically in cases presenting hypoglycemia (including but not limited to insulin or sulfonylurea overdose), during refractory bradycardia (during cardiogenic shock or β-blocker overdose) and as a GI relaxant during endoscopy, among other uses in emergency medicine [522; 523], and superactive analogues of glucagon such as [D-Ser^2]glucagon$_{1-29}$ described here may be used at lower doses to achieve the same results. Findings suggest that DPIV inhibition will likely also preserve bioactive glucagon; the net effect of postprandial DPIV inhibition is to reduce glycemic excursions [381; 382; 418], however, the effect of DPIV during fasting has not been examined, nor has the relative contribution of glucagon to the postprandial glycemic profile during DPIV inhibition.

In point form, the salient results from the current thesis are:

1. Desensitization of βTC-3 cells to GIP occurs at the level of the receptor, and at distal steps of the stimulus-secretion cascade.

2. Desensitization of the GIP receptor parallels receptor sequestration kinetics in transfected cells.

3. Receptor phosphorylation was implicated in both receptor desensitization and internalization, however, the specific sites appeared to be different, but may overlap.

4. Protein kinase C was implicated in the regulation of GIP responsiveness in βTC-3 cells and of the transfected receptor.

5. Fluorescent methods were developed to track GIP receptor internalization, and may be further used to delineate endocytic and recycling pathways.

6. Inactivation of GIP by dipeptidyl peptidase IV was confirmed: GIP_{3-42} bound to the GIP receptor with high affinity, but was unable to promote cyclic AMP production at concentrations as high as 10 μM.

7. A series of DPIV-resistant GIP analogues were generated, which serve to further our understanding of the importance of GIP's amino terminus for receptor activation, as well as permitting demonstration of enhanced bioactivity of enzyme resistant peptides *in vivo*. $[D-Ala^2]GIP_{1-42}$ was antidiabetogenic in normal and obese diabetic rats.

8. Parallel comparison of GIP and GLP-1 analogues *in vitro* and *in vivo* indicated that the potency of these peptides were not dramatically different, lending support for the use of both peptides as therapeutic agents.

9. Inactivation of glucagon by DPIV was shown. Fragments arising from DPIV cleavage were partial agonists *in vitro*, but ineffective *in vivo*. DPIV-resistant analogues were generated, and $[D-Ser^2]glucagon$ showed similar *in vitro* potency to native GIP, but enhanced *in vivo* biological activity.

From an academic standpoint, there is still much we don't know about GIP receptor physiology. Its regulation has only begun to be examined. Phosphorylation was implicated by the current work as a potential regulatory mechanism. A more detailed examination of individual phosphorylation sites would further clarify the importance of each site in either desensitization or internalization; alanine substitution was employed here, but substitution of negatively charged residues may mimic phosphorylation, and provide some insight. G-protein coupled receptor kinases, in particular GRK-2, have been implicated in the phosphorylation of the GIP receptor, although specific phosphorylation sites were not identified. Perhaps more interesting is the potential cross-talk between receptors, possibly mediating heterologous desensitization, a subject which has not been studied for the GIP receptor. The diversity of GIP

receptor signalling has been recently addressed [293; 294; 296; 300; 302], however, full characterization of these pathways has yet to be done. The role of receptor sequestration and/or interaction with cytoskeletal scaffold proteins in the activation of pleiotropic signal transduction cascades should be performed; MAP kinases may feedback on signalling molecules GRK-2 and/or β-arrestin to alter desensitization [524-535]. It is not clear whether the recent demonstration of G-protein switching for the adrenergic receptor [536; 537] and interacting molecules capable of altering the selectivity of the CGRP receptor [538; 539] may be applied to other G-protein coupled receptors such as those for incretin hormones.

The role of GIP receptor down-regulation in the etiology of type 2 diabetes needs to be further characterized. Supportive evidence has been found from *in vivo* studies in animal models of type 2 diabetes [379]. In order to fully understand the reasons for greater responsiveness to GLP-1, but diminished responsiveness to GIP may be accomplished by gene expression array technology comparing donor tissue from normal and diabetic islets. Furthermore, the underlying mechanisms for improved β-cell sensitivity in sulphonylurea treated diabetics may similarly be assessed [464]. Study of GIP receptor expression will likely yield agents capable of increasing GIP receptor expression, and thus reverse the ineffectiveness of the hormone in diabetes. In the meantime, a full pharmacokinetic study should be undertaken to characterize fully the dose-response relationship of GIP in healthy and diabetic humans. This will provide useful information regarding the feasibility of GIP and GIP analogues for the potential treatment of diabetes. In the current thesis, comparison of a completely resistant GIP analogue ([D-Ala^2]GIP) to a partially resistant analogues ([Ser^2]GIP) clearly demonstrated the benefit of greater DPIV resistance for enhanced *in vivo* potency (Chapter 4). Unfortunately, most of the completely DPIV-resistant analogues generated in the current study suffered compromised activity at the cloned receptor. Thus effort to obtain completely resistant GIP analogues with complete DPIV resistance would be worthwhile. Clinical testing of [D-Ala^2]GIP in healthy individuals and type

2 diabetes seems clear to proceed; recently, a preliminary report of use of DPIV-resistant [Tyr^1-glucitol]GIP in humans has been presented in abstract form [540].

With the finding that dipeptidyl peptidase IV is also capable of degrading glucagon [453; 456], there are many potential future directions. Perhaps the first and most important direction would be the development of analytical techniques to simultaneously measure glucagon and truncated fragments in serum. Use of immunoprecipitation combined with mass spectroscopy may be the most rapid method at this point [61], however, development of N-terminally specific antibodies would be equally effective, but perhaps more difficult [60; 417; 433; 448]. Thus it would be possible to examine the effects of DPIV inhibition on normal glucagon metabolism. Combination of glucagon antagonists and DPIV inhibitors may allow quantification of the relative contribution of glucagon to the postprandial glycemic profile in animals thus treated.

The role that peptide hormones play in the regulation of glucose homeostasis continues to be better understood with well designed experimental evidence. However, with each question that is answered, many more questions arise. It is hoped that this thesis has both answered many questions regarding GIP receptor physiology and regulation of insulinotropic hormones by enyzmatic inactivation, as well as provided insight for future studies in the field. GIP was the only known physiological incretin during the 1970s [3], but upon the discovery of GLP-1 [100], GLP-1 has been the focus of intense study by many groups for two decades, while GIP has been relatively neglected [511]. It seems now that we are in the beginning of a renaissance of interest in GIP in normal physiology, disease and as a therapeutic possibility.

Appendix A

Table 12: Predicted and measured molecular masses of synthetic peptides

Mass spectrometry was performed by Dr. S. Manhart, Probiodrug, Halle (Saale), Germany. Peptides were purified by HPLC to greater than 92-95%.

Synthetic Peptide:	Molecular Weight (Daltons)		Synthetic Peptide:	Molecular Weight (Daltons)	
	Expected	Measured		Expected	Measured
GIP(1-42OH)	4984.3	4984.7	[Ala^{14}]1-14OH	1507.7	1506.0
1-6NH2	685.7	686.9	[D-Ala^2]1-14OH	1567.8	1570.6
1-7NH2	798.9	800.2	[Pro^3]1-14OH	1535.8	1536.0
1-13OH	1436.5	1438.2	[Y^{1}A^{2}ψ(CH$_2$NH)]1-14OH	1552.9	1554.2
1-13NH2	1435.6	1435.6	[BTD]1-14OH	1766.8	1769.5
1-14OH	1567.8	1569.3			
1-14NH2	1566.8	1569.7	[D-Ala^2]1-42OH	5002.7	4998.6
1-15OH	1682.8	1680.3	[D-Ala^2]1-30NH2	3552.0	3553.8
1-15NH2	1681.9	1682.6	[Y^{1}A^{2}ψ(CH$_2$NH)]1-30NH2	3537.1	3539.0
1-30NH2	3552.0	3553.3	[Gly^2]1-30NH2	3537.0	3539.1
7-30NH2	2882.3	2886.9	[Ser^2]1-30NH2	3567.1	3568.0
15-42OH	3433.8	3434.4	[(P)Ser^2]1-30NH2	3647.1	3646.9
15-30NH2	2001.3	2003.3	[Val^2]1-30NH2	3579.1	3580.7
16-30NH2	1886.3	1887.6	[Pro^3]1-30NH2	3519.1	3522.9
17-30NH2	1758.1	1761.1	[N-MeGlu^3]1-30NH2	3565.1	3566.1
19-30NH2	1488.7	1489.8	[Cyclo(K^{16},D^{21})]1-30NH2	3533.1	3524.6
3-42OH	4749.4	4751.4			
[Ala^1]1-14OH	1475.7	1475.2	GLP-1$_{[7-36NH2]}$	3297.7	3298.4
[Ser^2]1-14OH	1583.8	1583.2	[Ser^2]GLP-1$_{[7-36NH2]}$	3313.9	3314.3
[Ala^3]1-14OH	1509.7	1511.4	[(P)Ser^2]GLP-1$_{[7-36NH2]}$	3393.7	3394.3
[Ala^4]1-14OH	1581.8	1586.8			
[Ala^5]1-14OH	1537.7	1533.2	Glucagon$_{1-29}$	3482.8	3482.9
[Ala^6]1-14OH	1491.7	1487.7	Glucagon$_{3-29}$	3258.6	3256.7
[Ala^7]1-14OH	1525.7	1526.1	[pGlu^3]glucagon$_{3-29}$	3241.6	3242.2
[Ala^8]1-14OH	1551.8	1546.6	Glucagon$_{5-29}$	3073.4	3074.9
[Ala^9]1-14OH	1523.7	1523.3	[D-Ser^2]glucagon$_{1-29}$	3482.8	3485.2
[Ala^{10}]1-14OH	1475.7	1477.8	[(P)Ser^2]glucagon$_{1-29}$	3562.8	3564.1
[Ala^{11}]1-14OH	1551.8	1553.6	[Gly^2]glucagon$_{1-29}$	3451.8	3452.0
[Ala^{12}]1-14OH	1525.7	1525.4	[D-Gln^3]glucagon$_{1-29}$	3482.8	3483.9
[Tyr^{13}]1-14OH	1659.9	1648.2			

References

[1] Sherwood, N. M., Krueckl, S. L., and McRory, J. E. (2000). The origin and function of the pituitary adenylate cyclase-activating polypeptide. *Endocr Rev*, **21**:619-670.

[2] Campbell, R. M., and Scanes, C. G. (1992). Evolution of the growth hormone-releasing factor (GRF) family of peptides. *Growth Regulation*, **2**:175-191.

[3] Pederson, R. A. (1994). Gastric Inhibitory Polypeptide, *in* J. H. Walsh, and G. J. Dockray, eds., Gut Peptides: Biochemistry and Physiology: New York, Raven Press Ltd., p. 217-259.

[4] McIntosh, C. H. S., Wheeler, M. B., Gelling, R. W., Brown, J. C., and Pederson, R. A. (1996). GIP receptors and signal-transduction mechanisms. *Acta Physiol Scand*, **157**:361-365.

[5] Lefkowitz, R. J. (2000). The superfamily of heptahelical receptors. *Nat Cell Biol*, **2**:E133-E116.

[6] Dixon, R. A., Kobilka, B. K., Strader, D. J., Benovic, J. L., Dohlman, H. G., Frielle, T., Bolanowski, M. A., Bennett, C. D., Rands, E., and Diehl, R. E. (1986). Cloning of the gene and cDNA for mammalian beta-adrenergic receptor and homology with rhodopsin. *Nature*, **321**:75-9.

[7] Ishihara, T., Nakamura, S., Kaziro, Y., Takahashi, T., Takahashi, K., and Nagata, S. (1991). Molecular cloning and expression of a cDNA encoding the secretin receptor. *EMBO J*, **10**:1635-1641.

[8] Thorens, B. (1992). Expression cloning of the pancreatic beta cell receptor for the gluco-incretin hormone glucagon-like peptide 1. *Proc Natl Acad Sci USA*, **89**:8641-8645.

[9] Svoboda, M., Ciccarelli, E., Tastenoy, M., Robberecht, P., and Christophe, J. (1993). A cDNA construct allowing the expression of rat hepatic glucagon receptors. *Biochem Biophys Res Commun*, **192**:135-142.

[10] Jenlinek, L. J., Lok, S., Rosenberg, G. B., Smith, R. A., Grant, F. J., Biggs, S., Bensch, P. A., Kuijper, J. L., Sheppard, P. O., and Sprecher, C. A. (1993). Expression cloning and signalling properties of the rat glucagon receptor. *Science*, **259**:1614-1616.

[11] Usdin, T. B., Mezey, É., Button, D. C., Brownstein, M. J., and Bonner, T. I. (1993). Gastric inhibitory polypeptide receptor, a member of the secretin-vasoactive intestinal peptide receptor family, is widely distributed in peripheral organs and the brain. *Endocrinology*, **133**:2861-2870.

[12] Brown, J. C., Pederson, R. A., Jorpes, E., and Mutt, V. (1969). Preparation of highly active enterogastrone. *Can J Physiol Pharmacol*, **47**:113-114.

[13] Brown, J. C., and Pederson, R. A. (1970). A multiparameter study on the action of preparations containing cholecystokinin-pancreozymin. *Scand J Gastroenterol*, **5**:537-541.

[14] Brown, J. C., Mutt, V., and Pederson, R. A. (1970). Further purification of a polypeptide demonstrating enterogastrone activity. *J Physiol*, **209**:57-64.

[15] Pederson, R. A., and Brown, J. C. (1972). Inhibition of histamine-, pentagastrin-, and insulin-stimulated canine gastric secretion by pure "gastric inhibitory polypeptide". *Gastroenterology*, **62**:393-400.

[16] Kosaka, T., and Lim, R. K. S. (1930). Demonstration of the humoral agent in fat inhibition of gastric secretion. *Proc Soc Exptl Biol NY*, **27**:890-891.

[17] Brown, J. C. (1971). A gastric inhibitory polypeptide. I. The amino acid composition and the tryptic peptides. *Can J Biochem*, **49**:255-261.

[18] Brown, J. C., and Dryburgh, J. R. (1971). A gastric inhibitory polypeptide II: The complete amino acid sequence. *Can J Biochem*, **49**:867-872.

[19] Jörnvall, H., Carlquist, M., Kwauk, S., Otte, S. C., McIntosh, C. H. S., Brown, J. C., and Mutt, V. (1981). Amino acid sequence and heterogeneity of gastric inhibitory polypeptide (GIP). *FEBS Lett*, **123**:205-210.

[20] Moody, A. J., Thim, L., and Valverde, I. (1984). The isolation and sequencing of human gastric inhibitory peptide (GIP). *FEBS Lett*, **172**:142-148.

[21] Carlquist, M., Maletti, M., Jörnvall, H., and Mutt, V. (1984). A novel form of gastric inhibitory polypeptide (GIP) isolated from bovine intestine using a radioreceptor assay. Fragmentation with staphylococcal protease results in GIP 1-3 and GIP 4-42, fragmentation with enterokinase in GIP 1-16 and GIP 17-42. *Eur J Biochem*, **145**:573-577.

[22] Takeda, J., Seino, Y., Tanaka, K-I., Fukumoto, H., Kayano, T., Takahashi, H., Mitani, T., Kurono, M., Suzuki, T., Tobe, T., and Imura, H. (1987). Sequence of an intestinal cDNA encoding human gastric inhibitory plolypeptide precursor. *Proc Natl Acad Sci USA*, **84**:7005-7008.

[23] Inagaki, N., Seino, Y., Takeda, J., Yano, H., Yamada, Y., Bell, G. I., Eddy, R. L., Fukushima, Y., Byers, M. G., Shows, T. B., and Imura, H. (1989). Gastric inhibitory polypeptide: structure and chromosomal localization of the human gene. *Mol Endocrinol*, **3**:1014-1021.

[24] Higashimoto, Y., Simchock, J., and Liddle, R. A. (1992). Molecular cloning of rat glucose-dependent insulinotropic peptide (GIP). *Biochim Biophys Acta*, **1132**:72-74.

[25] Higashimoto, Y., and Liddle, R. A. (1993). Isolation and characterization of the gene encoding rat glucose-dependent insulinotropic polypeptide. *Biochem Biophys Res Commun*, **193**:182-190.

[26] Tseng, C-C., Jarboe, L. A., Landau, S. B., Williams, E. K., and Wolfe, M. M. (1993). Glucose-dependent insulinotropic peptide: structure of the precursor and tissue-specific expression in rat. *Proc Natl Acad Sci USA*, **90**:1992-1996.

[27] Sharma, S. K., Austin, C., Howard, A., Lo, G., Nicholl, C. G., and Legon, S. (1992). Characterization of rat gastric inhibitory peptide cDNA. *J Mol Endocrinol*, **9**:265-272.

[28] Schieldrop, P. J., Gelling, R. W., Elliot, R., Hewitt, J., Kieffer, T. J., McIntosh, C. H. S., and Pederson, R. A. (1996). Isolation of a murine glucose-dependent insulinotropic polypeptide (GIP) cDNA from a tumor cell line (STC$_{6-14}$) and quantification of glucose-induced increases in GIP mRNA. *Biochim Biophys Acta*, **1308**:111-113.

[29] Yeung, C-M., Wong, C. K. C., Chung, S. K., Chung, S. S. M., and Chow, B. K. C. (1999). Glucose-dependent insulinotropic polypeptide gene expression in the stomach: revealed by a trangenic mouse study, in situ hybridization and immunohistochemical staining. *Mol Cell Endocrinol*, **154**:161-170.

[30] Lewis, T. B., Saenz, M., O'Connell, P., and Leach, R. J. (1994). Localization of glucose-dependent insulinotropic polypeptide (GIP) to a gene cluster on chromosome 17q. *Genomics*, **19**:589-591.

[31] Anderson, L. A., Friedman, L., Osborne-Lawrence, S., Lynch, E., Weissenbach, J., Bowcock, A., and King, M. C. (1993). High-density genetic map of the BRCA1 region of chromosome 17q12-q21. *Genomics*, **17**:618-623.

[32] Rossowski, W. J., Zacharia, S., Mungan, Z., Ozmen, V., Ertan, A., Baylor, L. M., Jiang, N-Y., and Coy, D. H. (1992). Reduced gastric acid inhibitory effect of a pGIP(1-30)NH2 fragment with potent pancreatic amylase inhibitory activity. *Regul Pept*, **39**:9-17.

[33] Someya, Y., Inagaki, N., Maekawa, T., Seino, Y., and Ishii, S. (1993). Two 3',5'-cyclic-adenosine monophosphate response elements in the promoter region of the human gastric inhibitory polypeptide gene. *FEBS Lett*, **317**:67-73.

[34] Boylan, M. O., Jepeal, L. I., Jarboe, L. A., and Wolfe, M. M. (1997). Cell-specific expression of the glucose-dependent insulinotropic polypeptide gene in a mouse neuroendocrine tumor cell line. *J Biol Chem*, **272**:17438-17443.

[35] Tseng, C-C., Boylan, M. O., Jarboe, L. A., Williams, E. K., Sunday, M. E., and Wolfe, M. M. (1995). Glucose-dependent insulinotropic polypeptide (GIP) gene expression in the rat salivary gland. *Mol Cell Endocrinol*, **115**:13-19.

[36] Higashimoto, Y, and Liddle, R. A. (1994). Developmental expression of the glucose-dependent insulinotropic polypeptide gene in rat intestine. *Biochem Biophys Res Commun*, **201**:964-972.

[37] Higashimoto, Y., Opara, E. C., and Liddle, R. A. (1995). Dietary regulation of glucose-dependent insulinotropic peptide (GIP) gene expression in rat small intestine. *Comp Biochem Physiol*, **110C**:207-214.

[38] Tseng, C-C., Jarboe, L. A., and Wolfe, M. M. (1994). Regulation of glucose-dependent insulinotropic peptide gene expression by a glucose meal. *Am J Physiol*, **266**:G887-G891.

[39] Berghöfer, P., Peterson, R. G., Schneider, K., Fehmann, H-C., and Göke, B. (1997). Incretin hormone expression in the gut of diabetic mice and rats. *Metabolism*, **46**:261-267.

[40] Wolfe, M. M., Zhao, K-B., Glazier, K. D., Jarboe, L. A., and Tseng, C-C. (2000). Regulation of glucose-dependent insulinotropic polypeptide release by protein in the rat. *Am J Physiol*, **279**:G561-566.

[41] Buchan, A. M. J., Polak, J. M., Capella, C., Solcia, C. E., and Pearse, A. G. E. (1978). Electronimmunocytochemical evidence for the K cell localization of gastric inhibitory polypeptide (GIP) in man. *Histochemistry*, **56**:37-44.

[42] Polak, J. M., Bloom, S. R., Kuzio, M., Brown, J. C., and Pearse, A. G. E. (1973). Cellular localization of gastric inhibitory polypeptide in the duodenum and jejunum. *Gut*, **14**:284-288.

[43] Buffa, R., Polak, J. M., Pearse, A. G. E., Solcia, C. E., Grimelius, L., and Capella, C. (1975). Identification of the intestinal cell storing gastric inhibitory peptide. *Histochemistry*, **43**:249-255.

[44] Mortensen, K., Petersen, L. L., and Ørskov, C. (2000). Colocalization of GLP-1 and GIP in human and porcine intestine. *Ann NY Acad Sci*, **921**:469-472.

[45] Damholt, A. B., Kofod, H., and Buchan, A. M. J. (1999). Immunocytochemical evidence for a paracrine interaction between GIP and GLP-1-producing cells in canine small intestine. *Cell Tissue Res*, **298**:287-293.

[46] Cheung, A. T., Dayanandan, B., Lewis, J. T., Korbutt, G. S., Rajotte, R. V., Bryer-Ash, M., Boylan, M. O., Wolfe, M. M., and Kieffer, T. J. (2000). Glucose-dependent insulin release from genetically engineered K cells. *Science*, **290**:1959-1962.

[47] Steinhoff, M., Hesse, H., Göke, B., Steinhoff, A., Eissele, R., and Slater, E. P. (2001). Indirect RT-PCR in-situ hybridization: a novel non-radioactive method for detecting glucose-dependent insulinotropic peptide. *Regul Pept*, **97**:187-194.

[48] Kieffer, T. J., Buchan, A. M. J., Barker, H., Brown, J. C., and Pederson, R. A. (1994). Release of gastric inhibitory polypeptide from cultured canine endocrine cells. *Am J Physiol*, **267**:E489-E496.

[49] Chow, B. K.-C., Morrow, G. W., Ho, M., Pederson, R. A., McIntosh, C. H. S., Brown, J. C., and MacGillivray, R. T. A. (1990). Expression of recombinant human glucose-dependent insulinotropic polypeptide in Escherichia coli by sequence-specific proteolysis of a protein A fusion protein. *Peptides*, **11**:1069-1074.

[50] Kieffer, T. J., Huang, Z., McIntosh, C. H. S., Buchan, A. M. J., Brown, J. C., and Pederson, R. A. (1995). Gastric inhibitory polypeptide release from a tumor-derived cell line. *Am J Physiol*, **269**:E316-E322.

[51] Kuzio, M., Dryburgh, J. R., Malloy, K. M., and Brown, J. C. (1974). Radioimmunoassay for gastric inhibitory polypeptide. *Gastroenterology*, **66**:357-364.

[52] Alam, M. J., and Buchanan, K. D. (1993). Conflicting gastric inhibitory polypeptide data: possible causes. *Diabetes Res Clin Prac*, **19**:93-101.

[53] Krarup, T. (1988). Immunoreactive gastric inhibitory polypeptide. *Endocr Rev*, **9**:122-134.

[54] Amland, P. F., Jorde, R., Revhaug, A., Myhre, E. S., Burhol, P. G., and Giercksky, K.-E. (1984). Fasting and postprandial GIP values in pigs, rats, dogs, and man measured with five different GIP antisera. *Scand J Gastroent*, **19**:1095-1098.

[55] Krarup, T., Holst, J. J., and Larsen, K. L. (1985). Responses and molecular heterogeneity of IR-GIP after intraduodenal glucose and fat. *Am J Physiol*, **249**:E195-E200.

[56] Jorde, R., Burhol, P. G., and Schulz, T. B. (1983). Fasting and postprandial plasma GIP values in man measured with seven different antisera. *Regul Pept*, **7**:87-94.

[57] Brown, J. C., Dahl, M., Kwauk, S., McIntosh, C. H. S., Otte, S. C., and Pederson, R. A. (1981). Actions of GIP. *Peptides*, **2 (Suppl. 2)**:241-245.

[58] Mentlein, R., Gallwitz, B., and Schmidt, W. E. (1993). Dipeptidyl-peptidase IV hydrolyses gastric inhibitory polypeptide, glucagon-like peptide-1 (7-36)amide, peptide histidine methionine and is responsible for their degradation in human serum. *Eur J Biochem*, **214**:829-835.

[59] Kieffer, T. J., McIntosh, C. H. S., and Pederson, R. A. (1995). Degradation of glucose-dependent insulinotropic polypeptide and truncated glucagon-like peptide 1 in vitro and in vivo by dipeptidyl peptidase IV. *Endocrinology*, **136**:3585-3596.

[60] Deacon, C. F., Nauck, M. A., Meier, J. J., Hücking, K., and Holst, J. J. (2000). Degradation of endogenous and exogenous gastric inhibitory polypeptide in healthy and in type 2 diabetic subjects as revealed using a new assay for the intact peptide. *J Clin Endocrinol Metab*, **85**:3575-3581.

[61] Wolf, R., Rosche, F., Hoffmann, T., and Demuth, H-U. (2001). Immunoprecipitation and liquid chromatographic-mass spectrometric determination of the peptide glucose-dependent insulinotropic polypeptides GIP1-42 and GIP3-42 from human plasma samples. New sensitive method to analyse physiological concentrations of peptide hormones. *J Chromatogr A*, **926**:21-27.

[62] Amland, P. F., Jorde, R., Burhol, P. G., and Giercksky, K-E. (1984). Similar plasma GIP responses in obese and lean subjects after an oral test meal and after intraduodenal stimulation with fat and glucose. *Int J Obes*, **8**:649-653.

[63] Greenberg, G. R., and Pokol-Daniel, S. (1994). Neural modulation of glucose-dependent insulinotropic peptide (GIP) and insulin secretion in conscious dogs. *Pancreas*, **9**:531-535.

[64] Ebert, R., Illmer, K., and Creutzfeldt, W. (1979). Release of gastric inhibitory polypeptide (GIP) by intraduodenal acidification in rats and humans and abolishment of the incretin effect of acid by GIP-antiserum in rats. *Gastroenterology*, **76**:515-523.

[65] Flaten, O. (1981). The effect of adrenoceptor blockade on the release of gastric inhibitory polypeptide after intraduodenal glucose in humans. *Scand J Gastroent*, **16**:641-645.

[66] Flaten, O. (1981). Radioimmunoassay of gastric inhibitory polypeptide (GIP) and the effect of intraduodenal acidification on glucose-stimulated and unstimulated GIP release in humans. *Scand J Gastroent*, **16**:545-554.

[67] Knapper, J. M. E., Heath, A., Fletcher, J. M., Morgan, L. M., and Marks, V. (1995). GIP and GLP-1(7-36)amide secretion in response to intraduodenal infusions of nutrients in pigs. *Comp Biochem Physiol*, **111C**:445-450.

[68] Bryer-Ash, M., Cheung, A., and Pederson, R. A. (1994). Feedback regulation of glucose-dependent insulinotropic polypeptide (GIP) secretion by insulin in conscious rats. *Regul Pept*, **51**:101-109.

[69] Nelson, R. L., Go, V. L. W., McCullough, A. J., Ilstrup, D. M., and Service, F. J. (1986). Lack of a direct effect of the autonomic nervous system on glucose-stimulated gastric inhibitory polypeptide (GIP) secretion in man. *Dig Dis Sci*, **31**:929-935.

[70] O'Dorisio, T. M., Spaeth, J. T., Martin, E. W. Jr., Sirinek, K. R., Thomford, N. R., Mazzaferri, E. L., and Cataland, S. (1978). Mannitol and glucose: effects on gastric acid secretion by endogenous gastric inhibitory polypeptide. *Dig Dis Sci*, **23**:1079-1083.

[71] Lavin, J. H., Wittert, G. A., Andrews, J., Yeap, B., Wishart, J. M., Morris, H. A., Morley, J. E., Horowitz, M., and Read, N. W. (1998). Interaction of insulin, glucagon-like peptide 1, gastric inhibitory polypeptide, and appetite in response to intraduodenal carbohydrate. *Am J Clin Nutr*, **68**:591-598.

[72] LeRioth, D., Spitz, I. M., Ebert, R., Liel, Y., Odes, S., and Creutzfeldt, W. (1980). Acid-induced gastric inhibitory polypeptide secretion in man. *J Clin Endocrinol Metab*, **51**:1385-1389.

[73] Ohneda, A., Kobayashi, T., Nihei, J., Imamura, M., Naito, H., and Tsuchiya, T. (1985). Role of vagus nerve in secretion of gastric inhibitory polypeptide in dogs. *Tohuku J Exp Med*, **147**:183-190.

[74] Lucey, M. R., Fairclough, P. D., Wass, J. A. H., Kwasowski, P., Medbak, S., Webb, J., and Rees, L. H. (1984). Response of circulating somatostatin, insulin, gastrin and GIP, to intraduodenal infusion of nutrients in normal man. *Clin Endocrinol*, **21**:209-217.

[75] Thomas, F. B., Shook, D. F., O'Dorisio, T. M., Cataland, S., Mekhjian, H. S., Caldwell, J. H., and Mazzaferri, E. L. (1977). Localization of gastric inhibitory polypeptide release by intestinal glucose perfusion in man. *Gastroenterology*, **72**:49-54.

[76] Sykes, S., Morgan, J., English, J., and Marks, V. (1980). Evidence for preferential stimulation of gastric inhibitory polypeptide secretion by the rat by actively transported carbohydrates and their analogues. *J Endocrinol*, **5**:210-217.

[77] Sirinek, K. R., Levine, B. A., O'Dorisio, T. M., and Cataland, S. (1983). Gastric inhibitory polypeptide (GIP) release by actively transported, structurally similar carbohydrates. *Proc Soc Exp Biol Med*, **173**:379-385.

[78] O'Dorisio, T. M., Cataland, S., Stevenson, M., and Mazzaferri, E. L. (1976). Gastric inhibitory polypeptide (GIP): intestinal distribution and stimulation by amino acids and medium-chain triglycerides. *Dig Dis Sci*, **21**:761-765.

[79] Sirinek, K. R., Crockett, S. E., Mazzaferri, E. L., Cataland, S., and Thomford, N. R. (1974). Release of gastric inhibitory polypeptide. Comparison of glucose and fat as stimuli. *Surg Forum*, **25**:361-363.

[80] Creutzfeldt, W., and Ebert, R. (1985). New developments in the incretin concept. *Diabetologia*, **28**:565-573.

[81] Ebert, R., and Creutzfeldt, W. (1984). Evidence that fat induced secretion of gastric inhibitory polypeptide is coupled to chylomicron formation (abstract). *Eur J Clin Invest*, **14**:9A.

[82] Pederson, R. A., Schubert, H. E., and Brown, J. C. (1975). Gastric inhibitory polypeptide, its physiologic release and insulinotropic action in dog. *Diabetes*, **24**:1050-1056.

[83] Thomas, F. B., Sinar, D., Mazzaferri, E. L., Cataland, S., Mekhjian, H. S., Caldwell, J. H., and Fromkes, J. J. (1978). Selective release of gastric inhibitory polypeptide by intraduodenal amino acid perfusion in man. *Gastroenterology*, **74**:1261-1265.

[84] Schulz, T. B., Jorde, R., and Burhol, P. G. (1982). Gastric inhibitory polypeptide release into the portal vein in response to intraduodenal amino acid loads in anesthetized rats. *Scand J Gastroenterol*, **17**:709-713.

[85] Thomas, F. B., Mazzaferri, E. L., Crockett, S. E., Mekhjian, H. S., Gruemer, H. D., and Cataland, S. (1976). Stimulation of secretion of gastric inhibitory polypeptide and insulin by intraduodenal amino acid perfusion. *Gastroenterology*, **70**:523-527.

[86] Sirinek, K. R., Pace, W. G., Crockett, S. E., O'Dorisio, T. M., Mazzaferri, E. L., and Cataland, S. (1978). Insulin-induced attenuation of glucose-stimulated gastric inhibitory polypeptide secretion. *Am J Surg*, **135**:151-155.

[87] Verdonk, C. A., Rizza, R. A., Nelson, R. L., Go, V. L. W., Gerich, J. E., and Service, F. J. (1980). Interaction of fat-stimulated gastric inhibitory polypeptide on pancreatic alpha and beta cell function. *J Clin Invest*, **65**:1119-1125.

[88] Creutzfeldt, W., Talaulicar, M., Ebert, R., and Willms, B. (1980). Inhibition of gastric inhibitory polypeptide (GIP) release by insulin and glucose in juvenile diabetes. *Diabetes*, **29**:140-145.

[89] Dryburgh, J. R., Hampton, S. M., and Marks, V. (1980). Endocrine pancreatic control of the release of gastric inhibitory polypeptide. A possible physiological role for C-peptide. *Diabetologia*, **19**:397-401.

[90] McIntosh, C. H. S. (1985). Gastrointestinal somatostatin: distribution, secretion and physiological significance. *Life Sci*, **37**:2043-2058.

[91] Schmid, R., Schusdziarra, V., Aulehner, R., Weigert, N., and Classen, M. (1990). Comparison of GLP-1 (7-36amide) and GIP on release of somatostatin-like

immunoreactivity and insulin from the isolated rat pancreas. *Z Gastroenterol*, **28**:280-284.

[92] Jia, X., Brown, J. C., Kwok, Y. N., Pederson, R. A., and McIntosh, C. H. S. (1994). Gastric inhibitory polypeptide and glucagon-like peptide-1(7-36) amide exert similar effects on somatostatin secretion but opposite effects on gastrin secretion from the rat stomach. *Can J Physiol Pharmacol*, **72**:1215-1219.

[93] Deacon, C. F., Wamberg, S., Bie, P., Hughes, T. E., and Holst, J. J. (2002). Preservation of active incretin hormones by inhibition of dipeptidyl peptidase IV suppresses meal-induced incretin secretion in dogs. *J Endocrinol*, **172**:355-362.

[94] Greenberg, G. R., Chan, B., McDonald, T. J., and Alleyne, J. (1985). The role of vagal integrity in gastrin releasing peptide stimulated gastroenteropancreatic hormone release and gastric acid secretion. *Regul Pept*, **10**:179-187.

[95] Williams, R. H., and Champagne, J. (1979). Effects of cholecystokinin, secretin, and pancreatic polypeptide on secretion of gastric inhibitory polypeptide, insulin, and glucagon. *Life Sci*, **25**:947-956.

[96] Sirinek, K. R., Cataland, S., O'Dorisio, T. M., Mazzaferri, E. L., Crockett, S. E., and Pace, W. G. (1977). Augmented gastric inhibitory polypeptide response to intraduodenal glucose by exogenous gastrin and cholecystokinin. *Surgery*, **82**:438-442.

[97] Kraenzlin, M. E., Ch'ng, J. L. C., Mulderry, P. K., Ghatei, M. A., and Bloom, S. R. (1985). Infusion of a novel peptide, calcitonin gene-related peptide (CGRP) in man. Pharmacokinetics and effects on gastric acid secretion and on intestinal hormones. *Regul Pept*, **10**:189-197.

[98] Bayliss, W. M., and Starling, E. H. (1902). The mechanism of pancreatic secretion. *J Physiol*, **28**:235-334.

[99] Holst, J. J., and Ørskov, C. (1994). Glucagon and other proglucagon-derived peptides, *in* J. H. Walsh, and G. J. Dockray, eds., Gut Peptides: Biochemistry and Physiology: New York, Raven Press Ltd., p. 305-340.

[100] Kieffer, T. J., and Habener, J. F. (1999). The glucagon-like peptides. *Endocr Rev*, **20**:876-913.

[101] Zhao, X. T., Walsh, J. H., Wong, H., Wang, L., and Lin, H. C. (1999). Intestinal fat-induced inhibition of meal-stimulated gastric acid secretion depends on CCK but not peptide YY. *Am J Physiol*, **276**:G550-G555.

[102] Lloyd, K. C. K., Maxwell, V., Kovacs, T. O. G., Miller, J., and Walsh, J. H. (1992). Cholecystokinin receptor antagonist MK-329 blocks intestinal fat-induced inhibition of meal-stimulated gastric acid secretion. *Gastroenterology*, **102**:131-138.

[103] Yamagishi, T., and Debas, H. T. (1980). Gastric inhibitory polypeptide (GIP) is not the primary mediator of the enterogastrone action of fat in the dog. *Gastroenterology*, **78**:931-936.

[104] El-Munshid, H. A., Håkanson, R., Lindberg, G., and Sundler, F. (1980). Effects of various gastrointestinal peptides on parietal cells and endocrine cells in the oxyntic mucosa of rat stomach. *J Physiol*, **305**:249-265.

[105] Soon-Shiong, P., Debas, H. T., and Brown, J. C. (1979). The evaluation of gastric inhibitory polypeptide (GIP) as the enterogastrone. *J Surg Res*, **26**:681-686.

[106] Maxwell, V., Shulkes, A., Brown, J. C., Solomon, T. E., Walsh, J. H., and Grossman, M. I. (1980). Effect of gastric inhibitory polypeptide on pentagastrin-stimulated acid secretion in man. *Dig Dis Sci*, **25**:113-116.

[107] McIntosh, C. H. S., Pederson, R. A., Koop, H., and Brown, J. C. (1981). Gastric inhibitory polypeptide stimulated secretion of somatostatinlike immunoreactivity from the stomach: inhibition by acetylcholine or vagal stimulation. *Can J Physiol Pharmacol*, **59**:468-472.

[108] Soon-Shiong, P., Debas, H. T., and Brown, J. C. (1984). Bethanechol prevents inhibition of gastric acid secretion by gastric inhibitory polypeptide. *Am J Physiol*, **247**:G171-G175.

[109] Holst, J. J., Jensen, S. L., Knuhtsen, S., Nielsen, O. V., and Rehfeld, J. F. (1983). Effect of vagus, gastric inhibitory polypeptide, and HCl on gastrin and somatostatin release from perfused pig antrum. *Am J Physiol*, **244**:G515-G522.

[110] Wolfe, M. M., Hocking, M. P., Maico, D. G., and McGuigan, J. E. (1982). Effects of antibodies to gastric inhibitory peptide on gastric acid secretion and gastrin release in the dog. *Gastroenterology*, **84**:941-948.

[111] McIntosh, C. H. S., Kwok, Y. N., Mordhorst, T., Nishimura, E., Pederson, R. A., and Brown, J. C. (1983). Enkephalinergic control of somatostatin secretion from the perfused rat stomach. *Can J Physiol Pharmacol*, **61**:657-663.

[112] McIntosh, C. H. S., Jia, X., and Kwok, Y. N. (1990). Characterization of the opioid receptor type mediating inhibition of rat gastric somatostatin secretion. *Am J Physiol*, **259**:G922-G927.

[113] Lloyd, K. C., and Walsh, J. H. (1994). Gastric Secretion, *in* J. H. Walsh, and G. J. Dockray, eds., Gut Peptides: Biochemistry and Physiology: New York, Raven Press Ltd., p. 633-654.

[114] Pederson, R. A., McIntosh, C. H. S., Meuller, M. K., and Brown, J. C. (1981). Absence of a relationship between immunoreactive-gastrin and somatostatin-like immunoreactivity secretion in the perfused rat stomach. *Regul Pept*, **2**:53-60.

[115] Schusdziarra, V., Bender, H., and Pfeiffer, E. F. (1983). Release of bombesin-like immunoreactivity from the isolated perfused rat stomach. *Regul Pept*, **7**:21-29.

[116] Villar, H. V., Fender, H. R., Rayford, P. L., Bloom, S. R., Ramus, N. I., and Thomson, J. C. (1976). Suppression of gastrin release and gastric secretion by gastric inhibitory polypeptide (GIP) and vasoactive intestinal polypeptide (VIP). *Ann Surg*, **184**:97-102.

[117] Wolfe, M. M., and Reel, G. M. (1986). Inhibition of gastrin release by gastric inhibitory peptide mediated by somatostatin. *Am J Physiol*, **250**:G331-G335.

[118] Chiba, T., and Yamada, T. (1994). Gut Somatostatin, *in* J. H. Walsh, and G. J. Dockray, eds., Gut Peptides: Biochemistry and Physiology: New York, Raven Press Ltd., p. 123-145.

[119] Rossowski, W. J., Cheng, B-L., Jiang, N-Y., and Coy, D. H. (1998). Examination of somatostatin involvement in the inhibitory action of GIP, GLP-1, amylin and adrenomedullin on gastric acid release using a new SRIF antagonist analogue. *Brit J Pharmacol*, **125:**1081-1087.

[120] Denniss, A. R., and Young, J. A. (1978). Modification of salivary duct electrolyte transport in rat and rabbit by physaleamin, VIP, GIP and other enterohormones. *Pflügers Arch Eur J Physiol*, **376:**73-80.

[121] Konturek, S. J., Bilski, J., Tasler, J., and Laskiewicz, J. (1985). Gut hormones in stimulation of gastroduodenal alkaline secretion in conscious dogs. *Am J Physiol*, **248:**G687-G691.

[122] Helman, C. A., and Barbezat, G. O. (1977). The effect of gastric inhibitory polypeptide on human jejunal water and electrolyte transport. *Gastroenterology*, **72:**376-379.

[123] Barbezat, G. O. (1986). The effect of luminal and hormonal factors on small intestinal water and electrolyte transport. *Schweiz Med Wochenschr*, **116:**946-949.

[124] Jensen, R. T., Lemp, G. F., Beinfeld, M. C., and Gardner, J. D. (1982). Actions of natural gastric inhibitory peptide on pancreatic acinar cells: due to contamination with cholecystokinin. *Gastroenterology*, **82:**20-25.

[125] Mueller, M. K., Demol, P., Goebell, H., Fladrich, G., and Brown, J. C. (1983). Natural purified porcine gastric inhibitory polypeptide (GIP) stimulates exocrine pancreas secretion due to contamination with a cholecystokinin-like substance. *Regul Pept*, **5:**307-315.

[126] Müller, M. K., Scheck, T., Demol, P., and Goebell, H. (1986). Interaction of acetylcholine and gastric inhibitory polypeptide on endocrine and exocrine rat pancreatic secretion: augmentation of acetylcholine-induced amylase and volume secretion by the insulinotropic action of gastric inhibitory polypeptide. *Digestion*, **33:**45-52.

[127] Mueller, M. K., Scheck, T., Dreesmann, V., Miodonski, A., and Goebell, H. (1987). GIP potentiates CCK stimulated pancreatic enzyme secretion: effect of GIP and CCK on amylase secretion. *Pancreas*, **2:**106-113.

[128] Cheeseman, C. I., and Tsang, R. (1996). The effect of GIP and glucagon-like peptides on intestinal basolateral membrane hexose transport. *Am J Physiol*, **271:**G477-G482.

[129] Cheeseman, C. I., and O'Neill, D. (1998). Basolateral D-glucose transport activity along the crypt-villus axis in rat jejunum and upregulation induced by gastric inhibitory peptide and glucagon-like peptide-2. *Exp Physiol*, **83:**605-616.

[130] Keinke, O., Ehrlein, H. J., and Wulschke, S. (1987). Mechanical factors regulating gastric emptying examined by the effects of exogenous cholecystokinin and secretin on canine gastroduodenal motility. *Can J Physiol Pharmacol*, **65**:287-292.

[131] Young, A. A., Gedulin, B. R., and Rink, T. J. (1996). Dose-responses for the slowing of gastric emptying in a rodent model by glucagon-like peptide (7-36)NH2, amylin, cholecystokinin, and other possible regulators of nutrient uptake. *Metabolism*, **45**:1-3.

[132] Fara, J. W., and Salazar, A. M. (1978). Gastric inhibitory polypeptide increases mesenteric blood flow. *Proc Soc Exp Biol Med*, **158**:446-448.

[133] Thor, P., Laskiewicz, J., Konturek, S. J., and Creutzfeldt, W. (1987). Role of GIP and insulin in glucose-induced changes in intestinal motility patterns. *Am J Physiol*, **252**:G8-G12.

[134] Castresana, M., Lee, K. Y., Chey, W. Y., and Yajima, H. (1978). Effects of motilin and octapeptide of cholecystokinin on antral and duodenal myoelectric activity in the interdigestive state and during inhibition by secretin and gastric inhibitory polypeptide. *Digestion*, **17**:300-308.

[135] Roberge, J. N., and Brubaker, P. L. (1993). Regulation of intestinal proglucagon-derived peptide secretion by glucose-dependent insulinotropic peptide in a novel enteroendocrine loop. *Endocrinology*, **133**:233-240.

[136] Damholt, A. B., Buchan, A. M. J., and Kofod, H. (1998). Glucagon-like-peptide-1 secretion from canine L-cells is increased by glucose-dependent-insulinotropic peptide but unaffected by glucose. *Endocrinology*, **139**:2085-2091.

[137] Brubaker, P. L. (1991). Regulation of intestinal proglucagon-derived peptide secretion by intestinal regulatory peptides. *Endocrinology*, **128**:3175-3182.

[138] Dumoulin, V., Dakka, T., Plaisancie, P., Chayvialle, J. A., and Cuber, J. C. (1995). Regulation of glucagon-like peptide-1-(7-36) amide by intestinal neurotransmitters and hormones in the isolated vascularly perfused rat colon. *Endocrinology*, **136**:5182-5188.

[139] Herrmann-Rinke, C., Voge, A., Hess, M., and Göke, B. (1995). Regulation of glucagon-like peptide-1 secreion from rat ileum by neurotransmitters and peptides. *J Endocrinol*, **147**:25-31.

[140] Brubaker, P. L., Schloos, J., and Drucker, D. J. (1998). Regulation of glucagon-like peptide-1 synthesis and secretion in the GLUTag enteroendocrine cell line. *Endocrinology*, **139**:4108-4114.

[141] Kogire, M., Inoue, K., Sumi, S., Doi, R., Takaori, K., Yun, M., Fujii, N., Yajima, H., and Tobe, T. (1988). Effects of synthetic human gastric inhibitory polypeptide on splanchnic circulation in dogs. *Gastroenterology*, **95**:1636-1640.

[142] Kogire, M., Inoue, K., Sumi, S., Doi, R., Yun, M., Kaji, H., and Tobe, T. (1992). Effects of gastric inhibitory polypeptide and glucagon on portal venous and hepatic arterial flow in conscious dogs. *Dig Dis Sci*, **37**:1666-1670.

[143] Svensson, A. M., Efendic, S., Östenson, C. G., and Jansson, L. (1997). Gastric inhibitory polypeptide and splanchnic blood perfusion: augmentation of the islet blood flow increase in hyperglycemic rats. *Peptides*, **18**:1055-1059.

[144] Elrick, H., Stimler, L., Hlad, C. J. Jr., and Arai, Y. (1964). Plasma insulin response to oral and intravenous glucose administration. *J Clin Endocrinol*, **24**:1076-1082.

[145] McIntyre, N., Holdsworth, C. D., and Turner, D. S. (1965). Intestinal factor in the control of insulin secretion. *J Clin Endocrinol Metab*, **25**:1317-1324.

[146] Perley, M. J., and Kipnis, D. M. (1967). Plasma insulin responses to oral and intravenous glucose. *J Clin Invest*, **46**:1954-1962.

[147] McIntyre, N., Holdsworth, C. D., and Turner, D. S. (1964). New interpretation of oral glucose tolerance. *Lancet*, **2**:20.

[148] Unger, R. H., and Eisentraut, A. M. (1969). Entero-insular axis. *Arch Intern Med*, **123**:261-266.

[149] Creutzfeldt, W. (1979). The incretin concept today. *Diabetologia*, **16**:75-85.

[150] Moore, B., Edie, E. S., and Abram, J. H. (1906). On the treatment of diabetes mellitus by acid extract of duodenal mucous membrane. *Biochem J*, **1**:28.

[151] Banting, F. G., and Best, C. H. (1922). The internal secretion of the pancreas. *J Lab Clin Med*, **7**:251-264.

[152] La Barre, J., and Still, E. V. (1930). Studies on the physiology of secretin. *Am J Physiol*, **91**:649-653.

[153] La Barre, J. (1932). Sur les possibilités d'un traitement due diabete par l'incretine. *Bull Acad Roy Méd Belg*, **12**:620-634.

[154] Zunz, E., and La Barre, J. (1929). Contributions à l'étude der variations physiologiques de la sécrétion interne du pancréas: relations entre les sécrétion externe du pancréas. *Arch Int Physiol Biochem*, **31**:20-44.

[155] Holst, J. J., and Ørskov, C (2001). Incretin hormones - an update. *Scand J Clin Lab Invest*, **61 (Suppl. 234)**:75-86.

[156] Rehfeld, J. F. (1972). Gastrointestinal hormones and insulin secretion. *Scand J Gastroent*, **7**:289-292.

[157] D'Alessio, D. (1997). Peptide hormone regulation of islet cells. *Rec Prog Horm Res*, **29**:297-300.

[158] Nauck, M. A. (1999). Is glucagon-like peptide 1 an incretin hormone? *Diabetologia*, **42**:373-379.

[159] Balkan, B., and Li, X. (2000). Portal GLP-1 administration in rats augments the insulin response to glucose via neuronal mechanisms. *Am J Physiol*, **279**:R1449-R1454.

[160] Dupré, J., and Beck, J. C. (1966). Stimulation of release of insulin by an extract of intestinal mucosa. *Diabetes*, **15**:555-559.

[161] Rabinovitch, A., and Dupré, J. (1972). Insulinotropic and glucagonotropic activities of crude preparations of cholecysokinin-pancreozymin (abstract). *Clin Res*, **20**:945.

[162] Dupré, J., Ross, S. A., Watson, D., and Brown, J. C. (1973). Stimulation of insulin secretion by gastric inhibitory polypeptide in man. *J Clin Endocrinol Metab*, **37**:826-828.

[163] Andersen, D. K., Elahi, D., Brown, J. C., Tobin, J. D., and Andres, R. (1978). Oral glucose augmentation of insulin secretion. Interactions of gastric inhibitory polypeptide with ambient glucose and insulin levels. *J Clin Invest*, **62**:152-161.

[164] Elahi, D., Andersen, D. K., Brown, J. C., Debas, H. T., Hershcopf, R. J., Raizes, G. S., Tobin, J. D., and Andres, R. (1979). Pancreatic α- and β-cell responses to GIP infusion in normal man. *Am J Physiol*, **237**:E185-E191.

[165] Pederson, R. A., and Brown, J. C. (1976). The insulinotropic action of gastric inhibitory polypeptide in the perfused isolated rat pancreas. *Endocrinology*, **99**:780-785.

[166] Schmidt, W. E., Siegel, E. G., Kümmel, H., Gallwitz, B., and Creutzfeldt, W. (1987). Commercially available preparations of porcine glucose-dependent insulinotropic polypeptide (GIP) contain a biologically inactive GIP-fragment and cholecystokinin-33/-39. *Endocrinology*, **120**:835-837.

[167] Schauder, P., Brown, J. C., Frerichs, H., and Creutzfeldt, W. (1975). Gastric inhibitory polypeptide: effect on glucose-induced insulin release from isolated rat pancreatic islets in vitro. *Diabetologia*, **11**:483-484.

[168] Schauder, P., Schindler, B., Panten, U., Brown, J. C., Frerichs, H., and Creutzfeldt, W. (1977). Insulin release from isolated rat pancreatic islets induced by alpha-ketoisocapronic acid, L-leucine, D-glucose or D-glyceraldehyde: effect of gastric inhibitory polypeptide or glucagon. *Mol Cell Endocrinol*, **7**:115-123.

[169] Fujimoto, W. Y. (1981). Effect of gut peptides on glucose-stimulated insulin release by monolayer cultures of neonatal rat islet cells. *Horm Met Res*, **13**:135-138.

[170] Szecówka, J., Grill, V., Sandberg, E., and Efendic, S. (1982). Effect of GIP on the secretion of insulin and somatostatin and the accumulation of cyclic AMP in vitro in the rat. *Acta Endocrinol*, **99**:416-421.

[171] Mazzaferri, E. L., Ciofalo, L., Waters, L. A., Starich, G. H., Groshong, J. C., and DePalma, L. (1983). Effects of gastric inhibitory polypeptide on leucine- and arginine-stimulated insulin release. *Am J Physiol*, **245**:E114-E120.

[172] Siegel, E. G., and Creutzfeldt, W. (1985). Stimulation of insulin release in isolated rat islets by GIP in physiological concentrations and its relation to islet cyclic AMP content. *Diabetologia*, **28**:857-861.

[173] Fujimoto, W. Y., Ensinck, J. W., Merchant, F. W., Williams, R. H., Smith, P. H., and Johnson, D. G. (1978). Stimulation by gastric inhibitory polypeptide of insulin and glucagon secretion by rat islet cultures. *Proc Soc Exp Biol Med*, **157**:89-93.

[174] Verchere, C. B. (1991). The role of gastric inhibitory polypeptide in the regulation of pancreatic endocrine secretion [Ph.D. Dissertation], University of British Columbia, Vancouver, 224 p.

[175] Amiranoff, B., Vauclin-Jacques, N., and Laburthe, M. (1984). Functional GIP receptors in a hamster pancreatic beta-cell line In111: specific binding and biological effects. *Biochem Biophys Res Commun*, **123**:671-676.

[176] Lu, M., Wheeler, M. B., Leng, X-H., and Boyd, A. E., 3rd (1993). The role of the free cytosolic calcium level in β-cell signal transduction by gastric inhibitory polypeptide and glucagon-like peptide I(7-37). *Endocrinology*, **132**:94-100.

[177] Fehmann, H-C., and Habener, J. F. (1991). Homologous desensitization of the insulinotropic glucagon-like peptide-I(7-37) receptor on insulinoma (HIT-T15) cells. *Endocrinology*, **128**:2880-2888.

[178] Kieffer, T. J., Verchere, C. B., Fell, C. D., Huang, Z., Brown, J. C., and Pederson, R. A. (1993). Glucose-dependent insulinotropic polypeptide stimulated insulin release from a tumour-derived β-cell lin (βTC3). *Can J Physiol Pharmacol*, **71**:917-922.

[179] Swanston-Flatt, S. K., and Flatt, P. R. (1988). Effects of amino acids, hormones and drugs on insulin release and ^{45}Ca uptake by transplantable rat insulinoma cells maintained in tissue culture. *Gen Pharmacol*, **19**:239-242.

[180] Montrose-Rafizadeh, C., Egan, J. M., and Roth, J. (1994). Incretin hormones regulate glucose-dependent insulin secretion in RIN 1046-38 cells: mechanisms of action. *Endocrinology*, **135**:589-594.

[181] O'Harte, F. P. M., Abdel-Wahab, Y. H., Conlon, J. M., and Flatt, P. R. (1998). Amino terminal glycation of gastric inhibitory polypeptide enhances its insulinotropic action on clonal pancreatic B-cells. *Biochim Biophys Acta*, **23**:319-327.

[182] Maletti, M., Altman, J. J., Hoa, D. H., Carlquist, M., and Rosselin, G. (1987). Evidence of functional gastric inhibitory polypeptide (GIP) receptors in human insulinoma. Binding of synthetic human GIP 1-31 and activation of adenylate cyclase. *Diabetes*, **36**:1336-1340.

[183] Ebert, R., Unger, H., and Creutzfeldt, W. (1983). Preservation of incretin activity after removal of gastric inhibitory polypeptide (GIP) from rat gut extracts by immunoadsorption. *Diabetologia*, **24**:449-454.

[184] Ebert, R., and Creutzfeldt, W. (1982). Influence of gastric inhibitory polypeptide antiserum on glucose-induced insulin secretion in rats. *Endocrinology*, **111**:1601-1606.

[185] Lewis, J. T., Dayanandan, B., Habener, J. F., and Kieffer, T. J. (2000). Glucose-dependent insulinotropic polypeptide confers early phase insulin release to oral glucose in rats: demonstration by a receptor antagonist. *Endocrinology*, **141**:3710-3716.

[186] Tseng, C-C., Kieffer, T. J., Jarboe, L. A., Usdin, T. B., and Wolfe, M. M. (1996). Postprandial stimulation of insulin release by glucose-dependent insulinotropic polypeptide (GIP). Effect of a specific glucose-dependent insulinotropic polypeptide receptor antagonist in the rat. *J Clin Invest*, **98**:2440-2445.

[187] Tseng, C-C., Zhang, X. Y., and Wolfe, M. M. (1999). Effect of GIP and GLP-1 antagonists on insulin release in the rat. *Am J Physiol*, **276**:E1049-E1054.

[188] Gault, V. A., O'Harte, F. P., Harriott, P., and Flatt, P. R. (2002). Characterization of the cellular and metabolic effects of a novel enzyme-resistant antagonist of glucose-dependent insulinotropic polypeptide. *Biochem Biophys Res Commun*, **290**:1420-1426.

[189] Miyawaki, K., Yamada, Y., Yano, H., Niwa, H., Ban, N., Ihara, Y., Kubota, A., Fujimoto, S., Kajikawa, M., Kuroe, A., Tsuda, K., Hashimoto, H., Yamashita, T., Jomori, T., Tashiro, F., Miyazaki, J., and Seino, Y. (1999). Glucose intolerance caused by a defect in the entero-insular axis: a study in gastric inhibitory polypeptide receptor knockout mice. *Proc Natl Acad Sci USA*, **96**:14843-14847.

[190] Ding, W. G., and Gromada, J. (1997). Protein kinase A-dependent stimulation of exocytosis in mouse pancreatic β-cells by glucose-dependent insulinotropic polypeptide. *Diabetes*, **46**:615-621.

[191] Gromada, J., Bokvist, K., Ding, W. G., Holst, J. J., Nielsen, J. H., and Rorsman, P. (1998). Glucagon-like peptide 1 (7-36) amide stimulates exocytosis in human pancreatic β-cells by both proximal and distal regulatory steps in stimulus-secretion coupling. *Diabetes*, **47**:57-65.

[192] Gromada, J., Holst, J. J., and Rorsman, P. (1998). Cellular regulation of islet hormone secretion by the incretin hormone glucagon-like peptide 1. *Pflügers Arch Eur J Physiol*, **435**:583-594.

[193] Béguin, P., Nagashima, K., Nishimura, M., Gonoi, T., and Seino, S. (1999). PKA-mediated phosphorylation of the human K(ATP) channel: separate roles of Kir6.2 and SUR1 subunit phosphorylation. *EMBO J*, **18**:4722-4732.

[194] Wahl, M. A., Plehn, R. J., Landsbeck, E. A., Verspohl, E. J., and Ammon, H. P. (1992). Are ionic fluxes of pancreatic beta cells a target for gastric inhibitory polypeptide? *Mol Cell Endocrinol*, **90**:117-123.

[195] Yajima, H., Komatsu, M., Schermerhorn, T., Aizawa, T., Kaneko, T., Nagai, M., Sharp, G. W., and Hashizume, K. (1999). cAMP enhances insulin secretion by an action on the ATP-sensitive K+ channel-independent pathway of glucose signaling in rat pancreatic islets. *Diabetes*, **48**:1006-1012.

[196] Suzuki, S., Kawai, K., Ohashi, S., Watanabe, Y., and Yamashita, K. (1992). Interaction of glucagon-like peptide-1(7-36) amide and gastric inhibitory polypeptide or

cholecystokinin on insulin and glucagon secretion from the isolated perfused rat pancreas. *Metabolism*, **41**:359-363.

[197] Fehmann, H-C., Göke, B., Göke, R., Trautmann, M. E., and Arnold, R. (1989). Synergistic stimulatory effect of glucagon-like peptide-1 (7-36) amide and glucose-dependent insulin-releasing polypeptide on the endocrine rat pancreas. *FEBS Lett*, **252**:109-112.

[198] Gallwitz, B., Witt, M., Folsch, U. R., Creutzfeldt, W., and Schmidt, W. E. (1993). Binding specificity and signal transduction of receptors for glucagon-like peptide-1(7-36)amide and gastric inhibitory polypeptide on RINm5F insulinoma cells. *J Mol Endocrinol*, **10**:259-268.

[199] Siegel, E. G., Schulze, A., Schmidt, W. E., and Creutzfeldt, W. (1992). Comparison of the effect of GIP and GLP-1 (7-36amide) on insulin release from rat pancreatic islets. *Eur J Clin Invest*, **22**:154-157.

[200] Verchere, C. B., Kwok, Y. N., and Brown, J. C. (1991). Modulation of acetylcholine-stimulated insulin release by glucose and gastric inhibitory polypeptide. *Pharmacology*, **42**:273-282.

[201] Sandberg, E., Ahrén, B., Tendler, D., and Efendic, S. (1988). Cholecystokinin-33 potentiates and vasoactive intestinal polypeptide inhibits gastric inhibitory polypeptide – induced insulin secretion in the perfused rat pancreas. *Acta Endocrinol*, **117**:545-551.

[202] Pederson, R. A., and Brown, J. C. (1978). Interaction of gastric inhibitory polypeptide, glucose, and arginine on insulin and glucagon secretion from the perfused rat pancreas. *Endocrinology*, **103**:610-615.

[203] Rasmussen, H., Zawalich, K. C., Ganesan, S., Calle, R., and Zawalich, W. S. (1990). Physiology and pathophysiology of insulin secretion. *Diabetes Care*, **13**:655-666.

[204] Zawalich, W. S., Zawalich, K. C., and Rasmussen, H. (1989). Interactions between cholinergic agonists and enteric factors in the regulation of insulin secretion from isolated perifused rat islets. *Acta Endocrinol*, **120**:702-707.

[205] McCullough, A. J., Marshall, J. B., Bingham, C. P., Rice, B. L., Manning, L. D., and Kalhan, S. C. (1985). Carbachol modulates GIP-mediated insulin release from rat pancreatic lobules in vitro. *Am J Physiol*, **248**:E299-E303.

[206] Brunicardi, F. C., Druck, P., Seymour, N. E., Sun, Y. S., Elahi, D., and Andersen, D. K. (1990). Selective neurohormonal interactions in islet cell secretion in the isolated perfused human pancreas. *J Surg Res*, **48**:273-278.

[207] Ma, H. T., Kato, M., and Tatemoto, K. (1996). Effects of pancreastatin and somatostatin on secretagogues-induced rise in intracellular free calcium in single rat pancreatic islet cells. *Regul Pept*, **61**:143-148.

[208] Silvestre, R. A., Salas, M., García-Hermida, O., Fontela, T., Dégano, P., and Marco, J. (1994). Amylin (islet amyloid polypeptide) inhibition of insulin release in the perfused rat pancreas: implication of the adenylate cyclase/cAMP system. *Regul Pept*, **50**:193-199.

217

[209] Rodríguez-Gallardo, J., Silvestre, R. A., and Marco, J. (1999). Inhibitory effect of enterostatin on the beta cell response to digestive insulinotropic peptides. *Int J Obes*, **23:**787-792.

[210] Miralles, P., Peiro, E., Silvestre, R. A., Villanueva, M. L., and Marco, J. (1988). Effects of galanin on islet cell secretory responses to VIP, GIP, 8-CCK, and glucagon by the perfused rat pancreas. *Metabolism*, **37:**766-770.

[211] Peiró, E., Miralles, P., Silvestre, R. A., Villanueva, M. L., and Marco, J. (1989). Pancreastatin inhibits insulin secretion as induced by glucagon, vasoactive intestinal peptide, gastric inhibitory peptide, and 8-cholecystokinin in the perfused rat pancreas. *Metabolism*, **38:**679-682.

[212] Ishizuka, J., Tatemoto, K., Cohn, D. V., Thompson, J. C., and Greeley, G. H., Jr. (1991). Effects of pancreastatin and chromogranin A on insulin release stimulated by various insulinotropic agents. *Regul Pept*, **34:**25-32.

[213] Lu, M., Wheeler, M. B., Leng, X.-H., and Boyd, A. E., 3rd (1993). Stimulation of insulin secretion and insulin gene expression by gastric inhibitory polypeptide. *Trans Assoc Am Phys*, **106:**42-53.

[214] Fehmann, H-C., and Göke, B. (1995). Characterization of GIP(1-30) and GIP(1-42) as stimulators of proinsulin gene transcription. *Peptides*, **16:**1149-1152.

[215] Schäfer, R., and Schatz, H. (1979). Stimulation of (Pro-)insulin biosynthesis and release by gastric inhibitory polypeptide in isolated islets of rat pancreas. *Acta Endocrinol*, **91:**493-500.

[216] Wang, Y., Montrose-Rafizadeh, C., Adams, L., Raygada, M., Nadiv, O., and Egan, J. M. (1996). GIP regulates glucose transporters, hexokinases, and glucose-induced insulin secretion in RIN 1046-38 cells. *Mol Cell Endocrinol*, **116:**81-87.

[217] Adrian, T. E., Bloom, S. R., Hermansen, K., and Iversen, J. (1978). Pancreatic polypeptide, glucagon and insulin secretion from the isolated perfused canine pancreas. *Diabetologia*, **14:**413-7.

[218] Ipp, E., Dobbs, R. E., Harris, V., Arimura, A., Vale, W., and Unger, R. H. (1977). The effects of gastrin, gastric inhibitory polypeptide, secretin, and the octapeptide of cholecystokinin upon immunoreactive somatostatin release by the perfused canine pancreas. *J Clin Invest*, **60:**1216-1219.

[219] Ding, W. G., Renström, E., Rorsman, P., Buschard, K., and Gromada, J. (1997). Glucagon-like peptide I and glucose-dependent insulinotropic polypeptide stimulate Ca2+-induced secretion in rat α-cells by a protein kinase A-mediated mechanism. *Diabetes*, **46:**792-800.

[220] Nauck, M. A., Heimesaat, M. M., Orskov, C., Holst, J. J., Ebert, R., and Creutzfeldt, W. (1993). Preserved incretin activity of glucagon-like peptide 1 [7-36 amide] but not of synthetic human gastric inhibitory polypeptide in patients with type-2 diabetes mellitus. *J Clin Invest*, **91:**301-307.

[221] Nauck, M., Schmidt, W. E., Ebert, R., Strietzel, J., Cantor, P., Hoffmann, G., and Creutzfeldt, W. (1989). Insulinotropic properties of synthetic human gastric inhibitory polypeptide in man: Interactions with glucose, phenylalanine, and cholecystokinin-8. *J Clin Endocrinol Metab*, **69**:654-662.

[222] Elahi, D., Raizes, G. S., Andres, R., Hershcopf, R. J., Muller, D. C., Tobin, J. D., and Andersen, D. K. (1982). Interaction of arginine and gastric inhibitory polypeptide on insulin release in man. *Am J Physiol*, **242**:E343-351.

[223] Yasuda, K., Inagaki, N., Yamada, Y., Kubota, A., Seino, S., and Seino, Y. (1994). Hamster gastric inhibitory polypeptide receptor expressed in pancreatic islets and clonal insulin-secreting cells: its structure and functional properties. *Biochem Biophys Res Commun*, **205**:1556-1562.

[224] Moens, K., Heimberg, H., Flamez, D., Huypens, P., Quartier, E., Ling, Z., Pipeleers, D., Gremlich, S., Thorens, B., and Schuit, F. (1996). Expression and functional activity of glucagon, glucagon-like peptide I, and glucose-dependent insulinotropic peptide receptors in rat pancreatic islet cells. *Diabetes*, **45**:257-261.

[225] Kaplan, A. M., and Vigna, S. R. (1994). Gastric inhibitory polypeptide (GIP) binding sites in rat brain. *Peptides*, **15**:297-302.

[226] Whitcomb, DC, O'Dorisio, TM, Nishikawara, MT, Shetzline, M, and Cataland, S (1984). Identification of target organs for gastric inhibitory polypeptide (GIP) with a new in vivo radioreceptor assay (abstract). *Dig Dis Sci*, **29** (**August Supplement**):95S.

[227] Madsbad, S., Kehlet, H., Hilsted, J., and Tronier, B. (1983). Discrepancy between plasma C-peptide and insulin response to oral and intravenous glucose. *Diabetes*, **32**:436-438.

[228] Nauck, M. A., Homberger, E., Siegel, E. G., Allen, R. C., Eaton, R. P., Ebert, R., and Creutzfeldt, W. (1986). Incretin effects of increasing glucose loads in man calculated from venous insulin and C-peptide responses. *J Clin Endocrinol Metab*, **63**:492-498.

[229] Ikeda, T., Yoshida, T., Honda, M., Ito, Y., Murakami, I., Mokuda, O., Tominaga, M., and Mashiba, H. (1987). Effect of intestinal factors on extraction of insulin in perfused rat liver. *Am J Physiol*, **253**:E603-E607.

[230] Hanks, J. B., Andersen, D. K., Wise, J. E., Putnam, W. S., Meyers, W. C., and Jones, R. S. (1984). The hepatic extraction of gastric inhibitory polypeptide and insulin. *Endocrinology*, **115**:1011-1018.

[231] Chap, Z., Ishida, T., Chou, J., Lewis, R., Hartley, C., Entman, M., and Field, J. B. (1985). Effects of atropine and gastric inhibitory polypeptide on hepatic glucose uptake and insulin extraction in conscious dogs. *J Clin Invest*, **76**:1174-1181.

[232] Matsumura, M., Akiyoshi, H., and Saito, S. (1980). Effects of somatostatin on gastrointestinal hormone-induced glycogenolysis and gluconeogenesis in cultured liver cells. *Gastroenterologia Japonica*, **15**:439-443.

[233] Hartmann, H., Ebert, R., and Creutzfeldt, W. (1986). Insulin-dependent inhibition of hepatic glycogenolysis by gastric inhibitory polypeptide (GIP) in perfused rat liver. *Diabetologia*, **29:**112-114.

[234] Ebert, R., and Creutzfeldt, W. (1987). Metabolic effects of gastric inhibitory polypeptide. *Front Horm Res*, **16:**175-185.

[235] Andersen, D. K., Sun, Y. S., Brunicardi, F. C., Berlin, S. A., Lebovitz, H. E., and Elahi, D. (1984). Regulation of hepatic glucose production by gastric inhibitory polypeptide (GIP), insulin (INS) and glucagon (GLUC). *Dig Dis Sci*, **29:**A5.

[236] Elahi, D., Meneilly, G. S., Minaker, K. L., Rowe, L. D., and Andersen, D. K. (1986). Regulation of glucose production by gastric inhibitory polypeptide in man (Abstracts presented at the Sixth International Symposium on Gastrointestinal Hormones. Vancouver, British Columbia, Canada, July 6-10, 1986). *Can J Physiol Pharmacol*, **65 (Suppl.):**18.

[237] Andersen, D. K., Putnam, W. S., Hanks, J. B., Wise, J. E., Lebovitz, H. E., and Jones, R. S. (1982). Gastric inhibitory polypeptide (GIP) suppression of hepatic glucose production [abstract]. *Regul Pept*, **1 (Suppl. 2):**4.

[238] Pederson, R. A., Schubert, H. E., and Brown, J. C. (1975). The insulinotropic action of gastric inhibitory polypeptide. *Can J Physiol Pharmacol*, **53:**217-223.

[239] O'Harte, F. P. M., Gray, A. M., and Flatt, P. R. (1998). Gastric inhibitory polypeptide and effects of glycation on glucose transport and metabolism in isolated mouse abdominal muscle. *J Endocrinol*, **156:**237-243.

[240] Yip, R. G., Boylan, M. O., Kieffer, T. J., and Wolfe, M. M. (1998). Functional GIP receptors are present on adipocytes. *Endocrinology*, **139:**4004-4007.

[241] McIntosh, C. H. S., Bremsak, I., Lynn, F. C., Gill, R., Hinke, S. A., Gelling, R., Nian, C., McKnight, G., Jaspers, S., and Pederson, R. A. (1999). Glucose-dependent insulinotropic polypeptide stimulation of lipolysis in differentiated 3T3-L1 cells: wortmannin-sensitive inhibition by insulin. *Endocrinology*, **140:**398-404.

[242] Ebert, R., Nauck, M., and Creutzfeldt, W. (1991). Effect of exogenous or endogenous gastric inhibitory polypeptide (GIP) on plasma triglyceride responses in rats. *Horm Met Res*, **23:**517-521.

[243] Jorde, R., Pettersen, J. E., and Burhol, P. G. (1984). Lack of effect of exogenous or endogenous gastric inhibitory polypeptide on the elimination rate of Intralipid in man. *Acta Med Scand*, **216:**19-23.

[244] Ohneda, A., Kobayashi, T., and Nihei, J. (1983). Effect of endogenous gastric inhibitory polypeptide (GIP) on the removal of triacylglycerol in dogs. *Regul Pept*, **6:**25-32.

[245] Wasada, T., McCorkle, K., Harris, V., Kawai, K., Howard, B., and Unger, R. H. (1981). Effect of gastric inhibitory polypeptide on plasma levels of chylomicron triglycerides in dogs. *J Clin Invest*, **68:**1106-1107.

[246] Eckel, R. H., Fujimoto, W. Y., and Brunzell, J. D. (1981). Effect of in-vitro lifespan of 3T3-L1 cells on hormonal responsiveness of lipoprotein lipase activity. *Int J Obes*, **5**:571-577.

[247] Eckel, R. H., Fujimoto, W. Y., and Brunzell, J. D. (1979). Gastric inhibitory polypeptide enhanced lipoprotein lipase activity in cultured preadipocytes. *Diabetes*, **28**:1141-1142.

[248] Knapper, J. M., Puddicombe, S. M., Morgan, L. M., and Fletcher, J. M. (1995). Investigations into the actions of glucose-dependent insulinotropic polypeptide and glucagon-like peptide-1(7-36)amide on lipoprotein lipase activity in explants of rat adipose tissue. *J Nutr*, **125**:183-188.

[249] Knapper, J. M., Puddicombe, S. M., Morgan, L. M., Fletcher, J. M., and Marks, V. (1993). Glucose dependent insulinotropic polypeptide and glucagon-like peptide-1(7-36)amide: effects on lipoprotein lipase activity. *Biochem Soc Trans*, **21**:135S.

[250] Beck, B., and Max, J. P. (1983). Gastric inhibitory polypeptide enhancement of the insulin effect on fatty acid incorporation into adipose tissue in the rat. *Regul Pept*, **7**:3-8.

[251] Miyawaki, K., Yamada, Y., Ban, N., Ihara, Y., Tsukiyama, K., Zhou, H., Fujimoto, S., Oku, A., Tsuda, K., Toyokuni, S., Hiai, H., Mizunoya, W., Fushiki, T., Holst, J. J., Makino, M., Tashita, A., Kobara, Y., Tsubamoto, Y., Jinnouchi, T., Jomori, T., and Seino, Y. (2002). Inhibition of gastric inhibitory polypeptide signalling prevents obesity. *Nat Med*, **8**:738-742.

[252] Starich, G. H., Bar, R. S., and Mazzaferri, E. L. (1985). GIP increases insulin receptor affinity and cellular sensitivity in adipocytes. *Am J Physiol*, **249**:E603-E607.

[253] Hauner, H., Glatting, G., Kaminska, D., and Pfeiffer, E. F. (1988). Effects of gastric inhibitory polypeptide on glucose and lipid metabolism of isolated rat adipocytes. *Ann Nutr Metab*, **32**:282-8.

[254] Oben, J., Morgan, L., Fletcher, J., and Marks, V. (1991). Effect of the entero-pancreatic hormones, gastric inhibitory polypeptide and glucagon-like polypeptide-1(7-36) amide, on fatty acid synthesis in explants of rat adipose tissue. *J Endocrinol*, **130**:267-272.

[255] Dupré, J., Greenidge, N., McDonald, T. J., Ross, S. A., and Rubinstein, D. (1976). Inhibition of actions of glucagon in adipocytes by gastric inhibitory polypeptide. *Metabolism*, **25**:1197-1199.

[256] Ottlecz, A., Samson, W. K., and McCann, S. M. (1985). The effects of gastric inhibitory polypeptide (GIP) on the release of anterior pituitary hormones. *Peptides*, **6**:115-119.

[257] Murphy, W. A., Lance, V. A., Sueiras-Diaz, J., and Coy, D. H. (1983). Effects of secretin and gastric inhibitory polypeptide on human pancreatic growth hormone-releasing factor(1-40)-stimulated growth hormone levels in the rat. *Biochem Biophys Res Commun*, **112**:469-474.

[258] Zhong, Q., Bollag, R. J., Dransfield, D. T., Gasalla-Herraiz, J., Ding, K. H., Min, L., and Isales, C. M. (2000). Glucose-dependent insulinotropic peptide signaling pathways in endothelial cells. *Peptides*, **21**:1427-1432.

[259] Bollag, R. J., Zhong, Q., Ding, K. H., Phillips, P., Zhong, L., Qin, F., Cranford, J., Mulloy, A. L., Cameron, R., and Isales, C. M. (2001). Glucose-dependent insulinotropic peptide is an integrative hormone with osteotropic effects. *Mol Cell Endocrinol*, **177**:35-41.

[260] Lacroix, A., Ndiaye, N., Tremblay, J., and Hamet, P. (2001). Ectopic and abnormal hormone receptors in adrenal Cushing's syndrome. *Endocr Rev*, **22**:75-110.

[261] Nussdorfer, G. G., Bahcelioglu, M., Neri, G., and Malendowicz, L. K. (2000). Secretin, glucagon, gastric inhibitory polypeptide, parathyroid hormone, and related peptides in the regulation of the hypothalamus- pituitary-adrenal axis. *Peptides*, **21**:309-324.

[262] Chabre, O., Liakos, P., Vivier, J., Bottari, S., Bachelot, I., Chambaz, E. M., Feige, J. J., and Defaye, G. (1998). Gastric inhibitory polypeptide (GIP) stimulates cortisol secretion, cAMP production and DNA synthesis in an adrenal adenoma responsible for food-dependent Cushing's syndrome. *Endocr Res*, **24**:851-856.

[263] Mazzocchi, G., Rebuffat, P., Meneghelli, V., Malendowicz, L. K., Tortorella, C., Gottardo, G., and Nussdorfer, G. G. (1999). Gastric inhibitory polypeptide stimulates glucocorticoid secretion in rats, acting through specific receptors coupled with the adenylate cyclase-dependent signaling pathway. *Peptides*, **20**:589-594.

[264] Bollag, R. J., Zhong, Q., Phillips, P., Min, L., Zhong, L., Cameron, R., Mulloy, A. L., Rasmussen, H., Qin, F., Ding, K. H., and Isales, C. M. (2000). Osteoblast-derived cells express functional glucose-dependent insulinotropic peptide receptors. *Endocrinology*, **141**:1228-1235.

[265] Maletti, M., Amiranoff, B., Laburthe, M., and Rosselin, G. (1983). Demonstration of specific receptors for gastric inhibitory peptide (GIP) [French]. *C R Acad Sc Paris(III)*, **297**:563-565.

[266] Maletti, M., Portha, B., Carlquist, M., Kergoat, M., Laburthe, M., Marie, J. C., and Rosselin, G. (1984). Evidence for and characterization of specific high affinity binding sites for the gastric inhibitory polypeptide in pancreatic β-cells. *Endocrinology*, **115**:1324-1331.

[267] Maletti, M., Carlquist, M., Portha, B., Kergoat, M., Mutt, V., and Rosselin, G. (1986). Structural requirements for gastric inhibitory polypeptide (GIP) receptor binding and stimulation of insulin release. *Peptides*, **1**:75-78.

[268] Whitcomb, D. C., O'Dorisio, T. M., Cataland, S., and Nishikawara, M. T. (1985). Theoretical basis for a new in vivo radioreceptor assay for polypeptide hormones. *Am J Physiol*, **249**:E555-E560.

[269] Whitcomb, D. C., O'Dorisio, T. M., Cataland, S., Shetzline, M., and Nishikawara, M. T. (1985). Identification of tissue insulin receptors: use of a unique in vivo radioreceptor assay. *Am J Physiol*, **249**:E561-E567.

[270] Couvineau, A., Amiranoff, B., Vauclin-Jacques, N., and Laburthe, M. (1984). The GIP receptor on pancreatic beta cell tumor: molecular identification by covalent cross-linking. *Biochem Biophys Res Commun*, **122**:283-288.

[271] Amiranoff, B., Couvineau, A., Vauclin-Jacques, N., and Laburthe, M. (1986). Gastric inhibitory polypeptide receptor in hamster pancreatic beta cells. Direct cross-linking, solubilization and characterization as a glycoprotein. *Eur J Biochem*, **159**:353-358.

[272] Amiranoff, B., Vauclin-Jacques, N., and Laburthe, M. (1985). Interaction of gastric inhibitory polypeptide (GIP) with the insulin-secreting pancreatic beta-cell line In 111: characteristics of GIP binding sites. *Life Sci*, **36**:807-813.

[273] Gallwitz, B., Witt, M., Paetzold, G., Morys-Wortmann, C., Folsch, U. R., and Schmidt, W. E. (1995). Binding characteristic of N-terminal GIP/GLP-1 hybrid peptides. *Endocrinol Metab*, **2**:39-46.

[274] Gallwitz, B., Witt, M., Morys-Wortmann, C., Folsch, U. R., and Schmidt, W. E. (1996). GLP-1/GIP chimeric peptides define the structural requirements for specific ligand-receptor interaction of GLP-1. *Regul Pept*, **63**:17-22.

[275] Lynn, F. C., Thomson, S. A., Pospisilik, J. A., Ehses, J. A., Hinke, S. A., Pamir, N., McIntosh, C. H. S., and Pederson, R. A. (2002). A novel pathway for regulation of glucose-dependent insulinotropic polypeptide (GIP) receptor expression in β-cells. *FASEB J*, **In press**.

[276] Wheeler, M. B., Gelling, R. W., McIntosh, C. H., Georgiou, J., Brown, J. C., and Pederson, R. A. (1995). Functional expression of the rat pancreatic islet glucose-dependent insulinotropic polypeptide receptor: ligand binding and intracellular signaling properties. *Endocrinology*, **136**:4629-4639.

[277] Gremlich, S., Porret, A., Hani, E. H., Cherif, D., Vionnet, N., Froguel, P., and Thorens, B. (1995). Cloning, functional expression, and chromosomal localization of the human pancreatic islet glucose-dependent insulinotropic polypeptide receptor. *Diabetes*, **44**:1202-1208.

[278] Volz, A., Göke, R., Lankat-Buttgereit, B., Fehmann, H-C., Bode, H. P., and Göke, B. (1995). Molecular cloning, functional expression, and signal transduction of the GIP-receptor cloned from a human insulinoma [erratum appears in FEBS Lett 1996 Mar 4;381(3):271.]. *FEBS Lett*, **373**:23-29.

[279] Xiao, Q., Jeng, W., and Wheeler, M. B. (2000). Characterization of glucagon-like peptide-1 receptor-binding determinants. *J Mol Endocrinol*, **25**:321-335.

[280] Gelling, R. W., Wheeler, M. B., Xue, J., Gyomorey, S., Nian, C., Pederson, R. A., and McIntosh, C. H. (1997). Localization of the domains involved in ligand binding and activation of the glucose-dependent insulinotropic polypeptide receptor. *Endocrinology*, **138**:2640-2643.

[281] Kubota, A., Yamada, Y., Hayami, T., Yasuda, K., Someya, Y., Ihara, Y., Kagimoto, S., Watanabe, R., Taminato, T., Tsuda, K., and Seino, Y. (1996). Identification of two

missense mutations in the GIP receptor gene: a functional study and association analysis with NIDDM: no evidence of association with Japanese NIDDM subjects. *Diabetes*, **45**:1701-1705.

[282] Yamada, Y., Hayami, T., Nakamura, K., Kaisaki, P. J., Someya, Y., Wang, C. Z., Seino, S., and Seino, Y. (1995). Human gastric inhibitory polypeptide receptor: cloning of the gene (GIPR) and cDNA. *Genomics*, **29**:773-776.

[283] Huypens, P., Ling, Z., Pipeleers, D., and Schuit, F. (2000). Glucagon receptors on human islet cells contribute to glucose competence of insulin release. *Diabetologia*, **43**:1012-1019.

[284] Boylan, M. O., Jepeal, L. I., and Wolfe, M. M. (1999). Structure of the rat glucose-dependent insulinotropic polypeptide receptor gene. *Peptides*, **20**:219-228.

[285] Frandsen, E. K., and Moody, A. J. (1980). Glucagon, GIP, VIP, and secretin activation of mouse islet adenylate cyclase [abstract]. *Diabetologia*, **19**:274.

[286] Gespach, C., Emami, S., and Rosselin, G. (1984). Gastric inhibitory peptide (GIP), pancreatic glucagon and vasoactive intestinal peptide (VIP) are cAMP-inducing hormones in the human gastric cancer cell line HGT-1. Homologous desensitization of VIP receptor activity. *Biochem Biophys Res Commun*, **120**:641-649.

[287] Gespach, C., Bataille, D., Dutrillaux, M. C., and Rosselin, G. (1982). The interaction of glucagon, gastric inhibitory peptide and somatostatin with cyclic AMP production systems present in rat gastric glands. *Biochim Biophys Acta*, **720**:7-16.

[288] Emami, S., Chastre, E., Bodere, H., Gespach, C., Bataille, D., and Rosselin, G. (1986). Functional receptors for VIP, GIP, glucagon-29 and -37 in the HGT-1 human gastric cancer cell line. *Peptides*, **1**:121-127.

[289] Rosselin, G. (1986). The receptors of the VIP family peptides (VIP, secretin, GRF, PHI, PHM, GIP, glucagon and oxyntomodulin). Specificities and identity. *Peptides*, **1**:89-100.

[290] Wheeler, M. B., Gelling, R. W., Hinke, S. A., Tu, B., Pederson, R. A., Lynn, F., Ehses, J., and McIntosh, C. H. S. (1999). Characterization of the carboxyl-terminal domain of the rat glucose-dependent insulinotropic polypeptide (GIP) receptor. A role for serines 426 and 427 in regulating the rate of internalization. *J Biol Chem*, **274**:24593-24601.

[291] Tseng, C-C., and Zhang, X. Y. (1998). The cysteine of the cytoplasmic tail of glucose-dependent insulinotropic peptide receptor mediates its chronic desensitization and down-regulation. *Molecular & Cellular Endocrinology*, **139**:179-186.

[292] Tseng, C-C., and Lin, L. (1997). A point mutation in the glucose-dependent insulinotropic peptide receptor confers constitutive activity. *Biochem Biophys Res Commun*, **232**:96-100.

[293] Trümper, A., Trümper, K., Trusheim, H., Arnold, R., Göke, B., and Hörsch, D. (2001). Glucose-dependent insulinotropic polypeptide is a growth factor for beta (INS-1) cells by pleiotropic signaling. *Mol Endocrinol*, **15**:1559-1570.

[294] Kashima, Y., Miki, T., Shibasaki, T., Ozaki, N., Miyazaki, M., Yano, H., and Seino, S. (2001). Critical role of cAMP-GEFII-Rim2 complex in incretin-potentiated insulin secretion. *J Biol Chem,* **276**:46046-46053.

[295] Zawalich, W. S. (1988). Synergistic impact of cholecystokinin and gastric inhibitory polypeptide on the regulation of insulin secretion. *Metabolism,* **37**:778-781.

[296] Ehses, J. A., Lee, S. S., Pederson, R. A., and McIntosh, C. H. (2001). A new pathway for glucose-dependent insulinotropic polypeptide (GIP) receptor signaling: evidence for the involvement of phospholipase A2 in GIP-stimulated insulin secretion. *J Biol Chem,* **276**:23667-23673.

[297] Lardinois, C. K., Richeson, R. B., 3rd, Starich, G. H., Mazzu, D., and Mazzaferri, E. L. (1990). Gastric inhibitory polypeptide mechanisms of augmenting insulin secretion. *Life Sci,* **47**:1015-1022.

[298] Straub, S. G., and Sharp, G. W. (1996). Glucose-dependent insulinotropic polypeptide stimulates insulin secretion via increased cyclic AMP and $[Ca^{2+}]_i$ and a wortmannin-sensitive signalling pathway. *Biochem Biophys Res Commun,* **224**:369-374.

[299] Kubota, A., Yamada, Y., Yasuda, K., Someya, Y., Ihara, Y., Kagimoto, S., Watanabe, R., Kuroe, A., Ishida, H., and Seino, Y. (1997). Gastric inhibitory polypeptide activates MAP kinase through the wortmannin-sensitive and -insensitive pathways. *Biochem Biophys Res Commun,* **235**:171-175.

[300] Ehses, J. A., Pellech, S. L., Pederson, R. A., and McIntosh, C. H. S. (2002). Glucose-dependent insulinotropic polypeptide (GIP) activates the Raf-Mek 1/2-ERK 1/2 module via a cyclic AMP/PKA/Rap1-mediated pathway. *J Biol Chem,* **277**:37088-37097.

[301] Susini, S., Van Haasteren, G., Li, S., Prentki, M., and Schlegel, W. (2000). Essentiality of intron control in the induction of c-fos by glucose and glucoincretin peptides in INS-1 beta-cells. *FASEB J,* **14**:128-136.

[302] Trümper, A, Trümper, K, and Hörsch, D (2002). Mechanisms of mitogenic and anti-apoptotic signaling by glucose-dependent insulinotropic polypeptide in β(INS-1)-cells. *J Endocrinol,* **174**:233-245.

[303] Lund, P. K., Goodman, R. H., Montminy, M. R., Dee, P. C., and Habener, J. F. (1983). Angler fish islet pre-proglucagon II. Nucleotide and corresponding amino acid sequence of the cDNA. *J Biol Chem,* **258**:3280-3284.

[304] Lund, P. K., Goodman, R. H., Dee, P. C., and Habener, J. F. (1982). Pancreatic preproglucagon cDNA contains two glucagon-related coding sequences arranged in tandem. *Proc Natl Acad Sci USA,* **79**:345-349.

[305] Lund, P. K., Goodman, R. H., and Habener, J. F. (1981). Intestinal glucagon mRNA identified by hybridization to a cloned isle cDNA encoding a precursor. *Biochem Biophys Res Commun,* **100**:1659-1666.

[306] Novak, U., Wilks, A., Beull, G., and McEwen, S. (1987). Identical mRNA for preproglucagon in pancreas and gut. *Eur J Biochem*, **164**:553-558.

[307] Lopez, L. C., Frazier, M. L., Su, C. J., Kumar, A., and Saunders, G. F. (1983). Mammalian pancreatic preproglucagon contains three glucagon-related peptides. *Proc Natl Acad Sci USA*, **80**:5485-5489.

[308] Bell, G. I., Santerre, R. F., and Mullenbach, G. T. (1983). Hamster proglucagon contains the sequence of glucagon and two related peptides. *Nature*, **302**:716-718.

[309] Drucker, D. J., and Brubaker, P. L. (1989). Proglucagon gene expression is regulated by a cyclic AMP-dependent pathway in rat intestine. *Proc Natl Acad Sci USA*, **86**:3953-3957.

[310] Heinrich, G., Gros, P., Lund, P. K., Bentley, R. C., and Habener, J. F. (1984). Preproglucagon messenger ribonucleic acid: nucleotide and encoded amino acid sequences of the rat pancreatic complementary deoxyriboneucleic acid. *Endocrinology*, **115**:2176-2181.

[311] Chiasson, J., and Cherrington, A. (1983). Glucagon and liver glucose output in vivo, *in* P. J. Lefèbvre, ed., Handbook of Experimental Pharmacology 66/I: New York, Springer-Verlag, p. 361-382.

[312] Drucker, D. J. (2002). Biological actions and therapeutic potential of the glucagon-like peptides. *Gastroenterology*, **122**:531-544.

[313] Thorens, B., Porret, A., Bühler, L., Deng, S. P., Morel, P., and Widmann, C. (1993). Cloning and functional expression of the human islet GLP-1 receptor: demonstration that exendin-4 is an agonist and exendin-(9-39) an antagonist of the receptor. *Diabetes*, **42**:1678-1682.

[314] Graziano, M. P., Hey, P. J., Borkowski, D., Chicci, C., and Strader, C. D. (1993). Cloning and functional expression of a human glucagon-like peptide-1 receptor. *Biochem Biophys Res Commun*, **196**:141-146.

[315] Yusta, B., Somwar, R., Wang, F., Munroe, D., Grinstein, S., Klip, A., and Drucker, D. J. (1999). Identification of glucagon-like peptide-2 (GLP-2)-activated signaling pathways in baby hamster kidney fibroblasts expressing the rat GLP-2 receptor. *J Biol Chem*, **274**:30459-30467.

[316] Li, J., Larocca, J. N., Rodriguez-Gabin, A. G., and Charron, M. J. (1997). Expression and signal transduction of the glucagon receptor in βTC3 cells. *Biochim Biophys Acta*, **24**:229-236.

[317] Gromada, J., Anker, C., Bokvist, K., Knudsen, L. B., and Wahl, P. (1998). Glucagon-like peptide-1 receptor expression in Xenopus oocytes stimulates inositol trisphosphate-dependent intracellular Ca2+ mobilization. *FEBS Lett*, **425**:277-280.

[318] Gromada, J., Rorsman, P., Dissing, S., and Wulff, B. S. (1995). Stimulation of cloned human glucagon-like peptide 1 receptor expressed in HEK 293 cells induces cAMP-

dependent activation of calcium-induced calcium release. [erratum appears in FEBS Lett. 1996 Mar 4;381(3):262.]. *FEBS Lett*, **373**:182-186.

[319] van Eyll, B., Lankat-Buttgereit, B., Bode, H. P., Göke, R., and Göke, B. (1994). Signal transduction of the GLP-1-receptor cloned from a human insulinoma. *FEBS Lett*, **348**:7-13.

[320] Widmann, C., Bürki, E., Dolci, W., and Thorens, B. (1994). Signal transduction by the cloned glucagon-like peptide-1 receptor: comparison with signaling by the endogenous receptors of β cell lines. *Mol Pharmacol*, **45**:1029-1035.

[321] Dillon, J. S., Tanizawa, Y., Wheeler, M. B., Leng, X. H., Ligon, B. B., Rabin, D. U., Yoo-Warren, H., Permutt, M. A., and Boyd, A. E., 3rd (1993). Cloning and functional expression of the human glucagon-like peptide-1 (GLP-1) receptor. *Endocrinology*, **133**:1907-10.

[322] Hansen, L. H., Gromada, J., Bouchelouche, P., Whitmore, T., Jelinek, L., Kindsvogel, W., and Nishimura, E. (1998). Glucagon-mediated Ca2+ signaling in BHK cells expressing cloned human glucagon receptors. *Am J Physiol*, **274**:C1552-C1562.

[323] Munroe, D. G., Gupta, A. K., Kooshesh, F., Vyas, T. B., Rizkalla, G., Wang, H., Demchyshyn, L., Yang, Z. J., Kamboj, R. K., Chen, H., McCallum, K., Sumner-Smith, M., Drucker, D. J., and Crivici, A. (1999). Prototypic G protein-coupled receptor for the intestinotrophic factor glucagon-like peptide 2. *Proc Natl Acad Sci USA*, **96**:1569-1573.

[324] Gelling, R. W. (1998). Structure-function studies of the gastric inhibitory polypeptide/glucose dependent insulinotropic polypeptide (GIP) receptor [Ph. D. Dissertation], University of British Columbia, Vancouver, 288 p.

[325] Zhou, A., Jiang, X., and Xu, X. (1997). Improved alkaline lysis method for rapid isolation of plasmid DNA. [see also later erratum]. *Biotechniques*, **23**:592-594.

[326] Efrat, S., Linde, S., Kofod, H., Spector, D., Delannoy, M., Grant, S., Hanahan, D., and Baekkeskov, S. (1988). Beta-cell lines derived from transgenic mice expressing a hybrid insulin gene-oncogene. *Proc Natl Acad Sci USA*, **85**:9037-9041.

[327] Poitout, V., Olson, L. K., and Robertson, R. P. (1996). Insulin-secreting cell lines: classification, characteristics and potential applications. *Diabet Metab (Paris)*, **22**:7-14.

[328] Hinke, S. A., Pospisilik, J. A., Demuth, H-U., Manhart, S., Kühn-Wache, K., Hoffmann, T., Nishimura, E., Pederson, R. A., and McIntosh, C. H. S. (2000). Dipeptidyl peptidase IV degradation of glucagon: characterization of glucagon degradation products and DPIV resistant analogs. *J Biol Chem*, **275**:3827-3834.

[329] Kühn-Wache, K., Manhart, S., Hoffmann, T., Hinke, S. A., Gelling, R., Pederson, R. A., McIntosh, C. H. S., and Demuth, H. U. (2000). Analogs of glucose-dependent insulinotropic polypeptide with increased dipeptidyl peptidase IV resistance. *Adv Exp Med Biol*, **477**:187-195.

[330] Kieffer, TJ (1994). Release and metabolism of gastric inhibitory polypeptide [Ph.D. Dissertation], University of British Columbia, Vancouver, 189 p.

[331] Motulsky, H. J. (1999). Analyzing data with graphpad prism: San Diego, GraphPad Software Inc., www.graphpad.com, 379 p.

[332] Kallal, L., Gagnon, A. W., Penn, R. B., and Benovic, J. L. (1998). Visualization of agonist-induced sequestration and down-regulation of a green fluorescent protein-tagged β2-adrenergic receptor. *J Biol Chem*, **272**:322-328.

[333] Petrou, C., Chen, L., and Tashjian, A. H. Jr. (1997). A receptor-G protein couplin-independent step in the internalization of the thyrotropin-releasing hormone receptor. *J Biol Chem*, **272**:2326-2333.

[334] Prado, G. N., Meirke, D. F., Pellegrini, M., Taylor, L., and Polgar, P. (1998). Motif mutation of bradykinin B2 receptor second intracellular loop and proximal C terminus is critical for signal transduction, internalization, and resensitization. *J Biol Chem*, **273**:33548-33555.

[335] Buggy, J. J., Heurich, R. O., MacDougall, M., Kelley, K. A., Livingston, J. N., Yoo-Warren, H., and Rossomando, A. J. (1997). Role of the glucagon receptor COOH-terminal domain in glucagon-mediated signaling and receptor internalization. *Diabetes*, **46**:1400-1405.

[336] Jia, X., Brown, J. C., Ma, P., Pederson, R. A., and McIntosh, C. H. S. (1995). Effects of glucose-dependent insulinotropic polypeptide and glucagon-like peptide-I-(7-36) on insulin secretion. *Am J Physiol*, **268**:E645-E651.

[337] Morrow, G. W., Kieffer, T. J., McIntosh, C. H., MacGillivray, R. T., Brown, J. C., St Pierre, S., and Pederson, R. A. (1996). The insulinotropic region of gastric inhibitory polypeptide; fragment analysis suggests the bioactive site lies between residues 19 and 30. *Can J Physiol Pharmacol*, **74**:65-72.

[338] Ferguson, S. S. G. (2001). Evolving concepts in G protein-coupled receptor endocytosis: the role in receptor desensitization and signaling. *Pharmacol Rev*, **53**:1-24.

[339] Morris, A. J., and Malbon, C. C. (1999). Physiological regulation of G protein-linked signalling. *Physiol Rev*, **79**:1373-1430.

[340] Claing, A., Laporte, S. A., Caron, M. G., and Lefkowitz, R. J. (2002). Endocytosis of G protein-coupled receptors: roles of G protein-coupled receptor kinases and β-arrestin proteins. *Prog Neurobiol*, **66**:61-79.

[341] Pierce, K. L., and Lefkowitz, R. J. (2001). Classical and new roles of β-arrestins in the regulation of G-protein-coupled receptors. *Nat Rev Neurosci*, **2**:727-733.

[342] Grady, E. F., Böhm, S. K., and Bunnett, N. W. (1997). Turning off the signal: mechanisms that attenuate signaling by G protein-coupled receptors. *Am J Physiol*, **273**:G586-G601.

[343] Tsao, P., Cao, T., and von Zastrow, M. (2001). Role of endocytosis in mediating downregulation of G-protein-coupled receptors. *Trends Pharmacol Sci*, **22**:91-96.

[344] Bünemann, M., and Hosey, M. M. (1999). G-protein coupled receptor kinases as modulators of G-protein signalling. *J Physiol*, **517**:5-23.

[345] Lefkowitz, R. J. (1998). G protein-coupled receptors. III. New roles for receptor kinases and β-arrestins in receptor signalling and desensitization. *J Biol Chem*, **273**:18677-18680.

[346] Tsao, P., and von Zastrow, M. (2000). Downregulation of G protein-coupled receptors. *Curr Opin Neurobiol*, **10**:365-369.

[347] Carman, C. V., and Benovic, J. L. (1998). G-protein-coupled receptors: turn-ons and turn-offs. *Curr Opin Neurobiol*, **8**:335-344.

[348] Böhm, S. K., Grady, E. F., and Bunnett, N. W. (1997). Regulatory mechanisms that modulate signalling by G-protein-coupled receptors. *Biochem J*, **322**:1-18.

[349] Dohlman, H. G., and Thorner, J. (1997). RGS proteins and signalling by heterotrimeric G proteins. *J Biol Chem*, **272**:3871-3874.

[350] Berman, D. M., and Gilman, A. G. (1998). Mammalian RGS proteins: barbarians at the gate. *J Biol Chem*, **273**:1269-1272.

[351] Chuang, D. M., and Costa, E. (1979). Evidence for internalization of the recognition site of β-adrenergic receptors during receptor subsensitivity in induced by (-)isoproterenol. *Proc Natl Acad Sci USA*, **76**:3024-3028.

[352] Harden, T. K., Cotton, C. U., Waldo, G. L., Lutton, J. K., and Perkins, J. P. (1980). Catecholamine-induced alteration in sedimentation behaviour of membrane bound β-adrenergic receptors. *Science*, **210**:441-443.

[353] Staehelin, M., and Simons, P. (1982). Rapid and reversible disappearance of β-adrenergic cell surface receptors. *EMBO J*, **1**:187-190.

[354] von Zastrow, M., and Kobilka, B. K. (1992). Ligand-regulated internalization and recycling of human β2-adrenergic receptors between the plasma membrane and endosomes containing transferrin receptors. *J Biol Chem*, **267**:3530-3538.

[355] Barak, L. S., Ferguson, S. S. G., Zhang, J., Martenson, C., Meyer, T., and Caron, M. G. (1997). Internal trafficking and surface mobility of a functionally intact b2-adrenergic receptor-green fluorescent protein conjugate. *Mol Pharmacol*, **51**:177-184.

[356] Pippig, S., Andexinger, S., and Lohse, M. J. (1995). Sequestration and recycling of the β2-adrenergic receptors permit receptor resensitization. *Mol Pharmacol*, **47**:666-676.

[357] Krueger, K. M., Daaka, Y., Pitcher, J. A., and Lefkowitz, R. J. (1997). The role of sequestration in G protein-coupled receptor resensitization: regulation of β2-adrenergic receptor dephosphorylation by vesicular acidification. *J Biol Chem*, **272**:5-8.

[358] Walker, J. K., Premont, R. T., Barak, L. S., Caron, M. G., and Shetzline, M. A. (1999). Properties of secretin receptor internalization differ from those of the β_2-adrenergic receptor. *J Biol Chem*, **274**:31515-31523.

[359] Shetzline, M. A., Premont, R. T., Walker, J. K., Vigna, S. R., and Caron, M. G. (1998). A role for receptor kinases in the regulation of class II G protein-coupled receptors. Phosphorylation and desensitization of the secretin receptor. *J Biol Chem*, **273**:6756-6762.

[360] Ulrich, C. D. II, Holtmann, M., and Miller, L. J. (1998). Secretin and vasoactive intestinal peptide receptors: members of a unique family of G protein-coupled receptors. *Gastroenterology*, **114**:382-397.

[361] Heurich, R. O., Buggy, J. J., Vandenberg, M. T., and Rossomando, A. J. (1996). Glucagon induces a rapid and sustained phosphorylation of the human glucagon receptor in Chinese hamster ovary cells. *Biochem Biophys Res Commun*, **220**:905-910.

[362] Gromada, J., Dissing, S., and Rorsman, P. (1996). Desensitization of glucagon-like peptide 1 receptors in insulin-secreting beta TC3 cells: role of PKA-independent mechanisms. *Brit J Pharmacol*, **118**:769-775.

[363] Fehmann, H-C., Jiang, J., Pitt, D., Schweinfurth, J., and Göke, B. (1996). Ligand-induced regulation of glucagon-like peptide-I receptor function and expression in insulin-secreting beta cells. *Pancreas*, **13**:273-282.

[364] Widmann, C., Dolci, W., and Thorens, B. (1995). Agonist-induced internalization and recycling of the glucagon-like peptide-1 receptor in transfected fibroblasts and in insulinomas. *Biochem J*, **310**:203-214.

[365] Göke, R., Richter, G., Göke, B., Trautmann, M., and Arnold, R. (1989). Internalization of glucagon-like peptide-1(7-36)amide in rat insulinoma cells. *Res Exp Med*, **189**:257-264.

[366] Widmann, C., Dolci, W., and Thorens, B. (1997). Internalization and homologous desensitization of the GLP-1 receptor depend on phosphorylation of the receptor carboxyl tail at the same three sites. *Mol Endocrinol*, **11**:1094-1102.

[367] Widmann, C., Dolci, W., and Thorens, B. (1996). Heterologous desensitization of the glucagon-like peptide-1 receptor by phorbol esters requires phosphorylation of the cytoplasmic tail at four different sites. *J Biol Chem*, **271**:19957-19963.

[368] Widmann, C., Dolci, W., and Thorens, B. (1996). Desensitization and phosphorylation of the glucagon-like peptide-1 (GLP-1) receptor by GLP-1 and 4-phorbol 12-myristate 13-acetate. *Mol Endocrinol*, **10**:62-75.

[369] Tseng, C-C., Boylan, M. O., Jarboe, L. A., Usdin, T. B., and Wolfe, M. M. (1996). Chronic desensitization of the glucose-dependent insulinotropic polypeptide receptor in diabetic rats. *Am J Physiol*, **270**:E661-E666.

[370] Hinke, S. A., Pauly, R. P., Ehses, J., Kerridge, P., Demuth, H-U., McIntosh, C. H. S., and Pederson, R. A. (2000). Role of glucose in chronic desensitization of isolated rat islets

and mouse insulinoma (βTC-3) cells to glucose-dependent insulinotropic polypeptide. *J Endocrinol*, **165**:281-291.

[371] Tseng, C-C., and Zhang, X. Y. (1998). Role of regulator of G protein signaling in desensitization of the glucose-dependent insulinotropic peptide receptor. *Endocrinology*, **139**:4470-4475.

[372] Tseng, C-C., and Zhang, X. Y. (2000). Role of G protein-coupled receptor kinases in glucose-dependent insulinotropic polypeptide receptor signaling. *Endocrinology*, **141**:947-952.

[373] Nauck, M., Stöckmann, F., Ebert, R., and Creutzfeldt, W. (1986). Reduced incretin effect in type 2 (non-insulin-dependent) diabetes. *Diabetologia*, **29**:46-52.

[374] Holst, J. J., Gromada, J., and Nauck, M. A. (1997). The pathogenesis of NIDDM involves a defective expression of the GIP receptor. *Diabetologia*, **40**:984-986.

[375] Elahi, D., McAloon-Dyke, M., Fukagawa, N. K., Meneilly, G. S., Sclater, A. L., Minaker, K. L., Habener, J. F., and Andersen, D. K. (1994). The insulinotropic actions of glucose-dependent insulinotropic polypeptide (GIP) and glucagon-like peptide-1 (7-37) in normal and diabetic subjects. *Regul Pept*, **51**:63-74.

[376] Jones, I. R., Owens, D. R., Moody, A. J., Luzio, S. D., Morris, T., and Hayes, T. M. (1987). The effects of glucose-dependent insulinotropic polypeptide infused at physiological concentrations in normal subjects and type 2 (non-insulin-dependent) diabetic patients on glucose tolerance and B-cell secretion. *Diabetologia*, **30**:707-712.

[377] Nauck, M. A., Kleine, N., Orskov, C., Holst, J. J., Willms, B., and Creutzfeldt, W. (1993). Normalization of fasting hyperglycaemia by exogenous glucagon-like peptide 1 (7-36 amide) in type 2 (non-insulin-dependent) diabetic patients. *Diabetologia*, **36**:741-744.

[378] Krarup, T., Saurbrey, N., Moody, A. J., Kühl, C., and Madsbad, S. (1987). Effect of porcine gastric inhibitory polypeptide on beta-cell function in type I and type II diabetes mellitus. *Metabolism*, **36**:677-682.

[379] Lynn, F. C., Pamir, N., Ng, E. H., McIntosh, C. H., Kieffer, T. J., and Pederson, R. A. (2001). Defective glucose-dependent insulinotropic polypeptide receptor expression in diabetic fatty Zucker rats. *Diabetes*, **50**:1004-1011.

[380] Pauly, R. P., Rosche, F., Wermann, M., McIntosh, C. H. S., Pederson, R. A., and Demuth, H. U. (1996). Investigation of glucose-dependent insulinotropic polypeptide-(1-42) and glucagon-like peptide-1-(7-36) degradation in vitro by dipeptidyl peptidase IV using matrix-assisted laser desorption/ionization-time of flight mass spectrometry. A novel kinetic approach. *J Biol Chem*, **271**:23222-23229.

[381] Pederson, R. A., White, H. A., Schlenzig, D., Pauly, R. P., McIntosh, C. H. S., and Demuth, H-U. (1998). Improved glucose tolerance in Zucker fatty rats by oral administration of the dipeptidyl peptidase IV inhibitor isoleucine thiazolidide. *Diabetes*, **47**:1253-1258.

[382] Pauly, R. P., Demuth, H-U., Rosche, F., Schmidt, J., White, H. A., Lynn, F., McIntosh, C. H., and Pederson, R. A. (1999). Improved glucose tolerance in rats treated with the dipeptidyl peptidase IV (CD26) inhibitor Ile-thiazolidide. *Metabolism*, **48**:385-389.

[383] Kesper, S., Rucha, J., Neye, H., Mazenot, C., and Verspohl, E. J. (1999). Galpha(i2)-mRNA and -protein regulation as a mechanism for heterologous sensitization and desensitization of insulin secretion. *Cell Signal*, **11**:759-768.

[384] Attramadal, H., Eikvar, L., and Hansson, V. (1988). Mechanisms of glucagon-induced homologous and heterologous desensitization of andenylate cyclase in membranes and whole sertoli cells of the rat. *Endocrinology*, **123**:1060-1068.

[385] Mundell, S. J., and Kelly, E. (1998). The effect of inhibitors of receptor internalization on the desensitization and resensitization of three Gs-coupled receptor responses. *Brit J Pharmacol*, **125**:1594-1600.

[386] Tartakoff, A. M. (1983). Perturbation of vesicular traffic with the carboxylic ionophore monensin. *Cell*, **32**:1026-1028.

[387] Mollenhauer, H. H., Morre, D. J., and Rowe, L. D. (1990). Alteration of intracellular traffic by monensin; mechanism, specificity and relationship to toxicity. *Biochim Biophys Acta*, **1031**:225-246.

[388] Ämmälä, C., Ashcroft, F. M., and Rorsman, P. (1993). Calcium-independent potentiation of insulin release by cyclic AMP in single β-cells. *Nature*, **363**:356-358.

[389] Renström, E., Eliasson, L., and Rorsman, P. (1997). Protein kinase A-dependent and -independent stimulation of exocytosis by cAMP in mouse pancreatic B-cells. *J Physiol*, **502**:105-118.

[390] Zhou, J., and Egan, J. M. (1997). SNAP-25 is phosphorylated by glucose and GLP-1 in RIN 1046-38 cells. *Biochem Biophys Res Commun*, **238**:297-300.

[391] De Vries, L., Zheng, B., Fischer, T., Elenko, E., and Farquar, M. G. (2000). The regulator of G protein signaling family. *Annu Rev Phamacol Toxicol*, **40**:235-271.

[392] Zheng, B., Ma, Y. C., Ostrom, R. S., Lavoie, C., Gill, G. N., Insel, P. A., Huang, X. Y., and Farquhar, M. G. (2001). RGS-PX1, a GAP for GalphaS and sorting nexin in vesicular trafficking. *Science*, **294**:1939-1942.

[393] Sinnarajah, S., Dessauer, C. W., Srikumar, D., Chen, J., Yuen, J., Yilma, S., Dennis, J. C., Morrison, E. E., Vodyanoy, V., and Kehrl, J. H. (2001). RGS2 regulates signal transduction in olfactory neurons by attenuating activation of adenylyl cyclase III. *Nature*, **409**:1051-1055.

[394] Houslay, M. D. (1991). 'Crosstalk': a pivotal role for protein kinase C in modulating relationships between signal transduction pathways. *Eur J Biochem*, **195**:9-27.

[395] Heuser, J. E., and Anderson, R. G. W. (1989). Hypertonic media inhibit receptor-mediated endocytosis by blocking clathrin-coated pit formation. *J Cell Biol*, **108**:389-400.

[396] Milligan, G. (1999). Exploring the dynamics of regulation of G protein-coupled receptors using green fluorescent protein. *Brit J Pharmacol*, **128**:501-509.

[397] Ferguson, S. S. G. (1998). Using green fluorescent protein to understand the mechanisms of G-protein-coupled receptor regulation. *Braz J Med Biol Res*, **31**:1471-1477.

[398] Tarasova, N. I., Stauber, R. H., Choi, J. K., Hudson, E. A., Czerwinski, G., Miller, J. L., Pavlakis, G. N., Michejda, C. J., and Wank, S. A. (1997). Visualization of G protein-coupled receptor trafficking with the aid of the green fluorescent protein: endocytosis and recycling of cholecystokinin receptor type A. *J Biol Chem*, **272**:14817-14824.

[399] Conway, B. R., Minor, L. K., Xu, J. Z., D'Andrea, M. R., Ghosh, R. N., and Demarest, K. T. (2001). Quantitative analysis of agonist-dependent parathyroid hormone receptor trafficking in whole cells using a functional green fluorescent protein conjugate. *J Cell Physiol*, **189**:341-355.

[400] Drmota, T., Gould, G. W., and Milligan, G. (1998). Real time visualization of agonist-mediated redistribution and internalization of a green fluorescent protein-tagged form of the thyrotropin-releasing hormone receptor. *J Biol Chem*, **272**:24000-24008.

[401] Awaji, T., Hirasawa, A., Kataoka, M., Shinoura, H., Nakayama, Y., Sugawara, T., Izumi, S., and Tsujimoto, G. (1998). Real-time optical monitoring of ligand-mediated internalization of α_{1b}-adrenoceptor with green fluorescent protein. *Mol Endocrinol*, **12**:1099-1111.

[402] Salapatek, A. M. F., MacDonald, P. E., Gaisano, H. Y., and Wheeler, M. B. (1999). Mutations to the third cytoplasmic domain of the glucagon-like peptide 1 (GLP-1) receptor can functionally uncouple GLP-1-stimulated insulin secretion in HIT-T15 cells. *Mol Endocrinol*, **13**:1305-1317.

[403] Gaudriault, G., Nouel, D., Dal Farra, C., Beaudet, A., and Vincent, J-P. (1997). Receptor-induced internalization of selective peptidic μ and δ opioid ligands. *J Biol Chem*, **272**:2880-2888.

[404] Grady, E. F., Slice, L. W., Brant, W. O., Walsh, J. H., Payan, D. G., and Bunnett, N. W. (1995). Direct observation of endocytosis of gastrin releasing peptide and its receptor. *J Biol Chem*, **270**:4603-4611.

[405] Brown, J. C., and Pederson, R. A. (1970). Cleavage of a gastric inhibitory polypeptide with cyanogen bromide and the physiological action of the C-terminal fragment. *J Physiol (Lond)*, **210**:52P.

[406] Schmidt, W. E., Siegel, E. G., Gallwitz, B., Kümmel, H., Ebert, R., and Creutzfeldt, W. (1986). Characterization of the insulinotropic activity of fragments derived from gastric inhibitory polypeptide (abstract). *Diabetologia*, **29**:591A.

[407] Yanaihara, N., Mochizuki, T., Yanaihara, C., Sakura, N., Hashimoto, T., Sakagami, M., Kaneko, T., Kanetoh, A., and Brown, J. C. (1978). Synthesis of GIP, *in* S. R. Bloom, ed., Gut Hormones: New York, Churchill Livingstone, p. 271-276.

[408] Moroder, L., Hallett, A., Thamm, P., Wilschowitz, L., Brown, J. C., and Wünsch, E. (1978). Studies on gastric inhibitory polypeptide: synthesis of the octatricontapeptide GIP(1-38) with full insulinotropic activity (abstract). *Scand J Gastroenterol*, **13 (Suppl. 49)**:129.

[409] Sandberg, E., Ahrén, B., Tendler, D., Carlquist, M., and Efendic, S. (1986). Potentiation of glucose-induced insulin secretion in the perfused rat pancreas by porcine GIP (gastric inhibitory polypeptide), bovine GIP, and bovine GIP(1-39). *Acta Physiol Scand*, **127**:323-326.

[410] Pederson, R. A., Mochizuki, T., Yanaihara, C., Yanaihara, N., and Brown, J. C. (1990). Reduced somatostatinotropic effect of a GIP fragment (pGIP[1-30]-NH2) with insulinotropic activity. *Digestion*, **46**:86.

[411] Taminato, T., Seino, Y., Goto, Y., Inoue, Y., and Kadowaki, S. (1977). Synthetic gastric inhibitory polypeptide. Stimulatory effect on insulin and glucagon secretion in the rat. *Diabetes*, **26**:480-484.

[412] Yajima, H., Kai, Y., Ogawa, H., Kubota, M., and Mori, Y. (1977). Structure-activity relationships of gastrointestinal hormones: motilin, GIP, and [27-TYR]CCK-PZ. *Gastroenterology*, **72**:793-796.

[413] Gelling, R. W., Coy, D. H., Pederson, R. A., Wheeler, M. B., Hinke, S., Kwan, T., and McIntosh, C. H. S. (1997). $GIP_{6-30amide}$ contains the high affinity binding region of GIP and is a potent inhibitor of GIP_{1-42} action in vitro. *Regul Pept*, **69**:151-154.

[414] Moody, A. J., Damm Jørgensen, K., and Thim, L. (1981). Structure-function relationships in porcine GIP (abstract). *Diabetologia*, **21**:306.

[415] Brown, J. C., Dahl, M., Kwauk, S., McIntosh, C. H. S., Muller, M., Otte, S. C., and Pederson, R. A. (1981). Properties and actions of GIP, *in* S. R. Bloom, and J. M. Polak, eds., Gut Hormones: New York, Churchill Livingstone, p. 248-255.

[416] Schmidt, W. E., Siegel, E. G., Ebert, R., and Creutzfeldt, W. (1986). N-terminal tyrosine-alanine is required for the insulin-releasing activity of glucose-dependent insulinotropic polypeptide (abstract). *Eur J Clin Invest*, **16**:A9.

[417] Deacon, C. F., Danielsen, P., Klarskov, L., Olesen, M., and Holst, J. J. (2001). Dipeptidyl peptidase IV inhibition reduces the degradation and clearance of GIP and potentiates its insulinotropic and antihyperglycemic effects in anesthetized pigs. *Diabetes*, **50**:1588-1597.

[418] Pauly, R. P., Demuth, H-U., Rosche, F., Schmidt, J., White, H. A., McIntosh, C. H. S., and Pederson, R. A. (1996). Inhibition of dipeptidyl peptidase IV (DP IV) in rat results in improved glucose tolerance (abstract). *Regul Pept*, **64**:148.

[419] Balkan, B., Kwasnik, L., Miserendino, R., Holst, J. J., and Li, X. (1999). Inhibition of dipeptidyl peptidase IV with NVP-DPP728 increases plasma GLP-1 (7-36 amide) concentrations and improves oral glucose tolerance in obese Zucker rats. *Diabetologia*, **42**:1324-1331.

[420] Hupe-Sodmann, K, McGregor, GP, Bridenbaugh, R, Göke, R, Göke, B, Thole, H, Zimmermann, B, and Voigt, K (1995). Characterisation of the processing by human neutral endopeptidase 24.11 of GLP-1(7-36) amide and comparison of the substrate specificity of the enzyme for other glucagon-like peptides. *Regul Pept*, **58**:149-156.

[421] Agerberth, B., Boman, A., Andersson, M., Jörnvall, H., Mutt, V., and Boman, H. G. (1993). Isolation of three antibacterial peptides from pig intestine: gastric inhibitory polypeptide (7-42), diazepam-binding inhibitor (32-86) and a novel factor, peptide 3910. *Eur J Biochem*, **216**:623-9.

[422] Sarson, D. L., Hayter, R. C., and Bloom, S. R. (1982). The pharmacokinetics of porcine glucose-dependent insulinotropic polypeptide (GIP) in man. *Eur J Clin Invest*, **12**:457-461.

[423] Sirinek, K. R., O'Dorisio, T. M., Gaskill, H. V., and Levine, B. A. (1984). Chronic renal failure: effect of hemodialysis on gastrointestinal hormones. *Am J Surg*, **148**:732-735.

[424] Jorde, R., Burhol, P. G., Gunnes, P., and Schulz, T. B. (1981). Removal of IR-GIP by the kidneys in man, and the effect of acute nephrectomy on plasma GIP in rats. *Scand J Gastroent*, **16**:469-471.

[425] O'Dorisio, T. M., Sirinek, K. R., Mazzaferri, E. L., and Cataland, S. (1977). Renal effects on serum gastric inhibitory polypeptide (GIP). *Metabolism*, **26**:651-656.

[426] Ørskov, C., Andreasen, J., and Holst, J. J. (1992). All products of proglucagon are elevated in plasma of uremic patients. *J Clin Endocrinol Metab*, **74**:379-384.

[427] Mentlein, R. (1999). Dipeptidyl-peptidase IV (CD26)--role in the inactivation of regulatory peptides. *Regul Pept*, **85**:9-24.

[428] Chap, Z., O'Dorisio, T. M., Cataland, S., and Field, J. B. (1987). Absence of hepatic extraction of gastric inhibitory polypeptide in conscious dogs. *Dig Dis Sci*, **32**:280-284.

[429] Kreymann, B., Ghatei, M. A., Williams, G., and Bloom, S. R. (1987). Glucagon-like peptide-1 (7-36): a physiological incretin in man. *Lancet*, **2**:1300-1304.

[430] Schjoldager, B. T., Mortensen, P. E., Christiansen, J., Ørskov, C., and Holst, J. J. (1989). GLP-1 (glucagon-like peptide 1) and truncated GLP-1, fragments of human proglucagon, inhibit gastric acid secretion in humans. *Dig Dis Sci*, **34**:703-708.

[431] Wettergren, A., Schjoldager, B. T., Mortensen, P. E., Myhre, J., Christiansen, J., and Holst, J. J. (1993). Truncated GLP-1 (proglucagon 78-107amide) inhibits gastric and pancreatic functions in man. *Dig Dis Sci*, **38**:665-673.

[432] Ørskov, C., Wettergren, A., and Holst, J. J. (1993). Biological effects and metabolic rates of glucagon-like peptide-1 7-36 amide and glucagon-like peptide-1 7-37 in healthy subjects are indistinguishable. *Diabetes*, **42**:658-661.

[433] Deacon, C. F., Pridal, L., Klarskov, L., Olesen, M., and Holst, J. J. (1996). Glucagon-like peptide 1 undergoes differential tissue-specific metabolism in the anesthetized pig. *Am J Physiol*, **271**:E458-E464.

[434] Pridal, L., Deacon, C. F., Kirk, O., Christensen, J. V., Carr, R. D., and Holst, J. J. (1996). Glucagon-like peptide-1(7-37) has a larger volume of distribution than glucagon-like peptide-1(7-36)amide in dogs and is degraded more quickly in vitro by dog plasma. *Eur J Drug Met Pharmacokinet*, **21**:51-59.

[435] Ruiz-Grande, C., Alarcón, C., Alcántara, A., Castilla, C., López Novoa, J. M., Villanueva-Penacarrillo, M. L., and Valverde, I (1993). Renal catabolism of truncated glucagon-like peptide-1. *Horm Metab Res*, **25**:612-616.

[436] Jaspan, J., Polonsky, K., Lewis, M., Pensler, J., Pugh, W., Moossa, A., and Rubinstein, A. (1981). Hepatic metabolism of glucagon in the dog: contribution of the liver to overall metabolic disposal of glucagon. *Am J Physiol*, **240**:E233-E244.

[437] Alford, F., Bloom, S., and Nabarro, J. (1976). Glucagon metabolism in man. Studies on the metabolic clearance rate and the plasma acute disappearance time of glucagon in normal and diabetic subjects. *J Clin Endocrinol Metab*, **42**:830-838.

[438] McDonald, J., Callahan, P., Zeitman, B., and Ellis, S. (1969). Inactivation and degradation of glucagon by dipeptidyl aminopeptidase I (cathepsin C) of rat liver. *J Biol Chem*, **244**:6199-6208.

[439] McDonald, J., Callahan, P., and Ellis, S. (1971). Polypeptide degradation by dipeptidyl aminopeptidase I (cathepsin C) and related peptidases, *in* A. Barrett, and J. Dingle, eds., Tissue Proteinases: Amsterdam, North-Holland Publishing, p. 69-107.

[440] Rao, N., Rao, G., and Hoidal, J. (1997). Human dipeptidyl peptidase I: gene characterization, localization and expression. *J Biol Chem*, **272**:10260-10265.

[441] Holst, J. J. (1991). Degradation of glucagons, *in* J. Henriksen, ed., Degradation of bioactive substances: physiology and pathophysiology: Boca Raton, CRC Press, p. 167-180.

[442] Hildebrandt, W., Blech, W., and Lohnert, K. (1991). Kinetic studies on hepatic handling of glucagon using the model of non recirculating perfused rat livers. *Horm Metab Res*, **23**:410-413.

[443] Lefèbvre, P., and Luyckx, A. (1983). The renal handling of glucagon, *in* P. J. Lefèbvre, ed., Handbook of Experimental Pharmacology 66/II: New York, Springer-Verlag, p. 389-396.

[444] Peterson, D. R., Green, E. A., Oparil, S., and Hjelle, J. T. (1986). Transport and hydrolysis of glucagon in the proximal nephron. *Am J Physiol*, **251**:F460-F467.

[445] Talor, Z., Emmanouel, D. S., and Katz, A. I. (1983). Glucagon degradation by luminal and basolateral rabbit tubular membranes. *Am J Physiol*, **244**:F297-F303.

[446] Buckley, D. I., and Lundquist, P. (1992). Analysis of the degradation of insulinotropin [GLP-1 (7-37)] in human plasma and production of degradation resistant analogs (abstract). *Regul Pept*, **40**:117.

[447] Deacon, C. F., Johnsen, A. H., and Holst, J. J. (1995). Degradation of glucagon-like peptide-1 by human plasma in vitro yields an N-terminally truncated peptide that is a major endogenous metabolite in vivo. *J Clin Endocrinol Metab*, **80**:952-957.

[448] Deacon, C. F., Nauck, M. A., Toft-Nielsen, M., Pridal, L., Willms, B., and Holst, J. J. (1995). Both subcutaneously and intravenously administered glucagon-like peptide I are rapidly degraded from the NH2-terminus in type II diabetic patients and in healthy subjects. *Diabetes*, **44**:1126-1131.

[449] Deacon, C. F., Hughes, T. E., and Holst, J. J. (1998). Dipeptidyl peptidase IV inhibition potentiates the insulinotropic effect of glucagon-like peptides 1 in the anesthetized pig. *Diabetes*, **47**:764-769.

[450] Wettergren, A., Wojdemann, M., and Holst, J. J. (1998). The inhibitory effect of glucagon-like peptide-1 (7-36)amide on antral motility is antagonized by its N-terminally truncated primary metabolite GLP-1 (9-36)amide. *Peptides*, **19**:877-882.

[451] Knudsen, L. B., and Pridal, L. (1996). Glucagon-like peptide-1-(9-36) amide is a major metabolite of glucagon-like peptide-1-(7-36) amide after in vivo administration to dogs, and it acts as an antagonist on the pancreatic receptor. *Eur J Pharmacol*, **318**:429-435.

[452] Hansen, L., Deacon, C. F., Orskov, C., and Holst, J. J. (1999). Glucagon-like peptide-1-(7-36)amide is transformed to glucagon-like peptide-1-(9-36)amide by dipeptidyl peptidase IV in the capillaries supplying the L cells of the porcine intestine. *Endocrinology*, **140**:5356-5363.

[453] Pospisilik, J. A., Hinke, S. A., Pederson, R. A., Hoffmann, T., Rosche, F., Schlenzig, D., Glund, K., Heiser, U., McIntosh, C. H. S., and Demuth, H-U. (2001). Metabolism of glucagon by dipeptidyl peptidase IV (CD26). *Regul Pept*, **96**:133-141.

[454] Märki, F. (1983). Stability of endogenous immunoreactive glucagon (IRG) in animal blood. *Horm Metab Res*, **15**:307-308.

[455] Hinke, S. A., Manhart, S., Pamir, N., Demuth, H-U., Gelling, R. W., Pederson, R. A., and Mcintosh, C. H. S. (2001). Identification of a bioactive domain in the amino-terminus of glucose-dependent insulinotropic polypeptide (GIP). *Biochim Biophys Acta*, **1547**:143-155.

[456] Hinke, S. A., Gelling, R. W., Pederson, R. A., Manhart, S., Nian, C., Demuth, H-U., and McIntosh, C. H. S. (2002). Dipeptidyl peptidase IV-resistant [D-Ala2]glucose-dependent insulinotropic polypeptide (GIP) improves glucose tolerance in normal and obese diabetic rats. *Diabetes*, **51**:652-661.

[457] Siegel, E. G., Scharf, G., Gallwitz, B., Mentlein, R., Morys-Wortmann, C., Folsch, U. R., and Schmidt, W. E. (1999). Comparison of the effect of native glucagon-like peptide 1 and dipeptidyl peptidase IV-resistant analogues on insulin release from rat pancreatic islets. *Eur J Clin Invest*, **29**:610-614.

[458] Deacon, C. F., Knudsen, L. B., Madsen, K., Wiberg, F. C., Jacobsen, O., and Holst, J. J. (1998). Dipeptidyl peptidase IV resistant analogues of glucagon-like peptide-1 which

have extended metabolic stability and improved biological activity. *Diabetologia*, **41**:271-278.

[459] Ritzel, U., Leonhardt, U., Ottleben, M., Ruhmann, A., Eckart, K., Spiess, J., and Ramadori, G. (1998). A synthetic glucagon-like peptide-1 analog with improved plasma stability. *J Endocrinol*, **159**:93-102.

[460] Unson, C. G., Gurzenda, E. M., Iwasa, K., and Merrifield, R. (1989). Glucagon antagonists: contribution to binding and activity of the amino-terminal sequence 1-5, position 12, and the putative alpha-helical segment 19-27. *J Biol Chem*, **264**:789-794.

[461] Holst, J. J. (1999). Glucagon-like peptide-1, a gastrointestinal hormone with pharmaceutical potential. *Curr Med Chem*, **6**:1005-1017.

[462] O'Harte, F. P. M., Mooney, M. H., and Flatt, P. R. (1999). NH_2-terminally modified gastric inhibitory polypeptide exhibits amino-peptidase resistance and enhanced antihyperglycemic activity. *Diabetes*, **48**:758-765.

[463] O'Harte, F. P. M., Mooney, M. H., Kelly, C. M. N., and Flatt, P. R. (2000). Improved glycaemic control in obese diabetic ob/ob mice using N-terminally modified gastric inhibitory polypeptide. *J Endocrinol*, **165**:639-648.

[464] Meneilly, G. S., Bryer-Ash, M., and Elahi, D. (1993). The effect of glyburide on β-cell sensitivity to glucose-dependent insulinotropic polypeptide. *Diabetes Care*, **16**:110-114.

[465] Nauck, M. A., Busing, M., Orskov, C., Siegel, E. G., Talartschik, J., Baartz, A., Baartz, T., Hopt, U. T., Becker, H. D., and Creutzfeldt, W. (1993). Preserved incretin effect in type 1 diabetic patients with end-stage nephropathy treated by combined heterotopic pancreas and kidney transplantation. *Acta Diabetol*, **30**:39-45.

[466] Creutzfeldt, W. O., Kleine, N., Willms, B., Orskov, C., Holst, J. J., and Nauck, M. A. (1996). Glucagonostatic actions and reduction of fasting hyperglycemia by exogenous glucagon-like peptide I(7-36) amide in type I diabetic patients. *Diabetes Care*, **19**:580-586.

[467] Dupré, J., Behme, M. T., Hramiak, I. M., McFarlane, P., Williamson, M. P., Zabel, P., and McDonald, T. J. (1995). Glucagon-like peptide I reduces postprandial glycemic excursions in IDDM. *Diabetes*, **44**:626-630.

[468] Blundell, T., and Wood, S. (1982). The conformation, flexibility, and dynamics of polypeptide hormones. *Ann Rev Biochem*, **51**:123-154.

[469] DaCambra, M. P., Yusta, B., Sumner-Smith, M., Crivici, A., Drucker, D. J., and Brubaker, P. L. (2000). Structural determinants for activity of glucagon-like peptide-2. *Biochemistry*, **39**:8888-8894.

[470] Wray, V., Nokihara, K., and Naruse, S. (1997). Solution structure comparison of the VIP/PACAP family of peptides by NMR spectroscopy. *Ann NY Acad Sci*, **865**:37-44.

[471] Barden, J. A., and Cuthbertson, R. M. (1993). Stabilized NMR structure of human parathyroid hormone(1-34). *Eur J Biochem*, **215**:315-321.

[472] Pellegrini, M, Royo, M, Rosenblatt, M, Chorev, M, and Mierke, DF (1998). Addressing the tertiary structure of human parathyroid hormone-(1-34). *J Biol Chem*, **273**:10420-10427.

[473] Barden, J. A., and Kemp, B. E. (1993). NMR solution structure of human parathyroid hormone(1-34). *Biochemistry*, **32**:7126-7132.

[474] Thornton, K, and Gorenstein, DG (1994). Structure of glucagon-like peptide(7-36) amide in a dodecylphosphocholine micelle as determined by 2D NMR. *Biochemistry*, **33**:3532-3539.

[475] Raufman, J-P. (1996). Bioactive peptides from lizard venoms. *Regul Pept*, **61**:1-18.

[476] Blankenfeldt, W., Nokihara, K., Naruse, S., Lessel, U., Schomburg, D., and Wray, V. (1996). NMR spectroscopic evidence that helodermin, unlike other members of the secretin/VIP family of peptides, is substantially structured in water. *Biochemistry*, **35**:5955-5962.

[477] Inooka, H., Ohtaki, T., Kitahara, O., Ikegami, T., Endo, S., Kitada, C., Ogi, K., Onda, H., Fujino, M., and Shirakawa, M. (2001). Conformation of a peptide ligand bound to its G-protein coupled receptor. *Nat Struct Biol*, **8**:161-165.

[478] Gascuel, O., and Golmard, J. L. (1988). A simple method for predicting the secondary structure of globular proteins: implications and accuracy. *Comput Appl Biosci*, **4**:357-365.

[479] Luck, MD, Carter, PH, and Gardella, TJ (1999). The (1-14) fragment of parathyroid hormone (PTH) activates intact and amino-terminally truncated PTH-1 receptors. *Mol Endocrinol*, **13**:670-680.

[480] Carter, P. H., Shimzu, M., Luck, M. D., and Gardella, T. J. (1999). The hydrophobic residues phenylalanine 184 and leucine 187 in the type-1 parathyroid hormone (PTH) receptor functionally interact with the amino-terminal portion of PTH-(1-34). *J Biol Chem*, **274**:31955-31960.

[481] Behar, V., Bisello, A., Bitan, G., Rosenblatt, M., and Chorev, M. (2000). Photoaffinity cross-linking identifies differences in the interactions of an agonist and an antagonist with the parathyroid hormone/parathyroid hormone-related protein receptor. *J Biol Chem*, **275**:9-17.

[482] Adams, A. E., Bisello, A., Chorev, M., Rosenblatt, M., and Suva, L. J. (1998). Arginine 186 in the extracellular N-terminal region of the human parathyroid hormone 1 receptor is essential for contact with position 13 of the hormone. *Mol Endocrinol,* **12**:1673-1683.

[483] Ohneda, A, Ohneda, K, Ohneda, M, Koizumi, F, Ohashi, S, Kawai, K, and Suzuki, S (1991). The structure-function relationship of GLP-1 related peptides in the endocrine function of the canine pancreas. *Tohuku J Exp Med*, **165**:209-221.

[484] Suzuki, S., Kawai, K., Ohashi, S., Mukai, H., and Yamashita, K. (1989). Comparison of the effects of various C-terminal and N-terminal fragment peptides of glucagon-like

peptide-1 on insulin and glucagon release from the isolated perfused rat pancreas. *Endocrinology*, **125:**3109-3114.

[485] Epand, R. M., and Grey, V. (1973). Conformational and biological properties of partial sequences of glucagon. *Can J Physiol Pharmacol*, **51:**243-248.

[486] Carrey, E. A., and Epand, R. M. (1983). Conformational and biological properties of glucagon fragments containing residues 1-17 and 19-29. *Int J Peptide Protein Res*, **22:**362-370.

[487] Fournier, A., Saunders, J. K., and St.-Pierre, S. (1984). Synthesis, conformational studies and biological activities of VIP and related fragments. *Peptides*, **5:**169-177.

[488] Gallwitz, B., Witt, M., Paetzold, G., Morys-Wortmann, C., Zimmermann, B., Eckart, K., Fölsch, U. R., and Schmidt, W. E. (1994). Structure/activity characterization of glucagon-like peptide-1. *Eur J Biochem*, **225:**1151-1156.

[489] Adelhorst, K., Hedegaard, B. B., Knudsen, L. B., and Kirk, O. (1994). Structure-activity studies of glucagon-like peptide-1. *J Biol Chem*, **269:**6275-6278.

[490] Shimizu, N., Guo, J., and Gardella, T. J. (2001). Parathyroid hormone (PTH)-(1-14) and -(1-11) analogs conformationally constrained by alpha-aminoisobutyric acid mediate full agonist responses via the juxtamembrane region of the PTH-1 receptor. *J Biol Chem*, **276:**49003-49012.

[491] Shimizu, M., Carter, P. H., Khatri, A., Potts, J. T., Jr., and Gardella, T. J. (2001). Enhanced activity in parathyroid hormone-(1-14) and -(1-11): novel peptides for probing ligand-receptor interactions. *Endocrinology*, **142:**3068-3074.

[492] Shimizu, M., Potts, J. T., Jr., and Gardella, T. J. (2000). Minimization of parathyroid hormone. Novel amino-terminal parathyroid hormone fragments with enhanced potency in activating the type-1 parathyroid hormone receptor. *J Biol Chem*, **275:**21836-21843.

[493] Carter, P. H., and Gardella, T. J. (2001). Zinc(II)-mediated enhancement of the agonist activity of histidine-substituted parathyroid hormone(1-14) analogues. *Biochim Biophys Acta*, **23:**2-3.

[494] Gershengorn, M. C., and Osman, R. (2001). Minireview: insights into G protein-coupled receptor function using molecular models. *Endocrinology*, **142:**2-10.

[495] Hjorth, S. A., and Schwartz, T. W. (1996). Glucagon and GLP-1 receptors: lessons from chimeric ligands and receptors. *Acta Physiol Scand*, **157:**343-345.

[496] Frohman, L. A., Downs, T. R., Heimer, E. P., and Felix, A. M. (1989). Dipeptidyl peptidase IV and trypsin-like enzymatic degradation of human growth hormone-releasing hormone in plasma. *J Clin Invest*, **83:**1533-1540.

[497] Heiman, M. L., Nekola, M. V., Murphy, W. A., Lance, V. A., and Coy, D. H. (1985). An extremely sensitive in vitro model for elucidating structure-activity relationships of growth hormone-releasing factor analogs. *Endocrinology*, **116:**410-415.

[498] Lance, V. A., Murphy, W. A., Sueiras-Diaz, J., and Coy, D. H. (1984). Super-active analogs of growth hormone-releasing factor (1-29)-amide. *Biochem Biophys Res Commun*, **119**:265-272.

[499] Sueiras-Diaz, J., Lance, V. A., Murphy, W. A., and Coy, D. H. (1984). Structure-activity studies on the N-terminal region of glucagon. *J Med Chem*, **27**:310-315.

[500] Xiao, Q., Giguere, J., Parisien, M., Jeng, W., St-Pierre, S. A., Brubaker, P. L., and Wheeler, M. B. (2001). Biological activities of glucagon-like peptide-1 analogues in vitro and in vivo. *Biochemistry*, **40**:2860-2869.

[501] Siegel, E. G., Gallwitz, B., Scharf, G., Mentlein, R., Morys-Wortmann, C., Fölsch, U. R., Schrezenmeir, J., Drescher, K., and Schmidt, W. E. (1999). Biological activity of GLP-1 analogues with N-terminal modifications. *Regul Pept*, **79**:93-102.

[502] Joseph, J. W., Kalitsky, J., St-Pierre, S., and Brubaker, P. L. (2000). Oral delivery of glucagon-like peptide-1 in a modified polymer preparation normalizes basal glycaemia in diabetic db/db mice. *Diabetologia*, **43**:1319-1328.

[503] Frohman, L. A., Downs, T. R., Williams, T. C., Heimer, E. P., Pan, Y. C., and Felix, A. M. (1986). Rapid enzymatic degradation of growth hormone-releasing hormone by plasma *in vitro* and *in vivo* to a biologically inactive product cleaved at the NH_2 terminus. *J Clin Invest*, **78**:906-913.

[504] Bitar, K. G., Somogyvari-Vigh, A., and Coy, D. H. (1994). Cyclic lactam analogues of ovine pituitary adenylate cyclase activating polypeptide (PACAP): discovery of potent type II receptor antagonists. *Peptides*, **15**:461-466.

[505] Barbier, J. R., MacLean, S., Morley, P., Whitfield, J. F., and Willick, G. E. (2000). Structure and activities of constrained analogues of human parathyroid hormone and parathyroid hormone-related peptide: implications for receptor-activating conformations of hormones. *Biochemistry*, **39**:14522-14530.

[506] Ahn, J. M., Gitu, P. M., Medieros, M., Swift, J. R., Trivedi, D., and Hruby, V. J. (2001). A new approach to search for the bioactive conformation of glucagon: positional cyclization scanning. *J Med Chem*, **44**:3109-3116.

[507] Parker, J. C., Andrews, K. M., Rescek, D. M., Massefski, W. Jr, Andrews, G. C., Contillo, L. G., Stevenson, R. W., Singleton, D. H., and Suleske, R. T. (1998). Structure-function analysis of a series of glucagon-like peptide-1 analogs. *J Peptide Res*, **52**:398-409.

[508] Amland, P. F., Jorde, R., Aanderud, S., Burhol, P. G., and Giercksky, K.-E. (1985). Effects of intravenously infused porcine GIP on serum insulin, plasma C-peptide, and pancreatic polypeptide in non-insulin-dependent diabetes. *Scand J Gastroenterol*, **20**:315-320.

[509] Jones, I. R., Owens, D. R., Luzio, S., and Hayes, T. M. (1989). Glucose dependent insulinotropic polypeptide (GIP) infused intravenously is insulinotropic in the fasting state in type 2 (non-insulin dependent) diabetes mellitus. *Horm Metabol Res*, **21**:23-26.

[510] Ritzel, R., Ørskov, C, Holst, J. J., and Nauck, M. A. (1995). Pharmacokinetic, insulinotropic, and glucagonostatic properties of GLP-1 [7-36 amide] after subcutaneous injection in healthy volunteers: dose-resopnse relationships. *Diabetologia*, **38**:720-725.

[511] Meier, J. J., Nauck, M. A., Schmidt, W. E., and Gallwitz, B. (2002). Gastric inhibitory polypeptide: the neglected incretin revisited. *Regul Pept*, **107**:1-13.

[512] Grondin, G., Hooper, N., and LeBel, D. (1999). Specific localization of membrane dipeptidase and dipeptidyl peptidase IV in secretion granules of two different pancreatic islet cells. *J Histochem Cytochem*, **47**:489-497.

[513] Pavoine, C., Brechler, V., Kervran, A., Blache, P., Le-Nguyen, D., Laurent, S., Bataille, D., and Pecker, F. (1991). Miniglucagon [glucagon-(19-29)] is a component of the positive inotropic effect of glucagon. *Am J Physiol*, **260**:C993-C999.

[514] Dalle, S., Smith, P., Blache, P., Le-Nguyen, D., Le Brigand, L., Bergeron, F., Ashcroft, F. M., and Bataille, D. (1999). Miniglucagon (glucagon 19-29), a potent and efficient inhibitor of secretagogue-induced insulin release through a Ca2+ pathway. *J Biol Chem*, **274**:10869-10876.

[515] Frandsen, E. K., Grønvald, F. C., Heding, L. G., Johansen, N. L. , Lundt, B. F., Moody, A. J., Markussen, J., and Volund, A. (1981). Glucagon: structure-function relationships investigated by sequence deletions. *Hoppe-Seyler's Z Physiol Chem*, **362**:665-678.

[516] Smith, R. A., Sisk, R., Lockhart, P., Mathewes, S., Gilbert, T., Walker, K., and Piggot, J. (1993). Isolation of glucagon antagonists by random molecular mutagenesis and screening. *Mol Pharmacol*, **43**:741-748.

[517] Robberecht, P., Damien, C., Moroder, L., Coy, D. H., Wunsch, E., and Cristophe, J. (1988). Receptor occupancy and adenylate cyclase activation in rat liver and heart membranes by 10 glucagon analogs modified in position 2, 3, 4, 25, 27, and/or 29. *Regul Pept*, **21**:117-128.

[518] Unson, C. G., and Merrifield, R. B. (1994). Identification of an essential serine residue in glucagon: implication for an active site triad. *Proc Natl Acad Sci USA*, **91**:454-458.

[519] Marguet, D, Baggio, L, Kobayashi, T, Bernard, A-M, Pierres, M, Nielsen, PF, Ribel, U, Watanabe, T, Drucker, DJ, and Wagtmann, N (2000). Enhanced insulin secretion and improved glucose tolerance in mice lacking CD26. *Proc Natl Acad Sci USA*, **97**:6874-6879.

[520] Creutzfeldt, W. (2001). The entero-insular axis in type 2 diabetes -- incretins as therpeutic agents. *Exp Clin Endocrinol Diabetes*, **109 (Suppl. 2)**:S288-S300.

[521] Holst, J. J., and Deacon, C. F. (1998). Inhibition of the activity of dipeptidylpeptidase IV as a treatment for type 2 diabetes. *Diabetes*, **47**:1663-1670.

[522] White, C. M. (1999). A review of potential cardiovascular uses of intravenous glucagon administration. *J Clin Pharmacol*, **39**:442-447.

[523] Pollack, C. V., Jr. (1993). Utility of glucagon in the emergency department. *J Emerg Med*, **11**:195-205.

[524] Fan, G., Shumay, E., Wang, H., and Malbon, C. C. (2001). The scaffold protein gravin (cAMP-dependent protein kinase-anchoring protein 250) binds the beta 2-adrenergic receptor via the receptor cytoplasmic Arg-329 to Leu-413 domain and provides a mobile scaffold during desensitization. *J Biol Chem*, **276**:24005-24014.

[525] Pierce, K. L., Tohgo, A., Ahn, S., Field, M. E., Luttrell, L. M., and Lefkowitz, R. J. (2001). Epidermal growth factor (EGF) receptor-dependent ERK activation by G protein-coupled receptors: a co-culture system for identifying intermediates upstream and downstream of heparin-binding EGF shedding. *J Biol Chem*, **276**:23155-23160.

[526] Jordan, B. A., Trapaidze, N., Gomes, I., Nivarthi, R., and Devi, L. A. (2001). Oligomerization of opioid receptors with beta 2-adrenergic receptors: a role in trafficking and mitogen-activated protein kinase activation. *Proc Natl Acad Sci USA*, **98**:343-348.

[527] Tang, H., Nishishita, T., Fitzgerald, T., Landon, E. J., and Inagami, T. (2000). Inhibition of AT1 receptor internalization by concanavalin A blocks angiotensin II-induced ERK activation in vascular smooth muscle cells. Involvement of epidermal growth factor receptor proteolysis but not AT1 receptor internalization. *J Biol Chem*, **275**:13420-13426.

[528] Elorza, A., Sarnago, S., and Mayor, F., Jr. (2000). Agonist-dependent modulation of G protein-coupled receptor kinase 2 by mitogen-activated protein kinases. *Mol Pharmacol*, **57**:778-783.

[529] Maudsley, S., Pierce, K. L., Zamah, A. M., Miller, W. E., Ahn, S., Daaka, Y., Lefkowitz, R. J., and Luttrell, L. M. (2000). The beta(2)-adrenergic receptor mediates extracellular signal-regulated kinase activation via assembly of a multi-receptor complex with the epidermal growth factor receptor. *J Biol Chem*, **275**:9572-9580.

[530] Pierce, K. L., Maudsley, S., Daaka, Y., Luttrell, L. M., and Lefkowitz, R. J. (2000). Role of endocytosis in the activation of the extracellular signal-regulated kinase cascade by sequestering and nonsequestering G protein-coupled receptors. *Proc Natl Acad Sci USA*, **97**:1489-1494.

[531] Pitcher, J. A., Tesmer, J. J., Freeman, J. L., Capel, W. D., Stone, W. C., and Lefkowitz, R. J. (1999). Feedback inhibition of G protein-coupled receptor kinase 2 (GRK2) activity by extracellular signal-regulated kinases. *J Biol Chem*, **274**:34531-34534.

[532] Schramm, N. L., and Limbird, L. E. (1999). Stimulation of mitogen-activated protein kinase by G protein-coupled alpha(2)-adrenergic receptors does not require agonist-elicited endocytosis. *J Biol Chem*, **274**:24935-24940.

[533] Lin, F. T., Miller, W. E., Luttrell, L. M., and Lefkowitz, R. J. (1999). Feedback regulation of β-arrestin1 function by extracellular signal-regulated kinases. *J Biol Chem*, **274**:15971-15974.

[534] Budd, D. C., Rae, A., and Tobin, A. B. (1999). Activation of the mitogen-activated protein kinase pathway by a Gq/11-coupled muscarinic receptor is independent of receptor internalization. *J Biol Chem*, **274:**12355-12360.

[535] Daaka, Y., Luttrell, L. M., Ahn, S., Della Rocca, G. J., Ferguson, S. S., Caron, M. G., and Lefkowitz, R. J. (1998). Essential role for G protein-coupled receptor endocytosis in the activation of mitogen-activated protein kinase. *J Biol Chem*, **273:**685-688.

[536] Luo, X., Zeng, W., Xu, X., Popov, S., Davignon, I., Wilkie, T. M., Mumby, S. M., and Muallem, S. (1999). Alternate coupling of receptors to Gs and Gi in pancreatic and submandibular gland cells. *J Biol Chem*, **274:**17684-17690.

[537] Daaka, Y., Luttrell, L. M., and Lefkowitz, R. J. (1997). Switching of the coupling of the β_2-adrenergic receptor to different G proteins by protein kinase A. *Nature*, **390:**88-91.

[538] Foord, S. M., and Marshall, F. H. (1999). RAMPs: accessory proteins for seven transmembrane domain receptors. *Trends Pharmacol Sci*, **20:**184-187.

[539] Sexton, P. M., Albiston, A., Morfis, M., and Tilakaratne, N. (2001). Receptor activity modifying proteins. *Cell Signal*, **13:**73-83.

[540] Lindsay, J. R., Au, S. T. B., Kelley, C. M., O'Harte, F. P., Flatt, P. R., and Bell, P. M. (2002). A novel amino-terminally glycated analogue of glucose-dependent insulinotropic polypeptide (GIP), with prolonged insulinotropic activity in type 2 diabetes mellitus (abstract 1394-P). *Diabetes*, **51 (Suppl. 2):**A341.